

Distribution Agreement

In presenting this thesis or dissertation as a partial fulfillment of the requirements for an advanced degree from Emory University, I hereby grant to Emory University and its agents the non-exclusive license to archive, make accessible, and display my thesis or dissertation in whole or in part in all forms of media, now or hereafter known, including display on the world wide web. I understand that I may select some access restrictions as part of the online submission of this thesis or dissertation. I retain all ownership rights to the copyright of the thesis or dissertation. I also retain the right to use in future works (such as articles or books) all or part of this thesis or dissertation.

Signature:

David B. Vogt

Date

Reductive Processes Enabled by Photoredox for the Synthesis and Modification of
Pharmaceutically Relevant Molecules

By

David B. Vogt

Doctor of Philosophy

Chemistry

Nathan Jui, Ph.D.
Advisor

Simon Blakey, Ph.D.
Committee Member

Dennis Liotta, Ph.D.
Committee Member

Accepted:

Dean of the Graduate School
Lisa A. Tedesco, Ph.D.

Date

Reductive Processes Enabled by Photoredox for the Synthesis and Modification of
Pharmaceutically Relevant Molecules

By

David B. Vogt

B.S., Furman University, 2011

Advisor: Nathan T. Jui, Ph.D.

An abstract of
A dissertation submitted to the Faculty of the
James T. Laney School of Graduate Studies of Emory University
in partial fulfillment of the requirements for the degree of
Doctor of Philosophy
in Chemistry
2020

Abstract

Reductive Processes Enabled by Photoredox for the Synthesis and Modification of Pharmaceutically Relevant Molecules

By: David B. Vogt

The generation and use of open shell species (radicals) has broadened reactivity and enabled novel disconnections repeatedly throughout history—often displaying orthogonal selectivity to their polar counterparts. Photoredox presents an ideal platform for studying and using these species as radicals can be generated in a catalytically and controlled fashion. Abstraction and radical chain mechanisms are rapid and uncontrolled and often limit the utility of the species being generated. Our group focuses on generating radical species via substrate reduction. Single electron transfer from a catalyst to the substrate results in a buildup of charge that then drives heterolytic cleavage of even strong bonds. A number of methods, including our own, utilize halogenated species for this reason; the weaker C–X bond allows for regiospecific cleavage and radical formation on a programmed atom upon halide expulsion.

We've developed a number of methods that focus on novel formation and reactivity of radicals. Detailed in Chapter 2 is the radical conjugate addition of heteroaryl radicals to an amino acid backbone for the practical and scalable synthesis of enantiopure unnatural amino acids. We later expanded the applicability of these radical additions to include neutral and rich olefins—uncovering along the way, important mechanistic principles that dictate the reactivity of heteroaryl radicals. Notably, we've also found that, under highly reducing photoredox conditions, that breaking and restoring aromaticity through the reduction of arenes, is a driving force strong enough to break benzylic C–F bonds. We've taken advantage of this cleavage mechanism to optimize conditions for alkylating trifluoromethyl aromatics—again through alkene addition. Lastly, we've explored these same conditions as a viable method for mineralizing (defluorinating) perfluorinated waste materials.

Reductive Processes Enabled by Photoredox for the Synthesis and Modification of
Pharmaceutically Relevant Molecules

By

David B. Vogt

B.S., Furman University, 2015

Advisor: Nathan T. Jui, Ph.D.

A dissertation submitted to the Faculty of the
James T. Laney School of Graduate Studies of Emory University
in partial fulfillment of the requirements for the degree of
Doctor of Philosophy
in Chemistry
2020

Acknowledgements

Autumn: You've kept me going through all rough patches and are an amazing companion and an incredible scientist. Thank you for putting up with my teasing and stupid questions regularly. I can't wait to marry you in a few short months and start our career and lives together. I couldn't ask for a better partner. Ily.

Mom and Dad: Having you nearby in grad school was a godsend. Escaping the city on the weekends kept me sane. I can begin to tell you how much I appreciate what you both have done for me my whole life and particularly in the last 5 years.

Nate: Working for you has been a truly rewarding experience. Your advice and mentoring over the last 5 years has completely reshaped me as a scientist. Thank you for letting me chase down crazy ideas and use your lab as a workshop. I hope we stay in contact as I start my career, I still have tons to learn from you.

Core 4: Man...its been a crazy 5 years. I'm grateful to have gone through grad school with you guys (relatively normal people). I know we'll stay in touch; can't wait to see what everyone accomplishes!

Ciaran: I didn't realize how valuable of a mentor you were to me until you were gone but I'm incredibly grateful for the training, discussions, and banter you gave in your short time here.

Hengbin: Working next to you for nearly a year was an interesting experience and I wouldn't trade it for anything. You left quite a legacy in the Jui lab and I appreciate all the help and guidance you gave me while you were here.

Simon: I've really enjoyed having you on my committee. You've helped me understand how to grow as a scientist and your commendation in my annual updates has given me a lot of confidence as a chemist.

Dennis: Your insight in my annual updates has been invaluable. I hope one day to know even half of what you know about chemistry.

Table of Contents

CHAPTER 1 INTRODUCTION TO PHOTOREDOX	1
1.1 DRIVING CHEMICAL REACTIONS WITH LIGHT	2
1.2 PHOTOREDOX CATALYSIS	3
1.2.1 Mechanisms of Catalysis.....	3
1.2.2 Catalyst Structures.....	5
1.2.3 The Photoredox Regime.....	9
CHAPTER 2 A PRACTICAL AND SCALABLE SYSTEM FOR HETEROARYL AMINO ACID SYNTHESIS	11
2.1 INTRODUCTION.....	12
2.2 RESULTS AND DISCUSSION.....	15
2.3 CONCLUSIONS	22
2.4 SUPPORTING INFORMATION.....	23
2.4.1 General Information	23
2.4.2 General Procedure.....	24
2.4.3 Optimization Details	25
2.4.4 Preparation of Starting Materials	28
2.4.5 Procedures and Characterization Data.....	45
2.4.6 Deprotection Procedures and Characterization Data.....	78
2.4.7 Chiral HPLC Data.....	84
2.4.8 Stern Volmer Fluorescence Quenching Experiments	86
2.4.9 Deuterium Incorporation Studies	88
CHAPTER 3 : RADICAL HYDROARYLATION OF FUNCTIONALIZED OLEFINS AND MECHANISTIC INVESTIGATION OF PHOTOCATALYTIC PYRIDYL RADICAL REACTIONS.....	89
3.1 INTRODUCTION.....	90

3.2 RESULTS AND DISCUSSION.....	93
3.2.1 Radical Hydroarylation of Olefinic Substrates.....	93
3.2.2 Mechanistic Investigation.....	99
3.3 CONCLUSIONS.....	109
3.4 SUPPORTING INFORMATION.....	110
3.4.1 General Information.....	110
3.4.2 General Procedures.....	111
3.4.3 Optimization Table.....	113
3.4.4 Preparation of Starting Materials.....	115
3.4.5 Procedures and Characterization Data.....	121
3.4.6 Scale-up Procedures.....	155
3.4.7 Mechanistic Investigation.....	157
3.4.8 Computational Details.....	177
3.4.9 Troubleshooting and Reaction Limitations.....	191

CHAPTER 4 : SELECTIVE C–F FUNCTIONALIZATION OF UNACTIVATED TRIFLUOROMETHYLARENES..... 194

4.1 INTRODUCTION.....	195
4.1.1 A Different Mode of Activation.....	195
4.1.2 Modification of Trifluoromethylaromatics.....	196
4.2 RESULTS AND DISCUSSION.....	200
4.3 CONCLUSIONS.....	211
4.4 SUPPORTING INFORMATION.....	212
4.4.1 General Information.....	212
4.4.2 General Procedures.....	213
4.4.3 Optimization Details.....	215
4.4.4 Preparation of Trifluoromethylarenes.....	219

<i>4.4.5 Procedures and Characterization Data</i>	231
<i>4.4.6 Computational Details</i>	281
<i>4.4.7 Fluorescence Quenching and Stern-Volmer Plots</i>	285

**CHAPTER 5 : REDUCTIVE MINERALIZATION OF
PERFLUOROALKYL SUBSTANCES USING VISIBLE LIGHT 289**

5.1 INTRODUCTION.....	290
5.2 RESULTS AND DISCUSSION.....	293
5.3 CONCLUSIONS	295
5.4 SUPPORTING INFORMATION.....	296
<i>5.4.1 General Information</i>	296
<i>5.4.2 General Analytical Information</i>	296
<i>5.4.3 Procedures and Characterization Data</i>	296

List of Figures

Figure 1.1 Energy Transfer Mechanisms.....	3
Figure 1.2 Outer Sphere Electron Transfer Mechanisms.....	4
Figure 1.3 Long lived triplet excited states of transition metal and metal-free photoredox catalysts.....	7
Figure 1.4 Limited light penetration of large scale photoredox reactions.....	10
Figure 2.1 Pyridine incorporation has a significant impact on physical and chemical properties of amino acids and peptide drugs.....	13
Figure 2.2 A proposed mechanism of heteroaryl radical conjugate addition to dehydroalanine.....	16
Figure 3.1 Catalytic intermolecular reactions of pyridyl radical intermediates.....	91
Figure 3.2 Enol acetate hydroarylation on a gram scale.....	98
Figure 3.3 Mechanistic proposal: the solvent dictates the nature of the pyridyl radical, imparting divergent chemoselectivity.....	100
Figure 3.4 Mechanisms of radical termination.....	106
Figure 3.5 Temporal evaluation of the reaction profile.....	108
Figure 3.6 Effect of water addition on chemoselectivity. Blue Squares represent RCA product. Red diamonds represent hydroarylation product.....	167
Figure 3.7 Superimposed NMR spectra for titration of 2-Bromopyridine into a HEH solution.....	170
Figure 3.8 Absorption spectrum for HEH and HEH + 2-bromopyridine.....	170
Figure 3.9 Temporal profile of hydroarylation reaction using blue LED array.....	171
Figure 3.10 Temporal profile using a single focused Blue LED.....	172
Figure 3.11 Temporal profile of reaction at various catalyst loadings.....	172

Figure 3.12 Typical set up for quantum yield measurement	174
Figure 3.13 Temporal Profile.....	176
Figure 3.14 UV/Vis spectra	176
Figure 4.1 Molecular editing of Ar-CF ³ groups via catalytic C-F	197
Figure 4.2 Radical C-F functionalization of Ar-CF ₃ substrates via photoredox catalysis ...	199
Figure 4.3 Optimization of the defluoroalkylation conditions.....	216
Figure 4.4 Deviation from the optimal conditions for defluoroalkylation.....	217
Figure 4.5 Thermodynamic Profile of C-F bond cleavage in Reduced Trifluoromethylaromatics	283
Figure 4.6 Characterization of the Ideal Substrate.....	284
Figure 4.7 Stern Volmer Plots of Select Trifluoromethylaromatics	286
Figure 4.8 Stern Volmer Plots of Other Reaction Components.....	288
Figure 5.1 Disposal of perfluorinated substances requires extremely high temperatures	292
Figure 5.2 Controlled decomposition and characterization of PFAS using photoredox	293
Figure 5.3 ¹⁹ F NMR of PFOA Degradation Products (DMSO, 100 °C, 24 hours)	301
Figure 5.4 ¹⁹ F NMR of PFOA Degradation Products (DMSO:MeCN, 100 °C, 8 hours)	301
Figure 5.5 ¹⁹ F NMR of PFOA Degradation Products (DMSO:MeCN, 100 °C, 8 hours) with added 1,1,1,2,2,3,3,4,4,5,5,6,6,7,7-pentadecafluoroheptane standard (no new peaks)	302

List of Schemes

Scheme 3.1 Anti-Markovnikov Vinyl Acetate Hydroarylation using HAT Catalysts ^a	93
Scheme 3.2 Proposed Mechanism of Reduction: PCET ^a	102
Scheme 3.3 Proposal for the Observed Solvent-Dependent Chemoselectivity of Pyridyl Radicals ^a	104
Scheme 3.4 Computationally derived reaction coordinate. All values in kcal/mol.....	178
Scheme 4.1 Activation of Stable C–F Bonds by Single-Electron Transfer using Photoredox Catalysis ^a	200
Scheme 4.2 Catalytic Defluoroalkylation in the Synthesis of Medicinal Building Blocks ...	206
Scheme 4.3 Catalytic or Direct HAT Mechanisms for Defluorofunctionalization of Trifluoromethyl Arenes	208

List of Tables

Table 2.1 Optimal conditions for pyridyl radical addition to a dehydroalanine substrate.....	17
Table 2.2 Catalytic amino acid synthesis: scope of the halogenated heteroarene ^a	18
Table 2.3 Radical conjugate addition: scope of the amino-substituted alkene coupling partner ^a	20
Table 2.4 Diastereoselective RCA to Karady–Beckwith Alkene ^a	21
Table 3.1 Anti-Markovnikov Hydroarylation with Pyridyl Radicals: Scope of the Functionalized Olefin ^a	95
Table 3.2 Scope of the Halogenated Pyridine ^a	97
Table 3.3	114
Table 3.4	114
Table 3.5 Solvent Screen	164
Table 3.6 Effect of EtOH additive. Use of TFE:EtOH mixtures resulted in a uniform decrease in yield.	165
Table 3.7 Effect of HFIP additive. Use of TFE:HFIP mixtures led to similar yields to the optimal system (71% isolated).....	165
Table 3.8 Effect of acidic additives. In this system, use of different acidic additives provided lower yields than with NH ₄ Cl. Use of stronger acids led to a more dramatic reduction in yield.....	165
Table 3.9 Effect of acidic additives on reaction with 4-bromopyridine.	166
Table 3.10 Effect of water on reaction efficiency.....	166
Table 3.11	167

Table 3.12 Effect of acidic additives on radical conjugate addition efficiency. Addition of stoichiometric amounts (2 equiv) of strong acid does not have any deleterious effect on the reaction yield in the RCA system.	168
Table 3.13 Effect of basic additives on hydroarylation.	169
Table 3.14 Reduction potentials for 2-bromopyridine with different levels of theory and solvation.....	178
Table 3.15	180
Table 3.16	192
Table 3.17 Failed and limited substrate scope.....	193
Table 4.1 Catalytic Defluoroalkylation: Scope of Unactivated Trifluoromethylaromatic Substrates ^a	202
Table 4.2 Scope of Olefinic Coupling Partner for Photocatalytic Difluoroalkylaromatic Synthesis ^a	204
Table 4.3 Substrate Scope for Hydrodefluorination ^a	210
Table 4.4 Optimization with N-(2-(trifluoromethyl)phenyl)acetamide.....	218

Chapter 1

Introduction to Photoredox

1.1 Driving Chemical Reactions with Light

Light induced chemical reactions are indeed older than life itself. One of the earliest terrestrial forms of photochemistry formed the ozone layer (photolysis of oxygen)—catering to the viability of early lifeforms.¹ Since then, visible light, and other forms of irradiation, have been driving an abundance of chemical reactions, helping to shape the world as we know it.

The beginnings of organic photochemistry (as a field of study) focused on chemistry uniquely enabled by light including a number of rearrangements, electrocyclizations, and radical reactions.² Later, many of the substrates in these reactions were revealed to react from their excited states (most often their triplet state). This culmination of principles from physics and organic chemistry was an important milestone in the field as it explained how light actually affected a change that enabled forward chemistry. Much of the chemistry described in the field's infancy relied on irradiation with ultraviolet light to reach an excited state as small pi systems typically absorb in this region of the electromagnetic spectrum.

This requirement was later negated with the advent of triplet sensitizers. These molecules—typically present in catalytic quantities—can be excited by visible light and then used to transfer energy to another molecule of interest, exciting it to the triplet state where it may then react.² Eventually, a second mode of reactivity for these sensitizers was observed where the excited sensitizer actually transfers an electron (or accepts one), through space, to/from the substrate. By this point the field of photoredox catalysis had been well-established.²

¹ Roth, H. D. The Beginnings of Organic Photochemistry. *Angew. Chemie Int. Ed. English* **1989**, 28 (9), 1193–1207

² Albini, A. *Photochemistry: Past, Present and Future*; Springer-Verlag: Berlin Heidelberg, 2016

1.2 Photoredox Catalysis

1.2.1 Mechanisms of Catalysis

Photoredox reactions can be classified in a number of ways but they differ primarily by the mechanism that takes place once the catalyst is excited. These mechanisms are dependent both on the structure of the catalyst being used as well as the presence or absence of other reagents in the system. An excited sensitizer can proceed through a number of characteristic mechanisms including energy transfer (which can be then subcategorized into Dexter or Förster energy transfer) and electron transfer (which can also be subcategorized based on how the excited state is quenched).

Dexter energy transfer mechanisms are both somewhat old (first characterized in the late 1950s)³ and still relatively unpredictable. Currently, many examples of this mode of reactivity are based on serendipitous discovery or the result of broad and extensive screening efforts.⁴ In a Dexter-type mechanism, an excited electron is transferred from a donor molecule to an acceptor molecule via a non-

radiative pathway. (Figure 1.1) In either a concerted or stepwise manner, a ground state electron from the acceptor is also transferred back to the donor molecule. This sequence effectively transfers the excited state of one molecule to another. Predictability for these donor acceptor pairs suffers mainly because wavefunction overlap is required between the two molecules, leaving little room for chemical intuition or even crude computational models to aid in pairing.⁵

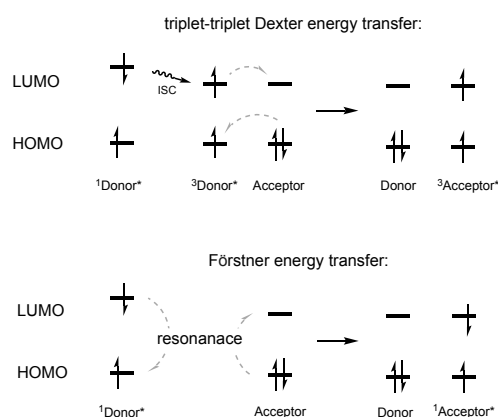


Figure 1.1 Energy Transfer Mechanisms

³ Dexter, D. L. A Theory of Sensitized Luminescence in Solids. *J. Chem. Phys.* **1953**, *21* (5), 836–850

⁴ Lima, C. G. S.; de M. Lima, T.; Duarte, M.; Jurberg, I. D.; Paixão, M. W. Organic Synthesis Enabled by Light-Irradiation of EDA Complexes: Theoretical Background and Synthetic Applications. *ACS Catal.* **2016**, *6* (3), 1389–1407

⁵ (a) Reineke, S.; Lindner, F.; Schwartz, G.; Seidler, N.; Walzer, K.; Lüssem, B.; Leo, K. White Organic Light-Emitting Diodes with Fluorescent Tube Efficiency. *Nature* **2009**, *459* (7244), 234–238; (b) Monguzzi, A.; Mezyk,

Förster energy transfer, unlike Dexter, is a radiative process. In this mode of substrate excitation, the excited sensitizer vibrationally relaxes to its lowest triplet state (according to Kasha's rule),⁶ where it then relaxes radiatively via fluorescence at a longer wavelength. In Förster energy transfer, the chosen acceptor molecule directly absorbs the photon emitted from this fluorescence, bringing the acceptor into its excited state.⁷ (Figure 1.1) The compatibility of these donor acceptor pairs are much more easily predicted as each is easily characterized by its absorption and emission spectra using a fluorimeter.

Electron transfers differ from Dexter energy transfer because the electrons are transferred to and from two separate molecules via two possible quenching mechanisms. (Figure 1.2) In its excited state, a catalyst that operates in this manner is concurrently reducing and oxidizing because of the excited electron and the resulting hole in the HOMO respectively.

If the excited catalyst were to first donate an electron (affect a reduction) the new species becomes even more oxidizing. To return to its original state, the catalyst must then accept an electron (affecting an oxidation) from a separate molecule. This sequence is referred to as an oxidative quenching cycle because the catalyst is oxidized directly

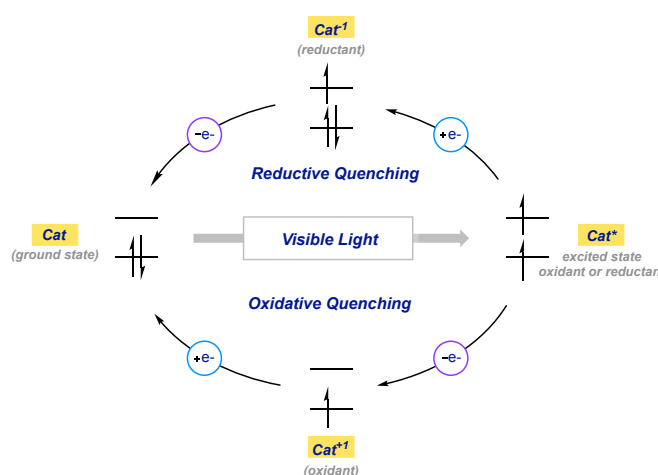


Figure 1.2 Outer Sphere Electron Transfer Mechanisms

J.; Scotognella, F.; Tubino, R.; Meinardi, F. Publisher's Note: Upconversion-Induced Fluorescence in Multicomponent Systems: Steady-State Excitation Power Threshold [Phys. Rev. B 78, 195112 (2008)]. *Phys. Rev. B* **2009**, *80* (3), 39904; (c) Chen, H.-C.; Hung, C.-Y.; Wang, K.-H.; Chen, H.-L.; Fann, W. S.; Chien, F.-C.; Chen, P.; Chow, T. J.; Hsu, C.-P.; Sun, S.-S. White-Light Emission from an Upconverted Emission with an Organic Triplet Sensitizer. *Chem. Commun.* **2009**, No. 27, 4064–4066 (d) Verhoeven, J. Glossary of Terms Used in Photochemistry (IUPAC Recommendations 1996). *Pure Appl. Chem.* **2009**, *68* (12), 2223–2286

⁶ Kasha, M. Characterization of Electronic Transitions in Complex Molecules. *Discuss. Faraday Soc.* **1950**, *9* (0), 14–19

⁷ Clegg, R. M. B. T.-L. T. in B. and M. B. Chapter 1 Förster Resonance Energy Transfer—FRET What Is It, Why Do It, and How It's Done. In *FRET and FRET Techniques*; Elsevier, 2009; Vol. 33, pp 1–57

after excitation. If instead the excited state first accepts an electron, it must then donate an electron to another molecule to return to its ground state. This is a reductive quenching cycle. These two mechanisms are targeted by the majority of modern photoredox methods because the catalysts are well developed, offer predictable properties, and are less substrate dependent for efficient reactivity.⁸ Specifically, an oxidative quenching mechanism will be the focus of this dissertation as the chemistry discussed herein is all reductive with respect to the substrate.

1.2.2 Catalyst Structures

Photoredox catalysts that operate via reductive or oxidative quenching cycles to oxidize or reduce substrate (respectively) are a relatively new technology. A subclass of these catalysts, those that operate with visible light, are even newer in terms of their use in organic chemistry. One of the first catalysts of this sort, Ru(bpy)₃²⁺, represents the end result of years of progress for use as a dye in solar cells and OLEDs.⁹ It wasn't until the early 2000s that Ru(bpy)₃²⁺ was popularized by the work of seminal photoredox groups like MacMillan, Yoon, Stephenson, and others. These transition metal complexes were an ideal starting point for photoredox in a number of aspects.⁸

First, it is highly absorbent of visible light (more specifically blue light) which negated the need for harsh ultraviolet irradiation, a prior requirement detrimental to the chemoselectivity and operational simplicity/safety of a given method. Second, a defining characteristic of these catalysts are their extremely long-lived excited state. These lifetimes are a function of carefully tuned ligands stabilizing the charge on the metal center in a process

⁸ Prier, C. K.; Rankic, D. A.; MacMillan, D. W. C. Visible Light Photoredox Catalysis with Transition Metal Complexes: Applications in Organic Synthesis. *Chem. Rev.* **2013**, *113* (7), 5322–5363

⁹ (a) Kalyanasundaram, K.; Grätzel, M. Applications of Functionalized Transition Metal Complexes in Photonic and Optoelectronic Devices. *Coord. Chem. Rev.* **1998**, *177* (1), 347–414; (b) Lowry, M. S.; Bernhard, S. Synthetically Tailored Excited States: Phosphorescent, Cyclometalated Iridium(III) Complexes and Their Applications. *Chem. – A Eur. J.* **2006**, *12* (31), 7970–7977; (c) Ulbricht, C.; Beyer, B.; Friebe, C.; Winter, A.; Schubert, U. S. Recent Developments in the Application of Phosphorescent Iridium(III) Complex Systems. *Adv. Mater.* **2009**, *21* (44), 4418–4441

called metal to ligand charge transfer (MLCT). In MLCT, upon excitation, an electron in one of the metal center's t_{2g} orbitals is excited directly to a π^* orbital in the ligand.¹⁰ (Figure 1.3A) In the case of $\text{Ru}(\text{bpy})_3^{2+}$, this results in an metal center that has been effectively oxidized to Ru(III) and an open shell ligand which undergoes intersystem crossing (ISC) to give the lowest energy triplet state.¹¹ In this triplet excited state, radiative relaxation—or fluorescence—is spin forbidden (in accord with the Pauli exclusion principle). These underlying principles are what afford these transition metal complexes the exceptionally long-lived excited states that they exhibit—a property that is largely responsible for their successful utility in organic chemistry. As reports of using these photocatalysts increased in popularity, a number of groups became interested in modifying the metal, ligand structure, and overall redox properties of catalysts in order to expand the scope of applicable organic reactions. With this came a number of iridium-based complexes (e.g. $\text{Ir}(\text{ppy})_3$, $[\text{Ir}(\text{dtbbpy})(\text{ppy})_2]$, and $[\text{Ir}\{\text{dFCF}_3\text{ppy}\}_2(\text{bpy})]$), all specifically designed with a property or purpose in mind.^{8,12}

¹⁰ Kalyanasundaram, K. Photophysics, Photochemistry and Solar Energy Conversion with Tris(Bipyridyl)Ruthenium(II) and Its Analogues. *Coord. Chem. Rev.* **1982**, *46*, 159–244

¹¹ McCusker, J. K. Femtosecond Absorption Spectroscopy of Transition Metal Charge-Transfer Complexes. *Acc. Chem. Res.* **2003**, *36* (12), 876–887

¹² (a) Lowry, M. S.; Goldsmith, J. I.; Slinker, J. D.; Rohl, R.; Pascal, R. A.; Malliaras, G. G.; Bernhard, S. Single-Layer Electroluminescent Devices and Photoinduced Hydrogen Production from an Ionic Iridium(III) Complex. *Chem. Mater.* **2005**, *17* (23), 5712–5719; (b) Slinker, J. D.; Gorodetsky, A. A.; Lowry, M. S.; Wang, J.; Parker, S.; Rohl, R.; Bernhard, S.; Malliaras, G. G. Efficient Yellow Electroluminescence from a Single Layer of a Cyclometalated Iridium Complex. *J. Am. Chem. Soc.* **2004**, *126* (9), 2763–2767; (c) Flamigni, L.; Barbieri, A.; Sabatini, C.; Ventura, B.; Barigelletti, F. Photochemistry and Photophysics of Coordination Compounds: Iridium BT - Photochemistry and Photophysics of Coordination Compounds II; Balzani, V., Campagna, S., Eds.; Springer Berlin Heidelberg: Berlin, Heidelberg, 2007; pp 143–203

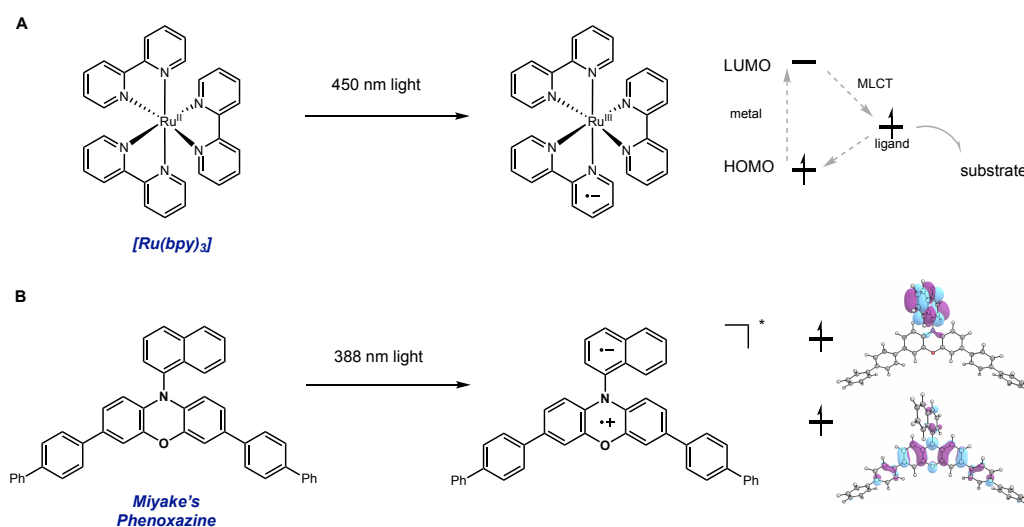


Figure 1.3 Long lived triplet excited states of transition metal and metal-free photoredox catalysts

Similar to metal-centered catalyst, metal-free photoredox catalysts have their roots in the field of organic dyes and stains. This classification of catalyst encompasses a vast variety of carbon backbones and functionalities and can offer benefits over their metal-containing counterparts in a number of ways. The exclusion of a transition metal is inherently better from a sustainability standpoint which goes hand and hand with their cost commercially. The use of carbon, for which there is an abundant supply, is also less toxic from a waste perspective. More importantly though, organophotoredox catalysts are not limited to the redox properties inherent to a metal center, but are instead limited only by the energy of the photons they absorb. Blue light for example, ($\lambda = 440 \text{ nm}$) is made up of photons containing 2.8 eV of energy.¹³ This represents the theoretical maximum of energy that can then be passed from the photocatalyst to a substrate assuming a single photon is absorbed and the internal relaxations and conversions are completely lossless.

Without the metal-ligand configuration that enables MLCT, many organic dyes only excite to a much shorter lived singlet excited state. A number of methodologies have been

¹³ Ghosh, I.; Ghosh, T.; Bardagi, J. I.; König, B. Reduction of Aryl Halides by Consecutive Visible Light-Induced Electron Transfer Processes. *Science*. **2014**, 346 (6210), 725 – 728

developed using singlet-excited photocatalysts,¹⁴ and in some cases singlet reactivity actually affords some advantages (e.g. no quenching from triplet oxygen, not air sensitive) but for more efficient and generalizable use, a longer lived (usually triplet) excited state lifetime is typically desired. To lengthen the lifetime of excited electrons, a barrier to fluorescence needs to be introduced. One strategy the field has adopted is the design of molecules that excite into a charge separated state. (Figure 1.3) When these catalysts are excited they exhibit what is effectively an intramolecular disproportionation that generates a radical cation and a radical anion within a single molecule. This is typically achieved by functional stabilization of charges into spatially separated orbitals. As the resulting singly occupied molecular orbitals (SOMOs) are separated in space (Figure 1.3), their relaxation (via fluorescence) is then faced with an energetic barrier.¹⁵ In addition, some catalyst scaffolds are amenable to ISC which results in a spatially separated triplet state and can drastically extend the excited state lifetime even further. In this context, many of the organic photocatalysts developed by the Mikaye group demonstrate high molar absorptivity of visible light, high quantum yield to a triplet state with spatially separated SOMOs that yield a high reduction potential and exceptionally long excited state lifetime.¹⁶ These properties make the catalysts ideal for developing methodologies with difficult reductions, some of which are featured in the following chapters.

¹⁴ For examples see: Discekici, E. H.; Treat, N. J.; Poelma, S. O.; Mattson, K. M.; Hudson, Z. M.; Luo, Y.; Hawker, C. J.; de Alaniz, J. R. A Highly Reducing Metal-Free Photoredox Catalyst: Design and Application in Radical Dehalogenations. *Chem. Commun.* **2015**, 51 (58), 11705–11708 and citing articles.

¹⁵ Lim, C.-H.; Ryan, M. D.; McCarthy, B. G.; Theriot, J. C.; Sartor, S. M.; Damrauer, N. H.; Musgrave, C. B.; Miyake, G. M. Intramolecular Charge Transfer and Ion Pairing in N,N-Diaryl Dihydrophenazine Photoredox Catalysts for Efficient Organocatalyzed Atom Transfer Radical Polymerization. *J. Am. Chem. Soc.* **2017**, 139 (1), 348–355

¹⁶ Pearson, R. M.; Lim, C.-H.; McCarthy, B. G.; Musgrave, C. B.; Miyake, G. M. Organocatalyzed Atom Transfer Radical Polymerization Using N-Aryl Phenoxazines as Photoredox Catalysts. *J. Am. Chem. Soc.* **2016**, 138 (35), 11399–11407

1.2.3 The Photoredox Regime

Light-driven reactions can offer unique reactivity and number of specific advantages when compared to chemical reductants and oxidants or electrochemical reactions. These benefits are matched by the technical challenges of supplying light to a reaction.

Historically, photoredox methods have been utilized for generation of open shell (radical) species while electrochemical methods have largely focused on closed cell, charged processes.^{8,17} This illustrates one of the main advantages of photoredox catalysis: the presence of reductant or oxidant in catalytic quantities. This is mandated both by the stoichiometry and the excited state lifetime of catalysts. At any given time, there is an extremely small concentration of active, excited state reductant or oxidant. Using a catalytic reduction as an example: the excited catalyst transfers an electron to the substrate, and then must fill the hole with an electron from the stoichiometric reductant, an entirely separate collision. This means that, unlike at the anode of an electrochemical cell, only a single electron can be transferred to the substrate per catalytic cycle. This makes consecutive substrate reductions to an anion extremely unlikely. Instead, the substrate is left as an open shell species which is likely to react before being reduced again. This phenomenon is an extremely enabling tool for the development of radical reactions because radicals can be generated in a controlled and catalytic manner.

These benefits, however, are met with a separate set of challenges. Light penetration is one of the inherently limiting factors of photochemistry. This limitation is most pronounced on large scale. Beer's law relates the absorption of light to physical properties of the material it is passing through.¹⁸ If 99.9% of the light in a 100 L photoredox reaction is absorbed by the outside 1 cm of the reaction vessel then the reaction will likely be very inefficient. (see Figure

¹⁷ Yan, M.; Kawamata, Y.; Baran, P. S. *Synthetic Organic Electrochemical Methods Since 2000: On the Verge of a Renaissance. Chem. Rev.* **2017**, *117* (21), 13230–13319

¹⁸ Beer. Bestimmung Der Absorption Des Rothen Lichts in Farbigen Flüssigkeiten. *Ann. Phys.* **1852**, *162* (5), 78–88

1.4 for example) To address this problem, a number of engineering solutions have been employed. Flow reactors can be instrumental in increasing a reactions light exposure by offering significantly increased exposed surface area, however, these solutions are often accompanied by problems of their own.¹⁹ In a practical context, these limitations must be balanced with the utility/safety/value of the reaction in question.

The following chapters contain methodologies that utilize photoredox as an enabling feature. It is a long-standing goal and philosophy of the Jui group to produce methods that are enabling and practically useful specifically to the pharmaceutical industry. Accordingly, in each of the following projects we've made an effort to demonstrate the realistic scope and limitations, robustness and scalability, and relevance of each reaction to drug design and modification. It is our hope that each of these reports have an actual impact on the pharmaceutical industry whether it be directly using our methods, or promoting general consideration of radical connectivity.



Figure 1.4 Limited light penetration of large scale photoredox reactions

¹⁹ Garlets, Z. J.; Nguyen, J. D.; Stephenson, C. R. J. The Development of Visible-Light Photoredox Catalysis in Flow. *Isr. J. Chem.* **2014**, *54* (4), 351–360

Chapter 2

A Practical and Scalable System for Heteroaryl Amino Acid Synthesis

Adapted and Reprinted in part with permission from *Chem. Sci.* **2017**, 8, 7998–8003
Copyright 2017 Royal Society of Chemistry

<https://doi.org/10.1039/C7SC03612D>

Abstract: A robust system for the preparation of β -heteroaryl α -amino acid derivatives has been developed using photoredox catalysis. This system operates via regiospecific activation of halogenated pyridines (or other heterocycles) and conjugate addition to dehydroalanine derivatives to deliver a wide range of unnatural amino acids. This process was conducted with good efficiency on large scale, the application of these conditions to amino ketone synthesis is shown, and a simple protocol is given for the preparation of enantioenriched amino acid synthesis, from a number of radical precursors.

2.1 Introduction

Amino acids play a central role in chemical and biological sciences. As primary members of the chiral pool, they are precursors to drugs,²⁰ chiral auxiliaries,²¹ and catalysts.²² In addition, they are fundamental building blocks for the construction of larger biomolecules like peptides. The use of peptides as therapeutic agents is attractive because in many examples they display extremely diverse, potent, and selective biological activities.²³ However, significant challenges exist for the design of peptide drugs. These include low metabolic

²⁰ Deacon, C. F. Dipeptidyl Peptidase-4 Inhibitors in the Treatment of Type 2 Diabetes: A Comparative Review. *Diabetes, Obes. Metab.* **2011**, *13* (1), 7–18

²¹ (a) *Asymmetric Synthesis: The Essentials, 2nd, Completely Revised Edition*; Christmann, Mathias; Brase, S., Ed.; Wiley and Sons, 2007; (b) Gnas, Y.; Glorius, F. Chiral Auxiliaries - Principles and Recent Applications. *Synthesis (Stuttg)*. **2006**, *2006* (12), 1899–1930

²² (a) Doyle, A. G.; Jacobsen, E. N. Small-Molecule H-Bond Donors in Asymmetric Catalysis. *Chem. Rev.* **2007**, *107* (12), 5713–5743; (b) Davie, E. A. C.; Mennen, S. M.; Xu, Y.; Miller, S. J. Asymmetric Catalysis Mediated by Synthetic Peptides. *Chem. Rev.* **2007**, *107* (12), 5759–5812; (c) Corey, E. J.; Helal, C. J. Reduction of Carbonyl Compounds with Chiral Oxazaborolidine Catalysts: A New Paradigm for Enantioselective Catalysis and a Powerful New Synthetic Method. *Angew. Chemie Int. Ed.* **1998**, *37* (15), 1986–2012; (d) Helmchen, G.; Pfaltz, A. Phosphinooxazolines A New Class of Versatile, Modular P,N-Ligands for Asymmetric Catalysis. *Acc. Chem. Res.* **2000**, *33* (6), 336–345; (e) Zhang, F.-L.; Hong, K.; Li, T.-J.; Park, H.; Yu, J.-Q. Functionalization of C–H Bonds Using a Transient Directing Group. *Science*. **2016**, *351* (6270), 252 – 256; (f) MacMillan, D. W. C. The Advent and Development of Organocatalysis. *Nature* **2008**, *455* (7211), 304–308; (g) Sakthivel, K.; Notz, W.; Bui, T.; Barbas, C. F. Amino Acid Catalyzed Direct Asymmetric Aldol Reactions: A Bioorganic Approach to Catalytic Asymmetric Carbon–Carbon Bond-Forming Reactions. *J. Am. Chem. Soc.* **2001**, *123* (22), 5260–5267; (h) Bertelsen, S.; Jørgensen, K. A. Organocatalysis—after the Gold Rush. *Chem. Soc. Rev.* **2009**, *38* (8), 2178–2189

²³ (a) Kaspar, A. A.; Reichert, J. M. Future Directions for Peptide Therapeutics Development. *Drug Discov. Today* **2013**, *18* (17), 807–817; (b) Fosgerau, K.; Hoffmann, T. Peptide Therapeutics: Current Status and Future Directions. *Drug Discov. Today* **2015**, *20* (1), 122–128

stability and poor physical properties like solubility. A proven strategy for overcoming these challenges involves substitution of the native residues with unnatural amino acids (synthetic mutagenesis).²⁴ Of these substitutions, nitrogen-containing heteroaromatics have become commonplace because of their ability to directly alter the solubility, metabolic stability, and binding affinity of the molecules that they comprise.²⁵ In consequence,

heteroarene-containing unnatural amino acids have become promising tools in the design of peptide therapeutics. In a number of specific examples, pyridine incorporation has had a dramatic impact on the properties of amino acids and peptides. Azatyrosine—a natural product that differs from the essential amino acid tyrosine by substitution of a single atom—displays potent antibiotic and antitumor properties.²⁶ Installation of the 3-pyridylalanine (3-pyr-Ala)

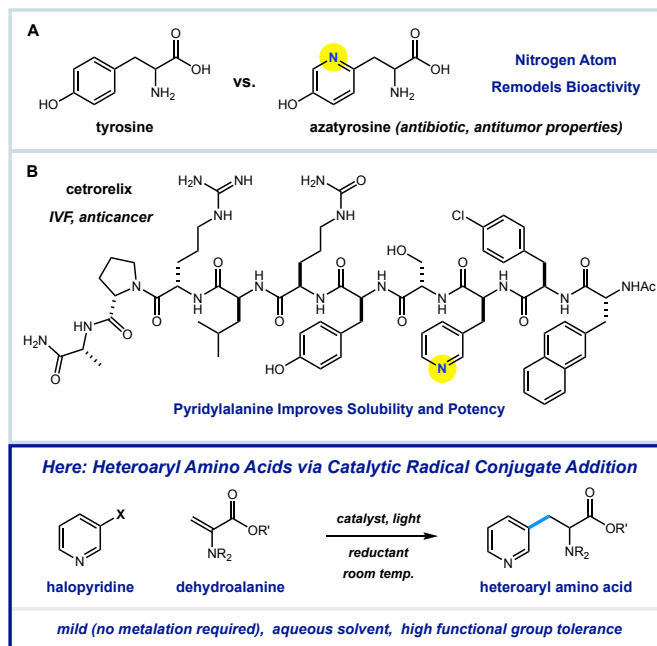


Figure 2.1 Pyridine incorporation has a significant impact on physical and chemical properties of amino acids and peptide drugs

²⁴ (a) Blaskovich, M. A. T. Unusual Amino Acids in Medicinal Chemistry. *J. Med. Chem.* **2016**, *59* (24), 10807–10836; For examples in synthetic peptide hormones, see: (b) Reissmann, T.; Schally, A. V.; Bouchard, P.; Riethmüller, H.; Engel, J. The LHRH Antagonist Cetorelix: A Review. *Hum. Reprod. Update* **2000**, *6* (4), 322–331; (c) Folkers, K.; Bowers, C. Y.; Kubiak, T.; Stepinski, J. Antagonists of the Luteinizing Hormone Releasing Hormone with Pyridyl-Alanines Which Completely Inhibit Ovulation at Nanogram Dosage. *Biochem. Biophys. Res. Commun.* **1983**, *111* (3), 1089–1095; (d) Asami, T.; Nishizawa, N.; Matsui, H.; Nishibori, K.; Ishibashi, Y.; Horikoshi, Y.; Nakayama, M.; Matsumoto, S.; Tarui, N.; Yamaguchi, M.; Matsumoto, H.; Ohtaki, T.; Kitada, C. Design, Synthesis, and Biological Evaluation of Novel Investigational Nonapeptide KISS1R Agonists with Testosterone-Suppressive Activity. *J. Med. Chem.* **2013**, *56* (21), 8298–8307

²⁵ (a) Vitaku, E.; Smith, D. T.; Njardarson, J. T. Analysis of the Structural Diversity, Substitution Patterns, and Frequency of Nitrogen Heterocycles among U.S. FDA Approved Pharmaceuticals. *J. Med. Chem.* **2014**, *57* (24), 10257–10274; (b) Ritchie, T. J.; Macdonald, S. J. F.; Peace, S.; Pickett, S. D.; Luscombe, C. N. The Developability of Heteroaromatic and Heteroaliphatic Rings – Do Some Have a Better Pedigree as Potential Drug Molecules than Others? *Medchemcomm* **2012**, *3* (9), 1062–1069

²⁶ (a) INOUE, S.; SHOMURA, T.; TSURUOKA, T.; OGAWA, Y.; WATANABE, H.; YOSHIDA, J.; NIIDA, T. L-β-(5-Hydroxy-2-Pyridyl)-Alanine and L-β-(3-Hydroxyureido)-Alanine from *Streptomyces*. *Chem. Pharm. Bull. (Tokyo)*. **1975**, *23* (11), 2669–2677; (b) Izawa, M.; Takayama, S.; Shindo-Okada, N.; Doi,

residue in the gonadotropin-releasing hormone antagonist cetorelix was found to improve both aqueous solubility and receptor affinity.²⁷ Similar effects were also observed in the development of other peptide hormones (not shown).^{24b-d}

In the time preceding this publication, the Jui group had developed a method for radical conjugate addition of pyridyl (and other heterocyclic) radicals to a number of Michael acceptors.²⁸ To expand this program, focusing on the catalytic functionalization of heteroaromatics, we next targeted the development of an impactful synthetic methods for the construction of novel β -heteroaryl α -amino acids. To accomplish this, we planned to invoke a similar radical conjugate addition mechanism.

In the past, we have found that pyridyl halide activation via single electron reduction using photoredox catalysts can be accomplished,²⁹ and that the intermolecular reactivity of the resulting radical species can be dictated by the reaction conditions.^{28,30} More specifically, we found that pyridyl radicals display nucleophilic reactivity in aqueous DMSO, and they readily couple with electron-poor alkenes. We questioned whether this approach could be translated to heteroaryl amino acid synthesis through radical conjugate addition to dehydroalanine derivatives. There are a number of powerful methods for the synthesis of unnatural β -heteroaryl

S.; Kimura, M.; Katsuki, M.; Nishimura, S. Inhibition of Chemical Carcinogenesis in Vivo by Azatyrosine. *Cancer Res.* **1992**, *52* (6), 1628 – 1630

²⁷ Beckers, T.; Bernd, M.; Kutscher, B.; Kühne, R.; Hoffmann, S.; Reissmann, T. Structure–Function Studies of Linear and Cyclized Peptide Antagonists of the GnRH Receptor. *Biochem. Biophys. Res. Commun.* **2001**, *289* (3), 653–663

²⁸ Aycock, R. A.; Wang, H.; Jui, N. T. A Mild Catalytic System for Radical Conjugate Addition of Nitrogen Heterocycles. *Chem. Sci.* **2017**, *8* (4), 3121–3125

²⁹ (a) Romero, N. A.; Nicewicz, D. A. Organic Photoredox Catalysis. *Chem. Rev.* **2016**, *116* (17), 10075–10166; (b) Prier, C. K.; Rankic, D. A.; MacMillan, D. W. C. Visible Light Photoredox Catalysis with Transition Metal Complexes: Applications in Organic Synthesis. *Chem. Rev.* **2013**, *113* (7), 5322–5363

³⁰ (a) Boyington, A. J.; Riu, M.-L. Y.; Jui, N. T. Anti-Markovnikov Hydroarylation of Unactivated Olefins via Pyridyl Radical Intermediates. *J. Am. Chem. Soc.* **2017**, *139* (19), 6582–6585; for other examples of photoredox catalysis in aryl radical chemistry, see: (b) Arora, A.; Weaver, J. D. Visible Light Photocatalysis for the Generation and Use of Reactive Azolyl and Polyfluoroaryl Intermediates. *Acc. Chem. Res.* **2016**, *49* (10), 2273–2283; (c) Ghosh, I.; Marzo, L.; Das, A.; Shaikh, R.; König, B. Visible Light Mediated Photoredox Catalytic Arylation Reactions. *Acc. Chem. Res.* **2016**, *49* (8), 1566–1577; (d) Nguyen, J. D.; D'Amato, E. M.; Narayanam, J. M. R.; Stephenson, C. R. J. Engaging Unactivated Alkyl, Alkenyl and Aryl Iodides in Visible-Light-Mediated Free Radical Reactions. *Nat. Chem.* **2012**, *4* (10), 854–859; (e) Discekici, E. H.; Treat, N. J.; Poelma, S. O.; Mattson, K. M.; Hudson, Z. M.; Luo, Y.; Hawker, C. J.; de Alaniz, J. R. A Highly Reducing Metal-Free Photoredox Catalyst: Design and Application in Radical Dehalogenations. *Chem. Commun.* **2015**, *51* (58), 11705–11708

α -amino acids, including malonate (or enolate) alkylation,³¹ cross-coupling of serine-derived organometallic reagents,³² and reduction of dehydroamino acid derivatives.³³ However, strategies based on radical addition to DHA derivatives are unique due to the highly-chemoselective nature of radical species, and the broad functional group tolerance that results.³⁴ Alkyl radical addition to DHA has been effectively accomplished even in the complex setting of intact proteins.³⁵ While this is a highly attractive attribute, a radical approach to heteroaryl amino acids is currently unknown. Here, we describe the successful translation of our reductive heteroarene activation system to amino acid synthesis.

2.2 Results and Discussion

Shown in Figure 2.2 is a mechanistic picture that is consistent with our observations.

Excitation of the photocatalyst $[\text{Ir}(\text{ppy})_2(\text{dtbbpy})]\text{PF}_6$ ($[\text{Ir}]^{1+}$), followed by reductive quenching

³¹ (a) Myers, A. G.; Gleason, J. L. A Practical Synthesis of L-Azatyrosine. *J. Org. Chem.* **1996**, *61* (2), 813–815; (b) Seebach, D.; Boes, M.; Naef, R.; Schweizer, W. B. Alkylation of Amino Acids without Loss of the Optical Activity: Preparation of α -Substituted Proline Derivatives. A Case of Self-Reproduction of Chirality. *J. Am. Chem. Soc.* **1983**, *105* (16), 5390–5398; (c) Kolar, P.; Petrič, A.; Tišler, M. Heteroarylalanines. *J. Heterocycl. Chem.* **1997**, *34* (4), 1067–1098

³² (a) Rilatt, I.; Caggiano, L.; Jackson, R. F. W. Development and Applications of Amino Acid Derived Organometallics. *Synlett* **2005**, *2005* (18), 2701–2719; (b) Huihui, K. M. M.; Caputo, J. A.; Melchor, Z.; Olivares, A. M.; Spiewak, A. M.; Johnson, K. A.; DiBenedetto, T. A.; Kim, S.; Ackerman, L. K. G.; Weix, D. J. Decarboxylative Cross-Electrophile Coupling of N-Hydroxyphthalimide Esters with Aryl Iodides. *J. Am. Chem. Soc.* **2016**, *138* (15), 5016–5019; (c) Lu, X.; Yi, J.; Zhang, Z.-Q.; Dai, J.-J.; Liu, J.-H.; Xiao, B.; Fu, Y.; Liu, L. Expedient Synthesis of Chiral α -Amino Acids through Nickel-Catalyzed Reductive Cross-Coupling. *Chem. – Eur. J.* **2014**, *20* (47), 15339–15343

³³ (a) Kreuzfeld, H. J.; Döbler, C.; Schmidt, U.; Krause, H. W. Synthesis of Non-Proteinogenic (D)- or (L)-Amino Acids by Asymmetric Hydrogenation. *Amino Acids* **1996**, *11* (3), 269–282; (b) Adameczyk, M.; Akireddy, S. R.; Reddy, R. E. Enantioselective Synthesis of (2-Pyridyl)Alanines via Catalytic Hydrogenation and Application to the Synthesis of l-Azatyrosine. *Org. Lett.* **2001**, *3* (20), 3157–3159; (d) Döbler, C.; Kreuzfeld, H.-J.; Michalik, M.; Krause, H. W. Unusual Amino Acids VII. Asymmetric Synthesis of 3- and 4- Pyridylalanines. *Tetrahedron: Asymmetry* **1996**, *7* (1), 117–125

³⁴ Hughes, A. B. *Amino Acids, Peptides and Proteins in Organic Chemistry: Building Blocks, Catalysis and Coupling Chemistry, Vol 3*; Wiley and Sons, 2011

³⁵ (a) Wright, T. H.; Bower, B. J.; Chalker, J. M.; Bernardes, G. J. L.; Wiewiora, R.; Ng, W.-L.; Raj, R.; Faulkner, S.; Vallée, M. R. J.; Phanumartwath, A.; Coleman, O. D.; Thézénas, M.-L.; Khan, M.; Galan, S. R. G.; Lercher, L.; Schombs, M. W.; Gerstberger, S.; Palm-Espling, M. E.; Baldwin, A. J.; Kessler, B. M.; Claridge, T. D. W.; Mohammed, S.; Davis, B. G. Posttranslational Mutagenesis: A Chemical Strategy for Exploring Protein Side-Chain Diversity. *Science*. **2016**, *354* (6312), aag1465; (b) Yang, A.; Ha, S.; Ahn, J.; Kim, R.; Kim, S.; Lee, Y.; Kim, J.; Söll, D.; Lee, H.-Y.; Park, H.-S. A Chemical Biology Route to Site-Specific Authentic Protein Modifications. *Science*. **2016**, *354* (6312), 623 – 626

of the excited state by Hantzsch ester (HEH) gives rise to the $[\text{Ir}]^0$ ($E_{1/2} = 1.51 \text{ V vs SCE}$).³⁶ Stern–Volmer quenching studies indicated that Hantzsch ester is the most significant excited state quencher (see Stern Volmer Fluorescence Quenching Experiments for details, pg. 86). Single electron reduction of halo pyridine I, followed by rapid mesolytic cleavage in polar solvents ($X = \text{Br}, \text{I}$)³⁷ affords heteroaryl radical intermediate II, which exhibits nucleophilic radical behavior in aqueous DMSO.²⁸ It is possible that halopyridine reduction is assisted by protonation, as each catalytic turnover produces an nominal equivalent of Hantzsch pyridinium bromide (HEH+ Br). Hydrodehalogenation (HDH) of the arene is observed as a common byproduct, but this undesired pathway can be suppressed by limiting the solubility of the

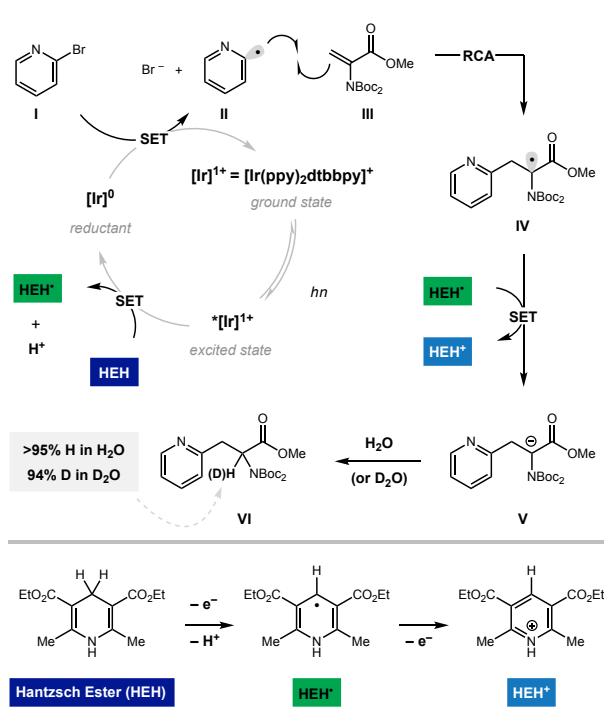


Figure 2.2 A proposed mechanism of heteroaryl radical conjugate addition to dehydroalanine

stoichiometric reductant, Hantzsch ester (HEH), in accord with our previous findings. Radical conjugate addition (RCA) to dehydroalanine III and subsequent single electron reduction of the nascent radical IV would deliver the corresponding enolate V. The intermediacy of V is supported by the fact that the a-H amino acid product VI is produced in the presence of H_2O as a cosolvent (regardless of H/D labeling of

³⁶ Lowry, M. S.; Goldsmith, J. I.; Slinker, J. D.; Rohl, R.; Pascal, R. A.; Malliaras, G. G.; Bernhard, S. Single-Layer Electroluminescent Devices and Photoinduced Hydrogen Production from an Ionic Iridium(III) Complex. *Chem. Mater.* **2005**, *17* (23), 5712–5719

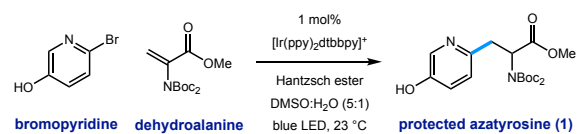
³⁷ (a) Andrieux, C. P.; Blocman, C.; Dumas-Bouchiat, J. M.; Saveant, J. M. Heterogeneous and Homogeneous Electron Transfers to Aromatic Halides. An Electrochemical Redox Catalysis Study in the Halobenzene and Halopyridine Series. *J. Am. Chem. Soc.* **1979**, *101* (13), 3431–3441; (b) Enemærke, R. J.; Christensen, T. B.; Jensen, H.; Daasbjerg, K. Application of a New Kinetic Method in the Investigation of Cleavage Reactions of Haloaromatic Radical Anions. *J. Chem. Soc. Perkin Trans. 2* **2001**, No. 9, 1620–1630

HEH). Conversely, when D₂O is used as a cosolvent, complete deuterium incorporation is obtained at the α-position.

As illustrated in Table 2.1, we identified conditions that efficiently unite 2-bromo-5-hydroxypyridine with the indicated dehydroalanine derivative (readily accessed on 35 g scale from Boc-Ser-OMe) to give the protected azatyrosine **1** in 98% NMR yield (entry 1). These conditions employ 1 mol% of the photosensitizer [Ir(ppy)₂(dtbbpy)]PF₆

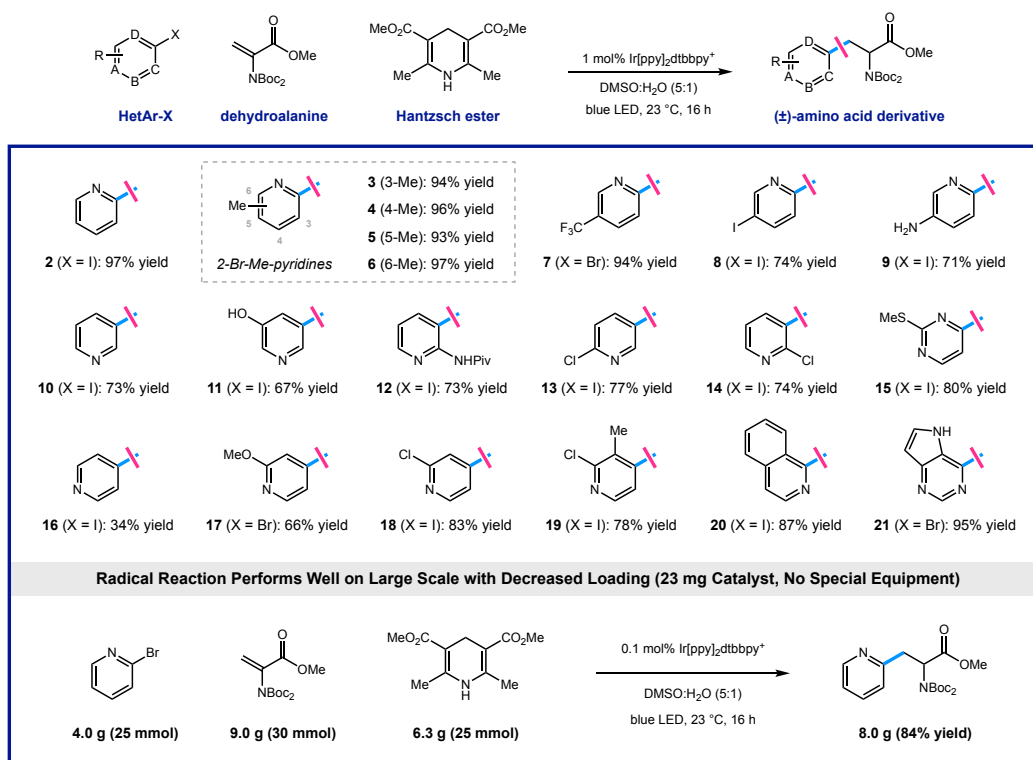
(excited by irradiation with a commercial blue LED) and Hantzsch ester (1.5 equiv.) as a stoichiometric reductant in aqueous DMSO. Control experiments indicated that all of these components are necessary for the reaction (entries 2–4, 0% yield), and that use of the prototypical Ru(bpy)₃²⁺ chromophore results in product formation, although with diminished efficiency (entry 5, 58% yield). Omission of water as a cosolvent was not well tolerated here (entry 6, 14% yield), a finding that is in consistent with our previous observations.²⁸ We found that other aqueous solvent mixtures can be used (entries 7 and 8, 35% and 71% yield, respectively), and that this photoredox system is remarkably robust; an experiment using bourbon as solvent (open to air) afforded the desired product in 93% yield (entry 9). Importantly, protection of the phenol O–H function was not required under these mild radical conditions.

Table 2.1 Optimal conditions for pyridyl radical addition to a dehydroalanine substrate



Entry	Deviation from Optimal Conditions	Yield of 1 ^b
1	none	98%
2	without Hantzsch ester	0%
3	without light	0%
4	without catalyst	0%
5	Ru(bpy) ₃ Cl ₂ as catalyst	58%
6	without H ₂ O	14%
7	DMF:H ₂ O (5:1) as solvent	35%
8	EtOH:H ₂ O (5:1) as solvent	71%
9	bourbon as solvent (open to air)	93%

^a Conditions: 2-bromo-5-hydroxypyridine (0.2 mmol), dehydroalanine (0.4 mmol), Ir(ppy)₂(dtbbpy)PF₆ (1 mol%), Hantzsch ester (0.3 mmol), H₂O (0.33 mL), DMSO (1.66 mL), blue LED, 23 °C, 16 h. ^b Yield determined by NMR.

Table 2.2 Catalytic amino acid synthesis: scope of the halogenated heteroarene^a

Using the optimized protocol outlined above, we found that the heteroaryl halide scope of this transformation is broad (as shown in Table 2.2). Some reactions are complete in as little as 2 hours, but each experiment was conducted overnight (16 h) for consistency and convenience without negatively impacting the yields. Regiospecific activation of each pyridyl position is possible via single electron reduction, and these conditions effectively delivered amino ester products from 2- and 3-iodopyridine (2 and 10), in 97% and 73% yield, respectively. Although less efficient, 4-iodopyridine also affords 4-pyridylalanine in useful yield (16, 34% yield), where reductive pyridine production is a significant alternative pathway. Methyl substitution is well-tolerated at all positions of 2-bromo pyridines, cleanly furnishing the corresponding pyridylalanines 3–6 in very high yield (93–97% yield). Reaction of 2-bromo-5-trifluoromethylpyridine (7) efficiently afforded product in 94% yield. Electron-donating groups are well-tolerated including amino (9, 71% yield), phenol (11, 67% yield), amide (12, 73% yield), and methoxy (17, 66% yield) groups. Dihalogenated pyridines can be

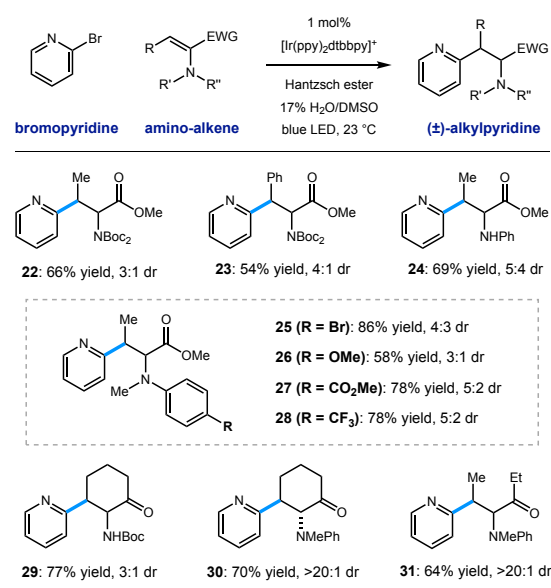
programmed for regiospecific radical formation and subsequent conjugate addition at any position, preserving 2-chloro-substituents in the presence of more reactive iodo-substituents. Coupling reactions of 2-chloro-3-iodo- (14), 2-chloro-4-iodo-(18), 2-chloro-5-iodo-(13), and 2-chloro-3-methyl-4-iodopyridine (19) each gave single pyridylalanine products in good yield (73–83% yield). 2,5-Diiodopyridine is selectively activated at the more electrophilic 2-position to afford the corresponding amino ester (8) as a single regioisomer in 74% yield. We found that halopyrimidines are also viable substrates in this process: 4-iodo-2-(methylthio)pyrimidine (15) and 4-bromodeazapurine (21) gave product in 80% and 95% yield respectively. This photoredox process is amenable to gram-scale preparation of heteroaryl amino acid synthesis, without the need for special equipment. We reacted 25 mmol of 2-bromopyridine with a slight excess (1.2 equivalents, 30 mmol) of the dehydroalanine substrate. In the presence of 1.0 equivalent of Hantzsch ester, in the presence of 1.0 equivalent of Hantzsch ester, and only 0.1 mol% (23 mg) of the iridium photoredox catalyst, the desired pyridylalanine derivative 2 was produced in 84% yield (8.0 g) after purification. As anticipated, selective unveiling of the amine and acid groups (in compound 2) using standard conditions went without issue. Hydrolysis of the methyl ester (2.0 equiv. of LiOH in THF/H₂O) occurred with preservation of both Boc groups. Exposure of 2 to trifluoroacetic acid in CH₂Cl₂ revealed the free amine as the TFA salt while leaving the methyl ester intact. Finally, sequential treatment of 2 with KOH in EtOH/H₂O followed by direct acidification of the reaction mixture with HCl afforded the fully deprotected 2-pyridylalanine as the double HCl salt. Each of these processes occurred in high yield at room temperature (see Deprotection Procedures and Characterization Data for details, pg. 78).

We conducted a brief evaluation of the scope of amino-substituted alkenes with the expectation that this reaction template could be flexibly utilized to deliver other amino acid or amino-carbonyl substructures. We found that dehydroamino acid substrates with methyl- and

phenyl-substituents in the β -position could be successfully employed, giving rise to products 22 and 23 in acceptable yield (66% and 54% yield, respectively) with modest diastereocontrol. Replacement of the -imide group in the alkene starting material (a structural artifact of dehydroalanine synthesis via Boc_2O -induced β -elimination) with an N-H aniline group or electronically diverse arylmethylamine groups was tolerated, although diastereoselectivity was low (25–28, 66–75% yield, #3 : 1 dr). These radical conjugate addition conditions directly translated to the synthesis of β -heteroaryl- α -amino ketone derivatives 29–31, giving the desired products in 64–77% yield. These results are notable because they show the ability of this mild radical system to accomplish the formation of other of α -aminocarbonyl classes.

We have demonstrated that this process is robust, scalable, and generally applicable for the synthesis of many heteroaryl amino acid and ketone derivatives. However, we recognize that the formation of products as racemic mixtures represents a main limitation of this method. To address this, we prepared the chiral tert-butyl oxazolidinone 32 that was described by Beckwith,³⁸ building on early work by Karady,³⁹ and Seebach.⁴⁰ In accord with early studies, we found that heteroaryl radical addition followed by diastereoselective

Table 2.3 Radical conjugate addition: scope of the amino-substituted alkene coupling partner^a



^aConditions as in Table 2.2. ^bDiastereomeric ratio (dr) determined by ¹H NMR.

³⁸ Beckwith, A. L. J.; Chai, C. L. L. Diastereoselective Radical Addition to Derivatives of Dehydroalanine and of Dehydrolactic Acid. *J. Chem. Soc. Chem. Commun.* **1990**, No. 16, 1087–1088

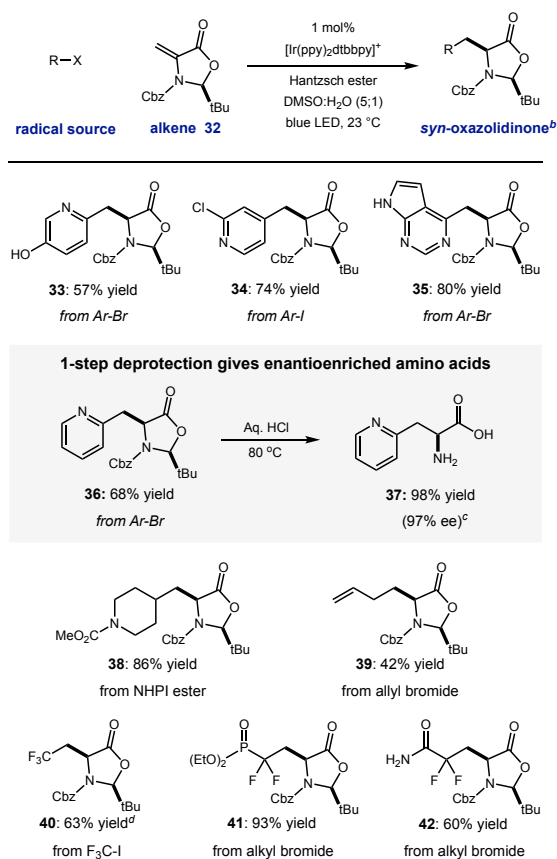
³⁹ Karady, S.; Amto, J. S.; Weinstock, L. M. Enantioselective Alkylation of Acyclic Amino Acids. *Tetrahedron Lett.* **1984**, 25 (39), 4337–4340

⁴⁰ Seebach, D.; Fadel, A. N,O-Acetals from Pivalaldehyde and Amino Acids for the α -Alkylation with Self-Reproduction of the Center of Chirality. Enolates of 3-Benzoyl-2-(Tert-Butyl)-1,3-Oxazolidin-5-Ones. *Helv. Chim. Acta* **1985**, 68 (5), 1243–1250

protonation from the less hindered Re-face could be achieved with a variety of haloheteroarenes, furnished syn-products 33–36 with complete diastereocontrol (57–80% yield, >20 : 1 dr). Concurrent carbamate cleavage and hemiaminal hydrolysis of 36 under acidic conditions cleanly afforded the amino acid 37 with retention of stereochemical purity (98% yield, 97% ee) (Table 2.4).

Other reducible radical precursors can be employed without modification of the reaction conditions to afford oxazolidinone adducts as single diastereomers. For example, the reaction of allyl bromide gives oxazolidinone 39 (42% yield). A redox-active N-hydroxyphthalimide ester⁴¹ reacted to give 39 in high yield (86% yield). Finally, reducible fluorinated alkyl halides operate within this manifold, affording oxazolidinone adducts 40–42 with good efficiency (60–93% yield). Deprotection of two of these products would directly yield fluorinated amino acids which have been enabling tools in a number of biomedical applications.⁴² For

Table 2.4 Diastereoselective RCA to Karady–Beckwith Alkene^a



^aConditions: Halogenated heteroarene (1.0 equiv), dehydroalanine (2.0 equiv), Ir(ppy)₂dtbbpy·PF₆ (1.0 mol%), Hantzsch ester (HEH, 1.3 mmol), DMSO/H₂O (5 : 1, 0.1 M), blue LED, 23 °C, 16 h, isolated yields shown. ^bThe *syn* isomer was observed with > 20 : 1 selectivity in all cases. ^cEnantiomeric excess (% ee) determined by chiral HPLC. ^dAlkene 32 used as limiting reagent

⁴¹ (a) Okada, K.; Okamoto, K.; Morita, N.; Okubo, K.; Oda, M. Photosensitized Decarboxylative Michael Addition through N-(Acyloxy)Phthalimides via an Electron-Transfer Mechanism. *J. Am. Chem. Soc.* **1991**, *113* (24), 9401–9402; (b) Pratsch, G.; Lackner, G. L.; Overman, L. E. Constructing Quaternary Carbons from N-(Acyloxy)Phthalimide Precursors of Tertiary Radicals Using Visible-Light Photocatalysis. *J. Org. Chem.* **2015**, *80* (12), 6025–6036; (c) Qin, T.; Cornella, J.; Li, C.; Malins, L. R.; Edwards, J. T.; Kawamura, S.; Maxwell, B. D.; Eastgate, M. D.; Baran, P. S. A General Alkyl-Alkyl Cross-Coupling Enabled by Redox-Active Esters and Alkylzinc Reagents. *Science*. **2016**, *352* (6287), 801 – 805; (d) Huihui, K. M. M.; Caputo, J. A.; Melchor, Z.; Olivares, A. M.; Spiewak, A. M.; Johnson, K. A.; DiBenedetto, T. A.; Kim, S.; Ackerman, L. K. G.; Weix, D. J. Decarboxylative Cross-Electrophile Coupling of N-Hydroxyphthalimide Esters with Aryl Iodides. *J. Am. Chem. Soc.* **2016**, *138* (15), 5016–5019

⁴² (a) Panigrahi, K.; Eggen, M.; Maeng, J.-H.; Shen, Q.; Berkowitz, D. B. The (E)-2,2-Difluorinated Phosphonate L-P-Ser-Analogue: An Accessible Chemical Tool for Studying Kinase- Dependent Signal

example, the difluorinated phosphonate L-pSer mimic (deprotected 41) is an important tool in the study of kinase-dependent signal transduction.^{42a} Because chiral alkene 32 is easily accessible from cysteine (detailed in Preparation of Starting Materials, pg. 28), and both enantiomers of this starting material are commercial, this strategy would enable access to either enantiomer of the unnatural heteroaryl amino acids (Table 2.4).

2.3 Conclusions

In summary, we have described an efficient catalytic system for the preparation of unnatural α -amino acids. This protocol is effective for regiospecific generation of a broad range of heteroaryl radicals, and intermolecular coupling with dehydroamino acid derivatives and α -aminoenones. We demonstrate that this photoredox system can be conducted on large scale using near stoichiometric conditions with good efficiency. We also show that diastereoselective radical conjugate addition to a chiral alkene is a viable strategy to access enantioenriched products, and that this process allows utilization of a range of radical precursors. The application of these findings to the synthesis of other valuable, highly complex products is a current aim of our program.

Transduction. *Chem. Biol.* **2009**, *16* (9), 928–936; (b) Dave, R.; Badet, B.; Meffre, P. γ -Fluorinated Analogues of Glutamic Acid and Glutamine. *Amino Acids* **2003**, *24* (3), 245–261

2.4 Supporting Information

2.4.1 General Information

General Reagent Information

All reactions were set up on the bench top and conducted under nitrogen atmosphere while subject to irradiation from blue LEDs (LEDwholesalers PAR38 Indoor Outdoor 16-Watt LED Flood Light Bulb, Blue; or PARsource PowerPAR LED Bulb-Blue 15 Watt/440 nm, available at www.eaglelight.com). Flash chromatography was carried out using Siliaflash® P60 silica gel obtained from Silicycle. Photoredox catalyst, $[\text{Ir}(\text{ppy})_2(\text{dtbbpy})]\text{PF}_6$, was prepared according to a literature procedure.⁴³ Halogenated heteroarenes were purchased from Aldrich Chemical Co., Alfa Aesar, Acros Organics, Combi-Blocks, or Oakwood Products and were used as received. Dehydroalanines were prepared according to the designated procedures in section IV, Preparation of Dehydroalanine Substrates. Molecular sieves were activated in a commercial microwave oven then cooled under high vacuum. DMSO was purified on a Pure Process Technologies solvent purification system. Reaction solvent was prepared by combining DMSO and tap water (5 : 1, V : V) which was degassed in a sidearm flask under weak vacuum while subject to sonication. Alcoholic beverages used as solvents for optimization screenings were purchased from a local package store and used as received.

General Analytical Information

All yields refer to isolated yields. New compounds were characterized by NMR, IR spectroscopy, HRMS, and melting point. NMR data were recorded on one of six spectrometers: Bruker 600 MHz, INOVA 600 MHz, INOVA 500 MHz, VNMR 400 MHz, INOVA 400 MHz, or Mercury 300 MHz. Chemical shifts (δ) are internally referenced to residual protio solvent (CDCl_3 : δ 7.26 ppm for ^1H NMR and 77.23 ppm for ^{13}C NMR; C_6D_6 : 7.15 ppm for ^1H NMR

⁴³ Lowry, M. S.; Hudson, W. R.; Pascal, R. A.; Bernhard, S. *J. Am. Chem. Soc.* **2004**, *126*, 14129.

and 128.4 ppm for ^{13}C NMR; CD_3OD : δ 3.31 ppm for ^1H NMR and 49.1 ppm for ^{13}C NMR, or D_2O). IR spectra were obtained with a Thermo Scientific Nicolet iS10 Fourier transform infrared spectrophotometer. Mass spectrometry data were obtained from the Emory Mass Spectrometry Center using a Thermo LTQ-FTMS high resolution mass spectrometer. Melting point data was obtained with a Thomas Hoover Unimelt capillary melting point apparatus. Adduct yields for optimization data were obtained via ^1H NMR with an Inova 400 MHz NMR using 1,3,5-trimethoxybenzene as internal standard, with relaxation delay set to 5 seconds. Hydrodehalogenated yields for optimization data were obtained via gas chromatography with an Agilent Technologies 7890B Gas Chromatography system (flame-ionization detection) equipped with an Agilent Technologies 19091J-413 HP-5 column (30 m x 0.320 mm x 0.25 μm , 5% phenyl methyl siloxane) and an Agilent Technologies G4513A autoinjector. Enantioenriched samples were analyzed on a 1100 Series Agilent HPLC on Daicel Chiralcel columns (250 x 4.6 mm ID). Optical rotations were measured at 20 $^\circ\text{C}$ using a Perkin Elmer Model 341 Polarimeter at $\lambda = 589$ nm.

2.4.2 General Procedure

A 20 mL screw-top test tube equipped with a stir bar was charged with Hantzsch ester (1.3 – 1.5 equiv), $[\text{Ir}(\text{ppy})_2(\text{dtbbpy})]\text{PF}_6$ (1 mol%), dehydroalanine (2 equiv), and halogenated heteroarene (1 equiv). The tube was sealed with PTFE/silicon septum and connected to a Schlenk line. The atmosphere was exchanged by applying vacuum and backfilling with N_2 (this process was conducted a total of three times). Under N_2 atmosphere, the tube was charged with degassed solvent (5 : 1 DMSO : H_2O , 10 mL/mmol heteroarene) by syringe. The resulting suspension was stirred under irradiation with blue LEDs for 16 hours while being cooled with a fan. The reaction was quenched with saturated sodium bicarbonate solution (60 mL) and extracted with ethyl acetate (3 x 40 mL). The extracts were combined, dried over magnesium

sulfate, filtered, and concentrated by rotary evaporation. The residue was purified by flash column chromatography using the indicated solvent mixture to afford the title compound.

2.4.3 Optimization Details

Procedure for In-Text Deviation from Optimal Conditions

A 15-mL screw-top test tube equipped with a stir bar was charged with Hantzsch ester (76 mg, 0.30 mmol, 1.5 equiv), [Ir(ppy)₂(dtbbpy)]PF₆ (1.8 mg, 0.002 mmol, 1 mol%), methyl-2-(di(*tert*-butoxycarbonyl)amino)but-2-enoate (120 mg, 0.4 mmol, 2 equiv), and 2-bromo-5-hydroxypyridine (34.8 mg, 0.20 mmol, 1 equiv). The tube was sealed with PTFE/silicon septum and connected to a Schlenk line. The atmosphere was exchanged by applying vacuum and backfilling with N₂ (this process was conducted a total of three times). Under N₂ atmosphere, the tube was charged degassed solvent (2.0 mL) by syringe. The resulting suspension was stirred under irradiation with blue LEDs for 16 hours while being cooled with a fan. The reaction was quenched with saturated sodium bicarbonate solution (10 mL) and extracted with ethyl acetate (5 x 5 mL). The extracts were combined and passed through a plug of silica which was flushed with additional ethyl acetate, and the solution was transferred to a 20-mL scintillation vial. The contents of the vial were concentrated via rotary evaporation and then subject to high vacuum for 2 hours. 1,3,5-trimethoxybenzene (33.6 mg, 1 equiv) was added, and the contents were thoroughly dissolved in CDCl₃. An aliquot was analyzed by ¹H NMR, and the integral values were used to calculate azatyrosine ester yield.

Optimization Procedure

A 15-mL screw-top test tube equipped with a stir bar was charged with Hantzsch ester (76 mg, 0.30 mmol, 1.5 equiv), photoredox catalyst (1 mol%), methyl-2-(di(*tert*-butoxycarbonyl)amino)but-2-enoate (120 mg, 0.4 mmol, 2 equiv), and 2-bromopyridine (31.6 mg, 0.20 mmol, 1 equiv). The tube was sealed with PTFE/silicon septum and connected to a Schlenk line. The atmosphere was exchanged by applying vacuum and backfilling with N₂ (this

process was conducted a total of three times). Under N₂ atmosphere, the tube was charged degassed solvent (2.0 mL) by syringe. The resulting suspension was stirred under irradiation with blue LEDs for 16 hours. The reaction was quenched with saturated sodium bicarbonate solution (10 mL) and extracted with ethyl acetate (5 x 5 mL). The extracts were combined and passed through a plug of silica which was flushed with additional ethyl acetate, and the solution was transferred to a 20-mL scintillation vial. An internal standard of dodecane (10 μL, 0.044 mmol) was delivered to the vial, and the contents were thoroughly mixed. A sample was analyzed by gas chromatography, and the integral values were used to calculate hydrodehalogenation product (pyridine) yield. The contents of the vial were concentrated via rotary evaporation and then subject to high vacuum for 2 hours. 1,3,5-trimethoxybenzene (33.6 mg, 1 equiv) was added, and the contents were thoroughly dissolved in CDCl₃. An aliquot was analyzed by H¹NMR, and the integral values were used to calculate pyridylalanine ester yield.

Gas Chromatography Method Conditions

The gas chromatography system hardware is reported in section I-B, General Analytical Information. The injection volume for each trial is 0.5 μL. The initial oven temperature was set to 50 °C, and the ramp rate was programmed to 20 °C/min until reaching 150 °C. With no hold time, the temperature ramp rate is adjusted to 25 °C/min until reaching the maximum temperature of 325 °C. Maximum temperature is held for one minute before concluding the run.

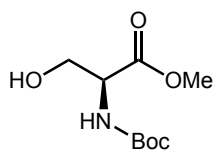
Optimization Table

c1ccncc1Br + COC(=O)C=CNC(=O)OC $\xrightarrow[\text{Hantzsch ester (1.3 equiv), solvent, blue LED}]{1 \text{ mol\% photocatalyst}}$ COC(=O)C(CNC(=O)OC)Cc1ccncc1 + c1ccncc1

2-bromopyridine **DHA (2.0 equiv)** **(±)-A** **B**

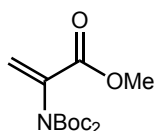
entry	photocatalyst	solvent	deviation	% yield A	% yield B	selectivity (A : B)
1	Ru(bpy) ₃ Cl ₂	MeCN (0.1 M)	-	0	0	-
2	Ir(ppy) ₃	MeCN (0.1 M)	-	48	2	24:1
3	Ir(dF(CF ₃)ppy) ₂ dtbbpy•PF ₆	MeCN (0.1 M)	-	50	2	25:1
4	Ir(ppy) ₂ dtbbpy•PF ₆	MeCN (0.1 M)	-	52	2	26:1
5	Ru(bpy) ₃ Cl ₂	DMSO (0.1 M)	-	54	2	27:1
6	Ir(ppy) ₃	DMSO (0.1 M)	-	65	2	33:1
7	Ir(dF(CF ₃)ppy) ₂ dtbbpy•PF ₆	DMSO (0.1 M)	-	81	11	7:1
8	Ir(ppy) ₂ dtbbpy•PF ₆	DMSO (0.1 M)	-	81	11	7:1
9	Ir(ppy) ₂ dtbbpy•PF ₆	DMF/H ₂ O (3:1, 0.1M)	-	34	2	17:1
10	Ir(ppy) ₂ dtbbpy•PF ₆	MeCN/H ₂ O (3:1, 0.1M)	-	27	3	9:1
11	Ir(ppy) ₂ dtbbpy•PF ₆	MeOH/H ₂ O (3:1, 0.1 M)	-	30	1	30:1
12	Ir(ppy) ₂ dtbbpy•PF ₆	DMSO/H ₂ O (3:1, 0.1 M)	-	85	3	28:1
13	Ir(ppy) ₂ dtbbpy•PF ₆	DMSO/H ₂ O (3:1, 0.03 M)	-	98	2	49:1
14	Ir(ppy) ₂ dtbbpy•PF ₆	DMSO/H ₂ O (5:1, 0.1 M)	-	98	2	49:1
15	Ir(ppy) ₂ dtbbpy•PF ₆	DMSO/H ₂ O (5:1, 0.1 M)	1.1 equiv DHA	93	7	13:1
16	Ir(ppy) ₂ dtbbpy•PF ₆	DMSO/H ₂ O (5:1, 0.1 M)	air-exposed	90	5	18:1
17	Ir(ppy) ₂ dtbbpy•PF ₆	DMSO/H ₂ O (5:1, 0.1 M)	1.1 equiv DHA, air-exposed	85	7	12:1
18	Ir(ppy) ₂ dtbbpy•PF ₆	DMSO/H ₂ O (5:1, 0.1 M)	no Hantzsch ester	0	0	-
19	Ir(ppy) ₂ dtbbpy•PF ₆	DMSO/H ₂ O (5:1, 0.1 M)	no light	0	0	-
20	none	DMSO/H ₂ O (5:1, 0.1 M)	-	0	0	-
21	Ir(ppy) ₂ dtbbpy•PF ₆	Grey Goose vodka (0.3 M)	-	85	12	7:1
22	Ir(ppy) ₂ dtbbpy•PF ₆	Bacardi white rum (0.3 M)	-	86	12	7:1
23	Ir(ppy) ₂ dtbbpy•PF ₆	Johnnie Walker Scotch (0.3 M)	-	84	12	7:1
24	Ir(ppy) ₂ dtbbpy•PF ₆	Woodford Reserve Bourbon (0.3 M)	-	93	4	23:1
25	Ir(ppy) ₂ dtbbpy•PF ₆	Seagram's gin (0.3 M)	-	94	4	24:1
26	Ir(ppy) ₂ dtbbpy•PF ₆	Redbull/Grey Goose (1:2, 0.3 M)	-	42	1	42:1

2.4.4 Preparation of Starting Materials



methyl (*tert*-butoxycarbonyl)-L-serinate:

To a stirring solution of L-serine, methyl ester hydrochloride (20.0g, 128 mmol, 1 equiv) in dichloromethane (130 mL) at 0 °C was added triethylamine (40 mL, 282 mmol, 2.2 equiv) and di-*tert*-butyl dicarbonate (37 mL, 135 mmol, 1.1 equiv). After stirring for 30 minutes, the solution was warmed to room temperature, and stirred for an additional 18 hours. The reaction mixture was concentrated by rotary evaporation, diluted with ethyl acetate, and washed with 1M HCl, saturated aqueous NaHCO₃, and brine. The organic phase was dried over sodium sulfate, filtered, and concentrated by rotary evaporation. The residue was passed through a silica plug (50% ethyl acetate in hexanes) to afford the product as a clear, colorless oil (37.2 g 94% yield). The physical properties and spectral data were consistent with the reported values.⁴⁴

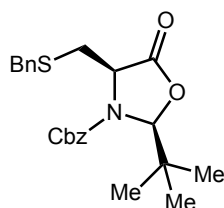


methyl-2-(di(*tert*-butoxycarbonyl)amino)but-2-enoate:

To a stirring solution of methyl (*tert*-butoxycarbonyl)-L-serinate (37.2, 120 mmol, 1.0 equiv) in acetonitrile (200 mL) at 0 °C was added di-*tert*-butyl dicarbonate (58.3 mL, 281 mmol, 2.2 equiv) and 4-dimethylaminopyridine (3.12 g, 25.6 mmol, 0.20 equiv). The resulting solution was warmed to room temperature and stirred for 8 hours. DBU (2.00 g, 12.8 mmol, 0.10 equiv) was added, and the resulting mixture was stirred for an additional 8 hours. The reaction was concentrated by rotary evaporation then diluted in ethyl acetate. The mixture was washed with

⁴⁴ Hiroaki, T. and Hisashi, Y. *J. Am. Chem. Soc.* **2016**, *138*, 14218.

1M HCl and saturated aqueous NaHCO₃, dried over sodium sulfate, filtered, and concentrated by rotary evaporation. The residue was purified by passing through a short plug of silica (5% – 15% ethyl acetate/hexanes) to afford the product (31.5 g, 89% yield) as a white solid. The physical properties and spectral data are consistent with the reported values.⁴⁵



benzyl (2*S*,4*R*)-4-((benzylthio)methyl)-2-(*tert*-butyl)-5-oxooxazolidine-3-carboxylate:

To a round bottom flask equipped with a stir bar was added *S*-benzyl-L-cysteine (10 g, 47 mmol, 1 equiv.), NaOH (1.8 g, 45 mmol, 0.95 equiv), and anhydrous MeOH (500 mL). The reaction was stirred at room temperature for 30 minutes or until nearly homogenous. Pivaldehyde (4.9 g, 57 mmol, 1.2 equiv) and activated 3 Å molecular sieves (50 g) were added to the reaction flask, each in one portion. The reaction was placed under nitrogen atmosphere and stirred at room temperature until the starting material had been consumed (determined by ¹H NMR of a filtered and concentrated aliquot of the reaction solution dissolved in D₃COD). The reaction was quickly filtered through celite and concentrated by rotary evaporation. The residue was dried under high vacuum for 4 hours to afford the imine as a white solid. The imine was dissolved in anhydrous DCM (500 mL) and cooled to 0 °C in an oversized, well-insulated ice bath. Benzyl chloroformate (10.1 mL, 71 mmol, 1.5 equiv) was added to the cooled reaction dropwise via syringe. The reaction was stirred at 0 °C for a full 18 hours then warmed to room temperature and stirred for an additional 6 hours. The mixture was washed with 1 M aqueous NaOH (1 x 250 mL). The organic layer was dried over sodium sulfate, filtered, and

⁴⁵ Adams, L. A.; Aggarwal, V. K.; Bonnert, R. V.; Bressel, B.; Cox, R. J.; Shepherd, J.; de Vicente, J.; Walter, M.; Whittingham, W. G.; and Winn, C. L. *J. Org. Chem.* **2003**, *68*, 9433.

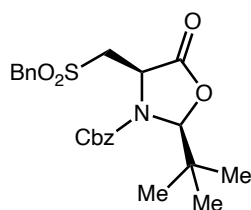
concentrated by rotary evaporation. The residue was purified by flash chromatography (5% – 15% ethyl acetate/hexanes) to afford the product (8.2 g, 42% yield) as a colorless oil.

¹H NMR (300 MHz, CDCl₃) δ 7.43 – 7.34 (m, 5H), 7.33 – 7.20 (m, 5H), 5.55 (s, 2H), 5.21 (dd, *J* = 16.6, 12.1 Hz, 2H), 4.55 (dd, *J* = 7.8, 6.2 Hz, 1H), 3.78 (q, *J* = 13.4 Hz, 1H), 2.94 (dd, *J* = 13.9, 8.0 Hz, 1H), 2.79 (dd, *J* = 13.9, 6.1 Hz, 1H) 0.93 (s, 9H).

¹³C NMR (75 MHz, CDCl₃) δ 171.1, 155.6, 137.6, 135.0, 128.9, 128.5, 128.4, 128.3, 127.0, 96.1, 68.3, 57.4, 36.7, 36.3, 33.1, 24.7.

FTIR (neat) ν_{max} : 33063, 3031, 2970, 1791, 1717, 1481, 1454, 1390, 1344, 1324, 1221, 1196, 1170, 1118, 1036, 1016, 968, 908, 728, and 697 cm⁻¹.

HRMS (NSI) *m/z*: [M+H]⁺ calcd. for C₂₃H₂₈O₄NS, 414.1733; found, 414.1731.



benzyl (2*S*,4*R*)-4-((benzylsulfonyl)methyl)-2-(*tert*-butyl)-5-oxooxazolidine-3-carboxylate:

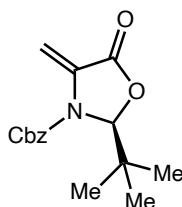
To a round bottom flask equipped with a stir bar was added benzyl (2*S*,4*R*)-4-((benzylthio)methyl)-2-(*tert*-butyl)-5-oxooxazolidine-3-carboxylate (2.4 g, 6 mmol, 1 equiv), *meta*-chloroperoxybenzoic acid (2.5 g, 15 mmol, 2.5 equiv), and DCM (200 mL). The reaction was stirred at room temperature for 18 hours. The reaction mixture was washed with 1 M aqueous sodium hydroxide (3 x 100 mL). The organic layer was dried over sodium sulfate, filtered, and concentrated by rotary evaporation. The residue was purified by flash chromatography (5% – 30% ethyl acetate/hexanes) to afford the product (2.5 g, 95% yield) as a white foam.

¹H NMR (400 MHz, CDCl₃) δ 7.47 – 7.22 (m, 10H), 5.60 (s, 1H), 5.30 – 5.14 (m, 2H), 5.07 (dd, *J* = 7.9, 4.0 Hz, 1H), 4.63 (d, *J* = 14.0 Hz, 1H), 4.40 (d, *J* = 14.0 Hz, 1H), 3.42 (dd, *J* = 15.3, 7.9 Hz, 1H), 3.15 (dd, *J* = 15.3, 4.0 Hz, 1H), 0.87 (s, 9H).

¹³C NMR (100 MHz, CDCl₃) δ 170.7, 155.3, 134.9, 129.0, 128.9, 128.7, 128.7, 128.7, 127.9, 96.8, 68.8, 60.2, 53.5, 52.6, 37.0, 24.5.

FTIR (neat) ν_{\max} : 3066, 3034, 2972, 2874, 2256, 1791, 1719, 1456, 1392, 1312, 1285, 1119, 1039, 966, 908, 725, and 696 cm⁻¹.

HRMS (NSI) *m/z*: [M+H]⁺ calcd. for C₂₄H₂₄O₂N₅S, 446.1645; found, 446.1640.

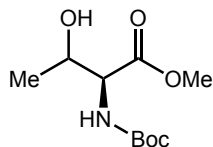


benzyl (*S*)-2-(*tert*-butyl)-4-methylene-5-oxooxazolidine-3-carboxylate (22):

To a round bottom flask equipped with a stir bar was added (benzyl (2*S*,4*R*)-4-((benzylsulfonyl)methyl)-2-(*tert*-butyl)-5-oxooxazolidine-3-carboxylate) (3.6g, 8 mmol, 1 equiv), and DCM (100 mL). The flask was chilled to 0 °C in an ice bath, and DBU (1.3 mL, 9 mmol, 1.1 equiv) was added dropwise via syringe. The reaction was stirred at 0 °C until the starting material had been consumed (determined by TLC, about 10 minutes). While still at 0 °C, the reaction mixture was quenched with saturated aqueous ammonium chloride (50 mL), the layers were separated, and the organic phase was washed with saturated aqueous ammonium chloride (3 x 100 mL). The organic layer was dried over sodium sulfate, filtered, and concentrated by rotary evaporation. The residue was purified by flash chromatography (5% – 15% ethyl acetate/ hexanes) to afford the product (2.0 g, 87% yield) as a colorless oil. The physical properties and spectral data are consistent with the reported values.⁴⁶ Chiral HPLC

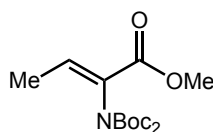
⁴⁶ Hargrave, J. D.; Bish, D.; Köhn, G. K.; and Frost, C. *G Org. Biomol. Chem.*, **2010**, *8*, 5120.

analysis of the alkene (OJ-H, 5% IPA/hexanes, 1.0 mL/min, 254 nm) indicated 97% ee for the major enantiomer (t_R (minor) = 11.800 min, t_R (major) = 13.225 min).



methyl (2S)-2-((tert-butoxycarbonyl)amino)-3-hydroxybutanoate:

To a stirring solution of L-threonine, methyl ester hydrochloride (8.2 g, 49 mmol, 1.0 equiv) in dichloromethane (80 mL) at 0 °C was added triethylamine (21 mL, 150 mmol, 3.0 equiv) and di-*tert*-butyl dicarbonate (12 g, 53 mmol, 1.1 equiv). After stirring 30 minutes, the solution was warmed to room temperature, and stirring was continued for an additional 18 hours. The reaction mixture was concentrated by rotary evaporation, diluted with ethyl acetate, and washed with 1M HCl, saturated aqueous NaHCO₃, and brine. The organic phase was dried over sodium sulfate, filtered, and concentrated by rotary evaporation. The residue was passed through a silica plug to afford the product (10.7 g, 95% yield) as a clear, colorless oil. The physical properties and spectral data are consistent with the reported values.⁴⁴



methyl-2-(di(tert-butoxycarbonyl)amino)but-2-enoate:

To a stirring solution of methyl (2S)-2-((tert-butoxycarbonyl)amino)-3-hydroxybutanoate (10.0 g, 42.9 mmol, 1.0 equiv) in acetonitrile (120 mL) at 0 °C was added di-*tert*-butyl dicarbonate (19.6 g, 90.1 mmol, 2.1 equiv) and DMAP (510 mg, 4.2 mmol, 0.10 equiv). The resulting solution was warmed to room temperature, and after stirring for 8 hours DBU (1.31 g, 8.59 mmol, 0.20 equiv) was added, and the resulting mixture was stirred for 8 hours. The reaction was concentrated by rotary evaporation then diluted in ethyl acetate. The mixture was

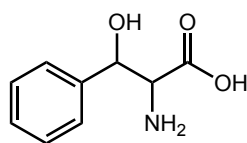
washed with 1M HCl and saturated aqueous NaHCO₃, dried over sodium sulfate, filtered, and concentrated by rotary evaporation. The residue was purified by passing through a short pad of silica (hexane/ethyl acetate = 30%) to afford the product (9.59 g , 71% yield) as a clear, colorless oil.

¹H NMR (300 MHz, CDCl₃) δ 6.93 – 6.68 (m, 1H), 3.72 (s, 3H), 1.72 (d, *J* = 7.1 Hz, 2H), 1.41 (d, *J* = 1.0 Hz, 18H).

¹³C NMR (75 MHz, CDCl₃) δ 164.3, 150.4, 136.5, 130.1, 82.7, 52.0, 27.8, 13.3.

FTIR (neat) ν_{\max} : 2980, 2953, 2935, 1792, 1757, 1727, 1368, 1270, 1250, 1152, 1093, 1044, and 730 cm⁻¹.

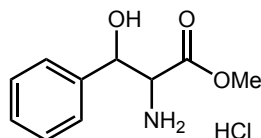
HRMS (NSI) *m/z*: [M+H]⁺ calcd. for C₁₅H₂₆NO₆, 316.1755; found, 316.1756.



2-amino-3-hydroxy-3-phenylpropanoic acid:

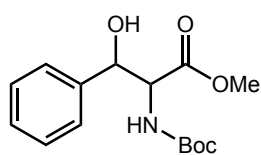
To a stirring solution of NaOH (10 g, 250 mmol, 4.5 equiv) in water (50 mL) was added glycine (5.7 mL, 56 mmol, 1.0 equiv). The solution was stirred 10 minutes, then benzaldehyde (10 g, 151 mmol, 2.9 equiv) was added. The solution was stirred for an additional 30 minutes as an off-white emulsion formed. The precipitant was broken apart in the flask, and concentrated HCl (aq) (130 mL) was added slowly while stirring until consumption of the solid was observed to give a clear yellow solution. After stirring an additional 10 minutes, a beige precipitate formed. The reaction mixture was cooled to 0 °C, and the precipitate was collected by vacuum filtration and washed with ether. The solid was dried under high vacuum to give the product as

an off-white solid (11.6 g, 72% yield). The physical properties and spectral data are consistent with the reported values.⁴⁷



methyl (2S)-2-amino-3-hydroxy-3-phenylpropanoate:

To a stirring solution of 3-hydroxyphenylalanine (3.62 g, 20 mmol, 1.0 equiv) in methanol (80 mL) at 0 °C was added thionyl chloride (3.5 g, 30 mmol, 1.5 equiv) dropwise via syringe, and the reaction mixture was stirred for 30 minutes while gradually warming to room temperature. Upon reaching room temperature, a reflux condenser was attached, and the reaction mixture was heated to 65 °C and stirred under reflux for an additional 5 hours. After cooling to room temperature, the reaction mixture was concentrated by rotary evaporation, diluted with chloroform, concentrated by rotary evaporation, washed with ether, and dried under high vacuum for 2 hours to afford the product as a white solid (4.6 g, 99% yield). The physical properties and spectral data are consistent with the reported values.⁴⁸



phenylalanine, N-[(1,1-dimethylethoxy)carbonyl]-β-hydroxy-, methyl ester:

To a stirring solution of methyl (2S)-2-amino-3-hydroxy-3-phenylpropanoate hydrochloride (5.8 g, 25 mmol, 1.0 equiv) in dichloromethane (70 mL) at 0 °C was added triethylamine (7.6 mL, 57 mmol, 2.5 equiv) and di-*tert*-butyl dicarbonate (5.5 mL, 25 mmol, 1.0 equiv). After

⁴⁷ Shiraiwa, T.; Saijoh, R.; Suzuki, M.; Yoshida, K.; Nishimura, S.; Nagasawa, H. *Chem. Pharm. Bull.* **2003**, *51*, 1363.

⁴⁸ Miyata, O.; Asai, H.; Naito, T. *Chem. Pharm. Bull.* **2005**, *53*, 355.

stirring 30 minutes, the solution was warmed to room temperature, and stirred for an additional 18 hours. The reaction mixture was concentrated by rotary evaporation, diluted with ethyl acetate, and washed with 1M HCl, saturated aqueous NaHCO₃, and brine. The organic phase was dried over sodium sulfate, filtered, and concentrated by rotary evaporation. The residue was passed through a silica plug (50% ethyl acetate/hexanes) to afford the product as a clear, colorless oil (5.10 g 91% yield). The physical properties and spectral data are consistent with the reported values.⁴⁹



methyl 2-(di(tert-butoxycarbonyl)amino)-3-phenylacrylate:

To a stirring solution of phenylalanine, *N*-[(1,1-dimethylethoxy)carbonyl]- β -hydroxy-, methyl ester (5.01 g, 16.9 mmol, 1.0 equiv) in acetonitrile (22 mL) at 0 °C was added di-*tert*-butyl dicarbonate (8.10 g, 37.2 mmol, 2.2 equiv) and DMAP (206 mg, 1.69 mmol, 0.10 equiv). The resulting solution was warmed to room temperature, and after stirring for 8 hours DBU (516 mg, 3.4 mmol, 0.2 equiv) was added, and the resulting mixture was allowed to continue stirring for an additional 8 hours. The reaction was concentrated by rotary evaporation then diluted with ethyl acetate. The organic layer was washed with 1M HCl and saturated aqueous NaHCO₃, dried over sodium sulfate, filtered, and concentrated by rotary evaporation. The residue was purified by flash column chromatography (5% – 15% ethyl acetate/hexanes) to afford the product, (5.17 g, 81% yield) as a clear, colorless oil.

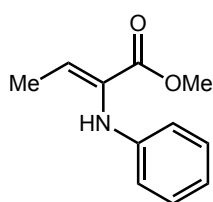
¹H NMR (300 MHz, CDCl₃) δ 7.52 (s, 1H), 7.50 – 7.45 (m, 2H), 7.40 – 7.35 (m, 3H), 3.83 (s, 3H), 1.30 (s, 18H).

⁴⁹ Bengtsson, C.; Nelander, H.; Almqvist, F. *Chem. Eur. J.*, **2013**, *19*, 9916.

^{13}C NMR (125 MHz, CDCl_3) δ 165.4, 150.0, 135.7, 133.0, 129.9, 129.6, 128.9, 127.1, 82.9, 52.4, 27.6.

FTIR (neat) ν_{max} : 2979, 2952, 2934, 1794, 1752, 1722, 1393, 1317, 1248, 1149, 1113, 1093, 1027, 850, and 780 cm^{-1} .

HRMS (NSI) m/z : $[\text{M}+\text{H}]^+$ calcd. for $\text{C}_{21}\text{H}_{24}\text{N}_2\text{O}_2$, 378.1925; found, 378.1919.



methyl 2-(phenylamino)but-2-enoate:

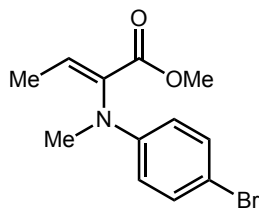
To a round-bottom flask equipped with stir bar was added methyl 2-oxobutanoate (6.1 g, 52 mmol, 1.0 equiv), aniline (4.8 g, 52 mmol, 1.0 equiv), *p*-toluenesulfonic acid monohydrate (494 mg, 2.6 mmol, 0.05 equiv), and benzene (150 mL). A Dean-Stark apparatus and reflux condenser were attached, and the mixture was heated to 95 $^{\circ}\text{C}$ while stirring for 24 hours. The reaction mixture was concentrated by rotary evaporation, and the residue was purified by flash column chromatography (5% – 50% ethyl acetate/hexanes) to afford the product (6.0 g, 59% yield) as an orange oil.

^1H NMR (300 MHz, CDCl_3) δ 7.30 – 7.19 (m, 2H), 6.86 (t, $J = 7.5$ Hz, 1H), 6.78 – 6.43 (m, 3H), 5.64 (s, 1H), 3.79 (s, 3H), 1.73 (d, $J = 7.3$ Hz, 2H).

^{13}C NMR (75 MHz, CDCl_3) δ 166.3, 144.2, 130.3, 129.0, 119.4, 115.3, 52.2, 14.5.

FTIR (neat) ν_{max} : 3375, 3053, 3026, 2971, 2951, 1708, 1647, 1599, 1497, 1434, 1266, 1244, 1175, 747, and 693 cm^{-1} .

HRMS (NSI) m/z : $[\text{M}+\text{H}]^+$ calcd. for $\text{C}_{11}\text{H}_{14}\text{O}_2\text{N}$, 192.1019; found, 192.1019.



methyl 2-((4-bromophenyl)(methyl)amino)but-2-enoate:

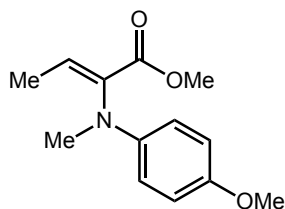
To a round-bottom flask equipped with stir bar was added methyl 2-oxobutanoate (2.3 g, 20 mmol, 2.0 equiv), 4-bromo-*N*-methylaniline (1.1 g, 10 mmol, 1.0 equiv), *p*-toluenesulfonic acid monohydrate (95 mg, 0.50 mmol, 0.05 equiv), and benzene (50 mL). A Dean-Stark apparatus and reflux condenser were attached, and the mixture was heated to 95 °C while stirring for 24 hours. The reaction mixture was concentrated by rotary evaporation, and the residue was purified by flash column chromatography (5% – 30% ethyl acetate/hexanes) to afford the product (1.6 g, 83% yield) as a clear, colorless oil.

¹H NMR (500 MHz, CDCl₃) δ 7.41 – 7.18 (m, 2H), 6.99 (q, *J* = 7.0 Hz, 1H), 6.49 (d, *J* = 9.0 Hz, 2H), 3.68 (d, *J* = 0.9 Hz, 3H), 3.04 (s, 3H), 1.81 – 1.70 (m, 3H).

¹³C NMR (125 MHz, CDCl₃) δ 165.6, 146.9, 138.2, 136.7, 131.7, 113.9, 109.5, 51.9, 38.0, 13.5.

FTIR (neat) ν_{max} : 2972, 2950, 2819, 1732, 1589, 1498, 1434, 1371, 1303, 1239, 1206, 808, and 747 cm⁻¹.

HRMS (NSI) *m/z*: [M+H]⁺ calcd. for C₁₂H₁₅O₂NBr, 284.0281; found, 284.0285.



methyl 2-((4-methoxyphenyl)(methyl)amino)but-2-enoate:

To a round-bottom flask equipped with stir bar was added methyl 2-oxobutanoate (2.3 g, 20 mmol, 2.0 equiv), 4-methoxy-*N*-methylaniline (1.4 g, 10 mmol, 1.0 equiv), *p*-toluenesulfonic

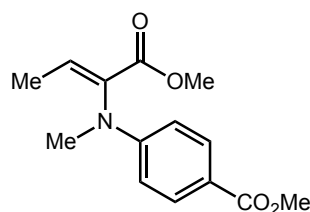
acid (95 mg, 0.50 mmol, 0.05equiv), and benzene (50 mL). A Dean-Stark apparatus and reflux condenser were attached, and the mixture was heated to 95 °C while stirring for 24 hours. The reaction mixture was concentrated by rotary evaporation, and the residue was purified by flash column chromatography (5% – 40% ethyl acetate/hexanes) to afford the product (1.6 g, 68% yield) as a clear, colorless oil.

¹H NMR (500 MHz, CDCl₃) δ 6.91 (q, J = 7.1 Hz, 1H), 6.81 (d, J = 9.0 Hz, 2H), 6.59 (d, J = 9.1 Hz, 2H), 3.75 (s, 3H), 3.67 (s, 3H), 3.05 (s, 3H), 1.79 (d, J = 7.1 Hz, 3H).

¹³C NMR (125 MHz, CDCl₃) δ 166.2, 151.9, 142.4, 137.6, 136.9, 114.7, 113.3, 55.6, 51.7, 38.3, 13.4.

FTIR (neat) ν_{max} : 2992, 2948, 2906, 2832, 1718, 1647, 1507, 1238, 1201, 1123, 1114, 1036, and 817 cm⁻¹.

HRMS (NSI) m/z : [M+H]⁺ calcd. for C₁₃H₁₈O₃N, 236.1281; found, 236.1278.



methyl 4-((1-methoxy-1-oxobut-2-en-2-yl)(methylamino)benzoate:

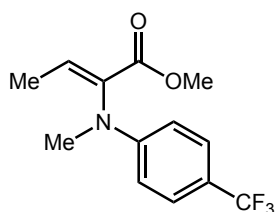
To a round-bottom flask equipped with stir bar was added methyl 2-oxobutanoate (2.3 g, 20 mmol, 1.0 equiv), methyl 4-(methylamino)benzoate (3.3 g, 20 mmol, 1.0 equiv), *p*-toluenesulfonic acid (190 mg, 1.0 mmol, 0.05 equiv), and benzene (50 mL). A Dean-Stark apparatus and reflux condenser were attached, and the mixture was heated to 95 °C while stirring for 24 hours. The reaction mixture was concentrated by rotary evaporation, and the residue was purified by flash column chromatography (5% – 50% ethyl acetate/hexanes) to afford the product (4.1 g, 77% yield) as a clear, colorless oil.

¹H NMR (500 MHz, CDCl₃) δ 7.87 (d, *J* = 8.5 Hz, 2H), 7.02 (q, *J* = 6.8 Hz, 1H), 6.57 (d, *J* = 8.5 Hz, 2H), 3.81 (s, 4H), 3.66 (s, 3H), 3.08 (s, 3H), 1.72 (d, *J* = 7.1 Hz, 3H).

¹³C NMR (125 MHz, CDCl₃) δ 167.1, 165.2, 151.4, 138.7, 136.2, 131.2, 118.6, 111.2, 52.0, 51.4, 38.0, 13.5.

FTIR (neat) ν_{max} : 2990, 2949, 2907, 1705, 1601, 1516, 1433, 1275, 1255, 1177, 1108, 1042, and 768 cm⁻¹.

HRMS (NSI) *m/z*: [M+H]⁺ calcd. for C₁₄H₁₈O₄N, 264.1230; found, 264.1227.



methyl 2-(methyl(4-(trifluoromethyl)phenyl)amino)but-2-enoate:

To a round-bottom flask equipped with stir bar was added methyl 2-oxobutanoate (2.3 g, 20 mmol, 2.0 equiv), 4-trifluoromethyl-*N*-methylaniline (1.8 g, 10 mmol, 1.0 equiv), *p*-toluenesulfonic acid monohydrate (95 mg, 0.5 mmol, 0.05 equiv), and benzene (50 mL). A Dean-Stark apparatus and reflux condenser were attached, and the mixture was heated to 95 °C while stirring for 24 hours. The reaction mixture was concentrated by rotary evaporation, and the residue was purified by flash column chromatography (5% – 40% ethyl acetate/hexanes) to afford the product (2.3 g, 84% yield) as a clear, colorless oil.

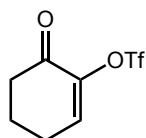
¹H NMR (500 MHz, CDCl₃) δ 7.44 (d, *J* = 9.1 Hz, 1H), 7.07 (q, *J* = 7.0 Hz, 0H), 6.65 (d, *J* = 8.9 Hz, 1H), 3.71 (s, 1H), 3.10 (s, 1H), 1.76 (d, *J* = 7.1 Hz, 1H).

¹³C NMR (75 MHz, CDCl₃) δ 165.3, 150.2, 139.0, 136.2, 126.5 (q, *J* = 4.2 Hz), 125.0 (q, *J* = 270.0 Hz), 118.7 (q, *J* = 33.1 Hz), 111.5, 52.0, 38.0, 13.4.

¹⁹F NMR (282 MHz, CDCl₃) δ -61.01.

FTIR (neat) ν_{\max} : 2994, 2953, 2912, 2825, 1720, 1650, 1613, 1524, 1321, 1257, 1205, 1193, 1102, 1067, 1043, 849, and 576 cm^{-1} .

HRMS (NSI) m/z : $[\text{M}+\text{H}]^+$ calcd. for $\text{C}_{13}\text{H}_{15}\text{O}_2\text{NF}_3$, 274.1049; found, 274.1050.



6-oxocyclohex-1-en-1-yl trifluoromethanesulfonate:

To a stirring solution of 1,2-cyclohexanedione (5.0 g, 45 mmol, 1.0 equiv) in dichloromethane (100 mL) at $-78\text{ }^{\circ}\text{C}$ was added triethylamine (5.5 g, 54 mmol, 1.2 equiv) and trifluoromethanesulfonic anhydride (12.7 g, 45 mmol, 1.0 equiv). The resulting solution was warmed to room temperature and stirred for an additional 3 hours. The reaction was concentrated by rotary evaporation then diluted with ethyl acetate. The organic layer was washed with 1M HCl and saturated aqueous sodium bicarbonate, dried over sodium sulfate, filtered, and concentrated by rotary evaporation. The residue was purified by flash column chromatography (10% – 30% ethyl acetate/hexanes) to afford the product (6.2 g, 57% yield) as a white crystalline, low-melting solid.

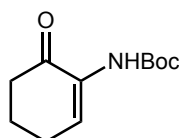
^1H NMR (600 MHz, CDCl_3) δ 6.93 (t, $J = 4.4$ Hz, 1H), 2.84 – 2.34 (m, 4H), 2.07 (p, $J = 7.4$, 6.9, 5.6, 5.6 Hz, 2H).

^{13}C NMR (150 MHz, CDCl_3) δ 189.8, 144.5, 139.5, 118.5 (q, $J = 320.1$ Hz), 37.6, 24.9, 21.8.

^{19}F NMR (282 MHz, CDCl_3) δ -73.99.

FTIR (neat) ν_{\max} : 2953, 1702, 1419, 1349, 1202, 1137, 1070, 914, and 809 cm^{-1} .

HRMS (NSI) m/z : $[\text{M}+\text{H}]^+$ calcd. for $\text{C}_7\text{H}_8\text{O}_4\text{S}$, 245.0090; found, 245.0087.



tert-butyl (6-oxocyclohex-1-en-1-yl)carbamate:

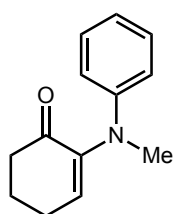
A three-neck round-bottom flask equipped with a stir bar was charged with 6-oxocyclohex-1-en-1-yl trifluoromethanesulfonate (4.0 g, 16.3 mmol, 1.0 equiv), tert-butyl carbamate (2.2 g, 19.6 mmol, 1.2 equiv), Pd₂(dba)₃ (372 mg, 0.41 mmol, 0.025 equiv), 2-di-tert-butylphosphino-2',4',6'-triisopropylbiphenyl (691 mg, 1.6 mmol, 0.10 equiv), and K₂CO₃ (5.5 g, 40.8 mmol, 2.5 equiv). A reflux condenser was connected, and each inlet was sealed with a rubber septum. The atmosphere was exchanged by applying vacuum and backfilling with N₂ (this process was conducted a total of three times). Under N₂ atmosphere, the tube was charged with degassed toluene (40 mL). The reaction mixture was heated to 80 °C and stirred under N₂ for 12 hours. After cooling to room temperature, the reaction was quenched with saturated ammonium chloride solution and extracted with dichloromethane (3 x 100 mL). The combined organic layers were dried over sodium sulfate, filtered, and concentrated by rotary evaporation. The residue was purified by flash column chromatography (10% – 70% ethyl acetate/hexanes) to afford the product (2.8 g, 80% yield) as a pale yellow oil.

¹H NMR (400 MHz, CDCl₃) δ 7.29 (t, *J* = 4.7 Hz, 1H), 7.05 (s, 1H), 2.56 – 2.28 (m, 4H), 2.00 – 1.76 (m, 2H), 1.39 (s, 9H).

¹³C NMR (75 MHz, CDCl₃) 193.7, 152.8, 132.4, 127.2, 80.1, 37.0, 28.1, 24.5, 22.4.

FTIR (neat) ν_{max} : 3402, 2977, 2933, 2871, 2832, 1784, 1721, 1672, 1638, 1507, 1355, 1227, 1151, 1042, 1020, 877, and 867 cm⁻¹.

HRMS (NSI) *m/z*: [M+H]⁺ calcd. for C₁₁H₁₈O₃N, 212.1281; found, 212.1279.

**2-(methyl(phenyl)amino)cyclohex-2-en-1-one:**

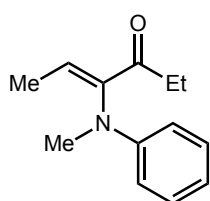
To a round-bottom flask equipped with stir bar was added cyclohexane-1,2-dione (2.2 g, 20 mmol, 2.0 equiv), *N*-methylaniline (1.1 g, 10 mmol, 1.0 equiv), *p*-toluenesulfonic acid (95 mg, 0.5 mmol, 0.05 equiv), and benzene (50 mL). A Dean-Stark apparatus and reflux condenser were attached, and the mixture was heated to 95 °C while stirring for 24 hours. The reaction mixture was diluted with ethyl acetate, washed with water (2 x 50 mL), dried over sodium sulfate, filtered, and concentrated by rotary evaporation. The residue was purified by flash column chromatography (5% – 30% ethyl acetate/hexanes) to afford the product (1.5 g, 80% yield) as a yellow oil.

¹H NMR (300 MHz, CDCl₃) δ 7.19 (dd, *J* = 8.7, 7.2 Hz, 2H), 6.83 – 6.76 (m, 2H), 6.75 – 6.68 (m, 2H), 3.07 (s, 3H), 2.54 (qd, *J* = 6.3, 3.8 Hz, 4H), 2.09 (p, *J* = 6.2 Hz, 2H).

¹³C NMR (75 MHz, CDCl₃) δ 196.4, 149.0, 144.6, 143.1, 128.8, 118.4, 114.7, 39.5, 39.3, 26.0, 22.9.

FTIR (neat) ν_{max} : 3058, 3024, 2942, 2874, 2813, 1680, 1596, 1497, 1323, 1128, 747, and 691 cm⁻¹.

HRMS (NSI) *m/z*: [M+H]⁺ calcd. for C₁₃H₁₆ON, 202.1226; found, 202.1225.



4-(methyl(phenyl)amino)hex-4-en-3-one:

To a round-bottom flask equipped with stir bar was added hexane-3,4-dione (5.5 g, 50 mmol, 5.0 equiv), *N*-methylaniline (1.1 g, 10 mmol, 1.0 equiv), *p*-toluenesulfonic acid (95 mg, 0.5 mmol, 0.05 equiv), and benzene (50 mL). A Dean-Stark apparatus and reflux condenser were attached, and the mixture was heated to 95 °C while stirring for 18 hours. The reaction mixture was diluted with ethyl acetate, washed with water (2 x 50 mL), dried over sodium sulfate,

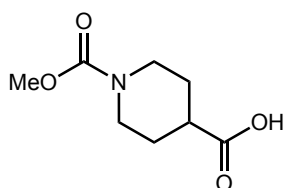
filtered, and concentrated by rotary evaporation. The residue was purified by flash column chromatography (5% – 30% ethyl acetate/hexanes) to afford the product (1.8 g, 91% yield) as a yellow oil.

¹H NMR (300 MHz, CDCl₃) δ 7.28 – 7.16 (m, 2H), 6.88 – 6.80 (m, 1H), 6.75 (tt, *J* = 7.3, 1.2 Hz, 1H), 6.60 (dd, *J* = 7.7, 1.1 Hz, 2H), 3.13 (s, 3H), 2.44 (q, *J* = 7.1 Hz, 2H), 1.75 (d, *J* = 7.1 Hz, 3H), 1.01 (t, *J* = 7.2 Hz, 3H).

¹³C NMR (75 MHz, CDCl₃) δ 201.5, 147.5, 145.0, 135.0, 129.3, 117.3, 111.9, 38.1, 31.8, 13.6, 7.9.

FTIR (neat) ν_{\max} : 3060, 2972, 2935, 2917, 1713, 1593, 1503, 1360, 746, and 691 cm⁻¹.

HRMS (NSI) *m/z*: [M+H]⁺ calcd. for C₁₃H₁₈ON, 204.1383; found, 204.1381.



1-(methoxycarbonyl)piperidine-4-carboxylic acid:

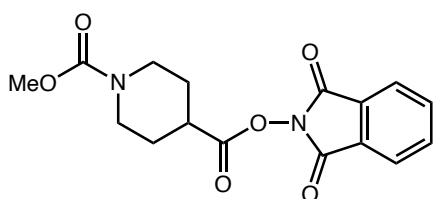
To a round bottom flask equipped with a stir bar was added piperidine-4-carboxylic acid (5.0 g, 39 mmol, 1 equiv), THF (100 mL), and saturated aqueous sodium bicarbonate (100 mL). Methyl chloroformate (6.0 mL, 77.0 mmol, 2 equiv) was then added dropwise via syringe. The reaction was allowed to stir at room temperature overnight. The reaction mixture was filtered over celite then concentrated to remove THF. The remaining solution was acidified to pH = 2 using 1 M HCl then extracted with ethyl acetate (3 x 100 mL). The combined extracts were dried over sodium sulfate, filtered, then concentrated by rotary evaporation. The residue was purified by flash chromatography (5% – 40% ethyl acetate/hexanes) to afford the product (5.65 g, 78% yield) as a white solid.

¹H NMR (500 MHz, CDCl₃) δ 11.46 (s, 1H), 4.01 (m, 2H), 3.65 (s, 3H), 2.89 (t, *J* = 11.5 Hz, 2H), 2.46 (tt, *J* = 10.8, 4.0 Hz, 1H), 1.88 (d, *J* = 11.5 Hz, 2H), 1.61 (qd, *J* = 11.2, 4.0 Hz, 2H).

¹³C NMR (125 MHz, CDCl₃) δ 179.6, 156.0, 52.8, 43.1, 40.6, 27.6.

FTIR (neat) ν_{max} : 3003, 2956, 2863, 1674, 1479, 1449, 1411, 1275, 1209, 1182, 1126, 1080, 1033, 930, 758, and 730 cm⁻¹.

HRMS (NSI) *m/z*: [M+H]⁺ calcd. for C₈H₁₄O₄N, 188.0917; found, 188.0916.



4-(1,3-dioxoisindolin-2-yl) 1-methyl piperidine-1,4-dicarboxylate:

To a round bottom flask equipped with a stir bar was added 1-(methoxycarbonyl)piperidine-4-carboxylic acid (5.7 g, 30 mmol, 1 equiv), *N*-hydroxyphthalamide (4.9 g, 30 mmol, 1 equiv), DMAP (369 mg, 3 mmol, 0.1 equiv), and DCM (300 mL). DIC (4.7 mL, 30 mmol, 1 equiv) was then added dropwise via syringe. The reaction was allowed to stir at this temperature until the starting material had been consumed (determined by TLC). The reaction mixture was filtered over celite and rinsed with an additional 50 mL of DCM. The filtrate was concentrated by rotary evaporation and the residue was purified by flash chromatography (5% – 40% ethyl acetate/hexanes) to afford the product (7.52 g, 75% yield) as a white solid.

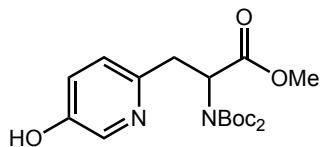
¹H NMR (400 MHz, CDCl₃) δ 7.85 (dd, *J* = 5.6, 3.0 Hz, 1H), 7.77 (dd, *J* = 5.6, 3.0 Hz, 1H), 4.13 – 3.90 (m, 1H), 3.68 (d, *J* = 1.4 Hz, 2H), 3.05 (t, *J* = 11.0 Hz, 2H), 2.91 (tt, *J* = 10.2, 4.0 Hz, 1H), 2.10 – 2.00 (m, 3H), 1.84 (ddt, *J* = 13.3, 10.2, 5.3 Hz, 3H).

¹³C NMR (101 MHz, CDCl₃) δ 170.5, 161.9, 155.8, 134.9, 128.8, 124.0, 52.7, 42.7, 38.3, 27.7.

FTIR (neat) ν_{max} : 2956, 2863, 1813, 1785, 1754, 1694, 1468, 1448, 1411, 1373, 1316, 1276, 1233, 1186, 1128, 1076, 1000, 968, 913, 877, 786, 767, 729, 695 cm⁻¹.

HRMS (NSI) m/z : $[M+H]^+$ calcd. for $C_{16}H_{17}O_6N_2$, 333.1081; found, 333.1081.

2.4.5 Procedures and Characterization Data



methyl 2-(di(*tert*-butoxycarbonyl)amino)-3-(5-hydroxypyridin-2-yl)propanoate (1):

Following the general procedure, the reaction of 6-bromopyridin-3-ol (174 mg, 1.00 mmol, 1 equiv), methyl 2-(di(*tert*-butoxycarbonyl)amino)acrylate (608 mg, 2.02 mmol, 2 equiv), $[Ir(ppy)_2(dtbbpy)]PF_6$ (10.4 mg, 0.011 mmol, 0.01 equiv) and Hantzsch ester (379 mg, 1.50 mmol, 1.5 equiv) provided the product (361 mg, 91% yield) as an off-white solid after purification by flash column chromatography (50% – 75% ethyl acetate/hexanes).

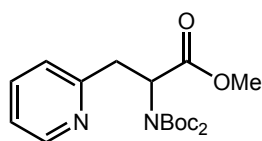
Mp: 163 °C (decomp.)

1H NMR (400 MHz, $CDCl_3$) δ 10.58 (s, 1H), 8.13 (d, $J = 2.9$ Hz, 1H), 7.15 (dd, $J = 8.5, 2.8$ Hz, 1H), 6.99 (d, $J = 8.4$ Hz, 1H), 5.29 (dd, $J = 10.2, 4.8$ Hz, 1H), 3.69 (s, 3H), 3.51 (dd, $J = 14.1, 4.9$ Hz, 1H), 3.26 (dd, $J = 14.2, 10.2$ Hz, 1H), 1.34 (s, 18H).

^{13}C NMR (100 MHz, $CDCl_3$) δ 170.5, 153.3, 151.5, 147.6, 136.5, 125.2, 125.0, 83.2, 58.4, 52.3, 36.8, 27.7.

FTIR (neat) ν_{max} : 3002, 2980, 2950, 2933, 2612, 1744, 1729, 1697, 1573, 1364, 1280, 1232, 1253, 1142, and 1115 cm^{-1} .

HRMS (NSI) m/z : $[M+H]^+$ calcd. for $C_{20}H_{31}O_6N_2$, 397.1969; found, 397.1967.



methyl 2-(di(*tert*-butoxycarbonyl)amino)-3-(pyridin-2-yl)propanoate (2):

1 mmol scale:

Following the general procedure, the reaction of 2-iodopyridine (207 mg, 1.01 mmol, 1 equiv), methyl 2-(di(*tert*-butoxycarbonyl)amino)acrylate (610 mg, 2.03 mmol, 2 equiv), [Ir(ppy)₂(dtbbpy)]PF₆ (9.9 mg, 0.011 mmol, 0.01 equiv) and Hantzsch ester (344 mg, 1.36 mmol, 1.3 equiv) provided the product (371 mg, 97% yield) as a clear, colorless crystalline solid after purification by flash column chromatography (10% – 50% ethyl acetate/hexanes).

25-mmol scale:

A 250-mL Schlenk flask equipped with a stir bar was charged with Hantzsch ester (6.33 g, 25 mmol, 1.0 equiv), [Ir(ppy)₂(dtbbpy)]PF₆ (22.9 mg, 0.025 mmol, 0.001 equiv), methyl-2-(di(*tert*-butoxycarbonyl)amino)but-2-enoate (9.03, 30 mmol, 1.2 equiv), 2-bromopyridine (3.95 g, 25 mmol, 1.0 equiv), and degassed DMSO/H₂O (5/1, V/V; 230 mL). The tube was connected to a N₂ line, and N₂ was streamed over the headspace of the reaction for 10 minutes before sealing with a rubber septum. The suspension was stirred under irradiation with blue LEDs for 18 hours while being cooled with a fan. The reaction was quenched with saturated sodium bicarbonate solution (1200 mL) and extracted with ethyl acetate (3 x 250 mL). The extracts were combined, passed through a silica plug, and concentrated by rotary evaporation. The residue was purified by flash column chromatography (5 – 60% ethyl acetate/hexanes) to afford the title compound (8.0 g, 84% yield) as a white crystalline solid.

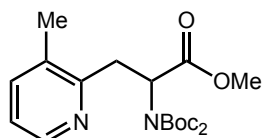
Mp: 49 – 51 °C

¹H NMR (300 MHz, CDCl₃) δ 8.45 (d, J = 4.8 Hz, 1H), 7.50 (td, J = 7.7, 1.9 Hz, 1H), 7.09 – 7.00 (m, 2H), 5.45 (dd, J = 9.3, 5.2 Hz, 1H), 3.65 (s, 3H), 3.57 (dd, J = 14.2, 5.1 Hz, 1H), 3.25 (dd, J = 14.2, 9.4 Hz, 1H), 1.34 (s, 18H).

¹³C NMR (75 MHz, CDCl₃) δ 170.8, 157.9, 151.5, 149.3, 136.1, 123.8, 121.4, 82.8, 58.1, 52.2, 38.7, 27.8.

FTIR (neat) ν_{max} : 3002, 2977, 2950, 2936, 1742, 1724, 1689, 1378, 1365, 12533, 1234, 1163, 1121, 1010, and 776 cm^{-1} .

HRMS (NSI) m/z : $[\text{M}+\text{H}]^+$ calcd. for $\text{C}_{19}\text{H}_{29}\text{O}_6\text{N}_2$, 381.2020; found, 381.2018.



methyl 2-(di(*tert*-butoxycarbonyl)amino)-3-(3-methylpyridin-2-yl)propanoate (3):

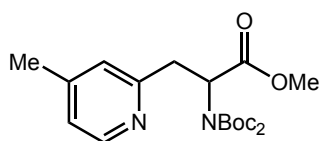
Following the general procedure, the reaction of 2-bromo-3-methylpyridine (175 mg, 1.02 mmol, 1 equiv), methyl 2-(di(*tert*-butoxycarbonyl)amino)acrylate (604 mg, 2.03 mmol, 2 equiv), $[\text{Ir}(\text{ppy})_2(\text{dtbbpy})]\text{PF}_6$ (9.9 mg, 0.011 mmol, 0.01 equiv) and Hantzsch ester (344 mg, 1.36 mmol, 1.3 equiv) provided the product (376 mg, 94% yield) as a pale yellow oil after purification by flash column chromatography (2% – 6% tetrahydrofuran/dichloromethane).

^1H NMR (300 MHz, CDCl_3) δ 8.33 – 8.29 (m, 1H), 7.38 – 7.28 (m, 1H), 6.97 (dd, $J = 7.6, 4.8$ Hz, 1H), 5.64 (dd, $J = 8.9, 5.1$ Hz, 1H), 3.69 (s, 3H), 3.58 (dd, $J = 14.8, 5.1$ Hz, 1H), 3.34 (dd, $J = 14.8, 8.9$ Hz, 1H), 2.27 (s, 3H), 1.38 (s, 18H).

^{13}C NMR (75 MHz, CDCl_3) δ 171.1, 156.4, 151.6, 146.6, 137.4, 131.6, 121.3, 82.8, 57.9, 52.2, 35.3, 27.8, 18.7.

FTIR (neat) ν_{max} : 2979, 2952, 2935, 1793, 1743, 1698, 1575, 1451, 1436, 1366, 1227, 1167, 1141, 1116, and 778 cm^{-1} .

HRMS (NSI) m/z : $[\text{M}+\text{H}]^+$ calcd. for $\text{C}_{20}\text{H}_{31}\text{O}_6\text{N}_2$, 395.2177; found, 395.2174.



methyl 2-(di(*tert*-butoxycarbonyl)amino)-3-(4-methylpyridin-2-yl)propanoate (4):

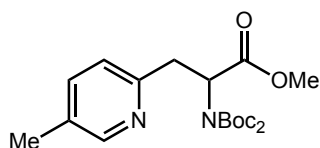
Following the general procedure, the reaction of 2-bromo-4-methylpyridine (173 mg, 1.01 mmol, 1 equiv), methyl 2-(di(*tert*-butoxycarbonyl)amino)acrylate (610 mg, 2.03 mmol, 2 equiv), [Ir(ppy)₂(dtbbpy)]PF₆ (9.6 mg, 0.011 mmol, 0.01 equiv) and Hantzsch ester (331 mg, 1.31 mmol, 1.3 equiv) provided the product (377 mg, 96% yield) as a pale yellow oil after purification by flash column chromatography (2% – 6% tetrahydrofuran/dichloromethane).

¹H NMR (300 MHz, CDCl₃) δ 8.33 (d, J = 5.8 Hz, 1H), 6.89 (s, 2H), 5.46 (dd, J = 9.3, 5.1 Hz, 1H), 3.68 (s, 3H), 3.55 (dd, J = 14.2, 5.1 Hz, 1H), 3.22 (dd, J = 14.2, 9.4 Hz, 1H), 2.24 (s, 3H), 1.37 (s, 18H).

¹³C NMR (75 MHz, CDCl₃) δ 170.9, 157.7, 151.5, 149.1, 147.1, 124.7, 122.4, 82.8, 58.2, 52.2, 38.6, 27.8, 20.8.

FTIR (neat) ν_{max}: 2978, 2952, 2935, 1794, 1740, 1606, 1366, 1270, 1251, 1227, 1166, 1138, 852, and 778 cm⁻¹.

HRMS (NSI) *m/z*: [M+H]⁺ calcd. for C₂₀H₃₁O₆N₂, 395.2177; found, 395.2175.



methyl 2-(di(*tert*-butoxycarbonyl)amino)-3-(5-methylpyridin-2-yl)propanoate (5):

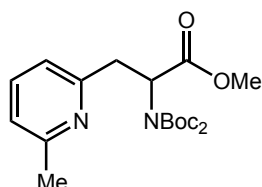
Following the general procedure, the reaction of 2-bromo-5-methylpyridine (175 mg, 1.02 mmol, 1 equiv), methyl 2-(di(*tert*-butoxycarbonyl)amino)acrylate (604 mg, 2.01 mmol, 2 equiv), [Ir(ppy)₂(dtbbpy)]PF₆ (9.2 mg, 0.010 mmol, 0.01 equiv) and Hantzsch ester (329 mg, 1.30 mmol, 1.3 equiv) provided the product (373 mg, 93% yield) as a pale yellow oil after purification by flash column chromatography (3% – 8% tetrahydrofuran/dichloromethane).

¹H NMR (300 MHz, CDCl₃) δ 8.38 – 8.24 (m, 1H), 7.45 – 7.31 (m, 1H), 6.98 (dd, J = 7.8, 0.8 Hz, 1H), 5.44 (dd, J = 9.4, 5.2 Hz, 1H), 3.69 (s, 3H), 3.56 (dd, J = 14.1, 5.2 Hz, 1H), 3.25 (dd, J = 14.1, 9.4 Hz, 1H), 2.24 (s, 3H), 1.38 (s, 18H).

^{13}C NMR (75 MHz, CDCl_3) δ 170.8, 154.9, 151.5, 149.7, 136.7, 130.6, 123.3, 82.8, 58.3, 52.2, 38.3, 27.8, 17.9.

FTIR (neat) ν_{max} : 2978, 2952, 2935, 1793, 174, 1710, 1366, 1270, 1167, 1137, and 808 cm^{-1} .

HRMS (NSI) m/z : $[\text{M}+\text{H}]^+$ calcd. for $\text{C}_{19}\text{H}_{30}\text{O}_6\text{N}_2$, 395.2177; found, 395.2173.



methyl 2-(di(*tert*-butoxycarbonyl)amino)-3-(6-methylpyridin-2-yl)propanoate (6):

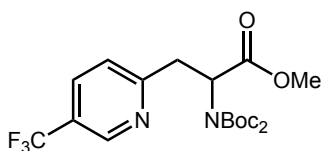
Following the general procedure, the reaction of 2-bromo-6-methylpyridine (175 mg, 1.02 mmol, 1 equiv), methyl 2-(di(*tert*-butoxycarbonyl)amino)acrylate (606 mg, 2.01 mmol, 2 equiv), $[\text{Ir}(\text{ppy})_2(\text{dtbbpy})]\text{PF}_6$ (10.1 mg, 0.011 mmol, 0.01 equiv) and Hantzsch ester (334 mg, 1.30 mmol, 1.3 equiv) provided the product (388 mg, 97% yield) as a pale yellow oil after purification by flash column chromatography (3% – 8% tetrahydrofuran/dichloromethane).

^1H NMR (400 MHz, CDCl_3) δ 7.42 (t, $J = 7.6$ Hz, 1H), 6.90 (dd, $J = 17.4, 7.6$ Hz, 2H), 5.44 (dd, $J = 9.7, 5.1$ Hz, 1H), 3.69 (s, 3H), 3.53 (dd, $J = 14.0, 5.1$ Hz, 1H), 3.26 (dd, $J = 13.9, 9.7$ Hz, 1H), 2.46 (s, 3H), 1.37 (d, $J = 0.9$ Hz, 18H).

^{13}C NMR (75 MHz, CDCl_3) δ 170.8, 157.8, 157.1, 136.4, 120.9, 120.8, 82.8, 58.3, 52.2, 38.6, 27.8, 24.4.

FTIR (neat) ν_{max} : 3000, 2980, 2957, 2933, 1743, 172, 1689, 1579, 1456, 1430, 1377, 1364, 1278, 1246, 1231, 1166, 1011, and 788 cm^{-1} .

HRMS (NSI) m/z : $[\text{M}+\text{H}]^+$ calcd. for $\text{C}_{20}\text{H}_{31}\text{O}_6\text{N}_2$, 395.2177; found, 395.2170.



methyl 2-(di(*tert*-butoxycarbonyl)amino)-3-(5-(trifluoromethyl)pyridin-2-yl)propanoate (7):

Following the general procedure, the reaction of 2-bromo-5-(trifluoromethyl)pyridine (225 mg, 1.00 mmol, 1 equiv), methyl 2-(di(*tert*-butoxycarbonyl)amino)acrylate (605 mg, 2.01 mmol, 2 equiv), [Ir(ppy)₂(dtbbpy)]PF₆ (9.6 mg, 0.011 mmol, 0.01 equiv) and Hantzsch ester (329 mg, 1.30 mmol, 1.3 equiv) provided the product (420 mg, 94% yield) as a pale yellow oil after purification by flash column chromatography (3% – 12% tetrahydrofuran/hexanes).

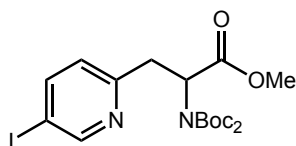
¹H NMR (300 MHz, CDCl₃) δ 8.76 – 8.68 (m, 1H), 7.76 (dd, *J* = 8.1, 2.2 Hz, 1H), 7.28 – 7.16 (m, 1H), 5.50 (dd, *J* = 8.7, 5.8 Hz, 1H), 3.71 – 3.59 (m, 4H), 3.34 (dd, *J* = 14.3, 8.8 Hz, 1H), 1.37 (s, 18H).

¹³C NMR (75MHz, CDCl₃) δ 177.5, 170.7, 151.9, 149.9, 147.1, 140.0, 128.8, 121.7, 83.3, 57.7, 52.3, 39.3, 32.4, 27.8, 27.4.

¹⁹F NMR (282 MHz, CDCl₃) δ -62.45.

FTIR (neat) ν_{max}: 2981, 2954, 2936, 1793, 1745, 1700, 1608, 1367, 1381, 1271, 1161, 1127, 1017, and 756 cm⁻¹.

HRMS (NSI) *m/z*: [M+H]⁺ calcd. for C₂₀H₂₈O₆N₂F₃, 449.1894; found, 449.1891.



methyl 2-(di(*tert*-butoxycarbonyl)amino)-3-(5-iodopyridin-2-yl)propanoate (8):

Following the general procedure, the reaction of 2,5-diiodopyridine (333 mg, 1.01 mmol, 1 equiv), methyl 2-(di(*tert*-butoxycarbonyl)amino)acrylate (601 mg, 2.00 mmol, 2 equiv), [Ir(ppy)₂(dtbbpy)]PF₆ (10.1 mg, 0.011 mmol, 0.01 equiv) and Hantzsch ester (321 mg, 1.27 mmol, 1.3 equiv) provided the product (378 mg, 74% yield) as white solid after purification by flash column chromatography (0% – 30% tetrahydrofuran/hexanes).

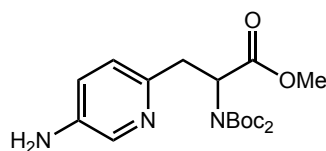
Mp: 59 – 62 °C

¹H NMR (300 MHz, CDCl₃) δ 7.74 8.66 (dd, *J* = 2.2, 0.7 Hz, 1H), 7.81 (dd, *J* = 8.1, 2.2 Hz, 1H), 6.90 (d, *J* = 8.2 Hz, 1H), 5.41 (dd, *J* = 9.0, 5.6 Hz, 1H), 3.66 (s, 3H), 3.51 (dd, *J* = 14.2, 5.6 Hz, 1H), 3.20 (dd, *J* = 14.2, 9.0 Hz, 1H), 1.37 (s, 18H).

¹³C NMR (75MHz, CDCl₃) δ 170.6, 156.9, 155.2, 151.5, 144.3, 125.7, 90.7, 83.0, 57.8, 52.3, 38.1, 27.8.

FTIR (neat) ν_{max} : 3005, 2980, 2968, 2945, 1746, 1728, 1697, 1363, 1273, 1163, 1128, and 760 cm⁻¹.

HRMS (NSI) *m/z*: [M+H]⁺ calcd. for C₁₉H₂₈O₆N₂I, 507.0987; found, 507.0976.



methyl 3-(5-aminopyridin-2-yl)-2-(di(*tert*-butoxycarbonyl)amino)propanoate (9):

Following the general procedure, the reaction of 6-iodopyridin-3-amine (220 mg, 1.00 mmol, 1 equiv), methyl 2-(di(*tert*-butoxycarbonyl)amino)acrylate (603 mg, 2.00 mmol, 2 equiv), [Ir(ppy)₂(dtbbpy)]PF₆ (9.2 mg, 0.011 mmol, 0.01 equiv) and Hantzsch ester (379 mg, 1.50 mmol, 1.5 equiv) provided the product (280 mg, 71% yield) as an off-white solid after purification by flash column chromatography (50% – 100% ethyl acetate/hexanes).

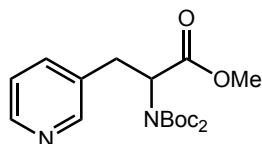
Mp: 80 – 82 °C

¹H NMR (500 MHz, CDCl₃) δ 7.95 (s, 1H), 6.82 (s, 2H), 5.33 (dd, *J* = 9.6, 5.1 Hz, 1H), 3.72 (s, 2H), 3.66 (s, 4H), 3.44 (dd, *J* = 14.2, 5.1 Hz, 1H), 3.14 (dd, *J* = 14.2, 9.6 Hz, 1H), 1.36 (s, 18H).

¹³C NMR (125 MHz, CDCl₃) δ 171.0, 151.5, 147.1, 141.0, 136.9, 123.8, 121.9, 82.8, 58.5, 52.1, 37.7, 27.8.

FTIR (neat) ν_{\max} : 3452, 3367, 2983, 2970, 2943, 1730, 1718, 1488, 1366, 1218, 1141, and 1115 cm^{-1} .

HRMS (NSI) m/z : $[\text{M}+\text{H}]^+$ calcd. for $\text{C}_{19}\text{H}_{30}\text{O}_6\text{N}_3$, 396.2129; found, 396.2113.



methyl 2-(di(*tert*-butoxycarbonyl)amino)-3-(pyridin-3-yl)propanoate (10):

Following the general procedure, the reaction of 3-iodopyridine (205 mg, 1.00 mmol, 1 equiv), methyl 2-(di(*tert*-butoxycarbonyl)amino)acrylate (609 mg, 2.02 mmol, 2 equiv), $[\text{Ir}(\text{ppy})_2(\text{dtbbpy})]\text{PF}_6$ (10.2 mg, 0.011 mmol, 0.01 equiv) and Hantzsch ester (379 mg, 1.50 mmol, 1.5 equiv) provided the product (279 mg, 73% yield) as a clear, colorless crystalline solid after purification by flash column chromatography (20% – 50% ethyl acetate/hexanes).

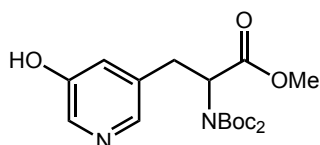
Mp: 76 – 78 $^{\circ}\text{C}$

^1H NMR (400 MHz, CDCl_3) δ 8.36 (dd, $J = 8.4, 3.5$ Hz, 2H), 7.44 (d, $J = 7.8$ Hz, 1H), 7.11 (dd, $J = 7.8, 4.8$ Hz, 1H), 5.06 (dd, $J = 10.3, 5.2$ Hz, 1H), 3.66 (s, 3H), 3.34 (dd, $J = 14.2, 5.2$ Hz, 1H), 3.15 (dd, $J = 14.3, 10.3$ Hz, 1H), 1.30 (s, 18H).

^{13}C NMR (100 MHz, CDCl_3) δ 170.3, 151.5, 150.7, 147.9, 136.9, 132.9, 123.1, 83.2, 58.6, 52.3, 33.3, 27.7.

FTIR (neat) ν_{\max} : 2975, 2951, 1793, 1739, 1392, 1368, 1138, 1112 1103, and 718 cm^{-1} .

HRMS (NSI) m/z : $[\text{M}+\text{H}]^+$ calcd. for $\text{C}_{19}\text{H}_{29}\text{O}_6\text{N}_2$, 381.2020; found, 381.2015.



methyl 2-(di(*tert*-butoxycarbonyl)amino)-3-(5-hydroxypyridin-3-yl)propanoate (11):

Following the general procedure, the reaction of 5-iodopyridin-3-ol (220 mg, 1.00 mmol, 1 equiv), methyl 2-(di(*tert*-butoxycarbonyl)amino)acrylate (610 mg, 2.03 mmol, 2 equiv), [Ir(ppy)₂(dtbbpy)]PF₆ (9.4 mg, 0.010 mmol, 0.01 equiv) and Hantzsch ester (371 mg, 1.47 mmol, 1.5 equiv) provided the product (265 mg, 67% yield) as an off-white solid oil after purification by flash column chromatography (50% – 100% ethyl acetate/hexanes).

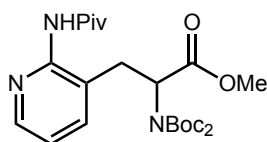
Mp: 112 – 116 °C

¹H NMR (300 MHz, CDCl₃) δ 8.10 (d, J = 2.6 Hz, 1H), 7.94 (d, J = 1.7 Hz, 1H), 7.12 (d, J = 2.2 Hz, 1H), 5.14 (dd, J = 10.2, 5.0 Hz, 1H), 3.74 (s, 3H), 3.41 (dd, J = 14.2, 5.0 Hz, 1H), 3.16 (dd, J = 14.2, 10.2 Hz, 1H), 1.38 (s, 18H).

¹³C NMR (75MHz, CDCl₃) δ 170.3, 154.8, 151.6, 140.2, 135.3, 134.9, 125.4, 83.6, 58.8, 52.4, 33.2, 27.7.

FTIR (neat) ν_{\max} : 2980, 2581, 1744, 1696, 1437, 1366, 1269, 1222, and 1166 cm⁻¹.

HRMS (NSI) m/z : [M+H]⁺ calcd. for C₁₉H₂₉O₇N₂, 397.1969; found, 397.1962.

**methyl 2-(di(*tert*-butoxycarbonyl)amino)-3-(2-pivalamidopyridin-3-yl)propanoate (12):**

Following the general procedure, the reaction of N-(3-iodopyridin-2-yl)pivalamide (302 mg, 0.99 mmol, 1 equiv), methyl 2-(di(*tert*-butoxycarbonyl)amino)acrylate (609 mg, 2.02 mmol, 2 equiv), [Ir(ppy)₂(dtbbpy)]PF₆ (9.9 mg, 0.010 mmol, 0.01 equiv) and Hantzsch ester (380 mg, 1.50 mmol, 1.5 equiv) provided the product (347 mg, 73% yield) as a white solid after purification by flash column chromatography (20% – 100% ethyl acetate/hexanes).

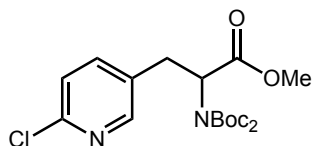
Mp: 104 – 107 °C

¹H NMR (300 MHz, CDCl₃) δ 8.56 (s, 1H), 8.30 (dd, *J* = 4.8, 1.8 Hz, 1H), 7.49 (dd, *J* = 7.6, 1.9 Hz, 1H), 7.05 (dd, *J* = 7.6, 4.8 Hz, 1H), 5.21 (dd, *J* = 8.5, 6.0 Hz, 1H), 3.66 (s, 3H), 3.46 (dd, *J* = 14.5, 6.0 Hz, 1H), 3.01 (dd, *J* = 14.5, 8.6 Hz, 1H), 1.34 (s, 18H), 1.29 (s, 9H).

¹³C NMR (75MHz, CDCl₃) δ 177.5, 170.7, 151.9, 149.9, 147.1, 140.0, 128.8, 121.7, 83.3, 57.7, 52.3, 39.3, 32.4, 27.8, 27.4.

FTIR (neat) ν_{\max} : 3160, 2970, 1749, 1738, 1697, 1437, 1365, and 1140 cm⁻¹.

HRMS (NSI) *m/z*: [M+H]⁺ calcd. for C₂₄H₃₈O₇N₃, 480.2704; found, 480.2694.



methyl 2-(di(*tert*-butoxycarbonyl)amino)-3-(6-chloropyridin-3-yl)propanoate (13):

Following the general procedure, the reaction of 2-chloro-5-iodopyridine (240 mg, 1.00 mmol, 1 equiv), methyl 2-(di(*tert*-butoxycarbonyl)amino)acrylate (610 mg, 2.03 mmol, 2 equiv), [Ir(ppy)₂(dtbbpy)]PF₆ (9.7 mg, 0.011 mmol, 0.01 equiv) and Hantzsch ester (379 mg, 1.50 mmol, 1.5 equiv) provided the product (318 mg, 77% yield) as a clear, colorless crystalline solid after purification by flash column chromatography (3% – 25% tetrahydrofuran/hexanes).

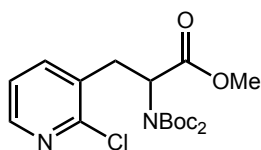
Mp: 87 – 90 °C

¹H NMR (300 MHz, CDCl₃) δ 8.18 (d, *J* = 1.9 Hz, 1H), 7.49 (dd, *J* = 8.2, 2.5 Hz, 1H), 7.22 (d, *J* = 7.8 Hz, 1H), 5.09 (dd, *J* = 10.0, 5.4 Hz, 1H), 3.73 (s, 3H), 3.38 (dd, *J* = 14.3, 5.4 Hz, 1H), 3.20 (dd, *J* = 14.2, 10.0 Hz, 1H), 1.39 (s, 18H).

¹³C NMR (75MHz, CDCl₃) δ 170.2, 151.7, 150.5, 149.8, 139.9, 132.0, 123.8, 83.5, 58.4, 52.4, 32.6, 27.8.

FTIR (neat) ν_{\max} : 3007, 1970, 1954, 2937, 2916, 2848, 1743, 1729, 1690, 1340, 1274, 1201, 1161, 1019, and 758 cm⁻¹.

HRMS (NSI) *m/z*: [M+H]⁺ calcd. for C₁₉H₂₈O₆N₂Cl, 415.1644; found, 415.1638.



methyl 2-(di(*tert*-butoxycarbonyl)amino)-3-(2-chloropyridin-3-yl)propanoate (14):

Following the general procedure, the reaction of 2-chloro-3-iodopyridine (239 mg, 1.00 mmol, 1 equiv), methyl 2-(di(*tert*-butoxycarbonyl)amino)acrylate (611 mg, 2.03 mmol, 2 equiv), [Ir(ppy)₂(dtbbpy)]PF₆ (10.2 mg, 0.011 mmol, 0.01 equiv) and Hantzsch ester (383 mg, 1.51 mmol, 1.5 equiv) provided the product (306 mg, 74% yield) as a white crystalline solid after purification by flash column chromatography (10% – 30% ethyl acetate/hexanes).

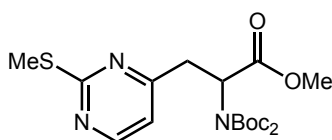
Mp: 71 – 74 °C

¹H NMR (300 MHz, CDCl₃) δ 8.23 – 8.18 (m, 1H), 7.45 (dd, *J* = 7.5, 1.9 Hz, 1H), 7.12 (dd, *J* = 7.5, 4.8 Hz, 1H), 5.24 (dd, *J* = 10.8, 4.3 Hz, 1H), 3.71 (s, 3H), 3.58 (dd, *J* = 14.2, 4.3 Hz, 1H), 3.26 (dd, *J* = 14.2, 10.8 Hz, 1H), 1.33 (s, 18H).

¹³C NMR (75MHz, CDCl₃) δ 170.2, 151.7, 151.2, 148.0, 140.4, 132.1, 122.5, 83.3, 56.9, 52.4, 33.7, 27.7.

FTIR (neat) ν_{\max} : 2980, 2952, 2936, 1794, 1745, 1696, 1367, 1137, 1126, and 748 cm⁻¹.

HRMS (NSI) *m/z*: [M+H]⁺ calcd. for C₁₉H₂₈O₆N₂Cl, 415.1630; found, 415.1623.



methyl 2-(di(*tert*-butoxycarbonyl)amino)-3-(2-(methylthio)pyrimidin-4-yl) propano-ate (15):

Following the general procedure, the reaction of 4-iodo-2-(methylthio)pyrimidine (249 mg, 0.99 mmol, 1 equiv), methyl 2-(di(*tert*-butoxycarbonyl)amino)acrylate (610 mg, 2.03 mmol, 2

equiv), [Ir(ppy)₂(dtbbpy)]PF₆ (9.4 mg, 0.010 mmol, 0.01 equiv) and Hantzsch ester (370 mg, 1.46 mmol, 1.5 equiv) provided the product (338 mg, 80% yield) as a white crystalline solid after purification by flash column chromatography (5% – 50% ethyl acetate/hexanes).

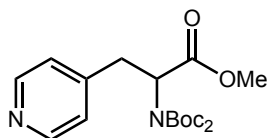
Mp: 71 – 75 °C

¹H NMR (400 MHz, CDCl₃) δ 8.32 (d, J = 5.0 Hz, 1H), 6.78 (d, J = 5.0 Hz, 1H), 5.46 (dd, J = 9.2, 5.4 Hz, 1H), 3.68 (s, 3H), 3.45 (dd, J = 14.2, 5.5 Hz, 1H), 3.19 (dd, J = 14.2, 9.2 Hz, 1H), 2.47 (s, 3H), 1.38 (s, 18H).

¹³C NMR (75 MHz, CDCl₃) δ 172.3, 170.4, 166.8, 156.9, 151.5, 116.2, 83.2, 57.0, 52.3, 37.9, 27.8, 13.9.

FTIR (neat) ν_{max} : 2983, 2940, 1948, 1703, 1565, 1550, 1451, 1296, 1162, 1136, and 778 cm⁻¹.

HRMS (NSI) m/z : [M+H]⁺ calcd. for C₁₇H₂₈O₆N₃S, 428.1850; found, 428.1841.



methyl 2-(di(*tert*-butoxycarbonyl)amino)-3-(pyridin-4-yl)propanoate (16):

Following the general procedure, the reaction of 4-iodopyridine (205 mg, 1.00 mmol, 1 equiv), methyl 2-(di(*tert*-butoxycarbonyl)amino)acrylate (609 mg, 2.02 mmol, 2 equiv), [Ir(ppy)₂(dtbbpy)]PF₆ (10.2 mg, 0.012 mmol, 0.01 equiv) and Hantzsch ester (376 mg, 1.50 mmol, 1.5 equiv) provided the product (129 mg, 34% yield) as a white crystalline solid after purification by flash column chromatography (10% – 80% ethyl acetate/hexanes).

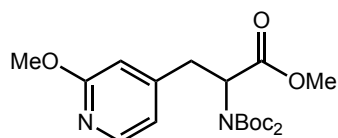
Mp: 97 – 100 °C

¹H NMR (500 MHz, CDCl₃) δ 8.49 – 8.41 (m, 2H), 7.10 (d, J = 5.7 Hz, 2H), 5.15 (dd, J = 10.1, 5.3 Hz, 1H), 3.72 (s, 3H), 3.40 (dd, J = 14.0, 5.3 Hz, 1H), 3.19 (dd, J = 14.0, 10.2 Hz, 1H), 1.37 (s, 18H).

^{13}C NMR (125 MHz, CDCl_3) δ 170.3, 151.6, 149.6, 146.7, 124.8, 83.3, 58.2, 52.4, 35.6, 27.8.

FTIR (neat) ν_{max} : 3005, 2970, 2948, 1748, 1736, 1690, 1366, 1228, 1217, and 1140 cm^{-1} .

HRMS (NSI) m/z : $[\text{M}+\text{H}]^+$ calcd. for $\text{C}_{19}\text{H}_{29}\text{O}_6\text{N}_2$, 381.2020; found, 381.2017.



methyl 2-(di(*tert*-butoxycarbonyl)amino)-3-(5-methoxypyridin-3-yl)propanoate (17):

Following the general procedure, the reaction of 4-bromo-2-methoxypyridine (195 mg, 1.04 mmol, 1 equiv), methyl 2-(di(*tert*-butoxycarbonyl)amino)acrylate (604 mg, 2.01 mmol, 2 equiv), $[\text{Ir}(\text{ppy})_2(\text{dtbbpy})]\text{PF}_6$ (9.2 mg, 0.010 mmol, 0.01 equiv) and Hantzsch ester (385 mg, 1.52 mmol, 1.5 equiv) provided the product (280 mg, 66% yield) as a white crystalline solid after purification by flash column chromatography (5% – 50% ethyl acetate/hexanes).

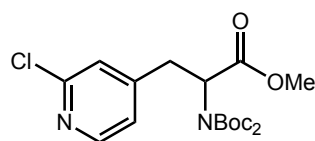
Mp: 69 – 72 $^{\circ}\text{C}$

^1H NMR (300 MHz, CDCl_3) δ 8.00 (dd, $J = 5.3, 0.7$ Hz, 1H), 6.67 (dd, $J = 5.3, 1.5$ Hz, 1H), 6.52 (dd, $J = 1.5, 0.7$ Hz, 1H), 5.12 (dd, $J = 10.2, 5.1$ Hz, 1H), 3.84 (s, 3H), 3.70 (s, 3H), 3.32 (dd, $J = 13.9, 5.1$ Hz, 1H), 3.12 (dd, $J = 13.9, 10.2$ Hz, 1H), 1.36 (s, 18H).

^{13}C NMR (75MHz, CDCl_3) δ 170.3, 164.3, 151.6, 149.3, 146.6, 118.1, 111.5, 83.2, 58.2, 53.2, 52.3, 35.4, 27.7.

FTIR (neat) ν_{max} : 2979, 2950, 1745, 1697, 1613, 1561, 1380, 1270, 1244, 1136, 1112, and 774 cm^{-1} .

HRMS (NSI) m/z : $[\text{M}+\text{H}]^+$ calcd. for $\text{C}_{20}\text{H}_{31}\text{O}_7\text{N}_2$, 411.2126; found, 411.2118.



methyl 2-(di(*tert*-butoxycarbonyl)amino)-3-(2-chloropyridin-4-yl)propanoate (18):

Following the general procedure, the reaction of 2-chloro-4-iodopyridine (244 mg, 1.02 mmol, 1 equiv), methyl 2-(di(*tert*-butoxycarbonyl)amino)acrylate (610 mg, 2.03 mmol, 2 equiv), [Ir(ppy)₂(dtbbpy)]PF₆ (9.2 mg, 0.010 mmol, 0.01 equiv) and Hantzsch ester (390 mg, 1.54 mmol, 1.5 equiv) provided the product (352 mg, 83% yield) as a white crystalline solid after purification by flash column chromatography (10% – 30% ethyl acetate/hexanes).

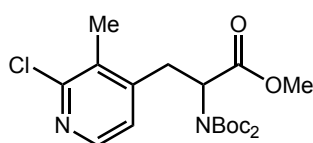
Mp: 104 – 108 °C

¹H NMR (400 MHz, CDCl₃) δ 8.23 (d, *J* = 5.1 Hz, 1H), 7.13 (s, 1H), 7.04 (dd, *J* = 5.1, 1.5 Hz, 1H), 5.12 (dd, *J* = 10.0, 5.4 Hz, 1H), 3.71 (s, 3H), 3.38 (dd, *J* = 14.0, 5.4 Hz, 1H), 3.18 (dd, *J* = 14.0, 10.0 Hz, 1H), 1.38 (s, 18H).

¹³C NMR (75MHz, CDCl₃) δ 170.0, 151.7, 151.4, 150.1, 149.4, 125.2, 123.6, 83.5, 57.9, 52.5, 35.3, 27.8.

FTIR (neat) ν_{\max} : 3054, 3001, 2982, 2972, 1743, 1727, 1692, 1596, 1375, 1275, 1139, 1128, and 1010 cm⁻¹.

HRMS (NSI) *m/z*: [M+H]⁺ calcd. for C₁₉H₂₈O₆N₂Cl, 415.1630; found, 415.1626.

**methyl 2-(di(*tert*-butoxycarbonyl)amino)-3-(2-chloro-3-methylpyridin-4-yl) propanoate (19):**

Following the general procedure, the reaction of 2-chloro-4-iodo-3-methylpyridine (250 mg, 0.99 mmol, 1 equiv), methyl 2-(di(*tert*-butoxycarbonyl)amino)acrylate (600 mg, 1.99 mmol, 2 equiv), [Ir(ppy)₂(dtbbpy)]PF₆ (9.0 mg, 0.010 mmol, 0.01 equiv) and Hantzsch ester (381 mg, 1.51 mmol, 1.5 equiv) provided the product (330 mg, 78% yield) as a white crystalline solid after purification by flash column chromatography (0% – 30% tetrahydrofuran/hexanes).

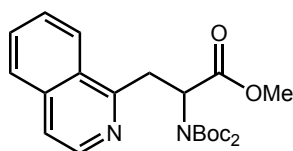
Mp: 83 – 86 °C

¹H NMR (300 MHz, CDCl₃) δ 8.05 (dd, *J* = 4.9, 0.7 Hz, 1H), 6.93 (d, *J* = 4.9 Hz, 1H), 5.10 (dd, *J* = 10.7, 4.7 Hz, 1H), 3.71 (s, 3H), 3.43 (dd, *J* = 14.1, 4.7 Hz, 1H), 3.28 (dd, *J* = 14.1, 10.7 Hz, 1H), 2.33 (s, 3H), 1.33 (s, 18H).

¹³C NMR (75MHz, CDCl₃) δ 170.0, 152.3, 151.6, 147.9, 146.1, 131.6, 124.7, 83.4, 57.4, 52.5, 33.7, 27.7, 15.6.

FTIR (neat) ν_{max} : 2996, 2980, 2955, 2936, 1752, 1741, 1706, 1365, 1249, 1136, 1113, and 1015 cm⁻¹.

HRMS (NSI) *m/z*: [M+H]⁺ calcd. for C₂₀H₃₀O₆N₂Cl, 429.1787; found, 429.1779.



methyl 2-(di(*tert*-butoxycarbonyl)amino)-3-(isoquinolin-1-yl)propanoate (20):

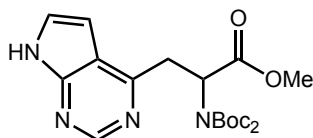
Following the general procedure, the reaction of 1-iodoisoquinoline (260 mg, 1.02 mmol, 1 equiv), methyl 2-(di(*tert*-butoxycarbonyl)amino)acrylate (610 mg, 2.03 mmol, 2 equiv), [Ir(ppy)₂(dtbbpy)]PF₆ (9.4 mg, 0.010 mmol, 0.01 equiv) and Hantzsch ester (371 mg, 1.47 mmol, 1.5 equiv) provided the product (381 mg, 87% yield) as a colorless oil after purification by flash column chromatography (1% – 10% tetrahydrofuran/dichloromethane).

¹H NMR (300 MHz, CDCl₃) δ 8.43 (d, *J* = 5.7 Hz, 1H), 8.14 (d, *J* = 8.4 Hz, 1H), 7.79 (d, *J* = 8.5 Hz, 1H), 7.71 – 7.62 (m, 1H), 7.57 (ddd, *J* = 8.3, 6.9, 1.3 Hz, 1H), 7.51 (d, *J* = 5.7 Hz, 1H), 5.77 (dd, *J* = 9.1, 4.7 Hz, 1H), 4.15 (dd, *J* = 15.1, 4.7 Hz, 1H), 3.93 (dd, *J* = 15.1, 9.1 Hz, 1H), 3.76 (s, 3H), 1.34 (s, 18H).

¹³C NMR (75MHz, CDCl₃) δ 171.0, 158.1, 151.7, 141.9, 136.1, 129.8, 127.5, 127.2, 127.1, 124.9, 119.4, 82.8, 58.2, 52.3, 35.1, 27.8.

FTIR (neat) ν_{\max} : 2978, 1793, 1741, 1696, 1366, 1381, 1273, 1251, 1226, 1135, 1109, and 764 cm^{-1} .

HRMS (NSI) m/z : $[\text{M}+\text{H}]^+$ calcd. for $\text{C}_{23}\text{H}_{31}\text{O}_6\text{N}_2$, 431.2177; found, 431.2168.



methyl 2-(di(*tert*-butoxycarbonyl)amino)-3-(7H-pyrrolo[2,3-d]pyrimidin-4-yl) propanoate (21):

Following the general procedure, the reaction of 4-bromo-7H-pyrrolo[2,3-d]pyrimidine (199 mg, 1.01 mmol, 1 equiv), methyl 2-(di(*tert*-butoxycarbonyl)amino)acrylate (611 mg, 2.03 mmol, 2 equiv), $[\text{Ir}(\text{ppy})_2(\text{dtbbpy})]\text{PF}_6$ (9.0 mg, 0.010 mmol, 0.01 equiv) and Hantzsch ester (381 mg, 1.51 mmol, 1.5 equiv) provided the product (401 mg, 95% yield) as an off-white crystalline solid after purification by flash column chromatography (5% – 50% ethyl acetate/hexanes).

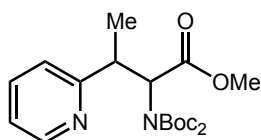
Mp: 112 – 114 °C

^1H NMR (300 MHz, CDCl_3) δ 11.84 (s, 1H), 8.82 (s, 1H), 7.35 (dd, $J = 3.6, 2.2$ Hz, 1H), 6.56 (dd, $J = 3.6, 1.8$ Hz, 1H), 5.72 (dd, $J = 9.0, 5.1$ Hz, 1H), 3.88 (dd, $J = 14.4, 5.2$ Hz, 1H), 3.72 (s, 3H), 3.67 (dd, $J = 14.4, 9.0$ Hz, 1H), 1.35 (s, 18H).

^{13}C NMR (75MHz, CDCl_3) δ 170.7, 159.1, 151.6, 151.4, 150.7, 125.5, 118.4, 99.5, 83.1, 57.5, 52.4, 36.0, 27.8.

FTIR (neat) ν_{\max} : 3127, 3002, 2974, 2852, 1745, 1691, 1583, 1379, 1346, 1142, 1119, 971, and 748 cm^{-1} .

HRMS (NSI) m/z : $[\text{M}+\text{H}]^+$ calcd. for $\text{C}_{20}\text{H}_{29}\text{O}_6\text{N}_4$, 421.2082; found, 421.2073.



methyl 2-(di(tert-butoxycarbonyl)amino)-3-(pyridin-2-yl)butanoate (22):

Following the general procedure, the reaction of 2-bromopyridine (161 mg, 1.02 mmol, 1 equiv), methyl-2-(di(tert-butoxycarbonyl)amino)but-2-enoate (638 mg, 2.02 mmol, 2 equiv), [Ir(ppy)₂(dtbbpy)]PF₆ (9.4 mg, 0.010 mmol, 0.01 equiv) and Hantzsch ester (329 mg, 1.30 mmol, 1.3 equiv) provided an inseparable 3:1 mixture of diastereomers (261 mg, 66% yield) as a white crystalline solid after purification by flash column chromatography (10% – 60% ethyl acetate/hexanes).

For the mixture of diastereomers:

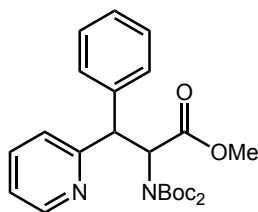
Mp: 84 – 88 °C

¹H NMR (600 MHz, CDCl₃) δ 8.56 – 8.49 (m, 1H_{dr1} + 1H_{dr2}), 7.60 (td, *J* = 7.6, 1.9 Hz, 1H_{dr1}), 7.55 (td, *J* = 7.6, 1.9 Hz, 1H_{dr2}), 7.25 (d, *J* = 7.9 Hz, 1H_{dr1}), 7.12 (d, *J* = 7.8 Hz, 1H_{dr2}), 7.09 (m, 1H_{dr1}+1H_{dr2}), 5.95 (d, *J* = 9.8 Hz, 1H_{dr1}), 5.17 (d, *J* = 9.7 Hz, 1H_{dr2}), 3.87 (dq, *J* = 9.7, 6.7 Hz, 1H_{dr2}), 3.76 (m, 1H_{dr1} + 3H_{dr2}), 3.58 (s, 3H_{dr1}), 1.58 (d, *J* = 7.2, 1H_{dr2}) 1.56 (s, 18H_{dr1}), 1.42 (s, 18H_{dr2}), 1.18 (d, *J* = 7.2 Hz, 3H_{dr1}).

¹³C NMR (150 MHz, CDCl₃) δ 171.0, 171.0, 164.2, 162.6, 152.3, 151.7, 149.3, 149.0, 136.1, 135.9, 123.2, 123.1, 121.3, 121.1, 83.1, 82.6, 62.1, 61.1, 52.1, 42.7, 28.0, 27.9, 20.2, 18.5

FTIR (neat) ν_{max}: 2979, 2936, 1793, 1745, 1699, 1523, 1365, 1143, 1122, 1104, 845, 758, and 749 cm⁻¹.

HRMS (NSI) *m/z*: [M+H]⁺ calcd. for C₂₀H₃₁O₆N₂, 395.2177; found, 395.2170.



methyl 2-(di(tert-butoxycarbonyl)amino)-3-phenyl-3-(pyridin-2-yl)propanoate (23):

Following the general procedure, the reaction of 2-bromopyridine (158 mg, 1.00 mmol, 1 equiv), methyl 2-(di(tert-butoxycarbonyl)amino)-3-phenylacrylate (750 mg, 2.00 mmol, 2 equiv), [Ir(ppy)₂(dtbbpy)]PF₆ (10.0 mg, 0.011 mmol, 0.01 equiv) and Hantzsch ester (340 mg, 1.34 mmol, 1.3 equiv) provided an inseparable 4:1 mixture of diastereomers (246 mg, 54% yield) as a colorless oil after purification by flash column chromatography (10% – 60% ethyl acetate/hexanes).

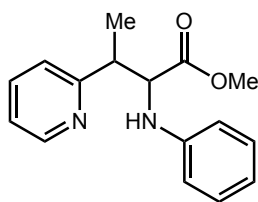
For the mixture of diastereomers:

¹H NMR (600 MHz, C₆D₆) δ 8.44 (ddd, *J* = 4.9, 1.9, 0.9 Hz, 1H_{dr1}), 8.40 (ddd, *J* = 4.8, 1.9, 0.9 Hz, 1H_{dr2}), 7.88 – 7.82 (m, 2H_{dr2}), 7.60 (d, *J* = 6.9 Hz, 2H_{dr1}), 7.27 (d, *J* = 10.2 Hz, 1H_{dr1}), 7.13 (t, *J* = 7.7 Hz, 2H_{dr2}), 7.10 (d, *J* = 7.9 Hz, 1H_{dr2}), 7.07 (t, *J* = 7.7 Hz, 2H_{dr1}), 7.01 (d, *J* = 8.1, 1H_{dr1}), 6.99 – 6.93 (m, 2H_{dr1} + 2H_{dr2}), 6.54 (ddd, *J* = 7.3, 4.9, 1.3 Hz, 1H_{dr1}), 6.50 (ddd, *J* = 7.5, 4.8, 1.2 Hz, 1H_{dr2}), 6.42 (d, *J* = 10.2 Hz, 1H_{dr2}), 5.46 (d, *J* = 10.3 Hz, 1H_{dr2}), 5.35 (d, *J* = 10.2 Hz, 1H_{dr1}), 3.19 (s, 3H_{dr1}), 3.17 (s, 3H_{dr2}), 1.38 (s, 18H_{dr2}), 1.34 (s, 18H_{dr1}).

¹³C NMR (150 MHz, C₆D₆) δ 170.4, 170.1, 161.9, 161.2, 152.4, 152.1, 149.0, 148.5, 142.3, 140.5, 135.8, 135.5, 129.3, 129.0, 128.2, 128.0, 126.6, 126.5, 124.2, 123.7, 120.9, 120.8, 81.7, 81.7, 61.7, 60.1, 54.8, 53.7, 51.2, 27.6, 27.6.

FTIR (neat) ν_{\max} : 2970, 2941, 1753, 1736, 1719, 1367, 1227, 1139, 1108, 770, and 755 cm⁻¹.

HRMS (NSI) *m/z*: [M+H]⁺ calcd. for C₂₅H₃₃O₆N₂, 457.2333; found, 457.2325.



methyl 2-(phenylamino)-3-(pyridin-2-yl)butanoate (24):

Following the general procedure, the reaction of 2-bromopyridine (158 mg, 1.00 mmol, 1.0 equiv), methyl 2-(phenylamino)but-2-enoate (380 mg, 2.00 mmol, 2.0 equiv), [Ir(ppy)₂(dtbbpy)]PF₆ (10.0 mg, 0.011 mmol, 0.01 equiv) and Hantzsch ester (325 mg, 1.28 mmol, 1.30 equiv) provided an inseparable 5:4 mixture of diastereomers (186 mg, 69% yield) as a yellow crystalline solid after purification by flash column chromatography (5% – 50% ethyl acetate/hexanes).

For the mixture of diastereomers:

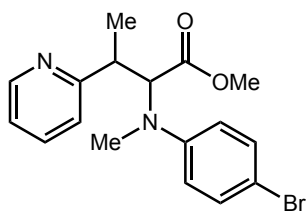
Mp: 62 – 64 °C

¹H NMR (500 MHz, CDCl₃) δ 8.64 – 8.54 (m, 1H_{dr1} + 1H_{dr2}), 7.65 – 7.52 (m, 1H_{dr1} + 1H_{dr2}), 7.23 – 7.07 (m, 4H_{dr1} + 4H_{dr2}), 6.70 (m, 1H_{dr1} + 1H_{dr2}), 6.63 (d, *J* = 7.6 Hz, 2H_{dr1}), 6.58 – 6.51 (d, *J* = 8.0 Hz, 2H_{dr2}), 4.97 (d, *J* = 8.9 Hz, 1H_{dr1}), 4.61 (d, *J* = 8.3 Hz, 1H_{dr2}), 4.42 (m, 1H_{dr1} + 1H_{dr2}), 3.62 (s, 3H_{dr1}), 3.59 (s, 3H_{dr2}), 3.53 – 3.40 (m, 1H_{dr1} + 1H_{dr2}), 1.49 (d, *J* = 7.1 Hz, 3H_{dr2}), 1.44 (d, *J* = 7.0 Hz, 3H_{dr1}).

¹³C NMR (125 MHz, CDCl₃) δ 173.8, 173.5, 161.7, 161.6, 149.2, 149.1, 147.2, 147.1, 136.5, 136.5, 129.2, 129.1, 122.4, 122.3, 121.9, 118.2, 117.8, 113.6, 113.2, 61.9, 61.7, 51.9, 51.8, 44.3, 43.7, 17.4, 15.4.

FTIR (neat) ν_{max} : 3373, 3053, 2969, 2950, 1732, 1601, 1590, 1507, 1149, 908, 729, and 691 cm⁻¹.

HRMS (NSI) *m/z*: [M+H]⁺ calcd. for C₁₆H₁₉O₂N₂, 271.1441; found, 271.1439



methyl 2-((4-bromophenyl)(methyl)amino)-3-(pyridin-2-yl)butanoate (25):

Following the general procedure, the reaction of 2-bromopyridine (160 mg, 1.01 mmol, 1 equiv), methyl 2-((4-bromophenyl)(methyl)amino)but-2-enoate (570 mg, 2.01 mmol, 2 equiv), [Ir(ppy)₂(dtbbpy)]PF₆ (9.1 mg, 0.010 mmol, 0.01 equiv) and Hantzsch ester (325 mg, 1.28 mmol, 1.3 equiv) provided an inseparable 4:3 mixture of diastereomers (311 mg, 86% yield) as a colorless oil after purification by flash column chromatography (10% – 50% ethyl acetate/hexanes).

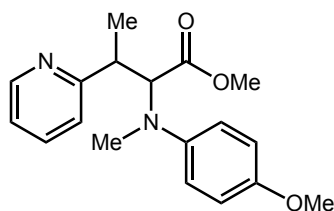
For the mixture of diastereomers:

¹H NMR (500 MHz, CDCl₃) 8.56 – 8.52 (m, 1H_{dr1}), 8.44 (m, 1H_{dr2}), 7.60 (td, *J* = 7.7, 1.8 Hz, 1H_{dr1}), 7.49 (td, *J* = 7.6, 1.8 Hz, 1H_{dr2}), 7.40 – 7.29 (m, 2H_{dr1}), 7.23 (d, *J* = 7.8 Hz, 1H_{dr1}), 7.18 (d, *J* = 9.0 Hz, 2H_{dr2}), 7.12 (ddd, *J* = 7.5, 4.9, 1.2 Hz, 1H_{dr1}), 7.06 (d, *J* = 7.8 Hz, 1H_{dr2}), 7.03 (ddd, *J* = 7.5, 4.8, 1.2 Hz, 1H_{dr2}), 6.85 (d, *J* = 9.1 Hz, 2H_{dr1}), 6.59 (d, *J* = 9.0 Hz, 2H_{dr2}), 4.98 (d, *J* = 10.8 Hz, 1H_{dr1}), 4.78 (d, *J* = 11.0 Hz, 1H_{dr2}), 3.72 (s, 3H_{dr2}), 3.67 – 3.57 (m, 1H_{dr1} + 1H_{dr2}), 3.46 (s, 3H_{dr1}), 2.93 (s, 3H_{dr1}), 2.72 (s, 3H_{dr2}), 1.32 (d, *J* = 6.7 Hz, 3H_{dr2}), 1.21 (d, *J* = 7.0 Hz, 3H_{dr1}).

¹³C NMR (125 MHz, CDCl₃) δ 171.4, 171.4, 162.7, 161.9, 149.3, 149.2, 148.8, 136.4, 136.2, 131.8, 131.4, 123.4, 122.4, 121.7, 121.6, 115.4, 115.0, 109.6, 109.5, 66.7, 65.5, 51.7, 51.5, 41.7, 41.6, 33.1, 32.7, 18.5, 18.2.

FTIR (neat) ν_{max} : 2990, 2948, 2904, 2817, 1718, 1648, 1490, 1434, 1252, 1202, 1120, 1108, 1042, 811, 776, and 766 cm⁻¹.

HRMS (NSI) *m/z*: [M+H]⁺ calcd. for C₁₇H₂₀O₂N₂Br, 363.0703; found, 363.0707.



methyl 2-((4-methoxyphenyl)(methyl)amino)-3-(pyridin-2-yl)butanoate (26):

Following the general procedure, the reaction of 2-bromopyridine (159 mg, 1.00 mmol, 1 equiv), methyl 2-((4-methoxyphenyl)(methyl)amino)but-2-enoate (477 mg, 2.03 mmol, 2 equiv), [Ir(ppy)₂(dtbbpy)]PF₆ (10.1 mg, 0.011 mmol, 0.01 equiv) and Hantzsch ester (335 mg, 1.32 mmol, 1.3 equiv) provided an inseparable 3:1 mixture of diastereomers (182mg, 58% yield) as a colorless oil after purification by flash column chromatography (5% – 40% ethyl acetate/hexanes).

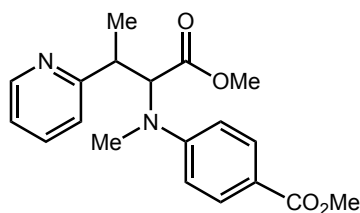
For the mixture of diastereomers:

¹H NMR (600 MHz, CDCl₃) δ 8.53 (ddd, *J* = 4.9, 1.9, 0.9 Hz, 1H_{dr2}), 8.49 (ddd, *J* = 4.9, 1.9, 0.9 Hz, 1H_{dr1}), 7.59 (td, *J* = 7.7, 1.9 Hz, 1H_{dr2}), 7.50 (td, *J* = 7.6, 1.8 Hz, 1H_{dr1}), 7.22 (dt, *J* = 7.8, 1.1 Hz, 1H_{dr2}), 7.13 – 7.07 (m, 1H_{dr1} + 1H_{dr2}), 7.04 (ddd, *J* = 7.6, 4.8, 1.1 Hz, 1H_{dr1}), 6.98 – 6.92 (m, 2H_{dr2}), 6.87 – 6.83 (m, 2H_{dr2}), 6.75 – 6.65 (m, 4H_{dr1}), 4.85 (d, *J* = 11.0 Hz, 1H_{dr2}), 4.68 (d, *J* = 11.1 Hz, 1H_{dr1}), 3.77 (s, 3H_{dr2}), 3.64 – 3.55 (m, 1H_{dr1} + 1H_{dr2}), 3.43 (s, 3H_{dr2}), 2.91 (s, 3H_{dr2}), 2.71 (s, 3H_{dr1}), 1.31 (d, *J* = 6.7 Hz, 3H_{dr1}), 1.27 (d, *J* = 7.0 Hz, 3H_{dr2}).

¹³C NMR (150 MHz, CDCl₃) δ 174.2, 174.1, 171.7, 163.1, 162.5, 152.4, 152.2, 149.2, 149.1, 144.9, 144.6, 136.3, 136.1, 123.4, 122.6, 121.5, 121.5, 116.2, 115.5, 114.6, 114.1, 83.3, 82.7, 68.5, 67.0, 55.6, 55.5, 52.9, 52.8, 51.4, 51.2, 41.6, 41.6, 33.3, 33.1, 25.7, 25.6, 18.4, 18.3, 8.0, 7.8.

FTIR (neat) ν_{max}: 3043, 2949, 2832, 1730, 1589, 1509, 1242, 1165, 1034, 991, 817, 786, and 749 cm⁻¹.

HRMS (NSI) *m/z*: [M+H]⁺ calcd. for C₁₈H₂₃O₃N₂, 315.1703; found, 315.1703.



methyl 4-((1-methoxy-1-oxo-3-(pyridin-2-yl)butan-2-yl)(methyl)amino)benzoate (27):

Following the general procedure, the reaction of 2-bromopyridine (158mg, 1.00 mmol, 1 equiv), methyl 4-((1-methoxy-1-oxobut-2-en-2-yl)(methyl)amino)benzoate (530 mg, 2.02 mmol, 2 equiv), [Ir(ppy)₂(dtbbpy)]PF₆ (9.1 mg, 0.010 mmol, 0.01 equiv) and Hantzsch ester (340 mg, 1.34 mmol, 1.3 equiv) provided an inseparable 5:2 mixture of diastereomers (267 mg, 78% yield) as a low-melting white solid after purification by flash column chromatography (5% – 50% ethyl acetate/hexanes).

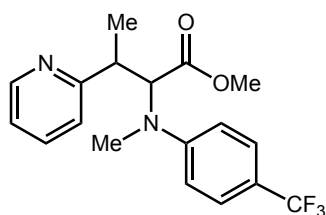
For the mixture of diastereomers:

¹H NMR (600 MHz, CDCl₃) δ 8.56 (ddd, *J* = 4.9, 1.8, 0.9 Hz, 1H_{dr1}), 8.40 (ddd, *J* = 4.9, 1.8, 0.9 Hz, 1H_{dr2}), 7.99 – 7.91 (m, 2H_{dr1}), 7.82 – 7.77 (m, 1H_{dr2}), 7.62 (td, *J* = 7.6, 1.8 Hz, 1H_{dr1}), 7.47 (td, *J* = 7.7, 1.8 Hz, 1H_{dr2}), 7.25 (d, *J* = 7.5 Hz, 1H_{dr1}), 7.14 (ddd, *J* = 7.6, 4.8, 1.1 Hz, 1H_{dr1}), 7.05 (dd, *J* = 7.7, 1.1 Hz, 1H_{dr1}), 7.00 (ddd, *J* = 7.6, 4.8, 1.1 Hz, 1H_{dr2}), 6.96 (d, *J* = 9.0 Hz, 2H_{dr1}), 6.69 (d, *J* = 9.0 Hz, 2H_{dr2}), 5.20 (d, *J* = 10.7 Hz, 1H_{dr1}), 4.96 (d, *J* = 10.9 Hz, 1H_{dr2}), 3.87 (s, 3H_{dr1}), 3.83 (s, 3H_{dr2}), 3.75 (s, 3H_{dr2}), 3.71 – 3.61 (m, 1H_{dr1} + 1H_{dr2}), 3.49 (s, 3H_{dr1}), 3.04 (s, 3H_{dr1}), 2.83 (s, 3H_{dr2}), 1.36 (d, *J* = 6.7 Hz, 3H_{dr2}), 1.19 (s, 3H_{dr1}).

¹³C NMR (150 MHz, CDCl₃) δ 171.3, 171.2, 167.2, 162.5, 161.5, 153.4, 152.9, 149.3, 149.2, 136.5, 136.3, 131.3, 130.9, 123.4, 122.3, 121.8, 121.7, 118.5, 118.4, 112.0, 111.9, 65.6, 64.7, 51.9, 51.7, 51.5, 51.5, 41.9, 41.7, 33.2, 32.9, 18.5, 18.1.

FTIR (neat) ν_{\max} : 2949, 2839, 1735, 1705, 1602, 1518, 1433, 1276, 1186, 1110, 769, and 747 cm⁻¹.

HRMS (NSI) *m/z*: [M+H]⁺ calcd. for C₁₉H₂₃O₄N₂, 343.1652; found, 343.1651.



methyl 2-(methyl(4-(trifluoromethyl)phenyl)amino)-3-(pyridin-2-yl)butanoate (28):

Following the general procedure, the reaction of 2-bromopyridine (158 mg, 1.00 mmol, 1 equiv), methyl 2-(methyl(4-(trifluoromethyl)phenyl)amino)but-2-enoate (551 mg, 2.02 mmol, 2 equiv), [Ir(ppy)₂(dtbbpy)]PF₆ (9.0 mg, 0.010 mmol, 0.01 equiv) and Hantzsch ester (329 mg, 1.30 mmol, 1.3 equiv) provided an inseparable 5:2 mixture of diastereomers (274 mg, 78% yield) as a colorless oil after purification by flash column chromatography (0% – 25% ethyl acetate/hexanes).

For the mixture of diastereomers:

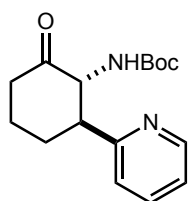
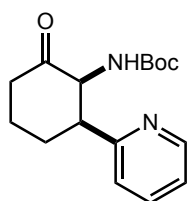
¹H NMR (600 MHz, CDCl₃) 8.55 (dd, *J* = 5.0, 1.7 Hz, 1H_{dr1}), 8.41 (dd, *J* = 4.9, 1.7 Hz, 1H_{dr2}), 7.62 (td, *J* = 7.6, 1.8 Hz, 1H_{dr1}), 7.50 (d, *J* = 8.6 Hz, 2H_{dr1} + 1H_{dr2}), 7.34 (d, *J* = 8.6 Hz, 2H_{dr2}), 7.27 – 7.22 (m, 1H_{dr1}), 7.16 – 7.12 (m, 1H_{dr2}), 7.01 (m, 2H_{dr1} + 1H_{dr2}), 6.74 (d, *J* = 8.6 Hz, 2H_{dr2}), 5.15 (d, *J* = 10.8 Hz, 1H_{dr1}), 4.92 (d, *J* = 11.0 Hz, 1H_{dr2}), 3.75 (s, 3H_{dr2}), 3.64 (dq, *J* = 10.5, 7.2 Hz, 1H_{dr1} + 1H_{dr2}), 3.49 (s, 3H_{dr1}), 3.02 (s, 3H_{dr1}), 2.80 (s, 3H_{dr2}), 1.35 (d, *J* = 6.7 Hz, 3H_{dr2}), 1.20 (d, *J* = 7.0 Hz, 3H_{dr1}).

¹³C NMR (150 MHz, CDCl₃) δ 171.3, 171.3, 162.5, 161.6, 152.3, 151.9, 149.3, 136.5, 136.3, 126.5 (q, *J* = 3.7 Hz), 126.0 (q, *J* = 3.7 Hz), 124.9 (q, *J* = 268.6), 124.9 (q, *J* = 268.7), 123.4, 122.4, 121.8, 118.9 (q, *J* = 32), 118.8 (q, *J* = 33), 112.5, 112.3, 65.9, 64.9, 51.9, 51.7, 41.8, 33.2, 32.8, 18.5, 18.2.

¹⁹F NMR (282 MHz, CDCl₃) δ -61.01.

FTIR (neat) ν_{max}: 2971, 2953, 2830, 1735, 1614, 1526, 1454, 1326, 1296, 1163, 1104, 1069, and 819 cm⁻¹.

HRMS (NSI) m/z : $[M+H]^+$ calcd. for $C_{18}H_{20}O_2N_2F_3$, 353.1471; found, 353.1480.

Major (\pm)Minor (\pm)

tert-butyl (2-oxo-6-(pyridin-2-yl)cyclohexyl)carbamate (29): Following the general procedure, 2-bromopyridine (160 mg, 1.01 mmol, 1 equiv) was reacted with tert-butyl (6-oxocyclohex-1-en-1-yl)carbamate (421 mg, 2.00 mmol, 2 equiv), $[Ir(ppy)_2(dtbbpy)]PF_6$ (9.0 mg, 0.010 mmol, 0.01 equiv) and Hantzsch ester (331 mg, 1.31 mmol, 1.3 equiv). Analysis of the crude 1H NMR spectrum indicated a mixture of stereoisomers (cis:trans = 2:9), and purification by flash column chromatography (5% – 100% ethyl acetate/hexanes) provided the title compounds (trans, 170 mg, 59% yield; cis, 52 mg, 18% yield).

Major isomer (trans):

R_f: 0.3 (50% ethyl acetate/hexanes)

Mp: 181 – 185 °C

1H NMR (300 MHz, $CDCl_3$) δ 8.67 – 8.31 (m, 1H), 7.59 (td, $J = 7.7, 1.8$ Hz, 1H), 7.20 (d, $J = 7.9$ Hz, 1H), 7.12 (ddd, $J = 7.5, 4.8, 1.1$ Hz, 1H), 5.00 (s, 1H), 4.69 – 4.51 (m, 1H), 2.97 – 2.83 (m, 1H), 2.63 – 2.43 (m, 2H), 2.32 – 1.89 (m, 3H), 1.74 (dddd, $J = 16.9, 9.9, 8.6, 4.1$ Hz, 1H), 1.21 (s, 9H).

^{13}C NMR (75 MHz, $CDCl_3$) δ 207.1, 160.2, 155.1, 149.2, 136.3, 122.3, 121.9, 79.3, 62.5, 54.6, 41.0, 31.5, 28.0, 26.1.

FTIR (neat) ν_{max} : 3206, 3025, 2978, 2935, 2864, 1737, 1714, 1686, 1555, 169, 1014, 785, and 735 cm^{-1} .

HRMS (NSI) m/z : $[M+H]^+$ calcd. for $C_{116}H_{23}O_3N_2$, 291.1703; found, 291.1699.

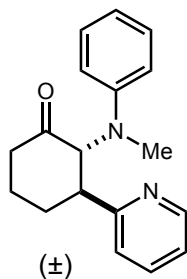
Minor isomer (cis):**R_f**: 0.7 (50% ethyl acetate/hexanes)**Mp**: 92 – 95 °C

¹H NMR (300 MHz, CDCl₃) δ 8.52 – 8.22 (m, 1H), 7.58 (td, *J* = 7.7, 1.9 Hz, 1H), 7.09 (dtd, *J* = 7.5, 5.2, 1.1 Hz, 2H), 5.48 (d, *J* = 7.3 Hz, 1H), 4.44 (ddd, *J* = 7.2, 5.7, 1.2 Hz, 1H), 3.98 (dt, *J* = 5.9, 3.9 Hz, 1H), 2.74 – 2.50 (m, 1H), 2.46 – 2.12 (m, 2H), 2.09 – 1.88 (m, 1H), 1.73 (dq, *J* = 11.2, 3.3 Hz, 2H), 1.34 (s, 9H).

¹³C NMR (75 MHz, CDCl₃) δ 206.0, 160.80, 155.7, 148.2, 136.5, 123.3, 121.5, 79.3, 60.0, 48.7, 40.2, 30.7, 28.2, 20.8.

FTIR (neat) ν_{max} : 3448, 3005, 2969, 2944, 1737, 1719, 1694, 1494, 1365, 1352, 1229, and 770 cm⁻¹.

HRMS (NSI) *m/z*: [M+H]⁺ calcd. for C₁₆H₂₃O₃N₂, 291.1703; found, 291.1698.



2-(methyl(phenyl)amino)-3-(pyridin-2-yl)cyclohexan-1-one (30): Following the general procedure, the reaction of 2-bromopyridine (160 mg, 1.01 mmol, 1 equiv), 2-(methyl(phenyl)amino)cyclohex-2-en-1-one (401 mg, 2.00 mmol, 2 equiv), [Ir(ppy)₂(dtbbpy)]PF₆ (9.5 mg, 0.010 mmol, 0.01 equiv) and Hantzsch ester (330 mg, 1.30 mmol, 1.3 equiv) provided the product (196 mg, 70% yield) as a white solid after purification by flash column chromatography (10% – 80% ethyl acetate/hexanes).

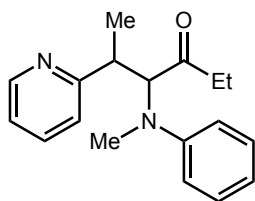
Mp: 111 – 115 °C

¹H NMR (300 MHz, CDCl₃) δ 8.52 – 8.37 (m, 1H), 7.48 (tdd, J = 7.7, 1.9, 1.0 Hz, 1H), 7.13 – 6.90 (m, 4H), 6.59 (td, J = 7.3, 1.0 Hz, 1H), 6.57 – 6.53 (m, 2H), 4.97 (d, J = 11.6 Hz, 1H), 3.60 – 3.27 (m, 1H), 2.77 (d, J = 1.0 Hz, 3H), 2.63 – 2.47 (m, 2H), 2.26 – 2.09 (m, 3H), 1.86 – 1.72 (m, 1H).

¹³C NMR (75 MHz, CDCl₃) δ 196.4, 149.0, 144.6, 143.1, 128.8, 118.4, 114.7, 39.5, 39.3, 26.0, 22.9.

FTIR (neat) ν_{\max} : 2950, 2933, 2866, 1710, 1596, 1505, 745, and 690 cm⁻¹.

HRMS (NSI) m/z : [M+H]⁺ calcd. for C₁₈H₂₁ON₂, 281.1648; found, 281.1647.



4-(methyl(phenyl)amino)-5-(pyridin-2-yl)hexan-3-one (31):

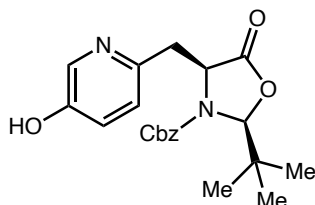
Following the general procedure, the reaction of 2-bromopyridine (159 mg, 1.00 mmol, 1 equiv), 4-(methyl(phenyl)amino)hex-4-en-3-one (406 mg, 2.00 mmol, 2 equiv), [Ir(ppy)₂(dtbbpy)]PF₆ (9.2 mg, 0.010 mmol, 0.01 equiv) and Hantzsch ester (325 mg, 1.28 mmol, 1.3 equiv) provided the product (180 mg, 64% yield) as a yellow oil after purification by flash column chromatography (0% – 30% ethyl acetate/hexanes).

¹H NMR (400 MHz, CDCl₃) δ 8.46 (ddd, J = 4.9, 1.9, 0.9 Hz, 1H), 7.57 (td, J = 7.8, 1.8 Hz, 1H), 7.36 – 7.26 (m, 2H), 7.24 (dd, J = 7.7, 1.1 Hz, 1H), 7.06 (ddd, J = 7.6, 4.9, 1.3 Hz, 1H), 7.00 (d, J = 8.2 Hz, 2H), 6.84 – 6.70 (m, 1H), 5.24 (d, J = 10.6 Hz, 1H), 3.62 (dq, J = 10.6, 7.1 Hz, 1H), 2.81 (s, 3H), 2.37 (dq, J = 17.7, 7.3 Hz, 1H), 2.21 (dq, J = 17.7, 7.3 Hz, 1H), 1.14 (d, J = 7.1 Hz, 3H), 0.96 – 0.70 (m, 3H).

¹³C NMR (100 MHz, CDCl₃) δ 208.4, 163.8, 149.8, 136.3, 129.4, 123.7, 121.2, 117.3, 112.7, 68.8, 39.6, 34.4, 32.6, 18.5, 7.4.

FTIR (neat) ν_{\max} : 3061, 3027, 2976, 2937, 2906, 2816, 1682, 1625, 1597, 1499, 1355, 1339, 1310, 1221, 1184, 1164, 1109, 747, and 692 cm^{-1} .

HRMS (NSI) m/z : $[\text{M}+\text{H}]^+$ calcd. for $\text{C}_{19}\text{H}_{23}\text{ON}_2$, 283.1805; found, 283.1804.



benzyl (2*S*,4*S*)-2-(*tert*-butyl)-4-((5-hydroxypyridin-2-yl)methyl)-5-oxooxazolidine-3-carboxylate (33):

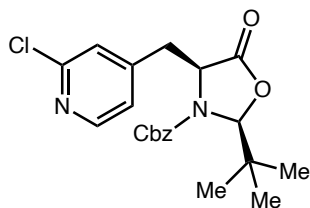
Following the general procedure, the reaction of 6-bromopyridin-3-ol (43 mg, 0.25 mmol, 1 equiv), **32** (145 mg, 0.50 mmol, 2 equiv), $[\text{Ir}(\text{ppy})_2(\text{dtbbpy})]\text{PF}_6$ (2 mg, 0.0025 mmol, 0.01 equiv) and Hantzsch ester (82 mg, 0.33 mmol, 1.3 equiv) provided the product (55 mg, 57% yield) as a colorless oil after purification by flash column chromatography (10% – 50% ethyl acetate/hexanes).

^1H NMR (500 MHz, CDCl_3) δ 8.06 (s, 1H), 7.36 – 7.27 (m, 3H), 7.24 – 7.20 (m, 2H), 7.12 (q, $J = 8.5$ Hz, 2H), 5.57 (s, 1H), 5.06 (d, $J = 12.0$ Hz, 1H), 4.91 (t, $J = 12.0$ Hz, 1H), 4.75 (t, $J = 6.9$ Hz, 1H), 3.32 (ddd, $J = 56.7, 14.1, 7.1$ Hz, 2H), 1.02 (s, 9H).

^{13}C NMR (125 MHz, CDCl_3) δ 171.8, 156.0, 153.2, 146.9, 136.0, 135.2, 128.7, 128.7, 128.5, 125.5, 125.3, 96.6, 68.5, 58.0, 39.5, 37.2, 25.1.

FTIR (neat) ν_{\max} : 3066, 3033, 2960, 2925, 2872, 1790, 1717, 1575, 1481, 1392, 1346, 1335, 1272, 1228, 1198, 1172, 1121, 1037, 976, 908, 839, 720, and 668 cm^{-1} .

HRMS (NSI) m/z : $[\text{M}+\text{H}]^+$ calcd. for $\text{C}_{23}\text{H}_{25}\text{O}_5\text{N}_2$, 385.1758; found, 385.17753.



benzyl (2*S*,4*S*)-2-(*tert*-butyl)-4-((2-chloropyridin-4-yl)methyl)-5-oxooxazolidine-3-carboxylate (**34**):

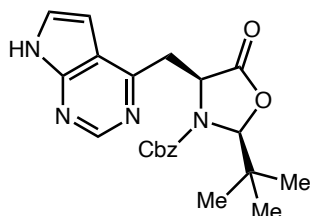
Following the general procedure, the reaction of 2-chloro-4-iodopyridine (60 mg, 0.25 mmol, 1 equiv), **32** (145 mg, 0.50 mmol, 2 equiv), [Ir(ppy)₂(dtbbpy)]PF₆ (2 mg, 0.0025 mmol, 0.01 equiv) and Hantzsch ester (82 mg, 0.33 mmol, 1.3 equiv) provided the product (75 mg, 75% yield) as a colorless oil after purification by flash column chromatography (5% – 30% ethyl acetate/hexanes).

¹H NMR (500 MHz, CDCl₃) δ 8.20 (d, *J* = 5.0 Hz, 1H), 7.41 – 7.38 (m, 3H), 7.27 (dd, *J* = 6.6, 2.8 Hz, 2H), 7.20 (s, 1H), 7.08 – 7.02 (m, 1H), 5.58 (s, 1H), 5.07 (dd, *J* = 70.4, 11.7 Hz, 2H), 4.43 (dd, *J* = 7.6, 5.4 Hz, 1H), 3.19 – 3.02 (m, 2H), 1.00 (s, 9H).

¹³C NMR (125 MHz, CDCl₃) δ 171.4, 155.7, 151.8, 149.7, 149.1, 134.8, 129.1, 129.0, 128.8, 125.1, 123.5, 96.6, 68.9, 58.1, 38.4, 37.3, 25.0.

FTIR (neat) ν_{max}: 3063, 3033, 2970, 2873, 1790, 1720, 1594, 1549, 1481, 1388, 1341, 1305, 1230, 1200, 1173, 1122, 1087, 1036, 980, 899, 878, 839, 746, and 698 cm⁻¹.

HRMS (NSI) *m/z*: [M+H]⁺ calcd. for C₂₁H₂₄O₄N₂Cl, 403.1419; found, 403.1414.



benzyl (2*S*,4*S*)-4-((7*H*-pyrrolo[2,3-*d*]pyrimidin-4-yl)methyl)-2-(*tert*-butyl)-5-oxooxazolidine-3-carboxylate (**35**):

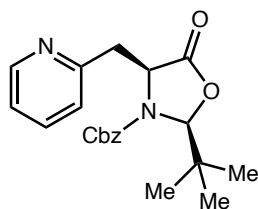
Following the general procedure, the reaction of 4-bromo-5*H*-pyrrolo[3,2-*d*]pyrimidine (50 mg, 0.25 mmol, 1 equiv), **32** (145 mg, 0.50 mmol, 2 equiv), [Ir(ppy)₂(dtbbpy)]PF₆ (2 mg, 0.0025 mmol, 0.01 equiv) and Hantzsch ester (82 mg, 0.33 mmol, 1.3 equiv) provided the product (82 mg, 80% yield) as a pale yellow oil after purification by flash column chromatography (20% – 70% ethyl acetate/hexanes).

¹H NMR (500 MHz, CDCl₃) δ 11.04 (s, 1H), 8.78 (s, 1H), 7.31 (dd, *J* = 3.4, 2.3 Hz, 1H), 7.25 (d, *J* = 2.9 Hz, 3H), 7.12 (s, 2H), 6.57 (s, 1H), 5.63 (s, 1H), 5.19 (t, *J* = 6.8 Hz, 1H), 5.02 (d, *J* = 12.1 Hz, 1H), 4.76 (d, *J* = 11.0 Hz, 1H), 3.70 – 3.51 (m, 2H), 1.07 (s, 9H).

¹³C NMR (125 MHz, CDCl₃) δ 171.8, 157.8, 155.8, 151.5, 150.9, 135.0, 128.6, 128.5, 128.3, 125.5, 117.9, 99.5, 96.7, 68.2, 56.7, 39.0, 37.3, 25.1.

FTIR (neat) ν_{max}: 3202, 3133, 2969, 1792, 1721, 1585, 1393, 1349, 1307, 1230, 1194, 1119, 1043, 976, 903, 733, and 698cm⁻¹.

HRMS (NSI) *m/z*: [M+H]⁺ calcd. for C₂₂H₂₅O₄N₄, 409.1870; found, 409.1866.



benzyl (2*S*,4*S*)-2-(*tert*-butyl)-5-oxo-4-(pyridin-2-ylmethyl)oxazolidine-3-carboxylate (36**):**

Following the general procedure, the reaction of 2-bromopyridine (39 mg, 0.25 mmol, 1 equiv), **32** (145 mg, 0.50 mmol, 2 equiv), [Ir(ppy)₂(dtbbpy)]PF₆ (2 mg, 0.0025 mmol, 0.01 equiv) and Hantzsch ester (82 mg, 0.33 mmol, 1.3 equiv) provided the product (63 mg, 68% yield) as a colorless oil after purification by flash column chromatography (10% – 40% ethyl acetate/hexanes).

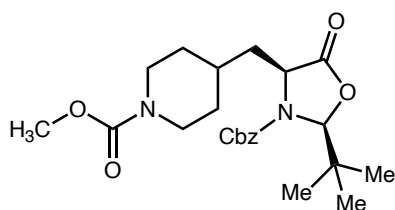
¹H NMR (500 MHz, CDCl₃) δ 8.49 (d, *J* = 4.2 Hz, 1H), 7.53 (td, *J* = 7.7, 1.8 Hz, 1H), 7.32 (td, *J* = 4.8, 1.8 Hz, 3H), 7.24 (dd, *J* = 6.9, 2.6 Hz, 2H), 7.16 (d, *J* = 7.7 Hz, 1H), 7.08 (dd, *J* = 7.1,

5.3 Hz, 1H), 5.59 (s, 1H), 5.08 (d, $J = 12.2$ Hz, 1H), 4.97 (t, $J = 6.9$ Hz, 1H), 4.85 (d, $J = 11.9$ Hz, 1H), 3.38 (dd, $J = 14.0, 6.9$ Hz, 1H), 3.30 (dd, $J = 14.0, 6.9$ Hz, 1H) 1.03 (s, 9H).

^{13}C NMR (125 MHz, CDCl_3) δ 172.0, 156.7, 155.9, 149.4, 136.2, 135.3, 128.6, 128.4, 128.3, 123.7, 121.9, 96.4, 68.1, 57.5, 41.4, 37.2, 25.0.

FTIR (neat) ν_{max} : 3064, 3034, 3010, 2970, 2873, 1791, 1716, 1593, 1475, 1438, 1391, 1347, 1305, 1231, 1173, 1190, 1121, 1036, 977, 932, 825, 731, and 697 cm^{-1} .

HRMS (NSI) m/z : $[\text{M}+\text{H}]^+$ calcd. for $\text{C}_{21}\text{H}_{25}\text{O}_4\text{N}_2$, 369.1809; found, 369.1804.



benzyl (2*S*,4*S*)-2-(*tert*-butyl)-4-((1-(methoxycarbonyl)piperidin-4-yl)methyl)-5-oxooxazolidine-3-carboxylate (**38**):

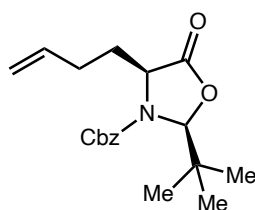
Following the general procedure, the reaction of 4-(1,3-dioxoisindolin-2-yl) 1-methyl piperidine-1,4-dicarboxylate (83 mg, 0.25 mmol, 1 equiv), **32** (145 mg, 0.5 mmol, 2 equiv), $[\text{Ir}(\text{ppy})_2(\text{dtbbpy})]\text{PF}_6$ (2 mg, 0.0025 mmol, 0.01 equiv) and Hantzsch ester (82 mg, 0.33 mmol, 1.3 equiv) provided the product (93 mg, 86% yield) as a white solid after purification by flash column chromatography (5% – 30% ethyl acetate/hexanes).

^1H NMR (500 MHz, CDCl_3) δ 7.39 – 7.34 (m, 5H), 5.59 – 5.39 (m, 3H), 4.66 (d, $J = 11.0$ Hz, 1H), 4.06 – 3.52 (m, 7H), 2.52 – 2.20 (m, 2H), 1.82 (dd, $J = 14.1, 7.6$ Hz, 1H), 1.65 – 1.35 (m, 3H), 1.06 (s, 9H), 0.93 – 0.66 (m, 1H).

^{13}C NMR (125 MHz, cdcl_3) δ 168.5, 156.0, 153.9, 134.6, 129.7, 129.1, 128.8, 95.6, 71.7, 68.1, 52.5, 44.1, 43.6, 38.8, 37.1, 31.5, 26.9.

FTIR (neat) ν_{max} : 2959, 2852, 1792, 1724, 1701, 1472, 1448, 1396, 1309, 1258, 1193, 1125, 1043, 966, 916, 757, 731, and 699 cm^{-1} .

HRMS (NSI) m/z : $[M+H]^+$ calcd. for $C_{23}H_{33}O_6N_2$, 433.2333; found, 433.2333.



benzyl (2*S*,4*S*)-4-(but-3-en-1-yl)-2-(*tert*-butyl)-5-oxooxazolidine-3-carboxylate (39):

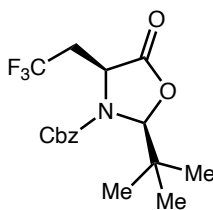
Following the general procedure, the reaction of 3-bromoprop-1-ene (22 μ L, 0.25 mmol, 1 equiv), **32** (145 mg, 0.50 mmol, 2 equiv), $[Ir(ppy)_2(dtbbpy)]PF_6$ (2 mg, 0.0025 mmol, 0.01 equiv) and Hantzsch ester (82 mg, 0.33 mmol, 1.3 equiv) provided the product (35 mg, 42% yield) as a colorless oil after purification by flash column chromatography (5% – 30% ethyl acetate/hexanes).

1H NMR (500 MHz, $CDCl_3$) δ 7.41 – 7.34 (m, 5H), 5.76 (td, $J = 16.7, 6.7$ Hz, 1H), 5.55 (s, 1H), 5.22 – 5.12 (td $J = 16.9, 11.9$ Hz, 2H), 5.06 (d, $J = 17.1$ Hz, 1H), 4.98 (d, $J = 11.2$ Hz, 1H), 4.30 (dd, $J = 7.8, 6.7$ Hz, 1H), 2.34 (m, 2H), 2.06 – 1.98 (m, 1H), 1.90 (m, 1H), 0.96 (s, 9H).

^{13}C NMR (125 MHz, $CDCl_3$) δ 172.7, 156.1, 137.0, 135.3, 128.8, 128.8, 128.6, 115.9, 96.4, 68.5, 56.5, 37.1, 32.5, 30.3, 25.0.

FTIR (neat) ν_{max} : 3068, 3034, 2960, 2873, 1790, 1716, 1641, 1391, 1324, 1282, 1195, 1117, 1041, 979, 914, and 968 cm^{-1} .

HRMS (NSI) m/z : $[M+H]^+$ calcd. for $C_{19}H_{26}O_4N$, 332.1856; found, 332.1859.



benzyl (2*S*,4*S*)-2-(*tert*-butyl)-5-oxo-4-(2,2,2-trifluoroethyl)oxazolidine-3-carboxylate (40):

A 20-mL screw-top test tube equipped with a stir bar was charged with **32** (289 mg, 1.0 mmol, 2 equiv), [Ir(ppy)₂(dtbbpy)]PF₆ (5 mg, 0.005 mmol, 0.01 equiv) and Hantzsch ester (164 mg, 0.65 mmol, 1.3 equiv). The tube was sealed PTFE/silicon septum and connected to a Schlenk line. The atmosphere was exchanged by applying vacuum and backfilling with N₂ (this process was conducted a total of three times). The reaction vial was disconnected from the nitrogen line and massed. The trifluoromethyl iodide lecture bottle outlet was fitted with a rubber septum, and a cannula needle (cooled to -78 °C) was used to condense trifluoromethyl iodide into the reaction tube. The reaction tube and contents were massed once more to measure the loading of trifluoromethyl iodide (861 mg, 4.4 mmol, 4.4 equiv). The reaction was then stirred for 18 hours under irradiation by blue LEDs. The reaction was quenched with aqueous sodium bicarbonate then extracted with ethyl acetate (5 x 25 mL). The combined extracts were dried over sodium sulfate then concentrated by rotary evaporation to provide the product (222 mg, 93% yield) as a colorless oil after purification by flash column chromatography (10% – 50% ethyl acetate/hexanes).

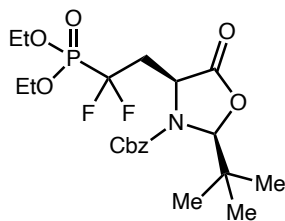
¹H NMR (500 MHz, DMSO-*d*₆, 80 °C) δ 7.44 – 7.34 (m, 7H), 5.43 – 5.34 (m, 2H), 4.92 (s, 1H), 3.58 (s, 1H), 3.43 (dq, *J* = 15.5, 10.2 Hz, 1H), 3.17 (s, 1H), 0.94 (s, 9H).

¹³C NMR (126 MHz, DMSO-*d*₆, 80 °C) δ 165.3, 152.5, 133.8, 128.4, 128.3, 128.1, 124.3 (q, *J* = 278.6 Hz), 95.9, 68.0, 66.7, 37.6, 33.8 (q, *J* = 28.5), 26.0.

¹⁹F NMR (282 MHz, cdcl₃) δ -59.92.

FTIR (neat) ν_{max}: 3035, 2965, 1799, 1732, 1483, 1394, 1333, 1290, 1230, 1200, 1138, 1117, 1044, 1018, 976, 916, 819, 798, 767, 755, and 696 cm⁻¹.

HRMS (NSI) *m/z*: [M+H]⁺ calcd. for C₁₇H₂₁O₄NF₃, 360.1417; found, 360.1421.



benzyl (2*S*,4*S*)-2-(*tert*-butyl)-4-(2-(diethoxyphosphoryl)-2,2-difluoroethyl)-5-oxooxazolidine-3-carboxylate (41):

Following the general procedure, the reaction of 2-bromo-2,2-diethyl (bromodifluoromethyl)phosphonate (89 μ L, 0.5 mmol, 1 equiv), **32** (289 mg, 1.0 mmol, 2 equiv), [Ir(ppy)₂(dtbbpy)]PF₆ (5 mg, 0.005 mmol, 0.01 equiv) and Hantzsch ester (164 mg, 0.65 mmol, 1.3 equiv) provided the product (222 mg, 93% yield) as a colorless oil after purification by flash column chromatography (10% – 50% ethyl acetate/hexanes).

¹H NMR (500 MHz, CDCl₃) δ 7.37 – 7.29 (m, 5H), 5.59 (s, 1H), 5.24 – 5.11 (m, 2H), 4.84 (t, J = 5.9 Hz, 1H), 4.24 (tddd, J = 12.4, 6.8, 5.2, 2.7 Hz, 4H), 2.77 – 2.48 (m, 2H), 1.35 (td, J = 7.0, 1.0 Hz, 6H), 0.95 (s, 9H).

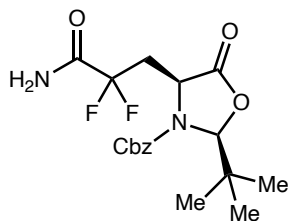
¹³C NMR (150 MHz, CDCl₃) δ 171.1, 155.6, 135.1, 128.6, 128.5, 121.0, 119.6, 119.3, 117.9, 117.6, 116.1, 96.8, 68.5, 64.9, 64.8, 64.8, 64.8, 51.1, 51.1, 51.0, 51.0, 37.3, 37.1, 37.0, 36.9, 24.8, 16.4, 16.3.

¹⁹F NMR (282 MHz, CDCl₃) δ -113.20 (dddd, J = 299.8, 103.3, 32.6, 7.5 Hz).

³¹P NMR (243 MHz, CDCl₃) δ 5.81 (tt, J = 104.4, 7.6 Hz).

FTIR (neat) ν_{max} : 2976, 2875, 1796, 1720, 1482, 1392, 1291, 1270, 1236, 1197, 1177, 1105, 1010, 977, 791, 732, and 698 cm⁻¹.

HRMS (NSI) m/z : [M+H]⁺ calcd. for C₂₁H₃₁O₇NF₂P, 478.1801; found, 478.1802.



benzyl (2*S*,4*S*)-4-(3-amino-2,2-difluoro-3-oxopropyl)-2-(*tert*-butyl)-5-oxooxazolidine-3-carboxylate (42):

Following the general procedure, the reaction of 2-bromo-2,2-difluoroacetamide (43 mg, 0.25 mmol, 1 equiv), **32** (145 mg, 0.50 mmol, 2 equiv), [Ir(ppy)₂(dtbbpy)]PF₆ (2 mg, 0.0025 mmol, 0.01 equiv) and Hantzsch ester (82 mg, 0.33 mmol, 1.3 equiv) provided the product (58 mg, 60% yield) as a colorless oil after purification by flash column chromatography (5% – 30% ethyl acetate/hexanes).

¹H NMR (500 MHz, CDCl₃) δ 7.40 – 7.31 (m, 5H), 6.40 (s, 1H), 6.13 (s, 1H), 5.58 (s, 1H), 5.26 – 5.08 (m, 2H), 4.70 (dd, *J* = 7.5, 5.9 Hz, 1H), 2.82 – 2.60 (m, 2H), 0.96 (s, 9H).

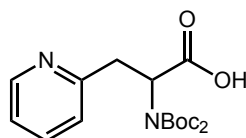
¹³C NMR (125 MHz, CDCl₃) δ 171.0, 165.4 (t, *J* = 29.0 Hz), 155.9, 135.1, 128.8, 128.8, 128.7, 116.0 (t, *J* = 254.8 Hz), 97.1, 68.8, 52.3, 37.0, 36.7 (t, *J* = 24.6 Hz), 24.9.

¹⁹F NMR (376 MHz, CDCl₃) δ -101.11 – -104.68 (m).

FTIR (neat) ν_{max}: 3446, 3354, 3198, 2964, 2875, 1793, 1719, 1607, 1394, 1319, 1196, 1037, 1014, 909, 731, and 698 cm⁻¹.

HRMS (NSI) *m/z*: [M+H]⁺ calcd. for C₁₈H₂₃O₅N₂F₂, 385.1570; found, 385.1570.

2.4.6 Deprotection Procedures and Characterization Data



methyl 2-(di(*tert*-butoxycarbonyl)amino)-3-(pyridin-2-yl)propanoic acid (2A):

To a stirring solution of methyl 2-(di(*tert*-butoxycarbonyl)amino)-3-(pyridin-2-yl)propanoate (**2**) (190 mg, 0.5 mmol, 1 equiv) in THF/H₂O (3:2, 5 mL) was added LiOH (24 mg, 1.0 mmol, 2.0 equiv). The resultant solution was stirred until consumption of starting material was observed by thin layer chromatography. The reaction mixture was extracted once with ethyl acetate, and the organic extract was discarded. The aqueous phase was gently acidified with 0.1 M HCl to pH 4 and extracted with ethyl acetate (5 x 5 mL). The combined extracts were dried over sodium sulfate, filtered, and concentrated to provide the product (172 mg, 94% yield) as a clear, colorless crystalline solid.

Mp: 164 °C (decomp.)

¹H NMR (300 MHz, CDCl₃) δ 8.53 (dt, $J = 5.0, 1.4$ Hz, 1H), 7.75 (td, $J = 7.7, 1.8$ Hz, 1H), 7.41 – 7.12 (m, 2H), 5.21 (dd, $J = 7.9, 4.7$ Hz, 1H), 3.93 (dd, $J = 15.3, 7.9$ Hz, 1H), 3.17 (dd, $J = 15.3, 4.7$ Hz, 1H), 1.45 (s, 18H).

¹³C NMR (75 MHz, CDCl₃) δ 171.6, 158.0, 152.0, 147.1, 138.6, 124.4, 122.4, 83.2, 58.2, 39.2, 27.9.

FTIR (neat) ν_{max} : 3456, 3068, 2970, 2930, 2853, 1748, 1708, 1366, 1108, 1062, and 778 cm⁻¹.

HRMS (NSI) m/z : [M+H]⁺ calcd. for C₁₈H₂₇O₆N₂, 367.1864; found, 367.1859.

methyl 2-(di(*tert*-butoxycarbonyl)amino)-3-(pyridin-2-yl)propanoic acid (2A):

To a stirring solution of methyl 2-(di(*tert*-butoxycarbonyl)amino)-3-(pyridin-2-yl)propanoate (**2**) (190 mg, 0.5 mmol, 1 equiv) in THF/H₂O (3:2, 5 mL) was added LiOH (24 mg, 1.0 mmol, 2.0 equiv). The resultant solution was stirred until consumption of starting material was observed by thin layer chromatography. The reaction mixture was extracted once with ethyl acetate, and the organic extract was discarded. The aqueous phase was gently acidified with 0.1 M HCl to pH 4 and extracted with ethyl acetate (5 x 5 mL). The combined extracts were

dried over sodium sulfate, filtered, and concentrated to provide the product (172 mg, 94% yield) as a clear, colorless crystalline solid.

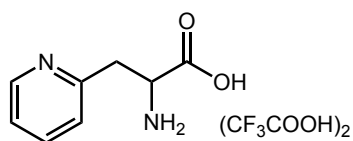
Mp: 164 °C (decomp.)

¹H NMR (300 MHz, CDCl₃) δ 8.53 (dt, J = 5.0, 1.4 Hz, 1H), 7.75 (td, J = 7.7, 1.8 Hz, 1H), 7.41 – 7.12 (m, 2H), 5.21 (dd, J = 7.9, 4.7 Hz, 1H), 3.93 (dd, J = 15.3, 7.9 Hz, 1H), 3.17 (dd, J = 15.3, 4.7 Hz, 1H), 1.45 (s, 18H).

¹³C NMR (75 MHz, CDCl₃) δ 171.6, 158.0, 152.0, 147.1, 138.6, 124.4, 122.4, 83.2, 58.2, 39.2, 27.9.

FTIR (neat) ν_{max} : 3456, 3068, 2970, 2930, 2853, 1748, 1708, 1366, 1108, 1062, and 778 cm⁻¹.

HRMS (NSI) m/z : [M+H]⁺ calcd. for C₁₈H₂₇O₆N₂, 367.1864; found, 367.1859.



2-(2-ammonio-3-methoxy-3-oxopropyl)pyridin-1-ium ditrifluoroacetate (2B):

To a stirring solution of of methyl 2-(di(*tert*-butoxycarbonyl)amino)-3-(pyridin-2-yl)propanoate (**2**) (190 mg, 0.5 mmol, 1 equiv) in dichloromethane (2 mL) was added trifluoroacetic acid (1.5 mL) dropwise. The resultant solution was allowed to continue stirring, and after 10 minutes consumption of starting material was observed by thin layer chromatography. The reaction mixture was concentrated directly by rotary evaporation. The solution was re-dissolved in dichloromethane and concentrated once more to quantitatively provide the product as a pale, yellow low-melting solid (203 mg, >99% yield).

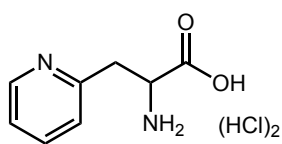
¹H NMR (300 MHz, D₃COD) δ 8.78 (dd, J = 5.7, 1.6 Hz, 1H), 8.44 (td, J = 7.9, 1.7 Hz, 1H), 7.96 (d, J = 8.0 Hz, 1H), 7.89 (td, J = 5.9, 2.8 Hz, 1H), 5.73 (s, 4H), 4.65 (t, J = 7.1 Hz, 1H), 3.77 (s, 3H), 3.69 (t, J = 7.2 Hz, 2H).

^{13}C NMR (75 MHz, D_3COD) δ 167.8, 159.8 (q, $J = 37.9$ Hz), 151.4, 144.9, 143.1, 127.4, 125.3, 117.6 (q, $J = 289.1$ Hz), 52.6, 51.5, 33.6, 26.2.

^{19}F NMR (282 MHz, D_3COD) δ -77.45.

FTIR (neat) ν_{max} : 2964, 2563, 2111, 1746, 1666, 1651, 1172, 1157, 1127, 836, 798, and 720 cm^{-1} .

HRMS (NSI) m/z : $[\text{M}+\text{H}]^+$ calcd. for $\text{C}_9\text{H}_{13}\text{O}_2\text{N}_2$, 181.0972; found, 181.0967.



2-amino-3-(pyridin-2-yl)propanoic acid dihydrochloride (2C):

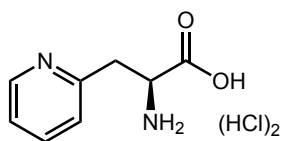
A 20-mL scintillation vial equipped with stir bar was charged with methyl 2-(di(*tert*-butoxycarbonyl)amino)-3-(pyridin-2-yl)propanoate (**2**) (190 mg, 0.5 mmol, 1 equiv), EtOH (5 mL) and 3N NaOH (5 mL), and the resultant solution was stirred until consumption of starting material was observed (~ 1 hour). The reaction mixture was acidified with 1M HCl and concentrated by rotary evaporation. The residue was reconstituted in EtOH, and precipitated NaCl was removed by vacuum filtration. The filtrate was concentrated under reduced pressure. Concentrated HCl (3 mL) was added dropwise to the residue and stirred 10 minutes. The mixture was concentrated directly to provide the product (119 mg, 96% yield) as a white crystalline solid.

^1H NMR (300 MHz, D_2O) δ 8.49 (d, $J = 6.0$ Hz, 1H), 8.32 (td, $J = 8.0, 1.7$ Hz, 1H), 7.83 (d, $J = 8.1$ Hz, 1H), 7.75 (dd, $J = 7.7, 6.1$ Hz, 1H), 4.34 (t, $J = 7.4$ Hz, 1H), 3.47 (d, $J = 7.4$ Hz, 2H).

^{13}C NMR (75 MHz, D_2O) δ 169.6, 149.6, 147.2, 141.4, 128.2, 126.1, 51.6, 33.2.

FTIR (neat) ν_{max} : 3399, 2780, 2934, 1702, 1567, 1477, 1403, 1367, 1243, 1139, 1102, 1101, 921, and 750 cm^{-1} .

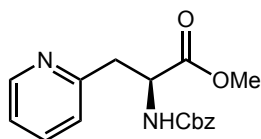
HRMS (NSI) m/z : $[\text{M}+\text{H}]^+$ calcd. for $\text{C}_8\text{H}_{11}\text{O}_2\text{N}_2$, 167.0815; found, 167.0811.



(S)-2-amino-3-(pyridin-2-yl)propanoic acid dihydrochloride (37):

To a round bottom flask equipped with a stir bar was added **23** (20.2 mg), and concentrated aqueous HCl (2 mL). The reaction was stirred at 80 °C for 30 minutes then concentrated by rotary evaporation to afford the product (12.8, 98%) as a white solid. The physical properties and spectral data are consistent with the values of the racemate (**2C**) reported herein, with the exception of optical rotation.

$[\alpha]_D^{20} +31.7$ (*c* 0.1, 1 M HCl) (lit.,⁵⁰ $+46.0$ (*c* 0.1, 1 M HCl))



methyl (S)-2-(((benzyloxy)carbonyl)amino)-3-(pyridin-2-yl)propanoate (37A):

To a round bottom flask equipped with a stir bar was added **24**, Et₂O (5 mL), and MeOH (5 mL). The reaction was placed under nitrogen atmosphere then cooled to 0 °C. (Trimethylsilyl)diazomethane solution (2.0 M in ether, 80 μL, 0.16 mmol, 2.0 equiv) was added dropwise via syringe and the reaction was warmed to room temperature and stirred for 30 minutes. The reaction was quenched with AcOH (2 mL) then concentrated by rotary evaporation. The residue was dissolved in saturated aqueous sodium bicarbonate (1 mL) and THF (1 mL). The solution was set to stir and chilled to 0 °C. Benzyl chloroformate (12.5 μL, 0.09 mmol, 1.1 equiv) was added dropwise via syringe, and the reaction was warmed to room temperature and stirred until HPLC indicated the starting material had been consumed. The

⁵⁰ Anaïs F. M. Noisier, Craig S. Harris, and Margaret A. Brimble *Chem. Commun.*, **2013**, 49, 7744.

reaction was concentrated to remove THF then diluted with water (1 mL). The aqueous solution was extracted with EtOAc (3 x 2 mL), and the combined extracts were concentrated by rotary evaporation. The residue was purified by preparative HPLC to afford the product as a colorless oil. Chiral HPLC analysis (OD-H, 15% IPA/hexanes, 1.0 mL/min, 254 nm) indicated 97% ee for the major enantiomer (t_R (major) = 14.949 min, t_R (minor) = 21.299 min).

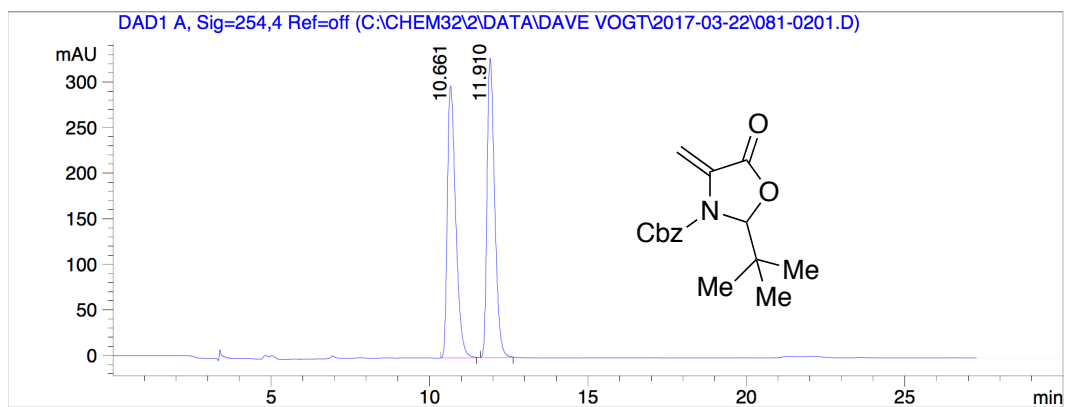
^1H NMR (500 MHz, CDCl_3) δ 8.47 (d, J = 4.7 Hz, 1H), 7.60 – 7.56 (m, 1H), 7.39 – 7.27 (m, 5H), 7.15 – 7.09 (m, 2H), 6.30 (d, J = 8.2 Hz, 1H), 5.15 – 5.05 (m, 2H), 4.76 (dt, J = 8.4, 5.3 Hz, 1H), 3.68 (s, 3H), 3.36 (dd, J = 14.9, 5.7 Hz 1H), 3.28 (dd, J = 14.9, 4.7 Hz 1H).

^{13}C NMR (125 MHz, CDCl_3) δ 172.1, 157.1, 156.1, 149.3, 136.7, 136.5, 128.5, 128.2, 128.2, 123.8, 121.9, 67.0, 53.4, 52.4, 39.0.

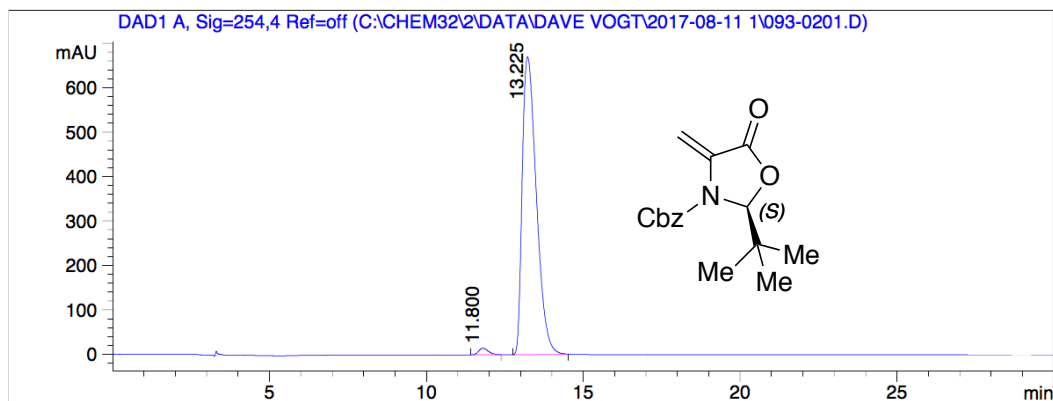
FTIR (neat) ν_{max} : 3333, 3032, 2951, 1716, 1593, 1507, 1436, 1340, 1210, 1050, 911, 752, and 670 cm^{-1} .

HRMS (NSI) m/z : $[\text{M}+\text{H}]^+$ calcd. for $\text{C}_{17}\text{H}_{19}\text{O}_4\text{N}_2$, 315.1339; found, 315.1335.

2.4.7 Chiral HPLC Data

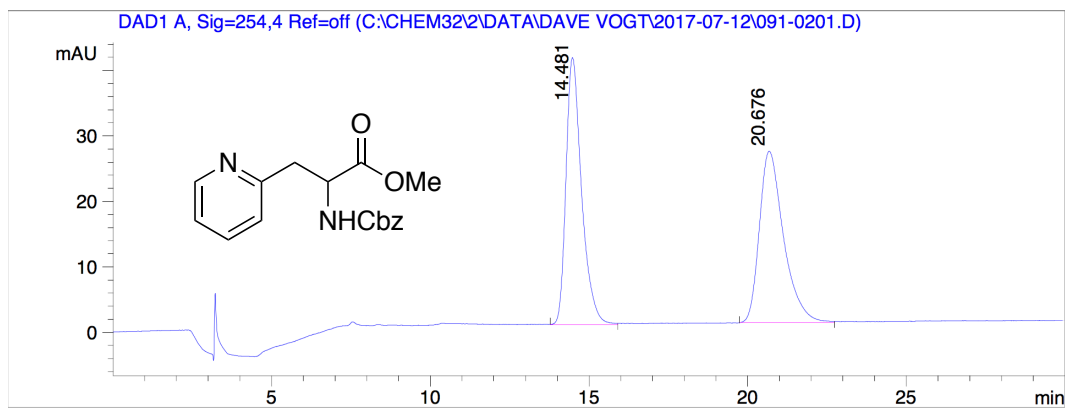


#	Compound Name	Amount	Resp.	Resp. %	Exp. RT	Meas. RT
1		0.000	5.459e3	49.955	0.000	10.661
2		0.000	5.469e3	50.045	0.000	11.910
Totals:		0.000				

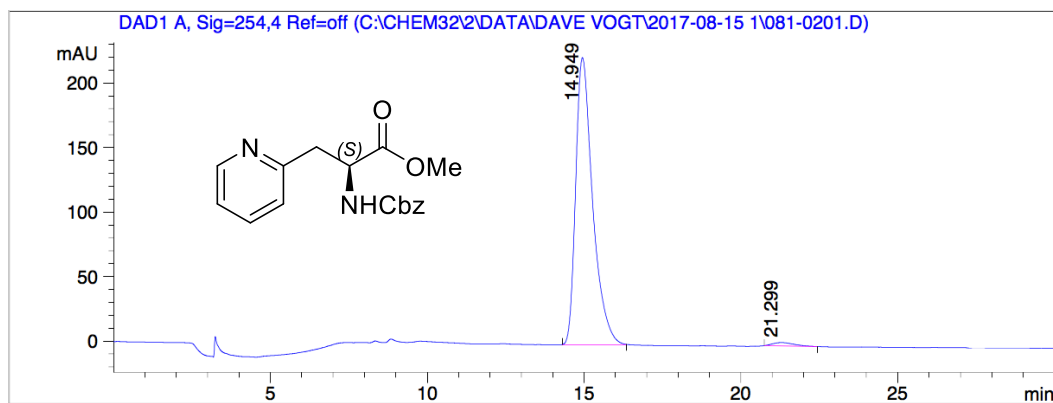


This is a result compounds table. Use the footer button in the table format dialog box to define the summations in the last table line.

#	Compound Name	Amount	Resp.	Resp. %	Exp. RT	Meas. RT
1		0.000	326.194	1.530	0.000	11.800
2		0.000	2.099e4	98.470	0.000	13.225
Totals:		0.000				



#	Compound Name	Amount	Resp.	Resp. %	Exp. RT	Meas. RT
1		0.000	1.399e3	50.170	0.000	14.481
2		0.000	1.389e3	49.830	0.000	20.676
Totals:		0.000				

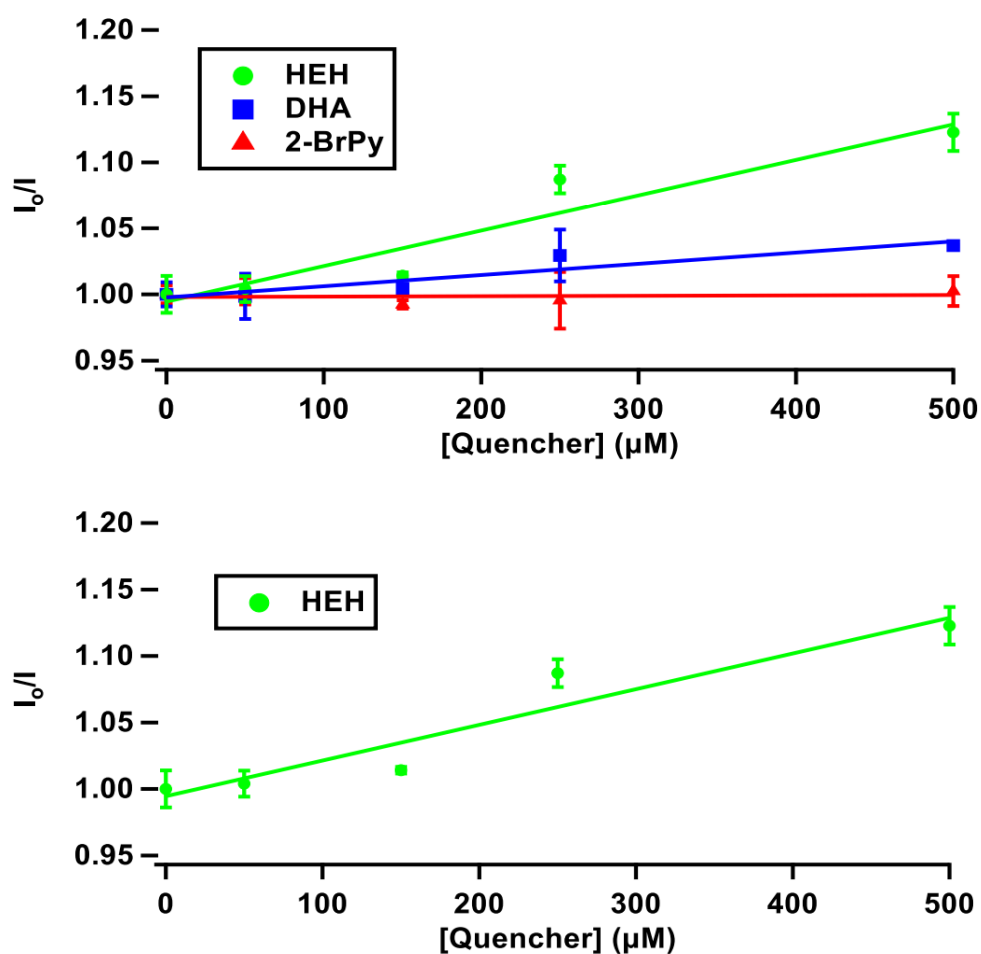


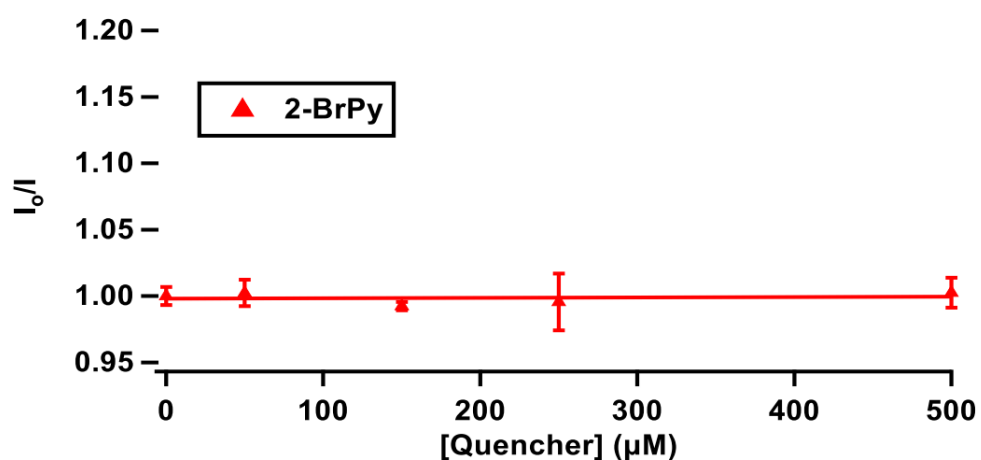
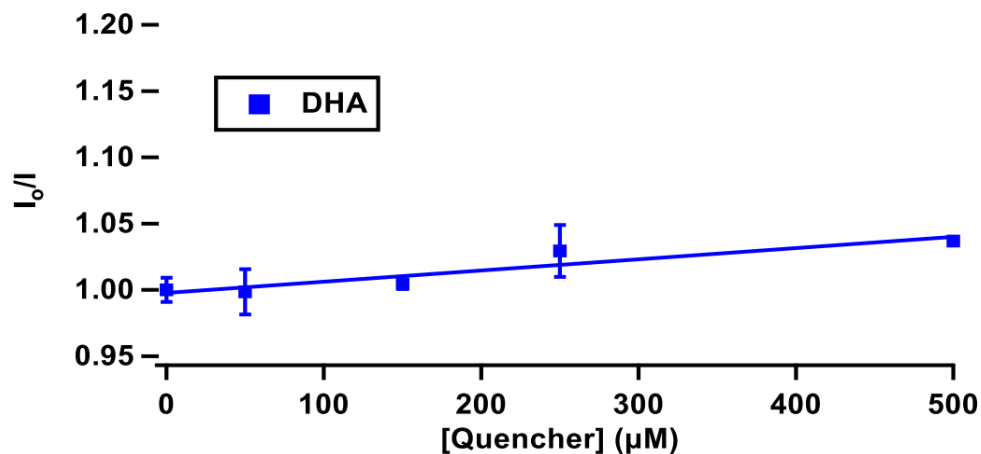
This is a result compounds table. Use the footer button in the table format dialog box to define the summations in the last table line.

#	Compound Name	Amount	Resp.	Resp. %	Exp. RT	Meas. RT
1		0.000	8.375e3	98.471	0.000	14.949
2		0.000	130.034	1.529	0.000	21.299
Totals:		0.000				

2.4.8 Stern Volmer Fluorescence Quenching Experiments

All fluorescence measurements were recorded using a Horiba Scientific Dual-FL Fluorometer. Quenching studies were conducted in DMSO:H₂O (5:1) at 20 ±0.5 °C (Peltier temperature controller) with an [Ir(ppy)₂(dtbbpy)]PF₆ concentration of 5 μM. Raw fluorescence intensity was measured at λ = 591 nm after excitation at λ = 450 nm in a quartz cuvette with a path length of 1 cm. Measurements using Hantzsch ester, dehydroalanine, or 2-bromopyridine as quenchers were taken in triplicate at concentrations of 0, 50, 100, 250, and 500 μM. At quencher concentration of 0 μM, additional duplicate measurements were collected prior to successive quenchers to maintain accuracy. SternVolmer plots were generated using Igor Pro 7; data points were fit with a linear trend line.



Measured Fluorescence Intensities at $\lambda = 591$ nm (counts)

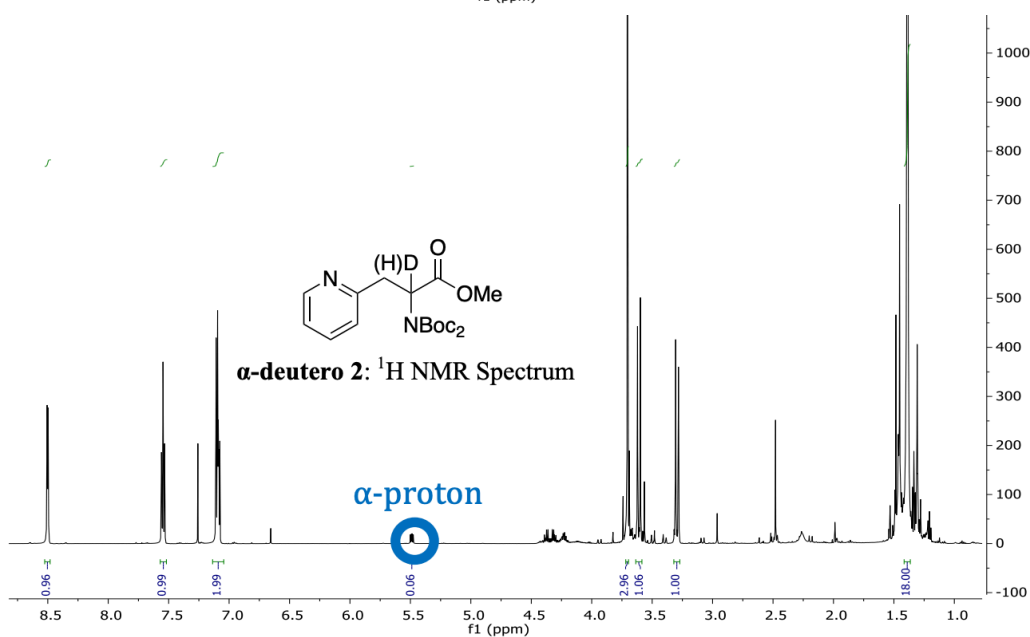
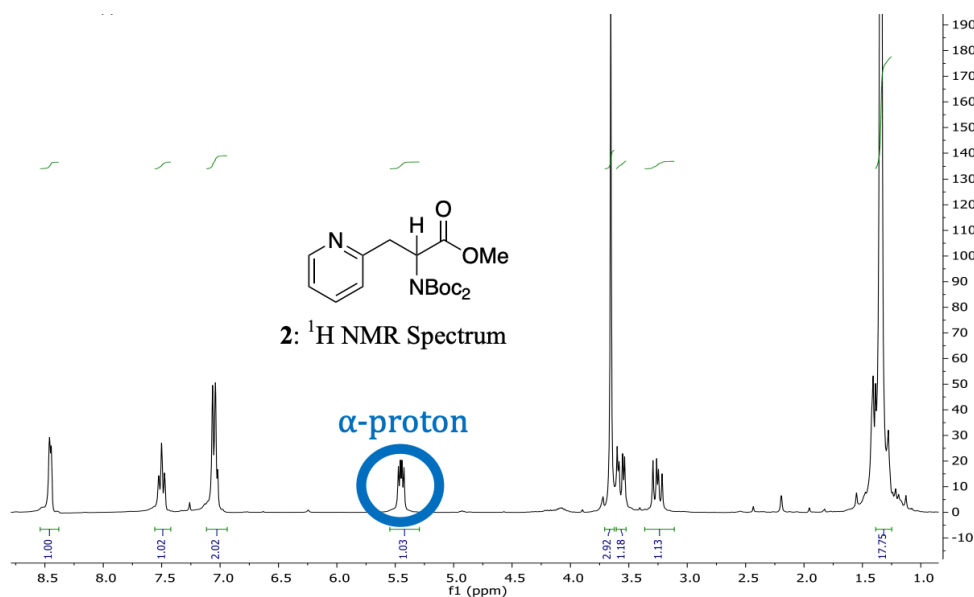
[HEH] (μM)	1	2	3	avg	stdev	I_0/I	error
0	5966.1219	5849.4855	-	5907.8037	82.4743	1.0000	0.0140
50	5819.8148	5929.6318	5902.7293	5884.0586	57.2398	1.0040	0.0098
100	5841.5493	5819.6902	5813.9702	5825.0699	14.5553	1.0142	0.0025
250	5374.5285	5468.2221	5461.4238	5434.7248	52.2422	1.0870	0.0104
500	5200.5652	5253.6675	5331.9516	5262.0614	66.0942	1.1227	0.0141

[DHA] (μM)	1	2	3	avg	stdev	I_0/I	error
0	5839.3979	5914.3043	5903.3400	5885.6807	40.4553	1.0519	0.0072
50	6095.6538	6197.9486	6307.0152	6200.2059	105.6987	0.9985	0.0170
100	6173.1678	6181.4130	6138.4126	6164.3311	22.8216	1.0043	0.0037
250	6057.7748	6100.8092	5884.9329	6014.5056	114.2576	1.0294	0.0196
500	5968.5599	5976.2475	5967.5891	5970.7988	4.7436	1.0369	0.0008

[2-BrPy] (μM)	1	2	3	avg	stdv	I_0/I	error
0	6151.0503	6231.0219	-	6191.0361	56.5485	0.9507	0.0087
50	5805.9303	5890.0415	5918.6204	5871.5308	58.5812	1.0024	0.0100
100	5951.2881	5923.7698	5915.9019	5930.3199	18.5802	0.9925	0.0031
250	5829.0025	5848.4549	6057.4723	5911.6432	126.6656	0.9956	0.0213
500	5840.9751	5825.5125	5946.4111	5870.9662	65.7930	1.0025	0.0112

2.4.9 Deuterium Incorporation Studies

Following the general procedure, the reaction of 2-bromopyridine (32 mg, 0.20 mmol, 1 equiv), methyl 2-(di(tert-butoxycarbonyl)amino)acrylate (120 mg, 0.40 mmol, 2 equiv), [Ir(ppy)₂(dtbbpy)]PF₆ (2.1 mg, 0.0021 mmol, 0.01 equiv) and Hantzsch ester (76 mg, 0.30 mmol, 1.3 equiv) provided the product (72 mg, 94% yield) as white solid after purification by flash column chromatography (5% – 40% ethyl acetate/hexanes). Integration of the alpha proton ¹H NMR signal was used to determine the percent of deuterium incorporation (94% D).



Chapter 3:

**Radical Hydroarylation of Functionalized
Olefins and Mechanistic Investigation of
Photocatalytic Pyridyl Radical Reactions**

Adapted and reprinted in part with permission from *J. Am. Chem. Soc.* **2018**, 15525-15534
Copyright 2018 American Chemical Society

<https://pubs.acs.org/doi/10.1021/jacs.8b10238>

Abstract: We've reported the photoredox alkylation of halopyridines using functionalized alkene and alkyne building blocks. Selective single-electron reduction of the halogenated pyridines provides the corresponding heteroaryl radicals, which undergo anti-Markovnikov addition to the alkene substrates. The system is shown to be mild and tolerant of a variety of alkene and alkyne subtypes. A combination of computational and experimental studies support a mechanism involving proton-coupled electron transfer followed by medium-dependent alkene addition and rapid hydrogen atom transfer mediated by a polarity-reversal catalyst.

3.1 Introduction

Beyond amino acids, functionalized pyridines are ubiquitous structural elements in bioactive molecules that span a wide range of applications.⁵¹ Accordingly, a number of powerful synthetic strategies have been developed to effectively access this heterocyclic family.⁵² In addition to classical methods for pyridine construction using acyclic precursors,⁵³ diversification of pyridine units using transition-metal-based cross-coupling⁵⁴ and C–H functionalization⁵⁵ strategies plays key roles in modern drug discovery, as do nucleophilic

⁵¹ (a) Guan, A.-Y.; Liu, C.-L.; Sun, X.-F.; Xie, Y.; Wang, M.-A. Discovery of Pyridine-Based Agrochemicals by Using Intermediate Derivatization Methods. *Bioorg. Med. Chem.* **2016**, *24* (3), 342–353; (b) Vitaku, E.; Smith, D. T.; Njardarson, J. T. Analysis of the Structural Diversity, Substitution Patterns, and Frequency of Nitrogen Heterocycles among U.S. FDA Approved Pharmaceuticals. *J. Med. Chem.* **2014**, *57* (24), 10257–10274; (c) Bakhite, E. A.; Abd-Ella, A. A.; El-Sayed, M. E. A.; Abdel-Raheem, S. A. A. Pyridine Derivatives as Insecticides. Part 1: Synthesis and Toxicity of Some Pyridine Derivatives Against Cowpea Aphid, *Aphis Craccivora* Koch (Homoptera: Aphididae). *J. Agric. Food Chem.* **2014**, *62* (41), 9982–9986

⁵² (a) Eicher, Theophil; Hauptmann, Siegfried; Speicher, A. *The Chemistry of Heterocycles: Structures, Reactions, Synthesis, and Applications*, 3rd ed.; Wiley-VCH: Weinheim, Germany, 2013; (b) Joule, J. A.; Mills, K. *Heterocyclic Chemistry*, 4th ed.; Blackwell: Malden, MA, 2000

⁵³ (a) Hill, M. D. Recent Strategies for the Synthesis of Pyridine Derivatives. *Chem. – A Eur. J.* **2010**, *16* (40), 12052–12062; (b) Boger, D. L. Diels-Alder Reactions of Heterocyclic Aza Dienes. Scope and Applications. *Chem. Rev.* **1986**, *86* (5), 781–793; (c) KRÖHNKE, F. The Specific Synthesis of Pyridines and Oligopyridines. *Synthesis (Stuttg.)*. **1976**, *1976* (01), 1–24

⁵⁴ (a) Schäfer, P.; Palacin, T.; Sidera, M.; Fletcher, S. P. Asymmetric Suzuki-Miyaura Coupling of Heterocycles via Rhodium-Catalysed Allylic Arylation of Racemates. *Nat. Commun.* **2017**, *8* (1), 15762; (b) Dick, G. R.; Woerly, E. M.; Burke, M. D. A General Solution for the 2-Pyridyl Problem. *Angew. Chemie Int. Ed.* **2012**, *51* (11), 2667–2672; (c) Billingsley, K. L.; Anderson, K. W.; Buchwald, S. L. A Highly Active Catalyst for Suzuki–Miyaura Cross-Coupling Reactions of Heteroaryl Compounds. *Angew. Chemie Int. Ed.* **2006**, *45* (21), 3484–3488

⁵⁵ (a) Bull, J. A.; Mousseau, J. J.; Pelletier, G.; Charette, A. B. Synthesis of Pyridine and Dihydropyridine Derivatives by Regio- and Stereoselective Addition to N-Activated Pyridines. *Chem. Rev.* **2012**, *112* (5), 2642–2713; (b) Nakao, Y.; Kanyiva, K. S.; Hiyama, T. A Strategy for C–H Activation of Pyridines: Direct C-2 Selective

aromatic substitution reactions.⁵⁶ In part because of the orthogonal reactivity of radical intermediates to acidic (i.e., X–H) or Lewis basic functional groups,⁵⁷ Minisci radical addition to pyridines remains a tremendously impactful retrosynthetic tool in complex pyridine synthesis.⁵⁸ However, the typical requirement for strong oxidants and the pronounced substrate-dependent regiocontrol limit the applicability of this strategy in many cases.⁵⁹

Among others, we have utilized an alternative approach to complex (hetero)arene synthesis that operates through single electron reduction of halogenated aryl units to give rise to aryl radicals in a regiospecific manner.^{28,30a} In contrast to arenediazonium salts, this approach draws from a vast collection of stable, often commercially available substrates as

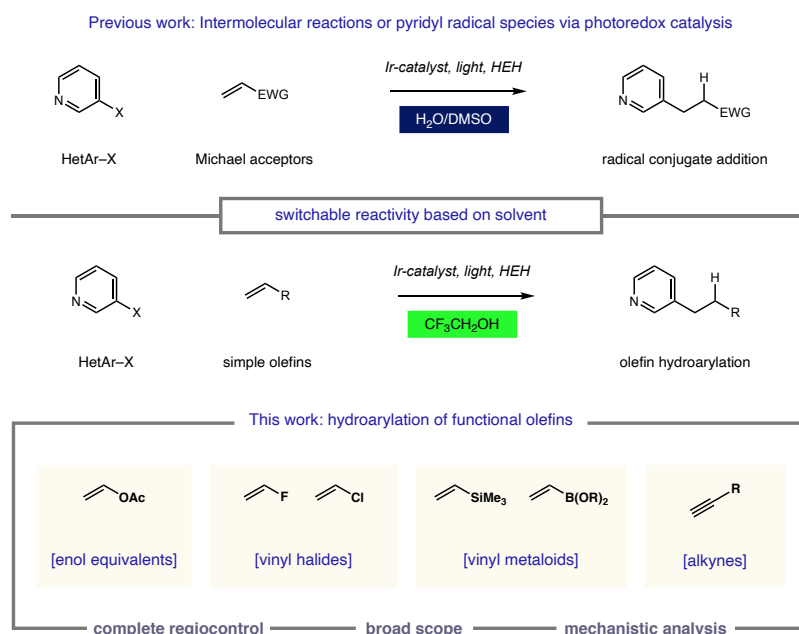


Figure 3.1 Catalytic intermolecular reactions of pyridyl radical intermediates.

Alkenylation of Pyridines by Nickel/Lewis Acid Catalysis. *J. Am. Chem. Soc.* **2008**, *130* (8), 2448–2449; (c) Cho, S. H.; Hwang, S. J.; Chang, S. Palladium-Catalyzed C–H Functionalization of Pyridine N-Oxides: Highly Selective Alkenylation and Direct Arylation with Unactivated Arenes. *J. Am. Chem. Soc.* **2008**, *130* (29), 9254–9256

⁵⁶ Bunnett, J. F.; Zahler, R. E. Aromatic Nucleophilic Substitution Reactions. *Chem. Rev.* **1951**, *49* (2), 273–412

⁵⁷ Yan, M.; Lo, J. C.; Edwards, J. T.; Baran, P. S. Radicals: Reactive Intermediates with Translational Potential. *J. Am. Chem. Soc.* **2016**, *138* (39), 12692–12714

⁵⁸ Punta, C.; Minisci, F. Minisci Reaction: A Friedel-Crafts Type Process with Opposite Reactivity and Selectivity. Selective Homolytic Alkylation, Acylation, Carboxylation and Carbamoylation of Heterocyclic Aromatic Bases. *Trends Heterocycl. Chem.* **2008**, *13*, 1–68

⁵⁹ (a) Duncton, M. A. J. Minisci Reactions: Versatile CH-Functionalizations for Medicinal Chemists. *Medchemcomm* **2011**, *2* (12), 1135–1161; (b) Minisci, F.; Citterio, A.; Giordano, C. Electron-Transfer Processes: Peroxydisulfate, a Useful and Versatile Reagent in Organic Chemistry. *Acc. Chem. Res.* **1983**, *16* (1), 27–32

radical precursors.⁶⁰ While arene activation in this manner requires the action of strong reductants, the introduction of photoredox catalysis has enabled the formation of highly reactive aryl radicals under mild conditions.⁶¹ Our studies in this area have centered on the intermolecular reaction of pyridyl radicals with an array of olefin subtypes. Interestingly, we have developed conditions that enforce divergent reactivity profiles of these typically ambiphilic radicals based solely on the reaction solvent (Figure 3.1) For example, in aqueous dimethyl sulfoxide (DMSO), pyridyl radicals selectively engage electron-poor alkenes through a radical conjugate addition (RCA) mechanism.²⁸ However, the use of 2,2,2-trifluoroethanol (TFE) as the solvent enables highly selective hydroarylation with simple electron-neutral olefins.^{30a} Importantly, this protocol delivers the desired pyridyl products with complete regiocontrol with respect to both the heterocyclic and olefinic subunits (anti-Markovnikov addition) as a complement to recent radical hydroarylation systems reported by Herzon⁶² and Shenvi⁶³ (Markovnikov addition). Here we describe the development of a system based on this mechanistic blueprint that allows for radical hydroarylation of a diverse collection of olefinic substrate classes. Many of these are shown for the first time as substrates under this synthetic disconnection, giving rise to densely functionalized alkylpyridines. In addition, we offer a mechanistic evaluation of these complementary pathways.

⁶⁰ Heinrich, M. R. Intermolecular Olefin Functionalisation Involving Aryl Radicals Generated from Arenediazonium Salts. *Chem. – A Eur. J.* **2009**, *15* (4), 820–833

⁶¹ Shaw, M. H.; Twilton, J.; MacMillan, D. W. C. Photoredox Catalysis in Organic Chemistry. *J. Org. Chem.* **2016**, *81* (16), 6898–6926

⁶² Ma, X.; Herzon, S. B. Intermolecular Hydroarylation of Unactivated Alkenes. *J. Am. Chem. Soc.* **2016**, *138* (28), 8718–8721

⁶³ (a) Green, S. A.; Matos, J. L. M.; Yagi, A.; Shenvi, R. A. Branch-Selective Hydroarylation: Iodoarene–Olefin Cross-Coupling. *J. Am. Chem. Soc.* **2016**, *138* (39), 12779–12782; (b) Green, S. A.; Vásquez-Céspedes, S.; Shenvi, R. A. Iron–Nickel Dual-Catalysis: A New Engine for Olefin Functionalization and the Formation of Quaternary Centers. *J. Am. Chem. Soc.* **2018**, *140* (36), 11317–11324

3.2 Results and Discussion

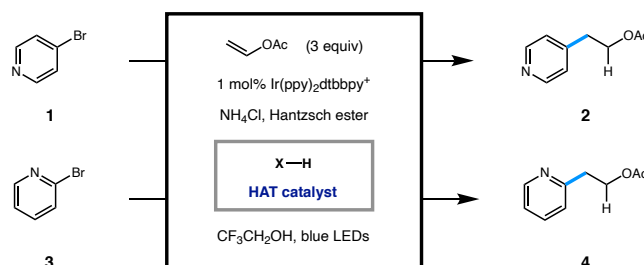
3.2.1 Radical Hydroarylation of Olefinic Substrates

At the outset of this investigation, we treated the feedstock reagent vinyl acetate with 4-bromopyridine (**1**) under conditions that we recently described for anti-Markovnikov hydroarylation of aliphatic olefins.^{30a} More specifically, we employed the commercial iridium-based photoredox catalyst $[\text{Ir}(\text{ppy})_2\text{dtbbpy}]\text{PF}_6$ (1 mol %) and Hantzsch ester (HEH) (1.3 equiv) as a stoichiometric reductant using TFE as the reaction solvent. We found that irradiation of this mixture for 16 h with blue light furnished the desired product 2-(4-pyridyl)ethyl acetate (**2**) in low yield (17%) and that the use of TFE was crucial for product formation. However, significant amounts of oligomeric byproducts where pyridyl units coupled with multiple vinyl acetate equivalents (pyridine:olefin ratios of 1:2, 1:3, etc.) were formed. We reasoned that increasing the rate of hydrogen atom transfer (HAT) to the nucleophilic α -oxy radical intermediate resulting from radical addition to vinyl acetate would preclude further olefin incorporation.⁶⁴

Therefore, we surveyed a number of electrophilic polarity-reversal catalysts (Scheme 3.1).

While the use of the nitroxyl-based HAT catalysts NHPI⁶⁵ and

Scheme 3.1 Anti-Markovnikov Vinyl Acetate Hydroarylation using HAT Catalysts^a



	with HAT catalyst: (5 mol%)	none	NHPI	HOBt	Cy-SH
yield of 2	17%	17%	18%	22%	63%
yield of 4	35%	35%	52%	38%	65%

^aPerformed with $[\text{Ir}(\text{ppy})_2(\text{dtbbpy})]\text{PF}_6$ (1 mol %), Hantzsch ester (1.3 equiv), halopyridine (1 equiv), vinyl acetate (3 equiv) in 2,2,2-trifluoroethanol (0.1 M) at 23 °C for 16 h. Yields were determined by ¹H NMR analysis. ⁴-Bromopyridine hydrochloride was used as the substrate.

⁶⁴ P. Roberts, B. Polarity-Reversal Catalysis of Hydrogen-Atom Abstraction Reactions: Concepts and Applications in Organic Chemistry. *Chem. Soc. Rev.* **1999**, 28 (1), 25–35

⁶⁵ Recupero, F.; Punta, C. Free Radical Functionalization of Organic Compounds Catalyzed by N-Hydroxyphthalimide. *Chem. Rev.* **2007**, 107 (9), 3800–3842

HOBT⁶⁶ did not significantly alter the reaction outcome, employing cyclohexanethiol (5 mol % loading) resulted in significantly improved production of 2 (63% yield).⁶⁷ Here a much cleaner reaction profile was observed, with pyridine production (via radical hydrodehalogenation) being the major alternative pathway. The beneficial effect of the thiol catalyst was also observed using the isomeric pyridyl radical precursor 3 as the limiting reagent, thus delivering the desired adduct 4 in 65% yield. A range of thiol HAT catalysts were surveyed, although no clear trend was observed between thiol electronics and reaction efficiency. Control reactions revealed that both the photocatalyst and light were necessary for effective conversion, and in line with our previous results, acidic additives such as AcOH or NH₄Cl increased the yield (see 3.4.3 Optimization Table for further details, pg. 113). We then applied our optimized conditions to a variety of functionalized alkenes (containing heteroatom substitution) that were absent from the current hydroarylation literature as well as common polymer feedstocks (Table 3.1).⁶⁸ Halogenated alkenes were particularly appealing because of the broad utility of the products for further functionalization. Vinyl bromide was an effective coupling partner under the reaction conditions, affording alkyl bromide 6 in 78% yield with no further reduction to the corresponding ethylpyridine. Exposure of the crude mixture to silica gel resulted in rapid quantitative conversion to the corresponding vinylpyridine, a product typically accessed through Stille cross-coupling with vinylstannane.⁶⁹ 2-Chloropropene was similarly effective,

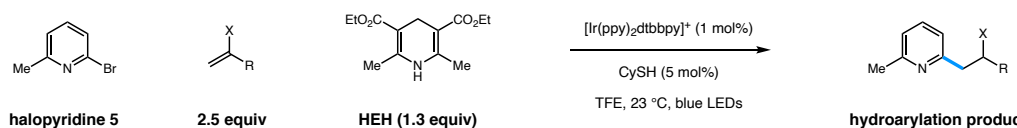
⁶⁶ Cooper, J. C.; Luo, C.; Kameyama, R.; Van Humbeck, J. F. Combined Iron/Hydroxytriazole Dual Catalytic System for Site Selective Oxidation Adjacent to Azaheterocycles. *J. Am. Chem. Soc.* **2018**, *140* (4), 1243–1246

⁶⁷ Dénès, F.; Pichowicz, M.; Povie, G.; Renaud, P. Thiyl Radicals in Organic Synthesis. *Chem. Rev.* **2014**, *114* (5), 2587–2693

⁶⁸ (a) Debuigne, A.; Caille, J.-R.; Jérôme, R. Highly Efficient Cobalt-Mediated Radical Polymerization of Vinyl Acetate. *Angew. Chemie Int. Ed.* **2005**, *44* (7), 1101–1104; (b) Percec, V.; Popov, A. V.; Ramirez-Castillo, E.; Monteiro, M.; Barboiu, B.; Weichold, O.; Asandei, A. D.; Mitchell, C. M. Aqueous Room Temperature Metal-Catalyzed Living Radical Polymerization of Vinyl Chloride. *J. Am. Chem. Soc.* **2002**, *124* (18), 4940–4941

⁶⁹ Over half of the reports on vinylpyridine synthesis from halopyridines come from stannanes. The remaining examples use mostly boron reagents (Scifinder 2018). For an example of Stille coupling to form vinylpyridines, see: Nuñez, A.; Abarca, B.; Cuadro, A. M.; Alvarez-Builla, J.; Vaquero, J. J. Ring-Closing Metathesis Reactions on Azinium Salts: Straightforward Access to Quinolininium Cations and Their Dihydro Derivatives. *J. Org. Chem.* **2009**, *74* (11), 4166–4176

Table 3.1 Anti-Markovnikov Hydroarylation with Pyridyl Radicals: Scope of the Functionalized Olefin^a

olefin	product	compound #: yield	olefin	product	compound #: yield
					
		6: 78%			13: 57%
		7: 70%			14: 72%
		8: 65% ^b			15: 62%
		9: 58% ^c			16: 72%
		10: 68%			17: 75%, 1:1 (E:Z)
		11: 41% ^b			18: 83%, 1:1 (E:Z)
		12: 52%			19: 66%, 1:1 (E:Z)

^aPerformed with [Ir(ppy)₂dtbbpy]PF₆ (1 mol %), Hantzsch ester (1.3 mmol), 2-bromo-6-methylpyridine (1 mmol), alkene (3 mmol), and CySH (5 mol %) in 2,2,2-trifluoroethanol (0.1 M) at 23 °C for 16 h. Isolated yields are shown. ^bThe reaction was performed on a 0.1 mmol scale. ^cThe reaction was performed on a 0.25 mmol scale.

providing secondary alkyl chloride **7** in 70% yield, again without undesired reduction of the resulting chloroalkane, and elimination during purification was not observed in this case. The reaction conditions were also tolerant of alkenyl fluorides, producing alkyl fluoride **8** in good yield. Robust methods for the synthesis of alkyl fluorides are highly prized, particularly where S_N2-type approaches are competitive with elimination byproducts.⁷⁰

⁷⁰ Nielsen, M. K.; Ugaz, C. R.; Li, W.; Doyle, A. G. PyFluor: A Low-Cost, Stable, and Selective Deoxyfluorination Reagent. *J. Am. Chem. Soc.* **2015**, *137* (30), 9571–9574

In a process complementary to the recently described work of Aggarwal,⁷¹ alkenylboronic esters also underwent the reaction smoothly under the reaction conditions. Homobenzylic alkylboronic ester **9** was effectively synthesized through this method (58%) without any undesired protodeboronation or oxidation. Alkenes substituted with main-group elements were also readily incorporated, despite relatively scarce examples of the hydroarylation of these moieties and a dearth of knowledge concerning the reactivity of the resulting α -heteroatomic radicals.⁷² Alkenes substituted with Si, P, and S were all tolerated, delivering **10**, **11**, and **12**, respectively, in good yields (41–68%). We envision this method to be applicable to the synthesis of novel bidentate P,N or S,N ligands that are nontrivial to access through other methods.⁷³

⁷¹ Noble, A.; Mega, R. S.; Pflästerer, D.; Myers, E. L.; Aggarwal, V. K. Visible-Light-Mediated Decarboxylative Radical Additions to Vinyl Boronic Esters: Rapid Access to γ -Amino Boronic Esters. *Angew. Chemie Int. Ed.* **2018**, *57* (8), 2155–2159

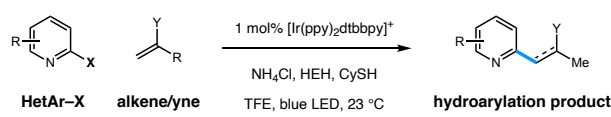
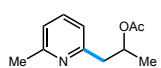
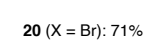
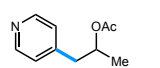
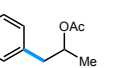
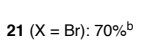
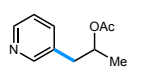
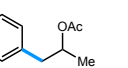
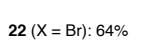
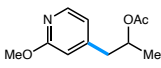
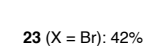
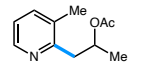
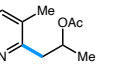
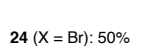
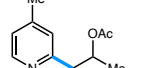
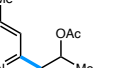
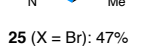
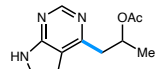
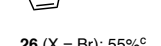
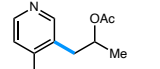
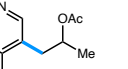
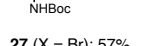
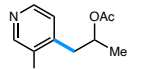
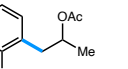
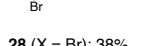
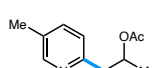
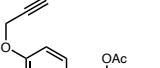
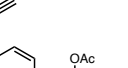
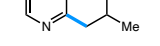
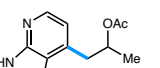
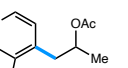
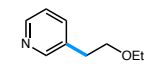
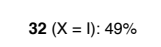
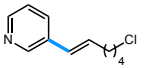
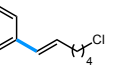
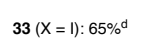
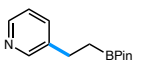
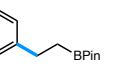
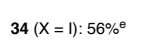
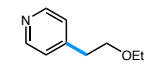
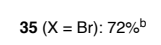
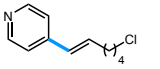
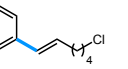
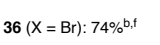
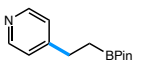
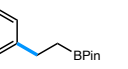
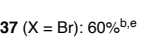
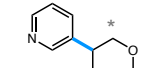
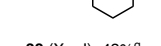
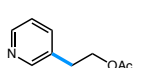
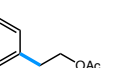
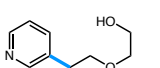
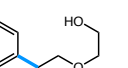
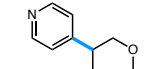
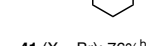
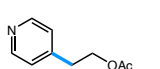
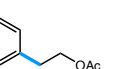
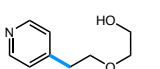
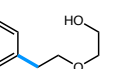
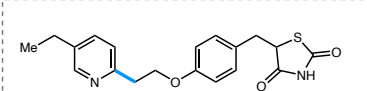
⁷² The reactivity of α -oxy and α -amino radicals is well-studied. For examples of the reactivity of α -oxy radicals, see: (a) Tang, X.; Studer, A. Sodium-Ketyl Radical Anions by Reverse Pinacol Reaction and Their Coupling with Iodoarenes. *Org. Lett.* **2016**, *18* (17), 4448–4450; (b) Zhang, W.-C.; Li, C.-J. Magnesium-Mediated Carbon–Carbon Bond Formation in Aqueous Media: Barbier–Grignard Allylation and Pinacol Coupling of Aldehydes. *J. Org. Chem.* **1999**, *64* (9), 3230–3236 (c) Jeffrey, J. L.; Terrett, J. A.; MacMillan, D. W. C. O–H Hydrogen Bonding Promotes H-Atom Transfer from α C–H Bonds for C-Alkylation of Alcohols. *Science*. **2015**, *349* (6255), 1532 – 1536; (d) Shaw, M. H.; Shurtleff, V. W.; Terrett, J. A.; Cuthbertson, J. D.; MacMillan, D. W. C. Native Functionality in Triple Catalytic Cross-Coupling: C–H Bonds as Latent Nucleophiles. *Science*. **2016**, *352* (6291), 1304 – 1308; (e) Ruiz Espelt, L.; McPherson, I. S.; Wiensch, E. M.; Yoon, T. P. Enantioselective Conjugate Additions of α -Amino Radicals via Cooperative Photoredox and Lewis Acid Catalysis. *J. Am. Chem. Soc.* **2015**, *137* (7), 2452–2455; For a recent example of degradation of α -halo radicals to aldehydes, see: (f) Ma, X.; Herzon, S. B. Synthesis of Ketones and Esters from Heteroatom-Functionalized Alkenes by Cobalt-Mediated Hydrogen Atom Transfer. *J. Org. Chem.* **2016**, *81* (19), 8673–8695

⁷³ Carroll, M. P.; Guiry, P. J. P,N Ligands in Asymmetric Catalysis. *Chem. Soc. Rev.* **2014**, *43* (3), 819–833

The polymer feedstocks vinyl acetate and ethyl vinyl ether both combined with bromopyridine 5 in good yields (57% and 62% yield, respectively), where the remainder of the mass balance was hydrodehalogenated 5 and not higher-order oligomers. Alkyl enol ethers smoothly participated in the reaction to give 14 and 16, both in 72% isolated yield. In addition to heteroatom-substituted alkenes, a number of alkynes were smoothly converted by this system to provide the corresponding vinylpyridines 17–19 as 1:1 mixtures of geometrical isomers (66%–83% yield). In particular, these transformations were unaffected by unprotected alcohols and primary alkyl chlorides. This method provides an alternative to classical Mizoroki–Heck chemistry, which is typically intolerant of such sensitive functionality.⁷⁴

We next explored the scope of the halopyridine component using isopropenyl

Table 3.2 Scope of the Halogenated Pyridine^a

		
HetAr-X	alkene/yne	hydroarylation product
		
20 (X = Br): 71%		
		
21 (X = Br): 70% ^b		
		
22 (X = Br): 64%		
		
23 (X = Br): 42%		
		
24 (X = Br): 50%		
		
25 (X = Br): 47%		
		
26 (X = Br): 55% ^c		
		
27 (X = Br): 57%		
		
28 (X = Br): 38%		
		
29 (X = Br): 50%		
		
30 (X = Br): 26%		
		
31 (X = Br): 38%		
		
32 (X = I): 49%		
		
33 (X = I): 65% ^d		
		
34 (X = I): 56% ^e		
		
35 (X = Br): 72% ^b		
		
36 (X = Br): 74% ^{b,f}		
		
37 (X = Br): 60% ^{b,e}		
		
38 (X = I): 43% ^g		
		
39 (X = I): 56%		
		
40 (X = I): 65%		
		
41 (X = Br): 76% ^b		
		
2 (X = Br): 62% ^b		
		
43 (X = Br): 45% ^b		
		
		Pioglitazone 44 (X = Br): 64%

^aThe reactions were conducted as in Table 3.1. Isolated yields are shown. ^b4-Bromopyridine-HCl was used as the starting material. ^cThe reaction was performed on a 0.5 mmol scale. ^dFormed as a 1.7:1 mixture of olefin isomers. ^eThe reaction was performed on a 0.25 mmol scale. ^fFormed as a 3:1 mixture of olefin isomers. ^gIsolated as a 1.2:1 mixture of regioisomers. The gray asterisk indicates the connectivity of the minor regioisomer.

⁷⁴ Primary alcohols can be oxidized under Heck conditions. For an example, see: Kim, B. H.; Lee, J. G.; Yim, T.; Kim, H.-J.; Lee, H. Y.; Kim, Y. G. Highly Efficient Two-Step Selective Synthesis of 2,6-Dimethylnaphthalene. *Tetrahedron Lett.* **2006**, 47 (44), 7727–7730

acetate as the olefinic coupling partner (as indicated in Table 3.2). The conditions were tolerant of alkyl substituents on the radical precursor (20, 24–25) in addition to other electron-donating groups, including alkoxy (23) and carbamate (27) functions, with only minor deviations in yield (42–57%). Alkyne-containing pyridine 30 could also be synthesized under the reaction conditions (26%), providing exclusive chemoselectivity for alkene addition, leaving a useful functional handle for further manipulation. Fused heterocycles were likewise tolerated, with pyrrolopyrimidine 26 and azaindole 31 being formed in moderate yields (38–55%). Moreover, 3,4-dibromopyridine underwent chemoselective reaction at the more electron-poor 4-position to provide alkylated bromopyridine 28 without subsequent reductive dehalogenation (38%). Here, radical anion fragmentation occurs selectively through cleavage of the weaker C–Br bond (at the 4-position), and 3-bromopyridine (formed via hydrodebromination) constituted the mass balance. To further illustrate the generality of the process for all pyridine regioisomers, representative members of the alkene scope were coupled to 3- and 4-halopyridines (Table 3.2, 32–43). To further demonstrate the scope of the alkene-coupling partner, the antidiabetic pioglitazone⁷⁵ was prepared in a short synthetic sequence (Table 3.2, 44, 64%) that utilized an aryl vinyl ether as olefinic partner. The unique disconnection afforded by this hydroarylation protocol allows for

a highly modular synthesis that would be appealing for early-stage discovery programs.⁷⁶ This photoredox process was amenable to gram-scale synthesis without erosion of the isolated yield (71

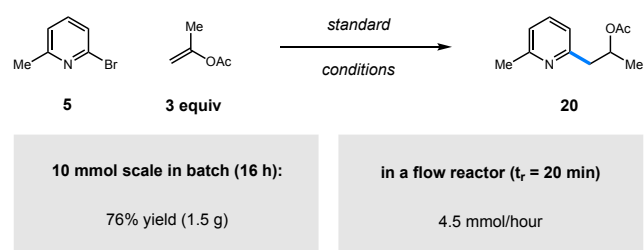


Figure 3.2 Enol acetate hydroarylation on a gram scale.

⁷⁵ SOHDA, T.; IKEDA, H.; MEGURO, K. Studies on Antidiabetic Agents. XII. Synthesis and Activity of the Metabolites of (±)-5-[p-[2-(5-Ethyl-2-Pyridyl)Ethoxy]Benzyl]-2, 4-Thiazolidinedione (Pioglitazone). *Chem. Pharm. Bull. (Tokyo)*. **1995**, *43* (12), 2168–2172

⁷⁶ Beeler, A. B.; Schaus, S. E.; Porco, J. A. Chemical Library Synthesis Using Convergent Approaches. *Curr. Opin. Chem. Biol.* **2005**, *9* (3), 277–284

vs 76%). Compound 20 was synthesized on a 10 mmol scale without any specialized equipment using only 0.1 mol % Ir catalyst (Figure 3.2). It has been well-demonstrated that scale-up of photocatalytic processes can be limited by light penetration;⁷⁷ a common solution to this issue is the use of continuous flow methods,⁷⁸ which have facilitated the large-scale production of active pharmaceutical ingredients.⁷⁹ To demonstrate that our method is amenable to such scale-up procedures, we performed the reaction in a custom-built flow reactor. By the use of a plug-flow regime with a residence time of 20 min, the alkylated product was formed in 75% yield, corresponding to a continuous flow production of 4.5 mmol/h. Further optimization of the flow reactor setup is ongoing within our laboratory.

3.2.2 Mechanistic Investigation.

Having established the utility of pyridyl radical intermediates in the hydroarylation of functionalized olefins, we were interested in gaining a deeper mechanistic understanding of this system. Of particular interest were the following two elements: (i) reductive activation of halopyridine substrates is efficient even in cases where single electron transfer (SET) would appear to be endergonic (as indicated by thermodynamic reduction potentials), and (ii) pyridyl radical species display remarkable chemoselectivity for different olefin types depending on the reaction solvent. Shown in Figure 3.3 is a proposed mechanistic scenario for the dual-catalytic hydroarylation process introduced above. Specifically, reductive quenching of the

⁷⁷ Tucker, J. W.; Zhang, Y.; Jamison, T. F.; Stephenson, C. R. J. Visible-Light Photoredox Catalysis in Flow. *Angew. Chemie Int. Ed.* **2012**, *51* (17), 4144–4147

⁷⁸ (a) Plutschack, M. B.; Pieber, B.; Gilmore, K.; Seeberger, P. H. The Hitchhiker's Guide to Flow Chemistry. *Chem. Rev.* **2017**, *117* (18), 11796–11893; (b) Lima, F.; Kabeshov, M. A.; Tran, D. N.; Battilocchio, C.; Sedelmeier, J.; Sedelmeier, G.; Schenkel, B.; Ley, S. V. Visible Light Activation of Boronic Esters Enables Efficient Photoredox C(Sp²)–C(Sp³) Cross-Couplings in Flow. *Angew. Chemie Int. Ed.* **2016**, *55* (45), 14085–14089

⁷⁹ (a) Beatty, J. W.; Douglas, J. J.; Miller, R.; McAtee, R. C.; Cole, K. P.; Stephenson, C. R. J. Photochemical Perfluoroalkylation with Pyridine N-Oxides: Mechanistic Insights and Performance on a Kilogram Scale. *Chem* **2016**, *1* (3), 456–472; (b) Caron, A.; Hernandez-Perez, A. C.; Collins, S. K. Synthesis of a Carprofen Analogue Using a Continuous Flow UV-Reactor. *Org. Process Res. Dev.* **2014**, *18* (11), 1571–1574; (c) Šterk, D.; Jukič, M.; Casar, Z. Application of Flow Photochemical Bromination in the Synthesis of a 5-Bromomethylpyrimidine Precursor of Rosuvastatin: Improvement of Productivity and Product Purity. *Org. Process Res. Dev.* **2013**, *17* (1), 145–151; (d) Lévesque, F.; Seeberger, P. H. Continuous-Flow Synthesis of the Anti-Malaria Drug Artemisinin. *Angew. Chemie Int. Ed.* **2012**, *51* (7), 1706–1709

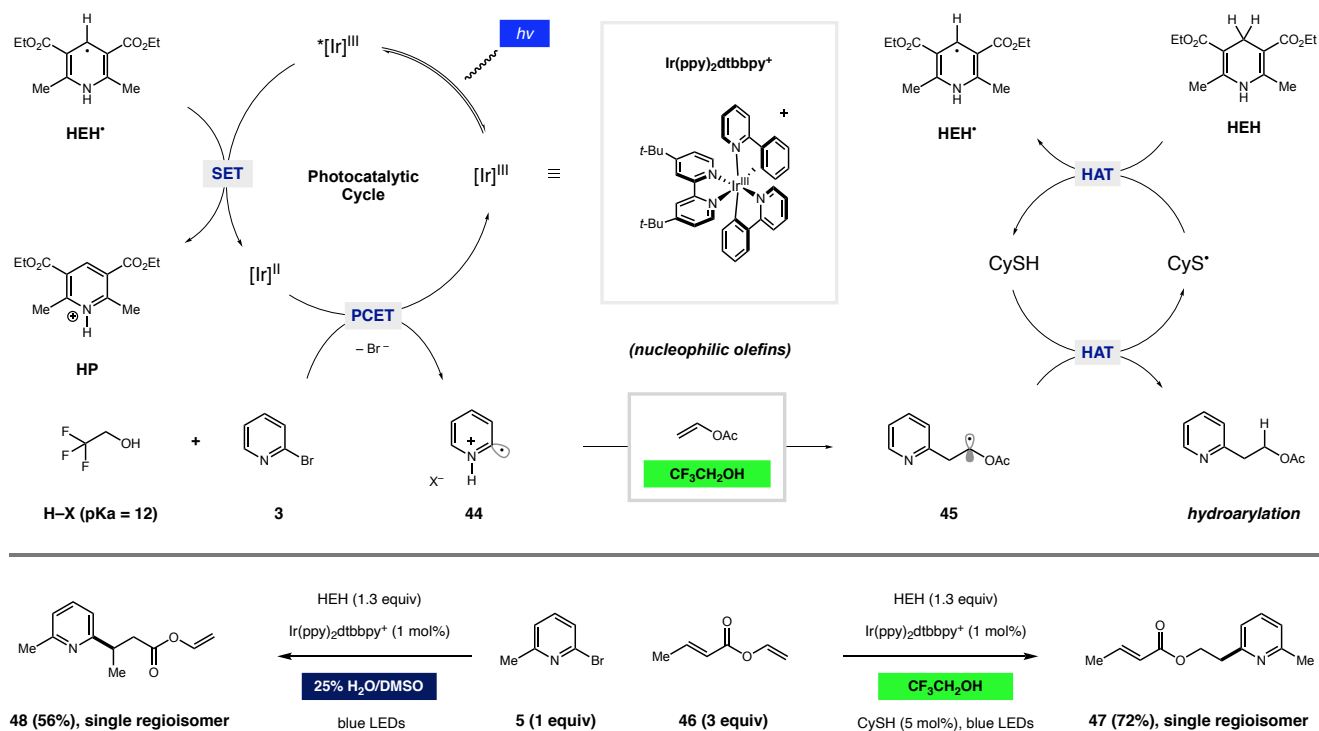


Figure 3.3 Mechanistic proposal: the solvent dictates the nature of the pyridyl radical, imparting divergent chemoselectivity.

photoexcited iridium catalyst ($^*[\text{Ir}]^{\text{III}}$) would give rise to the reducing $[\text{Ir}]^{\text{II}}$ species ($E^0_{1/2} = -1.51 \text{ V vs SCE}$). This mechanism would likely be initiated by oxidation of a sacrificial amount of HEH, as supported by Stern–Volmer quenching studies, in agreement with previous studies by Knowles.⁸⁰ Reduction of bromopyridine substrate **3** via proton-coupled electron transfer (PCET) (involving TFE as the proton source) followed by rapid mesolytic cleavage would provide protonated pyridine radical **44** and an equivalent of bromide. Regioselective radical addition to the terminal carbon of vinyl acetate (like other nucleophilic olefins) would furnish radical species **45**, which would undergo polarity-matched HAT from the thiol catalyst, concurrently producing the hydroarylation product and thiyl species. Regeneration of the HAT catalyst with HEH would deliver the corresponding dihydropyridine radical (HEH \cdot), a mild

⁸⁰ Rono, L. J.; Yayla, H. G.; Wang, D. Y.; Armstrong, M. F.; Knowles, R. R. Enantioselective Photoredox Catalysis Enabled by Proton-Coupled Electron Transfer: Development of an Asymmetric Aza-Pinacol Cyclization. *J. Am. Chem. Soc.* **2013**, *135* (47), 17735–17738

reductant that would close the photoredox catalytic cycle, delivering the corresponding pyridinium (HP).

Key to this electrophilic radical reactivity is the notorious H-bond-donating (but poorly H-bond-accepting) solvent TFE.⁸¹ Indeed, when the diene compound vinyl crotonate (46) was reacted in trifluoroethanol, the pyridyl radical derived from bromopyridine 5 engaged the nucleophilic alkene, giving rise to hydroarylation product 47 as a single regioisomer (72% yield). In contrast, activation of the same radical precursor with the same catalyst in aqueous DMSO as the solvent (25% v/v H₂O/ DMSO) resulted in exclusive radical conjugate addition to the Michael acceptor, affording 48 as a single regioisomer (56% yield). Regiochemical analysis in these experiments was conducted by GC and, in both cases, operates through different reactive intermediates, as dictated by the solvent.^{30a} Further evaluation of these scenarios is presented in the following sections.

Proton Coupled Electron Transfer

As indicated above, we propose that pyridyl radical formation occurs primarily through a reductive quenching pathway of the iridium photocatalyst. However, analysis of the salient reduction potentials in this system is complicated. Accurate measurement of the reduction potentials of halogenated pyridines remains a challenge because fragmentation of the resulting radical anions is rapid and pyridyl radicals readily undergo reduction to the corresponding anions. However, the reduction potential of 2-bromopyridine has been reported to be between -1.80^{82} and -2.29 V vs SCE,⁸³ which is significantly beyond the reducing ability of the Ir

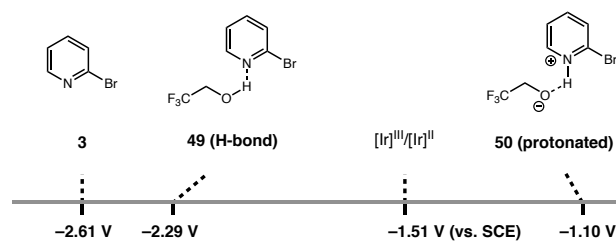
⁸¹ Bégué, J.-P.; Bonnet-Delpon, D.; Crousse, B. Fluorinated Alcohols: A New Medium for Selective and Clean Reaction. *Synlett* **2004**, 2004 (01), 18–29

⁸² Volke, J.; Holubek, J. Polarography of Heterocyclic Aromatic Compounds. XIII. Polarographic Fission of Carbon-Halogen Bonds in Monohalogenopyridines. *Collect. Czechoslov. Chem. Commun.* **1962**, 27, 680–692

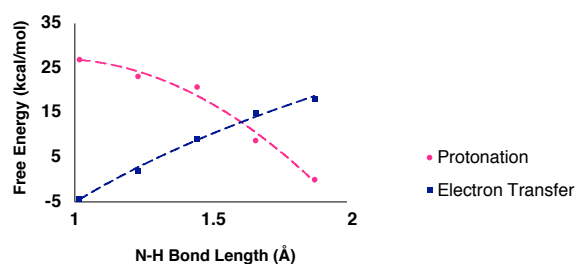
⁸³ (a) Enemærke, R. J.; Christensen, T. B.; Jensen, H.; Daasbjerg, K. Application of a New Kinetic Method in the Investigation of Cleavage Reactions of Haloaromatic Radical Anions. *J. Chem. Soc. Perkin Trans. 2* **2001**, No. 9, 1620–1630; (b) Andrieux, C. P.; Blocman, C.; Dumas-Bouchiat, J. M.; Saveant, J. M. Heterogeneous and Homogeneous Electron Transfers to Aromatic Halides. An Electrochemical Redox Catalysis Study in the Halobenzene and Halopyridine Series. *J. Am. Chem. Soc.* **1979**, 101 (13), 3431–3441

Scheme 3.2 Proposed Mechanism of Reduction: PCET^a

(A) Calculated reduction potentials of pertinent mechanistic component:



(B) Energetic consequences of bromopyridine (3) / TFE interaction



^aDFT calculations were performed at the uB3LYP/6-311+G(d,p)/CPCM=DMSO level of theory

catalyst ($E_{1/2}^0 = -1.51$ V vs SCE).

Although protonation of the halopyridine substrate would significantly decrease the reduction potential ($E_{1/2}^0 = -1.10$ V vs SCE), a cursory analysis of the pK_a values of TFE ($pK_a = 12$ in DMSO) and 2-bromopyridinium ($pK_a = 0.5$ in DMSO) does not support the formation of a discrete pyridinium salt. Thus, we reason that reductive activation of pyridine substrates in TFE occurs through a PCET mechanism.⁸⁴

The effect of pyridine protonation on the energetics of electron transfer has been well-studied, particularly within the context of CO₂ reduction.⁸⁵ However, reports detailing the exact impact of protonation on the pyridine reduction potential remain disparate. Because the complications associated with halopyridine reduction potential measurements (vide supra) are compounded by the fact that TFE has a narrow usable electrochemical window, we turned to density functional theory (DFT) calculations to further interrogate this step (Scheme 3.2A). At the uB3LYP level of theory, the reduction potential of 2-bromopyridine was calculated to be

⁸⁴ (a) Tarantino, K. T.; Liu, P.; Knowles, R. R. Catalytic Ketyl-Olefin Cyclizations Enabled by Proton-Coupled Electron Transfer. *J. Am. Chem. Soc.* **2013**, *135* (27), 10022–10025; (b) Weinberg, D. R.; Gagliardi, C. J.; Hull, J. F.; Murphy, C. F.; Kent, C. A.; Westlake, B. C.; Paul, A.; Ess, D. H.; McCafferty, D. G.; Meyer, T. J. Proton-Coupled Electron Transfer. *Chem. Rev.* **2012**, *112* (7), 4016–4093

⁸⁵ (a) Yan, Y.; Zeitler, E. L.; Gu, J.; Hu, Y.; Bocarsly, A. B. Electrochemistry of Aqueous Pyridinium: Exploration of a Key Aspect of Electrocatalytic Reduction of CO₂ to Methanol. *J. Am. Chem. Soc.* **2013**, *135* (38), 14020–14023; (b) Keith, J. A.; Carter, E. A. Theoretical Insights into Pyridinium-Based Photoelectrocatalytic Reduction of CO₂. *J. Am. Chem. Soc.* **2012**, *134* (18), 7580–7583

-2.61 V vs SCE,⁸⁶ and the potentials of H-bonded substrate 49 ($E_{1/2}^0 = -2.29$ V vs SCE; N-H-O bond length = 2 Å) and fully protonated substrate 50 ($E_{1/2}^0 = -1.1$ V vs SCE; bond length = 1.1 Å) were also computed. Indeed, the measured reduction potential of the [Ir]^{II} catalytic species ($E_{1/2}^0 = -1.51$ V vs SCE) lies squarely between these values.¹³ As shown in Scheme 3.2B, protonation of the neutral species with TFE is endergonic by 27 kcal/mol but is thermoneutral after reduction. Similarly, reduction of bromopyridine at 2 Å is endergonic by 18.1 kcal/mol but exergonic by 9.4 kcal/mol after protonation. The lowest energetic barrier (where the two curves intersect) was calculated to be 13 kcal/mol at a N-H bond length of 1.55 Å, a reasonable energetic barrier for the proposed PCET event. An endergonic electron transfer of this type is feasible from a ground-state reductant because of the highly exergonic heterolytic cleavage event that occurs immediately after reduction (i.e., the Curtin-Hammett principle). While this principle could account for a decoupled protonation/electron transfer sequence, we posit that a concerted mechanism is operative.

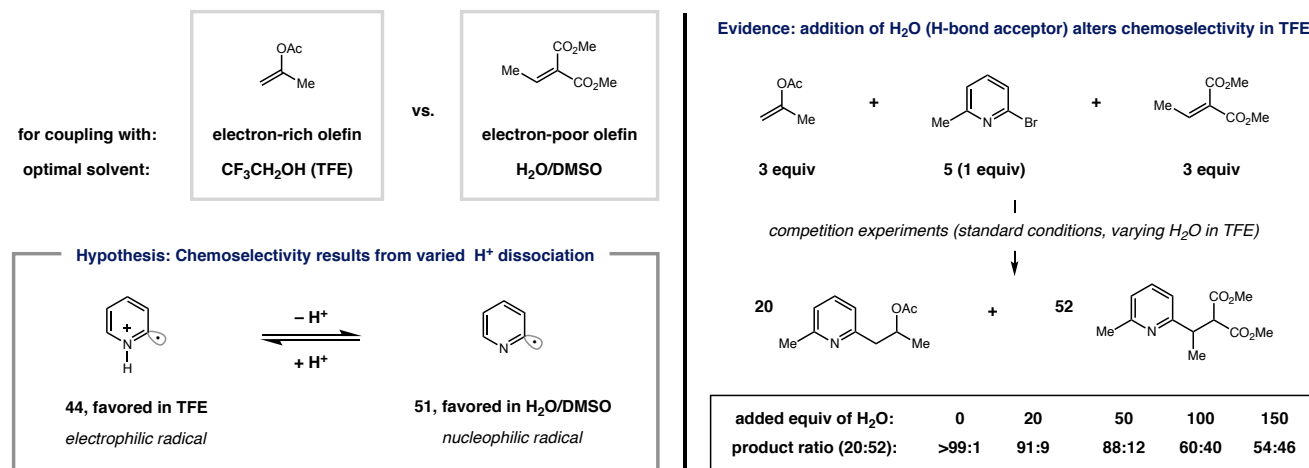
Chemoselective C-C Bond Formation

Among the most interesting features of this pyridyl-radical-based strategy is the highly pronounced chemoselectivity that is imparted by the chosen reaction solvent. Shown in Scheme 3.3 are two electronically diverse olefins along with the optimal reaction solvents for their intermolecular couplings with pyridyl radicals. Because high chemoselectivity for either electron-rich or -poor olefins has been observed (vide supra), we hypothesize that these complementary systems differ in the identity of the pertinent pyridyl radical species. More specifically, we propose that protonated, electrophilic radical species (e.g., 44) are active in

⁸⁶ DFT calculations were also performed at different levels of theory with different solvation parameters, giving a range of values for pyridine reduction potentials (see Table 3.14, pg. 182)

TFE, while proton dissociation in polar, H-bond-accepting solvents favors neutral, nucleophilic

Scheme 3.3 Proposal for the Observed Solvent-Dependent Chemoselectivity of Pyridyl Radicals^a



^aThe competition experiments were performed with [Ir(ppy)₂(dtbbpy)]PF₆ (1 mol %), Hantzsch ester (1.3 equiv), 2-bromo-6-methylpyridine (1 equiv), dimethylethylidene malonate (3 equiv), and isopropenyl acetate (3 equiv) in 2,2,2-trifluoroethanol (0.1 M) at 23 °C for 16 h.

aryl radicals (e.g., 51).⁸⁷

As an excellent H-bond donor and a weak H-bond acceptor, TFE has the ability to form strong H-bonding networks that effectively stabilize anions or protonate very weak bases.³³ As a result, the use of TFE as the reaction solvent has led to divergent selectivity profiles in other systems that are reminiscent of our findings.⁸¹ To investigate the relevance of this solvent property in our systems, we attempted to overturn the observed pyridyl radical chemoselectivity through a series of competition experiments. As indicated in Scheme 3.3, treatment of 5 with both electron-rich isopropenyl acetate and electron-poor dimethylethylidene malonate (3 equiv each) under standard conditions in TFE led to the exclusive production of 20. However, addition of various amounts of water was accompanied by increasingly significant formation of the radical conjugate addition product 52. With 150 equiv of H₂O, the two products were formed in nearly equal amounts, presumably resulting

⁸⁷ Joerg, S.; S. Drago, R.; Adams, J. Donor–Acceptor and Polarity Parameters for Hydrogen Bonding Solvents. *J. Chem. Soc. Perkin Trans. 2* **1997**, No. 11, 2431–2438

from increased dissociation of the proton from the pyridyl radical species by the H-bond acceptor H₂O.⁸⁸ Addition of acids to the same mixtures in DMSO did not have an impact on the chemoselectivity, which is also consistent with the suggestion that protons are highly dissociated from the pyridyl radical species in polar (aqueous) solvents.

An alternative set of reactive intermediates that could potentially account for the observed solvent-based complementary selectivity of this method could arise from differential rates of radical anion fragmentation depending on the solvent. In this scenario, an α -bromo, α -amino radical (resulting directly from PCET) would undergo C–C bond formation prior to bromide dissociation, presumably as an intermediate in radical conjugate addition (i.e., aqueous DMSO). Indeed, Weaver has proposed that the rate of radical anion fragmentation is responsible for altered selectivity in reductive photoredox processes of 2-haloazoles (where differential reactivity resulted from different halogens).⁸⁹ Along the same lines, it has been shown that the rate of 2-halopyridine (2-X-pyr) radical anion fragmentation decreases significantly in the series X = I > Br > Cl \gg F.^{83a} While the fluoropyridine-based radical anion persists long enough to observe reversible redox by CV, bromopyridine radical anion fragmentation is exceedingly rapid, as measured by Saveant and co-workers.⁹⁰ Solvent polarity has also been shown to alter the fragmentation rate to a lesser extent, but unimolecular fragmentation rates remain significantly higher than the relevant bimolecular addition rates for aryl radical addition to olefins.⁹¹

⁸⁸ Krishnan, R.; Fillingim, T. G.; Lee, J.; Robinson, G. W. Solvent Structural Effects on Proton Dissociation. *J. Am. Chem. Soc.* **1990**, *112* (4), 1353–1357

⁸⁹ (a) Arora, A.; Teegardin, K. A.; Weaver, J. D. Reductive Alkylation of 2-Bromoazoles via Photoinduced Electron Transfer: A Versatile Strategy to Csp²–Csp³ Coupled Products. *Org. Lett.* **2015**, *17* (15), 3722–3725; (b) Singh, A.; Arora, A.; Weaver, J. D. Photoredox-Mediated C–H Functionalization and Coupling of Tertiary Aliphatic Amines with 2-Chloroazoles. *Org. Lett.* **2013**, *15* (20), 5390–5393; (c) Arora, A.; Weaver, J. D. Photocatalytic Generation of 2-Azoly radicals: Intermediates for the Azoylation of Arenes and Heteroarenes via C–H Functionalization. *Org. Lett.* **2016**, *18* (16), 3996–3999

⁹⁰ Andrieux, C. P.; Robert, M.; Saveant, J.-M. Role of Environmental Factors in the Dynamics of Intramolecular Dissociative Electron Transfer. Effect of Solvation and Ion-Pairing on Cleavage Rates of Anion Radicals. *J. Am. Chem. Soc.* **1995**, *117* (36), 9340–9346

⁹¹ Giese, B. Formation of CC Bonds by Addition of Free Radicals to Alkenes. *Angew. Chemie Int. Ed. English* **1983**, *22* (10), 753–764

Radical Termination after Alkene Addition.

During our investigations of the addition of pyridyl radicals to olefins, we have observed different radical termination mechanisms that are highly dependent on the employed alkene subtype. While different reaction modes often lead to identical outcomes (e.g., Giese termination via HAT⁹² or a reduction/enolate protonation sequence⁹³), they could be expected to have discrete implications for photocatalyst turnover or, more importantly, the structural nature of the product. Using combinations of deuterium-labeled HEH and solvents, we have shown that dehydroalanine-derived **53** undergoes essentially exclusive reduction and enolate protonation to give the desired amino acid products.⁹⁴ In contrast, radicals **54** and **55** receive α -protons or deuterons primarily from HEH, indicating HAT as the primary termination events (>80% incorporation of the label from HEH rather than the solvent).^{28,30a} When

coupling to more nucleophilic vinyl heteroatoms is considered, both oxidation and HAT processes of the intermediate radical (e.g., **56** derived from vinyl acetate) are relevant, as they would likely be product-determining. For example, in a method described by Buchwald, a similar α -oxy radical generated by Meerwein addition to an enol acetate is efficiently

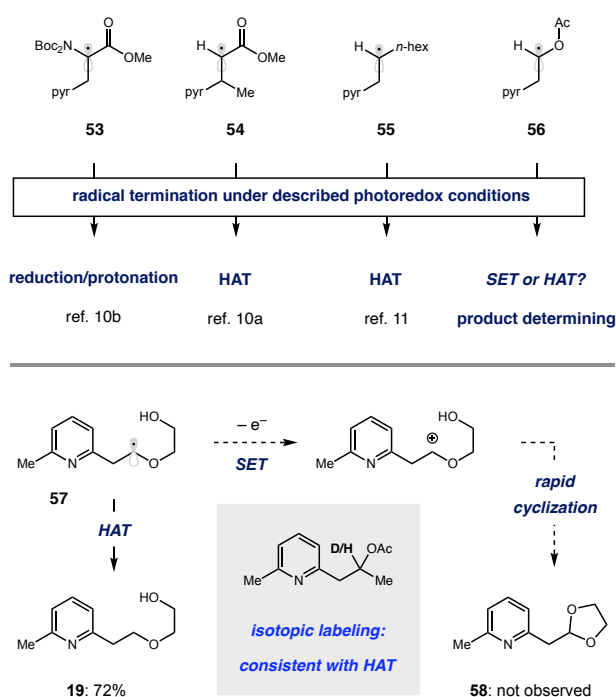


Figure 3.4 Mechanisms of radical termination.

⁹² Giese, B.; González-Gómez, J. A.; Witzel, T. The Scope of Radical CC-Coupling by the “Tin Method.” *Angew. Chemie Int. Ed. English* **1984**, *23* (1), 69–70

⁹³ Yin, Y.; Dai, Y.; Jia, H.; Li, J.; Bu, L.; Qiao, B.; Zhao, X.; Jiang, Z. Conjugate Addition–Enantioselective Protonation of N-Aryl Glycines to α -Branched 2-Vinylazaarenes via Cooperative Photoredox and Asymmetric Catalysis. *J. Am. Chem. Soc.* **2018**, *140* (19), 6083–6087

⁹⁴ Aycock, R. A.; Vogt, D. B.; Jui, N. T. A Practical and Scalable System for Heteroaryl Amino Acid Synthesis. *Chem. Sci.* **2017**, *8* (12), 7998–8003

oxidized by ferrocinium to provide an aldehyde product.⁹⁵ However, the conditions that are introduced here appear to enforce termination via HAT, even though single-electron oxidation of 56 would be facile ($E^0_{1/2} = 0.21$ V vs SCE).

Evidence for product formation via terminal HAT is offered in Figure 3.4, where the two potentially competing pathways involving radical intermediate 57 are illustrated. Work by Moeller⁹⁶ and Horner and Newcomb⁹⁷ indicates that oxidation to the corresponding cation would be followed by exceedingly rapid cyclization to form dioxolane 58. However, hydroarylation product 19 was delivered in 72% yield without any indication of 58 by NMR or GC–MS analysis. Furthermore, isotopic labeling experiments involving deuterated HEH and/or solvent were consistent with this proposal (see 3.4.7 Mechanistic Investigation for further details, pg. 157). The discrepancy between these results and the system reported by Buchwald⁹⁵ arises from effective concentration of the putative oxidant: 10 mol % Cp_2Fe^+ (generated through highly exergonic reduction of arenediazonium salts) versus the minute concentration of photooxidant.

Alternative Redox Pathways.

Although the mechanistic analyses that we have presented are consistent with experimental data, the observed results likely arise from an ensemble of related mechanistic pathways. For example, the proposed role of the stoichiometric reductant (HEH) is highly consistent with previous reports, facilitating product formation through sequential HAT and SET steps. However, the order of these events is experimentally ambiguous, as HEH

⁹⁵ Chernyak, N.; Buchwald, S. L. Continuous-Flow Synthesis of Monoarylated Acetaldehydes Using Aryldiazonium Salts. *J. Am. Chem. Soc.* **2012**, *134* (30), 12466–12469

⁹⁶ Campbell, J. M.; Xu, H.-C.; Moeller, K. D. Investigating the Reactivity of Radical Cations: Experimental and Computational Insights into the Reactions of Radical Cations with Alcohol and p-Toluene Sulfonamide Nucleophiles. *J. Am. Chem. Soc.* **2012**, *134* (44), 18338–18344

⁹⁷ Horner, J. H.; Taxil, E.; Newcomb, M. Laser Flash Photolysis Kinetic Studies of Enol Ether Radical Cations. Rate Constants for Heterolysis of α -Methoxy- β -Phosphatoxyalkyl Radicals and for Cyclizations of Enol Ether Radical Cations. *J. Am. Chem. Soc.* **2002**, *124* (19), 5402–5410

consumption via the same steps in reverse order (SET then HAT) would reasonably lead to the same experimental results.

To further evaluate the validity of the proposed photoredox pathway, we conducted a series of temporal studies. Under these conditions, hydroarylation of isopropenyl acetate (to give 20) exhibited zeroth-order kinetics with respect to the starting materials and catalyst in a manner that was highly dependent on the light source,⁹⁸ as shown in Figure 3.5. In conjunction with the finding that the

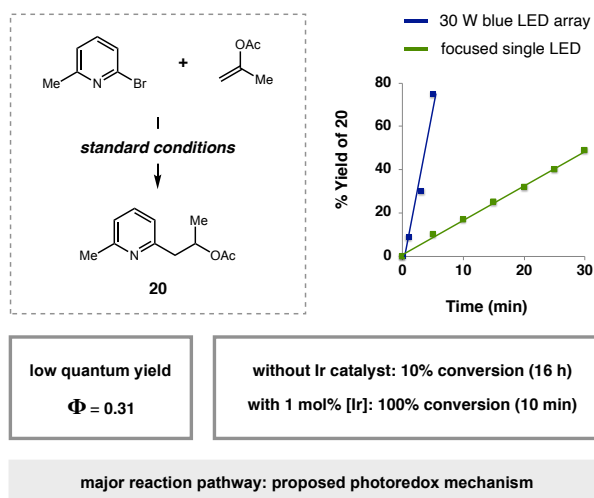


Figure 3.5 Temporal evaluation of the reaction profile.

benchmark reaction reached completion within 10 min, these results led us to question the degree of radical chain character of this process.⁹⁹ However, the relatively low quantum yield of this process ($\Phi = 0.31$) indicates that photosensitized processes are dominant. Control experiments showed that formation of 20 can occur in the absence of the iridium catalyst, but the reaction rate is considerably lower ($\sim 10\%$ yield after 16 h vs 72% yield after 10 min; see 3.4.7 Mechanistic Investigation for further details, pg.171). We suggest that the catalyst-free reaction arises from reduction of the halopyridine by the HEH excited state.¹⁰⁰ Charge transfer complexes between HEH and bromopyridine were not observed in either the ground state via ^1H NMR analysis or the excited state via UV/vis spectroscopy (see 3.4.7 Mechanistic

⁹⁸ Le, C. “Chip”; Wismer, M. K.; Shi, Z.-C.; Zhang, R.; Conway, D. V.; Li, G.; Vachal, P.; Davies, I. W.; MacMillan, D. W. C. A General Small-Scale Reactor To Enable Standardization and Acceleration of Photocatalytic Reactions. *ACS Cent. Sci.* **2017**, *3* (6), 647–653

⁹⁹ Cismesia, M. A.; Yoon, T. P. Characterizing Chain Processes in Visible Light Photoredox Catalysis. *Chem. Sci.* **2015**, *6* (10), 5426–5434

¹⁰⁰ Huang, W.; Cheng, X. Hantzsch Esters as Multifunctional Reagents in Visible-Light Photoredox Catalysis. *Synlett* **2017**, *28* (02), 148–158

Investigation for further details, pg. 169). Moreover, alteration of the catalyst properties had a noticeable impact on the overall reaction efficiency (see 3.4.7 Mechanistic Investigation for further details, pg. 172).⁹⁹ Taken in aggregate, these findings implicate the outlined catalytic manifold as the major contributor to product formation in this system.⁹⁹

3.3 Conclusions

A general and efficient method for the hydroarylation of electron-rich olefins has been developed. Addition of a thiol polarity-reversal catalyst promotes a rapid intermolecular HAT step that prevents side reactions such as olefin polymerization and single-electron oxidation to provide the anti-Markovnikov products exclusively. Investigation of the reaction mechanism revealed a solvent-dependent mechanistic divergence. Use of the highly coordinating solvent TFE leads to a protonated, electrophilic pyridyl radical that is polarity-matched for alkene addition with electron-rich olefins. Use of a H-bond-accepting medium such as aqueous DMSO leads to a dissociated, neutral pyridyl radical that is polarity-matched for electron-poor olefins. We believe that these data will provide a greater rationale for chemistries utilizing heteroaryl radicals and expand the scope and understanding of related radical–olefin couplings.

3.4 Supporting Information

3.4.1 General Information

General Reagent Information

All reactions were set up on the bench top and conducted under nitrogen atmosphere while subject to irradiation from blue LEDs (LEDwholesalers PAR38 Indoor Outdoor 16-Watt LED Flood Light Bulb, Blue; or Hydrofarm® PPB1002 PowerPAR LED Bulb-Blue 15W/E27 (available from Amazon)). Flash chromatography was carried out using Siliaflash® P60 silica gel obtained from Silicycle. Photoredox catalyst, $[\text{Ir}(\text{ppy})_2(\text{dtbbpy})]\text{PF}_6$, was prepared according to a literature procedure.¹ Halogenated heteroarenes and heteroalkenes were purchased from Aldrich Chemical Co., Alfa Aesar, Acros Organics, Combi-Blocks, or Oakwood Chemicals and were used as received. Non-commercial alkenes were prepared according to the designated procedures in section IV, Preparation of Starting Materials. Molecular sieves were activated in a commercial microwave oven then cooled under vacuum. 2,2,2-trifluoroethanol was purchased from Oakwood Chemicals and was degassed for 30 minutes prior to use by sonication under mild vacuum.

General Analytical Information

Unless otherwise noted, all yields refer to isolated yields. New compounds were characterized by NMR, IR spectroscopy, and high-resolution mass spectrometry (HRMS). NMR data were recorded on one of six spectrometers: Bruker 600 MHz, INOVA 600 MHz, INOVA 500 MHz, VNMR 400 MHz, INOVA 400 MHz, or Mercury 300 MHz. Chemical shifts (δ) are internally referenced to residual protio solvent (CDCl_3 : δ 7.26 ppm for ^1H NMR and 77.2 ppm for ^{13}C NMR; CD_3OD : δ 3.31 ppm for ^1H NMR and 49.1 ppm for ^{13}C NMR; THF-d_8 : δ 3.58 ppm for ^1H NMR and 67.6 ppm for ^{13}C NMR). ^{11}B NMR were obtained on an INOVA 600 MHz spectrometer using NaBH_4 in D_2O as an external reference. IR spectra were obtained with a

Thermo Scientific Nicolet iS10 Fourier transform infrared spectrophotometer. Mass spectrometry data were obtained from the Emory Mass Spectrometry Center using a Thermo LTQ-FTMS high-resolution mass spectrometer. Adduct yields for optimization data were obtained via H^1 NMR with an Inova 500 MHz NMR using 1,1,2,2-tetrachloroethane as internal standard, with relaxation delay set to 5 seconds. Preparative HPLC was performed using an Agilent 1260 HPLC using an Eclipse XDB-C18 Prep HT column. Eluents used were unmodified unless otherwise stated.

3.4.2 General Procedures

General Procedure A: Hydropyridylation of Alkenes

An oven-dried screw-top test tube equipped with a stir bar was sealed with a PTFE-faced silicon septa and cooled to room temperature under N_2 atmosphere. The tube was charged with $Ir(ppy)_2dtbbpy \cdot PF_6$ (1 mol%), Hantzsch ester (1.3 equiv), NH_4Cl (2 equiv), halopyridine (if solid, 1 equiv), and alkene (if solid, 3 equiv). The atmosphere was exchanged by applying vacuum and backfilling with N_2 (this process was conducted a total of three times). Under N_2 atmosphere, the tube was charged with alkene (if liquid, 3 equiv), halopyridine (if liquid, 1 equiv), cyclohexanethiol (5 mol%), and separately degassed 2,2,2-trifluoroethanol (0.1 M) via syringe. The resulting mixture was stirred at 1200 RPM for 16 hours under irradiation with a blue LED. The crude reaction mixture was quenched with saturated sodium bicarbonate and extracted with dichloromethane (3 x 20 mL). The extracts were combined, dried over sodium sulfate, filtered, and concentrated under reduced pressure. The residue was purified by flash column chromatography using the indicated solvent mixture to afford the title compound.

General Procedure B: Hydropyridylation of Alkenes with Hydrolytic Work Up

An oven-dried screw-top test tube equipped with a stir bar was sealed with a PTFE-faced silicon septa and cooled to room temperature under N₂ atmosphere. The tube was charged with Ir(ppy)₂dtbbpy•PF₆ (1 mol%), Hantzsch ester (1.3 equiv), NH₄Cl (2 equiv), halopyridine (if solid, 1 equiv), and alkene (if solid, 3 equiv). The atmosphere was exchanged by applying vacuum and backfilling with N₂ (this process was conducted a total of three times). Under N₂ atmosphere, the tube was charged with alkene (if liquid, 3 equiv), halopyridine (if liquid, 1 equiv), cyclohexanethiol (5 mol%), and separately degassed 2,2,2-trifluoroethanol (0.1 M) via syringe. The resulting mixture was stirred at 1200 RPM for 16 hours under irradiation with a blue LED. The crude reaction mixture was transferred to a 50 mL round-bottom flask. The solvent was removed in vacuo and the residue was reconstituted in 15 mL of tetrahydrofuran and 3 mL of water. A stir bar was added and the flask was charged with LiOH (6.5 equiv). A reflux condenser was attached, and the flask was heated to 60 °C in an oil bath with stirring for 2 hours to hydrolyze Hantzsch pyridine. Upon cooling to room temperature, the reaction was quenched with water (30 mL) and extracted with ethyl acetate (3 x 20 mL). The extracts were combined, dried over sodium sulfate, filtered, and concentrated under reduced pressure. The residue was purified by flash column chromatography using the indicated solvent mixture to afford the title compound.

General Procedure C: Hydropyridylation of Complex Alkenes for Reaction Optimization

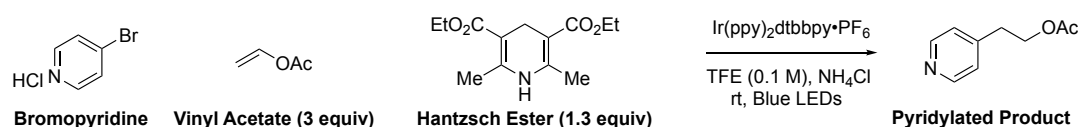
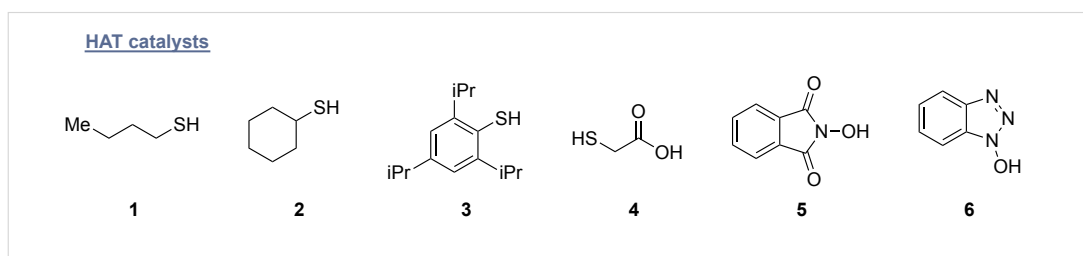
An oven-dried screw-top test tube equipped with a stir bar was sealed with a PTFE-faced silicon septa and cooled to room temperature under N₂ atmosphere. The tube was charged with Ir(ppy)₂dtbbpy•PF₆ (1 mol%), Hantzsch ester (1.3 equiv), NH₄Cl (2 equiv), 4-bromopyridine hydrochloride (1 equiv). The atmosphere was exchanged by applying vacuum and backfilling with N₂ (this process was conducted a total of three times). Under N₂ atmosphere, the tube was

charged with alkene (if liquid, 3 equiv), halopyridine (if liquid, 1 equiv) cyclohexanethiol (5 mol%), and separately degassed 2,2,2-trifluoroethanol (0.1 M) via syringe. The resulting mixture was stirred at 1200 RPM for 16 hours under irradiation with a blue LED. The crude reaction mixture was quenched with saturated sodium bicarbonate and extracted with dichloromethane (3 x 20 mL). The extracts were combined, dried over sodium sulfate, filtered, and concentrated under reduced pressure. 1,1,2,2-Tetrachloroethane (1 equiv) was added as an internal standard to the crude residue. The sample was then dissolved in CDCl₃ for ¹H NMR analysis.

3.4.3 Optimization Table

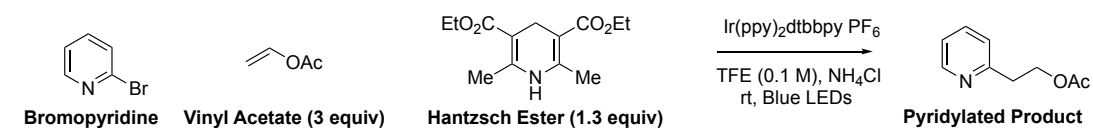
Initial optimization studies were performed on 6-bromopicoline with isopropenyl acetate as the reaction partner. This system was found to be relatively tolerant towards HAT catalyst and acidic modifier. The systems described below were chosen as more descriptive exemplars as they displayed significant variances in yield upon deviation of the reaction conditions. While thiol catalysts **3** and **4** showed a small improvement in yield for these substrates, we found that, overall, CySH performed better across a wide range of alkenes.

Table 3.3



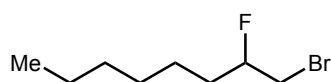
Entry	HAT Catalyst	Conditions	Yield (%)
1	none	as shown	17%
2	1	as shown	53%
3	2	as shown	63%
4	3	as shown	65%
5	4	as shown	62%
6	5	as shown	18%
7	6	as shown	22%
8	2	no photocatalyst	12%
9	2	no light	0%

Table 3.4



Entry	HAT Catalyst	Conditions	Yield (%)
1	none	as shown	35%
2	1	as shown	54%
3	2	as shown	65%
4	3	as shown	72%
5	4	as shown	67%
6	5	as shown	38%
7	6	as shown	52%

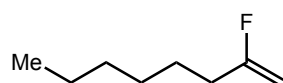
3.4.4 Preparation of Starting Materials



1-bromo-2-fluorooctane:

Prepared according to the procedure of Schlosser *et al.*¹⁰¹

To a round-bottomed flask charged with *N*-bromosuccinimide (2.1 g, 12 mmol) was added CH₂Cl₂ (5 mL) and 1-octene (1.56 mL, 1 equiv, 10 mmol). The suspension was cooled to 0 °C before the dropwise addition of triethylamine tris(hydrofluoride) (3.2 mL, 2 equiv, 20 mmol) in dichloromethane (5 mL) over the course of 15 min. After 2 h of additional stirring at 0 °C, the reaction mixture was absorbed directly onto silica gel (5 g) which was dried by evaporation before being loaded onto a column of silica gel. Elution with hexanes provided the desired product as a clear oil (1.8 g) that was taken directly into the next step.



2-fluorooct-1-ene:

Prepared according to the procedure of Schlosser *et al.*¹⁰¹

The 1-bromo-2-fluorooctane (1.8 g, 1 equiv, 8.6 mmol) was added to a solution of potassium *tert*-butoxide (1.34 g, 1.4 equiv, 12 mmol) in tetrahydrofuran (10 mL). After 5 h at 0 °C, the reaction mixture was passed through a thin plug of silica gel before being carefully concentrated at reduced pressure to provide the desired compound as a volatile colorless liquid (220 mg, 17 %).

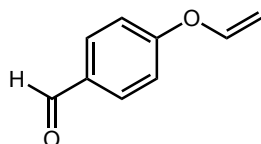
¹⁰¹ Suga, H.; Hamatani, T.; Guggisberg, Y.; Schlosser, M. Vicinal Bromofluoroalkanes: Their Regioselective Formation and Their Conversion to Fluoroolefins. *Tetrahedron* **1990**, *46* (12), 4255–4260

¹H NMR (500 MHz, CDCl₃) δ 4.48 (dd, *J* = 17.7, 2.6 Hz, 1H), 4.19 (dd, *J* = 50.5, 2.6 Hz, 1H), 2.25 – 2.08 (m, 2H), 1.55 – 1.45 (m, 2H), 1.31 (dddd, *J* = 20.4, 11.1, 7.2, 5.1 Hz, 6H), 0.89 (t, *J* = 6.9 Hz, 3H).

¹³C NMR (151 MHz, CDCl₃) δ 167.1 (d, ¹*J*_{C-F} = 256.6 Hz), 89.2 (d, ²*J*_{C-F} = 20.5 Hz), 31.8 (d, ²*J*_{C-F} = 27.1 Hz), 31.5, 28.6, 26.0 (d, ³*J*_{C-F} = 2.1 Hz), 22.5, 14.0.

¹⁹F NMR (565 MHz, CDCl₃) δ -94.65 (dq, *J* = 50.3, 16.5 Hz).

FTIR (neat) *v*_{max}: 2928, 2858, 1468, 1239, 1099 cm⁻¹.



4-(vinylloxy)benzaldehyde:

Prepared according to the procedure of Ishii *et al.*¹⁰²

To a toluene solution (15 mL) of [IrCl(cod)]₂ (100 mg, 1 mol%, 0.015 mmol) and Na₂CO₃ (945 mg, 0.6 equiv, 9 mmol) were added 4-hydroxybenzaldehyde (1830 mg, 1, equiv, 15 mmol) and vinyl acetate (2.8 mL, 2.6 g, 2 equiv, 30 mmol) under an atmosphere of Ar. The reaction mixture was stirred at 100 °C for 16 h. After quenching with wet ether, and concentration under reduced pressure, the residue was purified by column chromatography (silica gel, 0 – 5% hexane/EtOAc) to provide the desired compound as a clear oil (1.8 g, 81%).

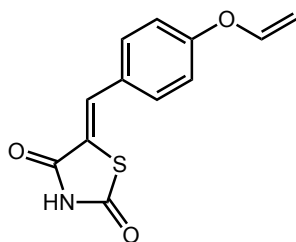
¹H NMR (600 MHz, CDCl₃) δ 9.93 (s, 1H), 7.93 – 7.71 (m, 2H), 7.18 – 7.08 (m, 2H), 6.70 (ddd, *J* = 13.6, 6.0, 0.7 Hz, 1H), 4.95 (ddd, *J* = 13.6, 1.9, 0.8 Hz, 1H), 4.63 (ddd, *J* = 6.0, 1.9, 0.7 Hz, 1H).

¹³C NMR (151 MHz, CDCl₃) δ 190.8, 161.7, 146.4, 132.0, 131.7, 116.8, 98.3.

FTIR (neat) *v*_{max}: 2828, 2740, 1691, 1592, 1503, 1237, 1156 cm⁻¹.

¹⁰² Okimoto, Y.; Sakaguchi, S.; Ishii, Y. Development of a Highly Efficient Catalytic Method for Synthesis of Vinyl Ethers. *J. Am. Chem. Soc.* **2002**, *124* (8), 1590–1591

HRMS (APCI) m/z : $[M+H]^+$ calcd. for $C_9H_9O_2$, 149.05971; found, 149.05961.



(Z)-5-(4-(vinylloxy)benzylidene)thiazolidine-2,4-dione:

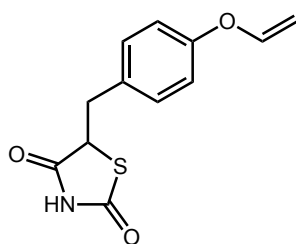
Prepared according to the procedure of Ishii *et al.*¹⁰²

To a round bottomed flask charged with 4-(vinylloxy)benzaldehyde (1.7 g, 1 equiv, 12 mmol) and 2,4-thiazolidinedione (2.2 g, 1.6 equiv, 19.2 mmol) was added piperidine (0.35 mL, 0.3 equiv, 3.6 mmol) and EtOH (48 mL). The reaction mixture was refluxed for 16 h. Upon cooling, the reaction mixture was poured onto ice water, leading to the precipitation of the desired product as a yellow solid. The yellow suspension was filtered and washed with cold methanol to provide the clean desired compound as an amorphous yellow solid (2.47g, 83%).

1H NMR (600 MHz, $CDCl_3$) δ 8.78 (s, 1H), 7.83 (s, 1H), 7.49 (d, $J = 8.8$ Hz, 2H), 7.17 – 7.03 (m, 2H), 6.68 (dd, $J = 13.6, 6.0$ Hz, 1H), 4.92 (dd, $J = 13.6, 1.9$ Hz, 1H), 4.60 (dd, $J = 6.0, 1.9$ Hz, 1H).

^{13}C NMR (151 MHz, $CDCl_3$) δ 167.2, 166.7, 158.8, 146.7, 134.0, 132.4, 127.8, 120.7, 117.4, 97.8.

FTIR (neat) ν_{max} : 2986 1691, 1678, 1590, 1426, 1343 cm^{-1} .



5-(4-(vinylloxy)benzyl)thiazolidine-2,4-dione

Prepared according to the procedure of Szelejewski *et al.*¹⁰³

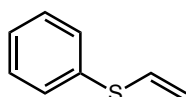
To a round bottomed flask charged with (Z)-5-(4-(vinylloxy)benzylidene)thiazolidine-2,4-dione (520 mg, 1 equiv, 2.1 mmol) in 2:1 MeOH/H₂O (15 mL) and 1 M sodium hydroxide solution (1.6 mL, 1.6 mmol), and the resultant mixture was stirred for 15 min at ca. 23 °C. Then, 1 mL of a CoCl₂-DMG complex solution (2 mg of CoCl₂·6H₂O and 13 mg of dimethylglyoxime in 5 mL of *N,N*-dimethylformamide) was added, and the stirring was continued. After 15 min, sodium borohydride (100 mg, 2.6 mmol) in water (2 mL) was added in a single portion. The blue-purple solution was warmed to 35 °C and stirred for 3 h. Then the reaction mixture was cooled to room temperature and brought to pH 6-7 with 1 M hydrochloric acid (70 mL), and the deposited precipitate of product was filtered off. The precipitate was diluted with CH₂Cl₂ (20 mL) and washed with H₂O (2 x 5 mL). The organics were passed through a plug of silica gel and concentrated under reduced pressure to provide the desired product as an amorphous off white solid (400 mg, 76%).

¹H NMR (600 MHz, CDCl₃) δ 7.83 (s, 1H), 7.19 (d, *J* = 8.2 Hz, 2H), 7.01 – 6.92 (m, 2H), 6.65 – 6.59 (m, 1H), 4.78 (dd, *J* = 13.6, 1.8 Hz, 1H), 4.52 (dd, *J* = 9.5, 4.0 Hz, 1H), 4.46 (dd, *J* = 6.0, 1.7 Hz, 1H), 3.48 (dd, *J* = 14.2, 4.0 Hz, 1H), 3.14 (dd, *J* = 14.2, 9.4 Hz, 1H).

¹³C NMR (151 MHz, CDCl₃) δ 174.2, 170.4, 156.5, 148.0, 132.4, 130.7, 117.5, 95.8, 53.6, 37.9.

FTIR (neat) ν_{\max} : 3039, 1665, 1658, 1641, 1591, 1333, 1247, 1168, 1144 cm⁻¹.

HRMS (APCI) *m/z*: [M+H]⁺ calcd. for C₁₂H₁₂O₃NS, 250.05324; found, 250.05325.



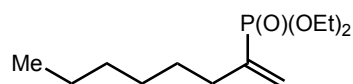
¹⁰³ Leś, A.; Pucko, W.; Szelejewski, W. Optimization of the Reduction of a 5-Benzylidenethiazolidine-2,4-Dione Derivative Supported by the Reaction Response Surface Analysis: Synthesis of Pioglitazone Hydrochloride. *Org. Process Res. Dev.* **2004**, *8* (2), 157–162

phenyl(vinyl)sulfane:

Synthesized according to the procedure of Ishii *et al.*¹⁰²

To a toluene solution (4.0 mL) of $[\text{IrCl}(\text{cod})]_2$ (28 mg, 1 mol%, 0.04 mmol) and NaOAc (10 mg, 3 mol%, 0.12 mmol) were added thiophenol (421 μL , 1 equiv, 4 mmol) and vinyl acetate (736 μL 2 equiv, 8 mmol) under Ar. The reaction mixture was stirred at 100 °C for 16 h. After quenching with wet ether, and concentration under reduced pressure, the crude residue was purified by column chromatography (silica gel, 0 – 5% hexane/EtOAc) to provide the desired compound as a pale yellow oil (610 mg, 85%). The physical properties and spectral data were consistent with the reported values.¹⁰²

¹H NMR (600 MHz, CDCl_3) δ 7.41 – 7.38 (m, 2H), 7.36 – 7.31 (m, 3H), 6.55 (ddd, $J = 16.6$, 9.6, 2.1 Hz, 1H), 5.38 – 5.33 (m, 2H).

**diethyl oct-1-en-2-ylphosphonate:**

Prepared according to the procedure of Han *et al.*¹⁰⁴

An oven-dried schlenk tube containing a stir bar was charged with $\text{Pd}_2(\text{dba})_3$ (2.3 mg, 0.5 mol%, 0.5 mmol), 1,3-bis(diphenylphosphino)propane (2.0 mg, 1 mol%, 0.5 mmol) and 0.5 mL toluene under N_2 atmosphere and stirred at room temperature for 10 min, then diethylphosphite (64 μL , 1 equiv, 0.5 mmol) and 1-octyne (74 μL , 1 equiv, 0.5 mmol) were added and the mixture was stirred at 100 °C overnight. After removal of the solvent the crude residue was purified by column chromatography (silica gel, chloroform) to provide the desired

¹⁰⁴ Chen, T.; Zhao, C.-Q.; Han, L.-B. Hydrophosphorylation of Alkynes Catalyzed by Palladium: Generality and Mechanism. *J. Am. Chem. Soc.* **2018**, *140* (8), 3139–3155

compound as a pale yellow oil (61 mg, 49%). The physical properties and spectral data were consistent with the reported values.¹⁰⁴

¹H NMR (600 MHz, CDCl₃) δ 7.41 – 7.38 (m, 2H), 7.36 – 7.31 (m, 3H), 6.55 (ddd, $J = 16.6, 9.6, 2.1$ Hz, 1H), 5.38 – 5.33 (m, 2H).

3.4.5 Procedures and Characterization Data



2-(pyridin-4-yl)ethan-1-ol:

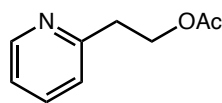
Prepared according to the General Procedure B using 4-bromopyridine hydrochloride (194 mg, 1 mmol, 1 equiv), and vinyl acetate (276 μ L, 258 mg, 3 mmol, 3 equiv), Hantzsch ester (329 mg, 1.3 mmol, 1.3 equiv) cyclohexanethiol (6 μ L, 0.05 mmol, 5 mol%), Ir[ppy]₂dtbbpy•PF₆ (9.1 mg, 0.01 mmol, 1 mol%), and NH₄Cl (106 mg, 2 mmol, 2 equiv). After 18 h, the reaction was purified according to the General Procedure B (silica gel, 40 – 100% EtOAc/hexanes, 1% Et₃N modifier then 10% MeOH/CH₂Cl₂) to provide the desired product as a yellow oil (76 mg, 62% yield).

¹H NMR (500 MHz, CDCl₃) δ 8.35 – 8.31 (m, 2H), 7.15 – 7.10 (m, 2H), 3.84 (t, J = 6.5 Hz, 2H), 3.55 (br. s, 1H), 2.81 (t, J = 6.4 Hz, 2H).

¹³C NMR (126 MHz, CDCl₃) δ 149.3, 148.9, 124.7, 62.1, 38.6.

FTIR (neat) ν_{max} : 3232, 2928, 1604, 1440, 1415, 1219 cm⁻¹.

HRMS (APCI) m/z : [M+H]⁺ calcd. for C₇H₁₀ON, 124.07569; found, 124.07564.



2-(pyridin-2-yl)ethyl acetate:

Prepared according to the General Procedure A using 2-bromopyridine (103 μ L, 156 mg, 1 mmol, 1 equiv), and vinyl acetate (276 μ L, 258 mg, 3 mmol, 3 equiv), Hantzsch ester (329 mg, 1.3 mmol, 1.3 equiv), cyclohexanethiol (6 μ L, 0.05 mmol, 5 mol%), Ir[ppy]₂dtbbpy•PF₆ (9.1 mg, 0.01 mmol, 1 mol%), and NH₄Cl (106 mg, 2 mmol, 2 equiv). After 18 h, the reaction was purified according to the General Procedure B (silica gel, 40 – 100% EtOAc/hexanes) to provide the desired product as a yellow oil (107 mg, 65% yield).

^1H NMR (600 MHz, CDCl_3) δ 8.57 (dd, $J = 5.0, 1.9$ Hz, 1H), 7.70 – 7.58 (m, 1H), 7.21 (d, $J = 7.8$ Hz, 1H), 7.18 (dd, $J = 7.5, 5.1$ Hz, 1H), 4.48 (t, $J = 6.8$ Hz, 2H), 3.14 (t, $J = 6.8$ Hz, 2H), 2.04 (s, 2H).

^{13}C NMR (151 MHz, CDCl_3) δ 171.2, 158.1, 149.5, 136.7, 123.6, 121.8, 63.7, 37.5, 21.1.

FTIR (neat) ν_{max} : 2964, 1732, 1592, 1570, 1437, 1365 cm^{-1} .

HRMS (ESI) m/z : $[\text{M}+\text{H}]^+$ calcd. for $\text{C}_9\text{H}_{12}\text{O}_2\text{N}$, 166.08626; found, 166.08627.



2-methyl-6-vinylpyridine:

An oven-dried screw-top test tube equipped with a stir bar was sealed with a PTFE-faced silicon septa and cooled to room temperature under N_2 atmosphere. The tube was charged with $\text{Ir}(\text{ppy})_2\text{dtbbpy}\cdot\text{PF}_6$ (9.1 mg, 1 mol%, 0.01 mmol), Hantzsch ester (329 mg, 1.3 mmol, 1.3 equiv) and NH_4Cl (106 mg, 2 mmol, 2 equiv). The atmosphere was exchanged by applying vacuum and backfilling with N_2 (this process was conducted a total of three times). 2-Bromo-6-methylpyridine (114 μL , 172 mg, 1 mmol, 1 equiv) and cyclohexanethiol (6 μL , 5 mol%, 0.05 mmol) were added via syringe.

Separately, vinyl bromide (207 μL , 3 equiv, 3 mmol) was condensed into a sealed vial at -78°C before the addition of separately degassed 2,2,2-trifluoroethanol (0.1 M) under a N_2 atmosphere via syringe. The vinyl bromide solution was transferred to the reaction vial and the resulting mixture was stirred at 1200 RPM for 16 hours under irradiation with a blue LED. The crude reaction mixture was quenched with saturated sodium bicarbonate and extracted with dichloromethane (3 x 20 mL). The extracts were combined, dried over sodium sulfate, filtered, and concentrated under reduced pressure. The residue was treated with silica gel for 15 min in

CH₂Cl₂ (10 mL) to afford the eliminated product. The resulting slurry was concentrated and purified by flash column chromatography (silica gel, 0 – 30% EtOAc/hexanes) then preparative HPLC (C₁₈, 30 – 99% MeCN/H₂O) to afford the title compound as a red-brown liquid (93 mg, 78 %).

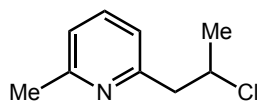
Isolation of the alkyl bromide product was found to be extremely difficult, with rapid elimination occurring under all conditions attempted.

¹H NMR (600 MHz, CDCl₃) δ 8.24 (t, *J* = 7.9 Hz, 1H), 7.86 (d, *J* = 8.1 Hz, 1H), 7.71 (dd, *J* = 17.6, 11.2 Hz, 1H), 7.52 (d, *J* = 7.7 Hz, 1H), 6.49 (d, *J* = 17.6 Hz, 1H), 6.00 (d, *J* = 11.1 Hz, 1H), 3.03 (s, 3H).

¹³C NMR (151 MHz, CDCl₃) δ 154.0, 150.9, 145.0, 127.7, 127.5, 126.0, 120.0, 19.7.

FTIR (neat) ν_{\max} : 1657, 1631, 1426, 1295, 1177 cm⁻¹.

HRMS (APCI) *m/z*: [M+H]⁺ calcd. for C₈H₁₀N, 120.08078; found, 120.08029.



2-(2-chloropropyl)-6-methylpyridine:

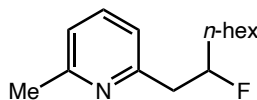
Prepared according to the General Procedure A using 2-Bromo-6-methylpyridine (114 μL, 172 mg, 1 mmol, 1 equiv), and 2-chloroprop-1-ene (254 μL, 228 mg, 3 mmol, 3 equiv), Hantzsch ester (329 mg, 1.3 mmol, 1.3 equiv), cyclohexanethiol (6 μL, 0.05 mmol, 5 mol%), Ir[ppy]₂dtbbpy•PF₆ (9.1 mg, 0.01 mmol, 1 mol%), and NH₄Cl (106 mg, 2 mmol, 2 equiv). After 18 h, the reaction was purified according to the General Procedure A (silica gel, 0 – 40% EtOAc/hexanes) to provide the desired product as a yellow oil (119 mg, 70% yield).

¹H NMR (600 MHz, CDCl₃) δ 7.50 (t, *J* = 7.6 Hz, 1H), 7.00 (dd, *J* = 10.8, 7.7 Hz, 2H), 4.56 – 4.37 (m, 1H), 3.12 (dd, *J* = 7.0, 3.8 Hz, 2H), 2.52 (s, 3H), 1.57 (d, *J* = 6.5 Hz, 3H).

¹³C NMR (151 MHz, CDCl₃) δ 158.2, 157.4, 136.7, 121.5, 121.2, 57.9, 48.9, 25.3, 24.6.

FTIR (neat) ν_{\max} : 2975, 2927, 1590, 1577, 1456, 1377 cm^{-1} .

HRMS (APCI) m/z : $[M+H]^+$ calcd. for $\text{C}_9\text{H}_{13}\text{NCl}$, 170.07310; found, 170.07306.



2-(2-fluorooctyl)-6-methylpyridine:

Prepared according to the General Procedure B using 2-bromo-6-methylpyridine (11.4 μL , 17.2 mg, 0.1 mmol, 1 equiv), and 2-fluorooct-1-ene (39 mg, 0.3 mmol, 3 equiv), Hantzsch ester (33 mg, 0.13 mmol, 1.3 equiv), cyclohexanethiol (0.6 μL , 0.005 mmol, 5 mol%), $\text{Ir}[\text{ppy}]_2\text{dtbbpy}\cdot\text{PF}_6$ (0.9 mg, 0.001 mmol, 1 mol%), and NH_4Cl (10.6 mg, 0.2 mmol, 2 equiv) in 1 mL of 2,2,2-trifluoroethanol (0.1 M). After 18 h, the reaction was purified according to the General Procedure B (preparative thin layer chromatography, silica gel, 20% EtOAc/hexanes) to provide the desired product as a colorless oil (14.5 mg, 65% yield).

^1H NMR (600 MHz, CDCl_3) δ 7.50 (t, $J = 7.6$ Hz, 1H), 7.01 (t, $J = 8.0$ Hz, 2H), 4.90 (dtt, $J = 49.1, 8.2, 3.9$ Hz, 1H), 3.11 – 2.94 (m, 1H), 2.53 (s, 3H), 1.77 – 1.56 (m, 2H), 1.56 – 1.47 (m, 1H), 1.45 – 1.21 (m, 9H), 0.88 (t, $J = 6.9$ Hz, 3H).

^{13}C NMR (126 MHz, CDCl_3) δ 157.9, 157.2 (d, $^3J_{\text{C-F}} = 4.2$ Hz), 136.5, 121.1, 120.9, 93.9 (d, $^1J_{\text{C-F}} = 169.5$ Hz), 44.2 (d, $^2J_{\text{C-F}} = 21.9$ Hz), 35.1 (d, $^2J_{\text{C-F}} = 20.7$ Hz), 31.7, 29.1, 25.0 (d, $^3J_{\text{C-F}} = 4.2$ Hz), 24.5, 22.5, 14.0.

^{19}F NMR (282 MHz, CDCl_3) δ -179.98 – -180.92 (m).

FTIR (neat) ν_{\max} : 2924, 2854, 1495, 1453, 1361, 1226, 1097 cm^{-1} .

HRMS (NSI) m/z : $[M+H]^+$ calcd. for $\text{C}_{14}\text{H}_{23}\text{NF}$, 224.18090; found, 224.18091.



2-(6-methylpyridin-2-yl)ethan-1-ol:

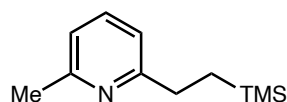
Prepared according to the General Procedure A using 2-bromo-6-methylpyridine (28 μL , 43 mg, 0.25 mmol, 1 equiv), and vinylboronic acid, pinacol ester (187 mg, 127 μL , 0.75 mmol, 3 equiv), Hantzsch ester (82 mg, 0.325 mmol, 1.3 equiv), cyclohexanethiol (1.6 μL , 0.0125 mmol, 5 mol%), Ir[ppy]₂dtbbpy•PF₆ (2.25 mg, 0.0025 mmol, 1 mol%), and NH₄Cl (26 mg, 0.5 mmol, 2 equiv). After 18 h, the reaction was quenched with saturated sodium bicarbonate solution and extracted with dichloromethane (3 x 10 mL). The combined extracts were concentrated under reduced pressure. Analysis of the crude residue showed a mixture of Hantzsch pyridine and the desired product (75% yield by NMR), which was confirmed by HRMS. The reaction mixture was then dissolved in 1:1 THF:H₂O before the addition of NaBO₃•4H₂O (956 mg, 6.25 mmol, 25 equiv). The resulting slurry was stirred for 14 h before being quenched upon the addition of Na₂S₂O₃ (saturated solution, 5 mL). The mixture was extracted with EtOAc (3 x 10 mL) and the combined organic layers dried over Na₂SO₄, filtered, and concentrated. Crude alcohol was purified by flash column chromatography (silica gel, 0 – 20% MeOH/CH₂Cl₂) to provide the desired product as a colorless oil (20 mg, 58% yield)

¹H NMR (600 MHz, CDCl₃) δ 7.51 (t, J = 7.6 Hz, 1H), 7.01 (d, J = 7.6 Hz, 1H), 6.95 (d, J = 7.7 Hz, 1H), 4.00 (t, J = 5.5 Hz, 2H), 2.97 (t, J = 5.5 Hz, 2H), 2.52 (s, 3H).

¹³C NMR (151 MHz, CDCl₃) δ 160.3, 157.6, 137.2, 121.2, 120.4, 62.1, 38.6, 24.5.

FTIR (neat) ν_{max} : 3349, 2925, 1596, 1578, 1459, 1235, 1046 cm⁻¹.

HRMS (NSI) m/z : [M+H]⁺ calcd. for C₈H₁₂ON, 138.09134; found, 138.09128.



2-methyl-6-(2-(trimethylsilyl)ethyl)pyridine:

Prepared according to the General Procedure A using 2-bromo-6-methylpyridine (114 μL , 172 mg, 1 mmol, 1 equiv), and trimethyl(vinyl)silane (306 mg, 3 mmol, 3 equiv), Hantzsch ester

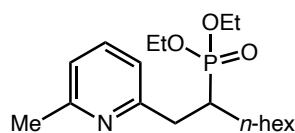
(329 mg, 1.3 mmol, 1.3 equiv), cyclohexanethiol (6 μ L, 0.05 mmol, 5 mol%), Ir[ppy]₂dtbbpy•PF₆ (9.1 mg, 0.01 mmol, 1 mol%), and NH₄Cl (106 mg, 2 mmol, 2 equiv). After 18 h, the reaction was purified according to the General Procedure A (silica gel, 0 – 30% EtOAc/hexanes) to provide the desired product as a yellow oil (109 mg, 65% yield).

¹H NMR (600 MHz, CDCl₃) δ 7.44 (t, J = 7.6 Hz, 1H), 6.95 (d, J = 7.7 Hz, 1H), 6.91 (d, J = 7.6 Hz, 1H), 2.81 – 2.69 (m, 2H), 2.50 (s, 3H), 0.97 – 0.86 (m, 2H), 0.00 (s, 9H).

¹³C NMR (151 MHz, CDCl₃) δ 164.1, 157.6, 136.6, 120.3, 118.7, 32.8, 24.7, 17.1, -1.6.

FTIR (neat) ν_{\max} : 2951, 1591, 1578, 1454, 1246 cm⁻¹.

HRMS (APCI) m/z : [M+H]⁺ calcd. for C₁₁H₂₀NSi, 194.13595; found, 194.13591.



diethyl (1-(6-methylpyridin-2-yl)octan-2-yl)phosphonate:

Prepared according to the General Procedure A using 2-bromo-6-methylpyridine (11.4 μ L, 17.2 mg, 0.1 mmol, 1 equiv), and diethyl oct-1-en-2-ylphosphonate (75 mg, 0.3 mmol, 3 equiv), Hantzsch ester (33 mg, 0.13 mmol, 1.3 equiv), cyclohexanethiol (0.6 μ L, 0.005 mmol, 5 mol%), Ir[ppy]₂dtbbpy•PF₆ (0.9 mg, 0.001 mmol, 1 mol%), and NH₄Cl (10.6 mg, 0.2 mmol, 2 equiv). After 18 h, the reaction was purified according to the General Procedure A (silica gel, 0 – 20% MeOH/CH₂Cl₂) to provide the desired product as a colorless oil (14 mg, 41% yield).

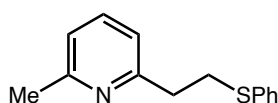
¹H NMR (500 MHz, CDCl₃) δ 7.47 (t, J = 7.6 Hz, 1H), 6.97 (dd, J = 7.7, 2.0 Hz, 2H), 4.10 – 4.00 (m, 4H), 3.18 (ddd, J = 14.2, 11.9, 5.4 Hz, 1H), 2.81 (td, J = 14.3, 9.0 Hz, 1H), 2.51 (s, 3H), 2.50 – 2.44 (m, 1H), 1.70 – 1.66 (m, 2H), 1.52 – 1.40 (m, 2H), 1.31 – 1.22 (m, 11H), 0.83 (t, J = 7.1 Hz, 3H).

^{13}C NMR (151 MHz, CDCl_3) δ 158.0 (d, $J_{\text{C-P}} = 13.9$ Hz), 156.8, 135.4, 119.8, 119.6, 60.6 – 60.3 (m), 36.2, 35.3, 34.4, 30.5, 28.2, 27.4 (d, $J_{\text{C-P}} = 3.6$ Hz), 26.4 (d, $J_{\text{C-P}} = 7.7$ Hz), 21.5, 15.4, 13.0.

^{31}P NMR (243 MHz, CDCl_3) δ 34.15.

FTIR (neat) ν_{max} : 2927, 2361, 2338, 1451, 1226, 1026 cm^{-1} .

HRMS (APCI) m/z : $[\text{M}+\text{H}]^+$ calcd. for $\text{C}_{18}\text{H}_{33}\text{O}_3\text{NP}$, 342.21926; found, 342.21991.



2-methyl-6-(2-(phenylthio)ethyl)pyridine:

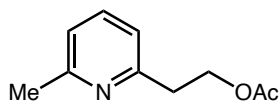
Prepared according to the General Procedure A using 2-bromo-6-methylpyridine (57 μL , 86 mg, 0.5 mmol, 1 equiv), and phenyl(vinyl)sulfane (204 mg, 1.5 mmol, 3 equiv), Hantzsch ester (164 mg, 0.65 mmol, 1.3 equiv), cyclohexanethiol (3 μL , 0.025 mmol, 5 mol%), $\text{Ir}[\text{ppy}]_2\text{dtbbpy}\cdot\text{PF}_6$ (9.1 mg, 0.005 mmol, 1 mol%), and NH_4Cl (53 mg, 1 mmol, 2 equiv) in 5 mL of 2,2,2-trifluoroethanol. After 18 h, the reaction was purified according to the General Procedure A (silica gel, 0 – 30% EtOAc/hexanes) to provide the desired product as a colorless oil (60 mg, 52% yield).

^1H NMR (400 MHz, CDCl_3) δ 7.46 (td, $J = 7.6, 0.8$ Hz, 1H), 7.38 – 7.31 (m, 2H), 7.29 – 7.23 (m, 2H), 7.18 – 7.12 (m, 1H), 7.00 – 6.86 (m, 2H), 3.30 (t, $J = 7.6$ Hz, 2H), 3.05 (t, $J = 7.1$ Hz, 2H), 2.51 (s, 3H).

^{13}C NMR (101 MHz, CDCl_3) δ 159.0, 158.1, 136.6, 136.4, 129.3, 128.9, 125.9, 121.1, 120.1, 37.8, 33.4, 24.5.

FTIR (neat) ν_{max} : 3057, 2922, 1590, 1576, 1480, 1454, 1156, 1090 cm^{-1} .

HRMS (APCI) m/z : $[\text{M}+\text{H}]^+$ calcd. for $\text{C}_{14}\text{H}_{16}\text{NS}$, 230.09980; found, 230.09993.



2-(6-methylpyridin-2-yl)ethyl acetate:

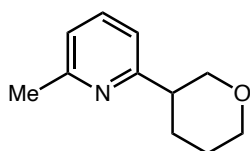
Prepared according to the General Procedure A using 2-bromo-6-methylpyridine (114 μL , 172 mg, 1 mmol, 1 equiv), vinyl acetate (276 μL , 258 mg, 3 mmol, 3 equiv), Hantzsch ester (329 mg, 1.3 mmol, 1.3 equiv), cyclohexanethiol (6 μL , 0.05 mmol, 5 mol%), Ir[ppy]₂dtbbpy•PF₆ (9.1 mg, 0.01 mmol, 1 mol%), and NH₄Cl (106 mg, 2 mmol, 2 equiv). After 18 h, the reaction was purified according to the General Procedure A (silica gel, 20 – 50% EtOAc/hexanes) to provide the desired product as a yellow oil (102 mg, 72% yield).

¹H NMR (400 MHz, CDCl₃) δ 7.44 (t, J = 7.7 Hz, 1H), 6.98 – 6.90 (m, 2H), 4.38 (t, J = 6.8 Hz, 2H), 3.02 (t, J = 6.8 Hz, 2H), 2.47 (s, 3H), 1.96 (s, 3H).

¹³C NMR (101 MHz, CDCl₃) δ 171.0, 158.1, 157.2, 136.6, 121.2, 120.2, 63.8, 37.4, 24.4, 20.9.

FTIR (neat) ν_{max} : 2960, 1735, 1593, 1578, 1458, 1364, 1231 cm⁻¹.

HRMS (APCI) m/z : [M+H]⁺ calcd. for C₁₀H₁₄O₂N, 180.10191; found, 180.10187.



2-methyl-6-(tetrahydro-2H-pyran-3-yl)pyridine:

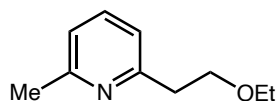
Prepared according to the General Procedure B using 2-bromo-6-methylpyridine (114 μL , 172 mg, 1 mmol, 1 equiv), and 3,4-dihydro-2H-pyran (254 μL , 252 mg, 3 mmol, 3 equiv), Hantzsch ester (329 mg, 1.3 mmol, 1.3 equiv), cyclohexanethiol (6 μL , 0.05 mmol, 5 mol%), Ir[ppy]₂dtbbpy•PF₆ (9.1 mg, 0.01 mmol, 1 mol%), and NH₄Cl (106 mg, 2 mmol, 2 equiv). After 18 h, the reaction was purified according to the General Procedure B (silica gel, 20 – 50% EtOAc/hexanes) to provide the desired product as a yellow oil (125 mg, 72% yield).

¹H NMR (400 MHz, CDCl₃) δ 7.47 (t, *J* = 7.7 Hz, 1H), 6.98 – 6.92 (m, 2H), 4.09 – 4.02 (m, 1H), 3.98 – 3.91 (m, 1H), 3.55 (t, *J* = 10.8 Hz, 1H), 3.47 (td, *J* = 11.2, 2.8 Hz, 1H), 2.97 (tt, *J* = 10.9, 4.0 Hz, 1H), 2.50 (s, 3H), 2.12 – 1.99 (m, 1H), 1.90 – 1.62 (m, 4H).

¹³C NMR (101 MHz, CDCl₃) δ 161.5, 158.0, 136.6, 121.2, 118.6, 93.5, 72.5, 68.2, 44.8, 29.5, 25.9, 24.7.

FTIR (neat) ν_{\max} : 2932, 2845, 1590, 1453, 1274, 1084 cm⁻¹.

HRMS (APCI) *m/z*: [M+H]⁺ calcd. for C₁₁H₁₆ON, 178.12264; found, 315.12357.



2-(2-ethoxyethyl)-6-methylpyridine:

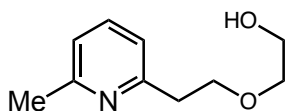
Prepared according to the General Procedure B using 2-bromo-6-methylpyridine (114 μL, 172 mg, 1 mmol, 1 equiv), and ethoxyethene (287 μL, 216 mg, 1 mmol, 1 equiv), Hantzsch ester (329 mg, 1.3 mmol, 1.3 equiv), cyclohexanethiol (6 μL, 0.05 mmol, 5 mol%), Ir[ppy]₂dtbbpy•PF₆ (9.1 mg, 0.01 mmol, 1 mol%), and NH₄Cl (106 mg, 2 mmol, 2 equiv). After 18 h, the reaction was purified according to the General Procedure B (silica gel, 20 – 50% EtOAc/hexanes) to provide the desired product as a yellow oil (103 mg, 62% yield).

¹H NMR (600 MHz, CDCl₃) δ 7.46 (t, *J* = 7.6 Hz, 1H), 7.00 (d, *J* = 7.7 Hz, 1H), 6.95 (d, *J* = 7.6 Hz, 1H), 3.75 (t, *J* = 7.0 Hz, 2H), 3.48 (q, *J* = 7.0 Hz, 2H), 3.01 (t, *J* = 7.0 Hz, 2H), 2.50 (s, 3H), 1.15 (t, *J* = 7.0 Hz, 3H).

¹³C NMR (151 MHz, CDCl₃) δ 158.6, 157.8, 136.5, 120.8, 120.3, 70.1, 66.2, 38.8, 24.5, 15.1.

FTIR (neat) ν_{\max} : 2973, 2859, 2951, 1591, 1578, 1453, 1375 cm⁻¹.

HRMS (APCI) *m/z*: [M+H]⁺ calcd. for C₁₀H₁₆ON, 166.12264; found, 166.12348.



2-(2-(6-methylpyridin-2-yl)ethoxy)ethan-1-ol:

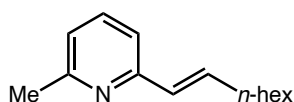
Prepared according to the General Procedure B using 2-bromo-6-methylpyridine (114 μL , 172 mg, 1 mmol, 1 equiv), and 2-(vinylloxy)ethan-1-ol (311 μL , 306 mg, 3 mmol, 3 equiv), Hantzsch ester (329 mg, 1.3 mmol, 1.3 equiv), cyclohexanethiol (6 μL , 0.05 mmol, 5 mol%), Ir[ppy]₂dtbbpy•PF₆ (9.1 mg, 0.01 mmol, 1 mol%), and NH₄Cl (106 mg, 2 mmol, 2 equiv). After 18 h, the reaction was purified according to the General Procedure B (silica gel, 20 – 100% EtOAc/hexanes) to provide the desired product as a yellow oil (130 mg, 72% yield).

¹H NMR (400 MHz, CDCl₃) δ 7.49 (t, J = 7.7 Hz, 1H), 6.99 (d, J = 7.7 Hz, 2H), 3.87 (t, J = 6.2 Hz, 2H), 3.75 – 3.66 (m, 2H), 3.63 – 3.57 (m, 2H), 3.02 (t, J = 6.2 Hz, 2H), 2.52 (s, 3H).

¹³C NMR (101 MHz, CDCl₃) δ 158.6, 157.9, 137.0, 121.2, 120.6, 72.2, 70.3, 61.9, 38.1, 24.3.

FTIR (neat) ν_{max} : 3304, 2923, 2864, 1716, 1593, 1578, 1460, 1377 cm⁻¹.

HRMS (ESI) m/z : [M+H]⁺ calcd. for C₉H₁₄O₂N, 168.10300; found, 168.10202.



(E)-2-methyl-6-(oct-1-en-1-yl)pyridine:

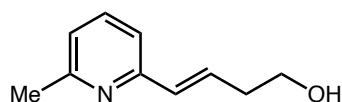
Prepared according to the General Procedure B using 2-bromo-6-methylpyridine (114 μL , 172 mg, 1 mmol, 1 equiv), and 1-octyne (441 μL , 330 mg, 3 mmol, 3 equiv), Hantzsch ester (329 mg, 1.3 mmol, 1.3 equiv), cyclohexanethiol (6 μL , 0.05 mmol, 5 mol%), Ir[ppy]₂dtbbpy•PF₆ (9.1 mg, 0.01 mmol, 1 mol%), and NH₄Cl (106 mg, 2 mmol, 2 equiv). After 18 h, the reaction was purified according to the General Procedure B (silica gel, 0 – 15% EtOAc/hexanes) to provide the desired product as colorless oil as a 1:1 mixture of olefin isomers (145 mg, 75% yield).

¹H NMR (600 MHz, CDCl₃) δ 7.50 (t, *J* = 7.7 Hz, 1H_{dr1}), 7.46 (t, *J* = 7.7 Hz, 1H_{dr2}), 7.06 (d, *J* = 7.8 Hz, 1H_{dr2}), 7.04 (d, *J* = 7.7 Hz, 1H_{dr1}), 6.94 (t, *J* = 7.9 Hz, 2H_{dr1+2}), 6.72 – 6.64 (m, 1H_{dr2}), 6.48 – 6.41 (m, 2H_{dr1+2}), 5.85 (dt, *J* = 11.9, 7.3 Hz, 1H_{dr1}), 2.53 (d, *J* = 6.7 Hz, 8H_{dr1+2}), 2.24 (q, *J* = 7.8, 7.3 Hz, 2H_{dr2}), 1.47 (dq, *J* = 20.0, 7.5 Hz, 4H_{dr1+2}), 1.39 – 1.22 (m, 12H_{dr1+2}), 0.87 (dt, *J* = 9.9, 6.8 Hz, 6H_{dr1+2}).

¹³C NMR (151 MHz, CDCl₃) δ ¹³C NMR (151 MHz, Chloroform-*d*) δ 157.9, 157.8, 156.2, 155.8, 136.9, 136.5, 136.1, 135.7, 130.2, 128.9, 121.0, 120.6, 120.6, 117.7, 32.9, 31.8, 31.7, 29.7, 29.1, 29.0, 29.0, 28.8, 24.7, 24.6, 22.6, 14.1, 14.1.

FTIR (neat) ν_{\max} : 2955, 2924, 2854, 1579, 1453, 1376, 1034 cm⁻¹.

HRMS (APCI) *m/z*: [M+H]⁺ calcd. for C₁₄H₂₂N, 204.17468; found, 204.17472.



4-(6-methylpyridin-2-yl)but-3-en-1-ol:

Prepared according to the General Procedure B using 2-bromo-6-methylpyridine (114 μL, 172 mg, 1 mmol, 1 equiv), and but-3-yn-1-ol (306 mg, 3 mmol, 3 equiv), Hantzsch ester (329 mg, 1.3 mmol, 1.3 equiv), cyclohexanethiol (6 μL, 0.05 mmol, 5 mol%), Ir[ppy]₂dtbbpy•PF₆ (9.1 mg, 0.01 mmol, 1 mol%), and NH₄Cl (106 mg, 2 mmol, 2 equiv). After 18 h, the reaction was purified according to the General Procedure B (silica gel, 30 – 100% EtOAc/hexanes) to provide the *cis* alkene as a pale yellow oil (67 mg, 41% yield) and the *trans* alkene as a pale yellow oil (69 mg, 42%, 83% combined yield).

Cis alkene

¹H NMR (600 MHz, CDCl₃) δ 7.53 (t, *J* = 7.7 Hz, 1H), 6.95 (dd, *J* = 12.1, 7.7 Hz, 2H), 6.46 (d, *J* = 11.8 Hz, 1H), 6.29 (s, 1H), 5.74 (dt, *J* = 12.0, 8.8 Hz, 1H), 3.68 (t, *J* = 5.5 Hz, 2H), 2.77 – 2.68 (m, 2H), 2.52 (s, 3H), 1.74 (dt, *J* = 11.0, 5.2 Hz, 2H).

^{13}C NMR (151 MHz, CDCl_3) δ 157.52, 155.56, 137.29, 136.16, 129.09, 121.82, 121.52, 59.71, 30.24, 24.42, 23.71.

FTIR (neat) ν_{max} : 3268, 2927, 2859, 1586, 1572, 1461, 1156 cm^{-1} .

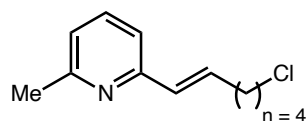
Trans alkene

^1H NMR (500 MHz, CDCl_3) δ 7.49 (t, $J = 7.7$ Hz, 1H), 7.07 (d, $J = 7.8$ Hz, 1H), 6.96 (d, $J = 7.6$ Hz, 1H), 6.70 (dt, $J = 15.8, 6.9$ Hz, 1H), 6.58 – 6.48 (m, 1H), 3.72 (t, $J = 6.5$ Hz, 2H), 2.53 (s, 3H), 2.42 – 2.30 (m, 2H), 1.79 (p, $J = 6.8$ Hz, 3H).

^{13}C NMR (126 MHz, CDCl_3) δ 158.2, 155.5, 136.7, 134.6, 130.9, 121.4, 118.0, 62.6, 32.0, 29.3, 24.7.

FTIR (neat) ν_{max} : 3349, 2925, 1587, 1461, 1451, 1060 cm^{-1} .

HRMS (APCI) m/z : $[\text{M}+\text{H}]^+$ calcd. for $\text{C}_{11}\text{H}_{16}\text{ON}$, 178.12264; found, 178.12261.



2-(6-chlorohex-1-en-1-yl)-6-methylpyridine:

Prepared according to the General Procedure A using 2-bromo-6-methylpyridine (114 μL , 172 mg, 1 mmol, 1 equiv), and 5-chlorohex-1-yne (360 mg, 3 mmol, 3 equiv). Hantzsch ester (329 mg, 1.3 mmol, 1.3 equiv), cyclohexanethiol (6 μL , 0.05 mmol, 5 mol%), $\text{Ir}[\text{ppy}]_2\text{dtbbpy}\cdot\text{PF}_6$ (9.1 mg, 0.01 mmol, 1 mol%), and NH_4Cl (106 mg, 2 mmol, 2 equiv). After 18 h, the reaction was purified according to the General Procedure A (silica gel, 0 – 10% EtOAc/hexanes (cis isomer) then preparative reverse phase HPLC 30 – 99% MeCN/ H_2O with 1% TFA modifier (trans isomer)) to provide the cis alkene as a pale yellow oil (70 mg, 36% yield) and the trans alkene as a pale yellow oil (60 mg, 31%) 66% combined yield.

Trans alkene

¹H NMR (600 MHz, CDCl₃) δ 7.49 (t, *J* = 7.7 Hz, 1H), 7.07 (d, *J* = 7.8 Hz, 1H), 6.96 (d, *J* = 7.6 Hz, 1H), 6.67 (dt, *J* = 15.9, 6.9 Hz, 1H), 6.49 (dd, *J* = 15.7, 1.6 Hz, 1H), 3.56 (t, *J* = 6.7 Hz, 2H), 2.53 (s, 3H), 2.29 (qd, *J* = 7.2, 1.5 Hz, 2H), 1.85 (p, *J* = 6.7 Hz, 2H), 1.73 – 1.62 (m, 2H).

¹³C NMR (151 MHz, CDCl₃) δ 158.1, 155.5, 136.7, 134.6, 131.0, 121.4, 118.0, 45.1, 32.2, 32.1, 26.3, 24.7.

FTIR (neat) ν_{\max} : 2928, 2860, 1581, 1571, 1453, 1157 cm⁻¹.

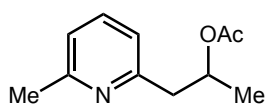
Cis alkene

¹H NMR (500 MHz, CDCl₃) δ 7.52 (t, *J* = 7.3 Hz, 1H), 7.02 (d, *J* = 7.7 Hz, 1H), 6.97 (d, *J* = 7.6 Hz, 1H), 6.45 (d, *J* = 10.7 Hz, 1H), 5.83 (dtd, *J* = 11.7, 7.4, 0.9 Hz, 1H), 3.55 (td, *J* = 6.6, 0.8 Hz, 2H), 2.63 (q, *J* = 7.6 Hz, 2H), 2.54 (s, 3H), 1.88 – 1.78 (m, 2H), 1.67 – 1.60 (m, 2H).

¹³C NMR (126 MHz, CDCl₃) δ 158.0, 156.1, 136.3, 136.0, 129.5, 120.9, 120.9, 45.1, 32.3, 27.9, 26.9, 24.8.

FTIR (neat) ν_{\max} : 2928, 2860, 1581, 1571, 1453, 1157 cm⁻¹.

HRMS (APCI) *m/z*: [M+H]⁺ calcd. for C₁₂H₁₇NCl, 210.10440; found, 210.10445.



1-(6-methylpyridin-2-yl)propan-2-yl acetate:

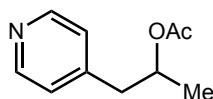
Prepared according to the General Procedure A using 2-bromo-6-methylpyridine (114 μL, 172 mg, 1 mmol, 1 equiv), and prop-1-en-2-yl acetate (325 μL, 300 mg, 1 mmol, 1 equiv), Hantzsch ester (329 mg, 1.3 mmol, 1.3 equiv), cyclohexanethiol (6 μL, 0.05 mmol, 5 mol%), Ir[ppy]₂dtbbpy•PF₆ (9.1 mg, 0.01 mmol, 1 mol%), and NH₄Cl (106 mg, 2 mmol, 2 equiv). After 18 h, the reaction was purified according to the General Procedure A (silica gel, 20 – 50% EtOAc/hexanes) to provide the desired product as a yellow oil (137 mg, 71% yield).

¹H NMR (400 MHz, CDCl₃) δ 7.42 (t, *J* = 7.7 Hz, 1H), 6.96 – 6.89 (m, 2H), 5.22 (ddt, *J* = 12.3, 7.7, 6.2 Hz, 1H), 2.99 (dd, *J* = 13.6, 7.7 Hz, 1H), 2.87 (dd, *J* = 13.6, 5.7 Hz, 1H), 2.46 (s, 3H), 1.91 (s, 3H), 1.22 (d, *J* = 6.3 Hz, 3H).

¹³C NMR (101 MHz, CDCl₃) δ 196.3, 170.4, 157.9, 157.2, 136.5, 121.1, 120.6, 70.8, 44.5, 24.4, 21.2, 19.9.

FTIR (neat) ν_{\max} : 2923, 2858, 1736, 1593, 1578, 1460, 1376 cm⁻¹.

HRMS (APCI) *m/z*: [M+H]⁺ calcd. for C₁₁H₁₆O₂N, 194.11756; found, 194.11854.



1-(pyridin-4-yl)propan-2-yl acetate:

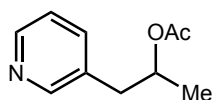
Prepared according to the General Procedure A using 4-bromopyridine hydrochloride (194 mg, 1 mmol, 1 equiv), and prop-1-en-2-yl acetate (325 μL, 300 mg, 1 mmol, 1 equiv), Hantzsch ester (329 mg, 1.3 mmol, 1.3 equiv), cyclohexanethiol (6 μL, 0.05 mmol, 5 mol%), Ir[ppy]₂dtbbpy•PF₆ (9.1 mg, 0.01 mmol, 1 mol%), and NH₄Cl (106 mg, 2 mmol, 2 equiv). After 18 h, the reaction was purified according to the General Procedure A (silica gel, 30 – 100% EtOAc/hexanes) to provide the desired product as a yellow oil (126 mg, 70% yield).

¹H NMR (600 MHz, CDCl₃) δ 8.46 (d, *J* = 6.1 Hz, 2H), 7.08 (d, *J* = 6.1 Hz, 2H), 5.14 – 5.01 (m, 1H), 2.85 (dd, *J* = 13.8, 7.2 Hz, 1H), 2.73 (dd, *J* = 13.8, 5.8 Hz, 1H), 1.94 (s, 3H), 1.19 (d, *J* = 6.3 Hz, 3H).

¹³C NMR (151 MHz, CDCl₃) δ 170.4, 149.8, 146.6, 124.7, 70.3, 41.5, 21.2, 19.6.

FTIR (neat) ν_{\max} : 2934, 1726, 1603, 1572, 1414, 1369 cm⁻¹.

HRMS (ESI) *m/z*: [M+H]⁺ calcd. for C₁₀H₁₄O₂N, 180.10300; found, 315.10208.



1-(pyridin-3-yl)propan-2-yl acetate:

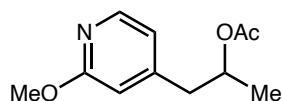
Prepared according to the General Procedure A using 3-iodopyridine (205 mg, 1 mmol, 1 equiv), and prop-1-en-2-yl acetate (325 μ L, 300 mg, 1 mmol, 1 equiv), Hantzsch ester (329 mg, 1.3 mmol, 1.3 equiv), cyclohexanethiol (6 μ L, 0.05 mmol, 5 mol%), Ir[ppy]₂dtbbpy•PF₆ (9.1 mg, 0.01 mmol, 1 mol%), and NH₄Cl (106 mg, 2 mmol, 2 equiv). After 18 h, the reaction was purified according to the General Procedure A (silica gel, 40 – 100% EtOAc/hexanes, 1% Et₃N modifier) to provide the desired product as a yellow oil (115 mg, 64% yield).

¹H NMR (400 MHz, CDCl₃) δ 8.48 (dd, J = 4.9, 1.7 Hz, 1H), 8.45 (d, J = 2.8 Hz, 1H), 7.53 (ddd, J = 7.8, 2.2, 1.7 Hz, 1H), 5.15 – 5.03 (m, 1H), 2.97 – 2.71 (m, 2H), 1.99 (s, 3H), 1.24 (d, J = 6.3 Hz, 3H).

¹³C NMR (101 MHz, CDCl₃) δ 170.4, 150.6, 148.0, 136.9, 133.1, 123.3, 70.7, 39.2, 21.2, 19.5.

FTIR (neat) ν_{max} : 2978, 1726, 1665, 1414, 1370, 1237 cm⁻¹.

HRMS (ESI) m/z : [M+H]⁺ calcd. for C₁₀H₁₄O₂N, 180.10191; found, 315.10103.

**1-(2-methoxypyridin-4-yl)propan-2-yl acetate:**

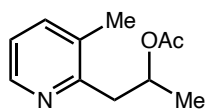
Prepared according to the General Procedure A using 4-bromo-2-methoxypyridine (188 mg, 1 mmol, 1 equiv), and prop-1-en-2-yl acetate (325 μ L, 300 mg, 1 mmol, 1 equiv), Hantzsch ester (329 mg, 1.3 mmol, 1.3 equiv), cyclohexanethiol (6 μ L, 0.05 mmol, 5 mol%), Ir[ppy]₂dtbbpy•PF₆ (9.1 mg, 0.01 mmol, 1 mol%), and NH₄Cl (106 mg, 2 mmol, 2 equiv). After 18 h, the reaction was purified according to the General Procedure A (silica gel, 10 – 50% EtOAc/hexanes) to provide the desired product as a clear oil (88 mg, 42% yield).

$^1\text{H NMR}$ (600 MHz, CDCl_3) δ 8.05 (dd, $J = 5.1, 0.7$ Hz, 1H), 6.73 – 6.68 (m, 1H), 6.57 – 6.54 (m, 1H), 5.10 (dt, $J = 7.1, 6.1$ Hz, 1H), 3.90 (d, $J = 0.6$ Hz, 3H), 2.84 (dd, $J = 13.8, 7.0$ Hz, 1H), 2.70 (dd, $J = 13.5, 6.0$ Hz, 1H), 1.98 (s, 3H), 1.21 (dd, $J = 6.3, 0.5$ Hz, 3H).

$^{13}\text{C NMR}$ (151 MHz, CDCl_3) δ 170.5, 164.6, 149.4, 146.8, 118.2, 111.5, 70.4, 53.5, 41.5, 21.4, 19.7.

FTIR (neat) ν_{max} : 2979, 2947, 1734, 1613, 1561, 1449, 1398 cm^{-1} .

HRMS (APCI) m/z : $[\text{M}+\text{H}]^+$ calcd. for $\text{C}_{11}\text{H}_{16}\text{O}_3\text{N}$, 210.11247; found, 210.11247.



1-(3-methylpyridin-2-yl)propan-2-yl acetate:

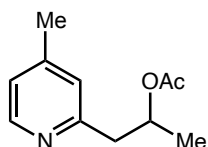
Prepared according to the General Procedure A using 2-bromo-3-methylpyridine (172 mg, 1 mmol, 1 equiv), and prop-1-en-2-yl acetate (325 μL , 300 mg, 1 mmol, 1 equiv), Hantzsch ester (329 mg, 1.3 mmol, 1.3 equiv), cyclohexanethiol (6 μL , 0.05 mmol, 5 mol%), $\text{Ir}[\text{ppy}]_2\text{dtbbpy}\cdot\text{PF}_6$ (9.1 mg, 0.01 mmol, 1 mol%), and NH_4Cl (106 mg, 2 mmol, 2 equiv). After 18 h, the reaction was purified according to the General Procedure A (silica gel, 10 – 50% EtOAc/hexanes) to provide the desired product as a yellow oil (96 mg, 50% yield).

$^1\text{H NMR}$ (600 MHz, CDCl_3) δ 8.35 (d, $J = 3.2$ Hz, 1H), 7.40 (d, $J = 7.6$ Hz, 0H), 7.03 (dd, $J = 7.6, 4.8$ Hz, 1H), 5.36 – 5.30 (m, 1H), 3.15 (dd, $J = 13.6, 7.2$ Hz, 1H), 2.91 (dd, $J = 13.6, 6.4$ Hz, 1H), 2.35 (s, 3H), 1.95 (s, 3H), 1.30 (d, $J = 6.3$ Hz, 3H).

$^{13}\text{C NMR}$ (151 MHz, CDCl_3) δ 170.4, 156.3, 146.7, 137.7, 131.8, 121.6, 70.5, 41.6, 21.3, 20.0, 18.9.

FTIR (neat) ν_{max} : 2931, 1732, 1574, 1449, 1370, 1173 cm^{-1} .

HRMS (APCI) m/z : $[\text{M}+\text{H}]^+$ calcd. for $\text{C}_{11}\text{H}_{16}\text{O}_2\text{N}$, 194.11756; found, 194.11756.



1-(4-methylpyridin-2-yl)propan-2-yl acetate:

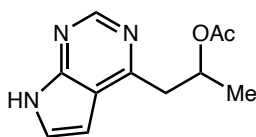
Prepared according to the General Procedure A using 2-bromo-4-methylpyridine (172 mg, 1 mmol, 1 equiv), and prop-1-en-2-yl acetate (325 μ L, 300 mg, 1 mmol, 1 equiv), Hantzsch ester (329 mg, 1.3 mmol, 1.3 equiv), cyclohexanethiol (6 μ L, 0.05 mmol, 5 mol%), Ir[ppy]₂dtbbpy•PF₆ (9.1 mg, 0.01 mmol, 1 mol%), and NH₄Cl (106 mg, 2 mmol, 2 equiv). After 18 h, the reaction was purified according to the General Procedure A (silica gel, 30 – 100% EtOAc/hexanes) to provide the desired product as a yellow oil (76 mg, 50% yield).

¹H NMR (500 MHz, CDCl₃) δ 8.37 (d, *J* = 5.1 Hz, 1H), 6.99 (s, 1H), 6.95 (d, *J* = 5.2 Hz, 1H), 5.33 – 5.20 (m, 1H), 3.04 (dd, *J* = 13.6, 7.1 Hz, 1H), 2.90 (dd, *J* = 13.5, 6.2 Hz, 1H), 2.31 (s, 3H), 1.98 (s, 3H), 1.26 (d, *J* = 6.3 Hz, 3H).

¹³C NMR (126 MHz, CDCl₃) δ 170.4, 157.6, 149.0, 147.3, 124.6, 122.6, 70.8, 44.4, 21.3, 21.0, 19.8.

FTIR (neat) ν_{max} : 2979, 2929, 1736, 1606, 1445, 1372, 1239 cm⁻¹.

HRMS (APCI) *m/z*: [M+H]⁺ calcd. for C₁₁H₁₆O₂N, 194.11756; found, 194.11753.



1-(7H-pyrrolo[2,3-d]pyrimidin-4-yl)propan-2-yl acetate:

Prepared according to the General Procedure A using 4-bromo-7H-pyrrolo[2,3-*d*]pyrimidine (99 mg, 0.5 mmol, 1 equiv), and prop-1-en-2-yl acetate (167 μ L, 150 mg, 1.5 mmol, 1 equiv), Hantzsch ester (165 mg, 0.65 mmol, 1.3 equiv), cyclohexanethiol (3 μ L, 0.025 mmol, 5 mol%), Ir[ppy]₂dtbbpy•PF₆ (4.6 mg, 0.005 mmol, 1 mol%), and NH₄Cl (53 mg, 1 mmol, 2 equiv).

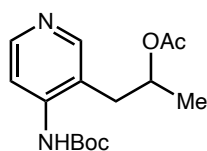
After 18 h, the reaction was purified according to the General Procedure A (silica gel, 30 – 100% EtOAc/hexanes) to provide the desired product as a yellow oil (60 mg, 55% yield).

¹H NMR (400 MHz, CDCl₃) δ 10.86 (br. s, 1H), 8.84 (s, 1H), 7.36 (dd, *J* = 3.6, 2.2 Hz, 1H), 6.69 (dd, *J* = 3.6, 1.8 Hz, 1H), 5.50 – 5.42 (m, 1H), 3.42 (dd, *J* = 13.3, 6.9 Hz, 1H), 3.19 (dd, *J* = 13.3, 6.3 Hz, 1H), 1.94 (s, 3H), 1.34 (d, *J* = 6.3 Hz, 3H).

¹³C NMR (151 MHz, CDCl₃) δ 172.6, 170.6, 159.1, 151.1, 125.3, 118.5, 100.3, 70.3, 42.2, 21.4, 20.2.

FTIR (neat) ν_{\max} : 2956, 2920, 2851, 1576, 1559, 1435, 1350 cm⁻¹.

HRMS (ESI) *m/z*: [M+Na]⁺ calcd. for C₁₁H₁₃O₂N₃Na, 242.09000; found, 242.09002.



1-(4-((tert-butoxycarbonyl)amino)pyridin-3-yl)propan-2-yl acetate:

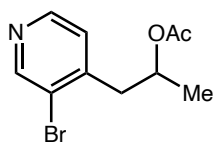
Prepared according to the General Procedure A using *tert*-butyl (3-bromopyridin-4-yl)carbamate (272 mg, 1 mmol, 1 equiv), and prop-1-en-2-yl acetate (325 μL, 300 mg, 1 mmol, 1 equiv). Hantzsch ester (329 mg, 1.3 mmol, 1.3 equiv), Ir[ppy]₂dtbbpy•PF₆ (9.1 mg, 0.01 mmol, 1 mol%), and NH₄Cl (106 mg, 2 mmol, 2 equiv). After 18 h, the reaction was purified according to the General Procedure A (silica gel, 20 – 100% EtOAc/hexanes) to provide the desired product as a colorless oil (78 mg, 27% yield).

¹H NMR (600 MHz, CDCl₃) δ 8.36 (d, *J* = 5.7 Hz, 1H), 8.20 (s, 1H), 8.07 (d, *J* = 5.6 Hz, 2H), 4.86 – 4.76 (m, 1H), 2.97 (dd, *J* = 14.5, 4.3 Hz, 1H), 2.62 (dd, *J* = 14.4, 7.8 Hz, 1H), 2.10 (s, 3H), 1.54 (s, 9H), 1.25 (d, *J* = 6.9 Hz, 3H).

¹³C NMR (151 MHz, CDCl₃) δ 171.4, 152.6, 151.8, 149.8, 145.0, 119.6, 113.0, 81.5, 71.1, 36.0, 28.3, 21.4, 19.0.

FTIR (neat) ν_{\max} : 2977, 2928, 1723, 1604, 1582, 1512, 1234, 1151 cm⁻¹.

HRMS (ESI) m/z : $[M+H]^+$ calcd. for $C_{15}H_{23}O_4N_2$, 295.16523; found, 295.16524.



1-(3-bromopyridin-4-yl)propan-2-yl acetate:

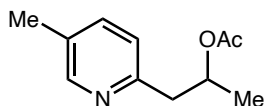
Prepared according to the General Procedure A using 3,4-dibromopyridine (236 mg, 1 mmol, 1 equiv), and prop-1-en-2-yl acetate (325 μ L, 300 mg, 1 mmol, 1 equiv), Hantzsch ester (329 mg, 1.3 mmol, 1.3 equiv), cyclohexanethiol (6 μ L, 0.05 mmol, 5 mol%), Ir[ppy]₂dtbbpy•PF₆ (9.1 mg, 0.01 mmol, 1 mol%), and NH₄Cl (106 mg, 2 mmol, 2 equiv). After 18 h, the reaction was purified according to the General Procedure A (silica gel, 30 – 100% EtOAc/hexanes) to provide the desired product as a yellow oil (97 mg, 38% yield).

¹H NMR (400 MHz, CDCl₃) δ 8.65 (s, 1H), 8.39 (dd, J = 4.9, 0.8 Hz, 1H), 7.15 (dd, J = 5.0, 0.8 Hz, 1H), 5.29 – 5.08 (m, 1H), 3.05 – 2.92 (m, 2H), 1.95 (s, 3H), 1.28 (dd, J = 6.3, 0.9 Hz, 3H).

¹³C NMR (101 MHz, CDCl₃) δ 170.3, 152.2, 148.1, 146.2, 126.2, 123.6, 69.4, 41.2, 21.2, 20.0.

FTIR (neat) ν_{\max} : 2979, 2930, 1734, 1584, 1399, 1371, 1234 cm⁻¹.

HRMS (APCI) m/z : $[M+H]^+$ calcd. for $C_{10}H_{13}O_2NBr$, 258.01242; found, 258.01248.



1-(5-methylpyridin-2-yl)propan-2-yl acetate:

Prepared according to the General Procedure A using 2-bromo-5-methylpyridine (172 mg, 1 mmol, 1 equiv), and prop-1-en-2-yl acetate (325 μ L, 300 mg, 1 mmol, 1 equiv). Hantzsch ester (329 mg, 1.3 mmol, 1.3 equiv), cyclohexanethiol (6 μ L, 0.05 mmol, 5 mol%), Ir[ppy]₂dtbbpy•PF₆ (9.1 mg, 0.01 mmol, 1 mol%), and NH₄Cl (106 mg, 2 mmol, 2 equiv).

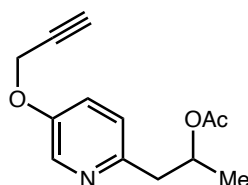
After 18 h, the reaction was purified according to the General Procedure A (silica gel, 30 – 100% EtOAc/hexanes) to provide the desired product as a yellow oil (90 mg, 47% yield).

¹H NMR (500 MHz, CDCl₃) δ 8.29 (s, 1H), 7.34 (dd, *J* = 7.5, 1.9 Hz, 1H), 7.00 (d, *J* = 7.9 Hz, 1H), 5.20 (dt, *J* = 12.4, 6.2 Hz, 1H), 2.98 (dd, *J* = 13.6, 7.3 Hz, 1H), 2.86 (dd, *J* = 13.6, 6.0 Hz, 1H), 2.23 (s, 3H), 1.90 (s, 3H), 1.20 (d, *J* = 6.3 Hz, 3H).

¹³C NMR (126 MHz, CDCl₃) δ 170.4, 154.9, 149.7, 136.8, 130.8, 123.1, 70.8, 44.1, 21.2, 19.8, 18.0.

FTIR (neat) ν_{max} : 2979, 2929, 1732, 1570, 1488, 1371, 1237, 1048 cm⁻¹.

HRMS (APCI) *m/z*: [M+H]⁺ calcd. for C₁₁H₁₆O₂N, 194.11756; found, 194.11756.



1-(5-(prop-2-yn-1-yloxy)pyridin-2-yl)propan-2-yl acetate:

Prepared according to the General Procedure A using 2-bromo-5-(prop-2-yn-1-yloxy)pyridine (210 mg, 1 mmol, 1 equiv), and prop-1-en-2-yl acetate (325 μL, 300 mg, 1 mmol, 1 equiv).

Hantzsch ester (329 mg, 1.3 mmol, 1.3 equiv), cyclohexanethiol (6 μL, 0.05 mmol, 5 mol%),

Ir[ppy]₂dtbbpy•PF₆ (9.1 mg, 0.01 mmol, 1 mol%), and NH₄Cl (106 mg, 2 mmol, 2 equiv).

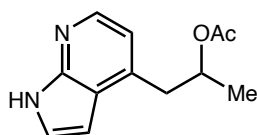
After 18 h, the reaction was purified according to the General Procedure A (silica gel, 20 – 100% EtOAc/hexanes) to provide the desired product as a pale yellow oil (62 mg, 26% yield).

¹H NMR (600 MHz, CDCl₃) δ 8.27 (d, *J* = 2.9 Hz, 1H), 7.21 (dd, *J* = 8.5, 3.0 Hz, 1H), 7.09 (d, *J* = 8.5 Hz, 1H), 5.22 (dt, *J* = 12.4, 6.2 Hz, 1H), 4.69 (d, *J* = 2.4 Hz, 2H), 3.01 (dd, *J* = 13.8, 7.3 Hz, 1H), 2.89 (dd, *J* = 13.8, 6.0 Hz, 1H), 2.54 (t, *J* = 2.4 Hz, 1H), 1.95 (s, 3H), 1.24 (d, *J* = 6.3 Hz, 3H).

^{13}C NMR (126 MHz, CDCl_3) δ 170.5, 152.4, 151.0, 137.6, 123.9, 122.4, 77.9, 76.4, 70.9, 56.3, 43.7, 21.4, 19.8.

FTIR (neat) ν_{max} : 3290, 2979, 2932, 1727, 1573, 1482, 1371, 1227 cm^{-1} .

HRMS (APCI) m/z : $[\text{M}+\text{H}]^+$ calcd. for $\text{C}_{13}\text{H}_{16}\text{O}_3\text{N}$, 234.11247; found, 315.11262.



1-(1H-pyrrolo[2,3-b]pyridin-4-yl)propan-2-yl acetate:

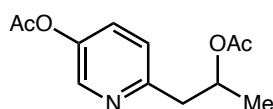
Prepared according to the General Procedure A using 4-bromo-1H-pyrrolo[2,3-*b*]pyridine (197 mg, 1 mmol, 1 equiv), and prop-1-en-2-yl acetate (325 μL , 300 mg, 1 mmol, 1 equiv), Hantzsch ester (329 mg, 1.3 mmol, 1.3 equiv), cyclohexanethiol (6 μL , 0.05 mmol, 5 mol%), Ir[ppy]₂dtbbpy•PF₆ (9.1 mg, 0.01 mmol, 1 mol%), and NH₄Cl (106 mg, 2 mmol, 2 equiv). After 18 h, the reaction was purified according to the General Procedure A (silica gel, 30 – 100% EtOAc/hexanes) to provide the desired product as a white solid (82 mg, 37% yield).

^1H NMR (600 MHz, CDCl_3) δ 11.96 (br. s, 1H), 8.26 (dd, $J = 4.9, 0.9$ Hz, 1H), 7.38 (d, $J = 3.4$ Hz, 1H), 6.92 (d, $J = 4.8$ Hz, 1H), 6.61 (dd, $J = 3.5, 1.0$ Hz, 1H), 5.52 – 5.08 (m, 1H), 3.27 (dd, $J = 13.5, 6.5$ Hz, 1H), 3.01 (dd, $J = 13.4, 6.9$ Hz, 1H), 1.98 (s, 3H), 1.25 (d, $J = 6.3$, 3H).

^{13}C NMR (151 MHz, CDCl_3) δ 170.7, 148.9, 142.3, 139.5, 125.1, 121.0, 116.5, 99.2, 70.6, 39.5, 21.4, 19.9.

FTIR (neat) ν_{max} : 2981, 2922, 1725, 1599, 1406, 1246, 1057 cm^{-1} .

HRMS (APCI) m/z : $[\text{M}+\text{H}]^+$ calcd. for $\text{C}_{12}\text{H}_{15}\text{O}_2\text{N}_2$, 219.11280; found, 219.11282.



6-(2-acetoxypropyl)pyridin-3-yl acetate:

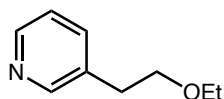
Prepared according to the General Procedure A using 6-bromopyridin-3-yl acetate (216 mg, 1 mmol, 1 equiv), and prop-1-en-2-yl acetate (325 μ L, 300 mg, 3 mmol, 3 equiv). Hantzsch ester (329 mg, 1.3 mmol, 1.3 equiv), cyclohexanethiol (6 μ L, 0.05 mmol, 5 mol%), Ir[ppy]₂dtbbpy•PF₆ (9.1 mg, 0.01 mmol, 1 mol%), and NH₄Cl (106 mg, 2 mmol, 2 equiv). After 18 h, the reaction was purified according to the General Procedure A (silica gel, 20 – 100% EtOAc/hexanes) to provide the desired product as a yellow oil (63 mg, 27% yield).

¹H NMR (500 MHz, CDCl₃) δ 8.32 (d, J = 2.7 Hz, 1H), 7.40 (dd, J = 8.4, 2.8 Hz, 1H), 7.20 (d, J = 8.4 Hz, 1H), 5.27 (dt, J = 7.2, 6.1 Hz, 1H), 3.08 (dd, J = 13.8, 7.3 Hz, 1H), 2.96 (dd, J = 13.8, 5.9 Hz, 1H), 2.31 (s, 3H), 1.97 (s, 3H), 1.27 (d, J = 6.3 Hz, 3H).

¹³C NMR (126 MHz, CDCl₃) δ 170.6, 169.1, 155.4, 146.0, 142.7, 129.6, 124.0, 70.7, 44.0, 21.4, 21.1, 19.9.

FTIR (neat) ν_{max} : 2980, 2934, 1765, 1731, 1482, 1370, 1240, 1187 cm⁻¹.

HRMS (NSI) m/z : [M+H]⁺ calcd. for C₁₂H₁₆O₄N, 238.10738; found, 238.10739.



3-(2-ethoxyethyl)pyridine:

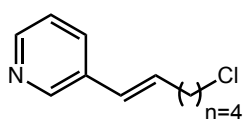
Prepared according to the General Procedure B using 3-iodopyridine (205 mg, 1 mmol, 1 equiv), and ethoxyethene (287 μ L, 216 mg, 1 mmol, 1 equiv), Hantzsch ester (329 mg, 1.3 mmol, 1.3 equiv), cyclohexanethiol (6 μ L, 0.05 mmol, 5 mol%), Ir[ppy]₂dtbbpy•PF₆ (9.1 mg, 0.01 mmol, 1 mol%), and NH₄Cl (106 mg, 2 mmol, 2 equiv). After 18 h, the reaction was purified according to the General Procedure B (silica gel, 50 – 100% EtOAc/hexanes) to provide the desired product as a pale yellow oil (69 mg, 49% yield).

¹H NMR (600 MHz, CDCl₃) δ 8.40 (d, *J* = 2.4 Hz, 1H), 8.36 (dd, *J* = 4.8, 1.7 Hz, 1H), 7.47 (dt, *J* = 7.7, 2.0 Hz, 1H), 7.12 (ddd, *J* = 7.8, 4.9, 1.0 Hz, 1H), 3.54 (t, *J* = 6.8 Hz, 2H), 3.39 (q, *J* = 6.9 Hz, 2H), 2.78 (t, *J* = 6.8 Hz, 2H), 1.09 (t, *J* = 6.9 Hz, 3H).

¹³C NMR (151 MHz, CDCl₃) δ 150.1, 147.5, 136.4, 134.7, 123.2, 70.6, 66.2, 33.4, 15.0.

FTIR (neat) ν_{max} : 2974, 2863, 1479, 1423, 1326, 1106 cm⁻¹.

HRMS (APCI) *m/z*: [M+H]⁺ calcd. for C₉H₁₄ON, 152.10699; found, 315.10774.



(E)-3-(6-chlorohex-1-en-1-yl)pyridine:

Prepared according to the General Procedure A using 3-iodopyridine (205 mg, 1 mmol, 1 equiv), and 5-chlorohex-1-yne (360 mg, 3 mmol, 3 equiv). Hantzsch ester (329 mg, 1.3 mmol, 1.3 equiv), cyclohexanethiol (6 μL, 0.05 mmol, 5 mol%), Ir[ppy]₂dtbbpy•PF₆ (9.1 mg, 0.01 mmol, 1 mol%), and NH₄Cl (106 mg, 2 mmol, 2 equiv). After 18 h, the reaction was purified according to the General Procedure A (silica gel, 20 – 60% EtOAc/hexanes) as a pale yellow oil. Compound was isolated as an inseparable mixture of cis:trans isomers in a 1:1.7 (127 mg, 65%).

Trans isomer

¹H NMR (600 MHz, CDCl₃) δ 8.48 (s, 1H), 8.36 (d, *J* = 4.8 Hz, 1H), 7.62 – 7.51 (m, 1H), 7.14 (dd, *J* = 8.0, 4.8 Hz, 1H), 6.31 (d, *J* = 15.8 Hz, 1H), 6.20 (dt, *J* = 15.6, 6.7 Hz, 1H), 3.50 (t, *J* = 6.6 Hz, 2H), 2.20 (q, *J* = 7.3 Hz, 2H), 1.80 – 1.72 (m, 2H), 1.62 – 1.54 (m, 2H).

¹³C NMR (151 MHz, CDCl₃) δ 148.1, 148.0, 133.3, 132.7, 132.6, 127.0, 44.9, 32.4, 32.1, 26.4.

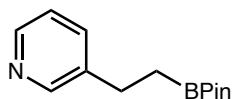
Cis isomer

¹H NMR (600 MHz, CDCl₃) δ 8.45 (s, 1H), 8.39 (d, *J* = 4.8 Hz, 1H), 7.49 (dd, *J* = 7.9, 1.9 Hz, 1H), 7.21 – 7.17 (m, 1H), 6.33 (d, *J* = 7.7 Hz, 1H), 5.71 (dt, *J* = 11.5, 7.3 Hz, 1H), 3.44 (t, *J* = 6.6 Hz, 2H), 2.26 (q, *J* = 7.4 Hz, 2H), 1.75 – 1.68 (m, 2H), 1.57 – 1.50 (m, 2H).

¹³C NMR (151 MHz, CDCl₃) δ 149.9, 147.7, 135.8, 134.6, 133.2, 126.0, 123.2, 44.8, 32.1, 27.9, 27.0.

FTIR (neat) ν_{\max} : 3024, 2935, 2860, 1651, 1567, 1414 cm⁻¹.

HRMS (APCI) *m/z*: [M+H]⁺ calcd. for C₁₁H₁₅NCl, 196.08875; found, 196.08888.



3-(2-(4,4,5,5-tetramethyl-1,3,2-dioxaborolan-2-yl)ethyl)pyridine:

Prepared according to the General Procedure A using 3-iodopyridine (41 mg, 0.2 mmol, 1 equiv), and vinylboronic acid, pinacol ester (102 μL, 92 mg, 0.75 mmol, 3 equiv), Hantzsch ester (66 mg, 0.26 mmol, 1.3 equiv), cyclohexanethiol (1.2 μL, 0.0125 mmol, 5 mol%), Ir[ppy]₂dtbbpy•PF₆ (1.8 mg, 0.002 mmol, 1 mol%), and NH₄Cl (21 mg, 0.4 mmol, 2 equiv). After 18 h, the reaction was purified according to the General Procedure A (preparative reverse phase HPLC, 30 – 99% MeCN/H₂O) to provide the desired product as a colorless oil (25 mg, 53%).

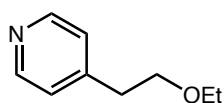
¹H NMR (600 MHz, CDCl₃) δ 8.50 – 8.45 (m, 1H), 8.40 (dd, *J* = 4.7, 1.6 Hz, 1H), 7.52 (dt, *J* = 7.8, 2.0 Hz, 1H), 7.17 (dd, *J* = 7.8, 4.8 Hz, 1H), 2.74 (t, *J* = 8.0 Hz, 2H), 1.20 (s, 12H), 1.14 (t, *J* = 8.1 Hz, 2H).

¹³C NMR (151 MHz, CDCl₃) δ 149.9, 147.2, 139.6, 135.6, 123.3, 83.4, 27.3, 24.9. Boron bearing carbon not observed.

¹¹B NMR (192 MHz, CDCl₃) δ 38.0.

FTIR (neat) ν_{\max} : 2977, 2928, 1425, 1370, 1310, 1143 cm⁻¹.

HRMS (APCI) m/z : $[M+H]^+$ calcd. for $C_{13}H_{21}O_2NB$, 234.16599; found, 234.16605.



4-(2-ethoxyethyl)pyridine:

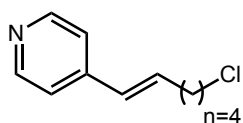
Prepared according to the General Procedure A using 4-bromopyridine hydrochloride (194 mg, 1 mmol, 1 equiv), and ethoxyethene (287 μ L, 216 mg, 1 mmol, 1 equiv), Hantzsch ester (329 mg, 1.3 mmol, 1.3 equiv), cyclohexanethiol (6 μ L, 0.05 mmol, 5 mol%), Ir[ppy]₂dtbbpy•PF₆ (9.1 mg, 0.01 mmol, 1 mol%), and NH₄Cl (106 mg, 2 mmol, 2 equiv). After 18 h, the reaction was purified according to the General Procedure A (silica gel, 40 – 80% EtOAc/hexanes, 1% Et₃N modifier) to provide the desired product as a colorless oil (108 mg, 72% yield).

¹H NMR (600 MHz, CDCl₃) δ 8.49 (d, J = 6.1 Hz, 2H), 7.15 (d, J = 6.0 Hz, 2H), 3.65 (t, J = 6.8 Hz, 2H), 3.48 (q, J = 7.0 Hz, 2H), 2.86 (t, J = 6.8 Hz, 2H), 1.18 (t, J = 7.0 Hz, 3H).

¹³C NMR (151 MHz, CDCl₃) δ 149.8, 124.4, 70.1, 66.5, 35.8, 15.2.

FTIR (neat) ν_{\max} : 2921, 2850, 1463, 1265 cm⁻¹.

HRMS (APCI) m/z : $[M+H]^+$ calcd. for $C_9H_{14}ON$, 152.10699; found, 152.10692.



(E)-4-(6-chlorohex-1-en-1-yl)pyridine:

Prepared according to the General Procedure A using 4-bromopyridine hydrochloride (196 mg, 1 mmol, 1 equiv), and 5-chlorohex-1-yne (360 mg, 3 mmol, 3 equiv). Hantzsch ester (329 mg, 1.3 mmol, 1.3 equiv), cyclohexanethiol (6 μ L, 0.05 mmol, 5 mol%), Ir[ppy]₂dtbbpy•PF₆ (9.1 mg, 0.01 mmol, 1 mol%), and NH₄Cl (106 mg, 2 mmol, 2 equiv). After 18 h, the reaction was purified according to the General Procedure A (silica gel, 20 – 60% EtOAc/hexanes) as a pale

yellow oil. Compound was isolated as an inseparable mixture of cis:trans isomers in a 1:3 ratio (144 mg, 74%).

Trans isomer

$^1\text{H NMR}$ (600 MHz, CDCl_3) δ 8.47 (d, $J = 5.2$ Hz, 2H), 7.17 (d, $J = 5.1$ Hz, 2H), 6.42 (dt, $J = 15.3, 6.8$ Hz, 1H), 6.31 (d, $J = 16.1$ Hz, 1H), 3.54 (t, $J = 6.6$ Hz, 2H), 2.25 (q, $J = 7.2$ Hz, 2H), 1.85 – 1.75 (m, 2H), 1.69 – 1.58 (m, 2H).

$^{13}\text{C NMR}$ (151 MHz, CDCl_3) δ 150.1, 145.0, 135.3, 128.4, 120.7, 44.8, 32.3, 32.1, 26.2.

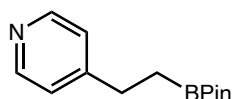
Cis isomer

$^1\text{H NMR}$ (600 MHz, CDCl_3) δ 8.53 (d, $J = 5.1$ Hz, 2H), 7.11 (d, $J = 5.2$ Hz, 2H), 6.33 (d, $J = 15.3$ Hz, 1H), 5.81 (dt, $J = 11.7, 7.3$ Hz, 1H), 3.49 (t, $J = 6.6$ Hz, 2H), 2.33 (qd, $J = 7.5, 1.7$ Hz, 2H), 1.82 – 1.71 (m, 2H), 1.64 – 1.55 (m, 2H).

$^{13}\text{C NMR}$ (151 MHz, CDCl_3) δ 149.8, 145.0, 136.3, 127.3, 123.5, 44.8, 32.1, 27.9, 26.9.

FTIR (neat) ν_{max} : 2936, 2861, 1650, 1594, 1549, 1414 cm^{-1} .

HRMS (APCI) m/z : $[\text{M}+\text{H}]^+$ calcd. for $\text{C}_{11}\text{H}_{15}\text{NCl}$, 196.08875; found, 196.08886.



4-(2-(4,4,5,5-tetramethyl-1,3,2-dioxaborolan-2-yl)ethyl)pyridine:

Prepared according to the General Procedure A using 4-bromopyridine hydrochloride (39 mg, 0.2 mmol, 1 equiv), and vinylboronic acid, pinacol ester (102 μL , 92 mg, 0.75 mmol, 3 equiv), Hantzsch ester (66 mg, 0.26 mmol, 1.3 equiv), cyclohexanethiol (1.2 μL , 0.0125 mmol, 5 mol%), $\text{Ir}[\text{ppy}]_2\text{dtbbpy}\cdot\text{PF}_6$ (1.8 mg, 0.002 mmol, 1 mol%), and NH_4Cl (21 mg, 0.4 mmol, 2 equiv). After 18 h, the reaction was purified according to the General Procedure A (preparative reverse phase HPLC, 30 – 99% $\text{MeCN}/\text{H}_2\text{O}$) to provide the desired product as a amorphous white solid (26 mg, 56%).

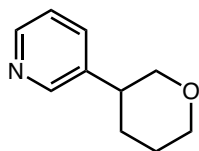
¹H NMR (600 MHz, CDCl₃) δ 8.45 (d, *J* = 5.2 Hz, 2H), 7.14 (d, *J* = 5.1 Hz, 2H), 2.73 (t, *J* = 8.1 Hz, 2H), 1.20 (s, 12H), 1.13 (t, *J* = 8.1 Hz, 2H).

¹³C NMR (151 MHz, CDCl₃) δ 153.5, 149.5, 123.7, 83.5, 29.4, 24.9. Boron bearing carbon not observed.

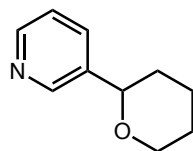
¹¹B NMR (192 MHz, CDCl₃) δ 38.1.

FTIR (neat) ν_{max} : 2986, 2923, 1625, 1433, 1379, 1090 cm⁻¹.

HRMS (APCI) *m/z*: [M+H]⁺ calcd. for C₁₃H₂₁O₂NB, 234.16599; found, 234.16619.



isomer A



isomer B

3-(tetrahydro-2H-pyran-3-yl)pyridine; 3-(tetrahydro-2H-pyran-2-yl)pyridine:

Prepared according to the General Procedure B using 3-iodopyridine (205 mg, 1 mmol, 1 equiv), and 3,4-dihydro-2*H*-pyran (254 μL, 252 mg, 3 mmol, 3 equiv), Hantzsch ester (329 mg, 1.3 mmol, 1.3 equiv), cyclohexanethiol (6 μL, 0.05 mmol, 5 mol%), Ir[ppy]₂dtbbpy•PF₆ (9.1 mg, 0.01 mmol, 1 mol%), and NH₄Cl (106 mg, 2 mmol, 2 equiv). After 18 h, the reaction was purified according to the General Procedure B (preparative thin layer chromatography, silica gel, 40% EtOAc/hexanes) to provide the isomer A as a pale yellow oil (32 mg, 23% yield), and isomer B as a pale yellow oil (37 mg, 20% yield, 43% combined yield).

Isomer A

¹H NMR (500 MHz, CDCl₃) δ 8.56 (d, *J* = 2.3 Hz, 1H), 8.48 (dd, *J* = 4.8, 1.8 Hz, 1H), 7.68 (dt, *J* = 7.8, 2.0 Hz, 1H), 7.27 – 7.23 (m, 1H), 4.35 (dd, *J* = 11.1, 2.3 Hz, 1H), 4.13 (ddd, *J* = 11.4, 4.2, 1.9 Hz, 1H), 3.60 (td, *J* = 11.6, 2.4 Hz, 1H), 1.98 – 1.89 (m, 1H), 1.83 (dt, *J* = 13.1, 2.3 Hz, 1H), 1.72 – 1.50 (m, 4H).

¹³C NMR (126 MHz, CDCl₃) δ 148.5, 147.7, 138.7, 133.4, 123.2, 77.7, 68.9, 33.8, 25.7, 23.7.

FTIR (neat) ν_{\max} : 2936, 2847, 1440, 1425, 1366, 1269 cm^{-1} .

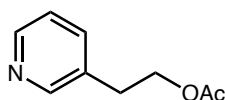
Isomer B

^1H NMR (500 MHz, CDCl_3) δ 8.49 (d, $J = 2.3$ Hz, 1H), 8.46 (dd, $J = 4.8, 1.6$ Hz, 1H), 7.53 (dt, $J = 7.9, 2.0$ Hz, 1H), 7.23 (dd, $J = 7.8, 4.8$ Hz, 1H), 3.97 (tdd, $J = 11.2, 4.4, 2.0$ Hz, 2H), 3.50 – 3.44 (m, 1H), 3.40 (t, $J = 10.9$ Hz, 1H), 2.87 (tt, $J = 10.9, 3.9$ Hz, 1H), 2.04 (ddt, $J = 9.3, 3.8, 2.1$ Hz, 1H), 1.82 – 1.68 (m, 3H).

^{13}C NMR (126 MHz, CDCl_3) δ 149.4, 148.2, 138.1, 134.8, 123.5, 73.3, 68.3, 40.6, 30.3, 25.9.

FTIR (neat) ν_{\max} : 2932, 2847, 1424, 1279 cm^{-1} .

HRMS (APCI) m/z : $[\text{M}+\text{H}]^+$ calcd. for $\text{C}_{10}\text{H}_{14}\text{ON}$, 164.10699; found, 164.10690.



2-(pyridin-3-yl)ethyl acetate:

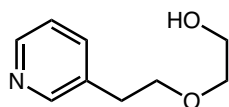
Prepared according to the General Procedure A using 3-iodopyridine (205 mg, 1 mmol, 1 equiv), and vinyl acetate (276 μL , 258 mg, 3 mmol, 3 equiv), Hantzsch ester (329 mg, 1.3 mmol, 1.3 equiv), cyclohexanethiol (6 μL , 0.05 mmol, 5 mol%), $\text{Ir}[\text{ppy}]_2\text{dtbbpy}\cdot\text{PF}_6$ (9.1 mg, 0.01 mmol, 1 mol%), and NH_4Cl (106 mg, 2 mmol, 2 equiv). After 18 h, the reaction was purified according to the General Procedure A (silica gel, 40 – 100% EtOAc/Hexanes, 1% Et_3N modifier) to provide the desired product as a yellow oil (86 mg, 56% yield).

^1H NMR (600 MHz, CDCl_3) δ 8.46 (d, $J = 2.8$ Hz, 2H), 7.52 (dt, $J = 7.8, 2.0$ Hz, 1H), 7.21 (dd, $J = 7.8, 4.8$ Hz, 1H), 4.25 (t, $J = 6.9$ Hz, 2H), 2.91 (t, $J = 6.8$ Hz, 2H), 2.00 (s, 3H).

^{13}C NMR (151 MHz, CDCl_3) δ 171.0, 150.4, 148.2, 136.4, 133.5, 123.5, 64.3, 32.4, 21.0.

FTIR (neat) ν_{\max} : 2978, 1729, 1579, 1424, 1371, 1236 cm^{-1} .

HRMS (APCI) m/z : $[\text{M}+\text{H}]^+$ calcd. for $\text{C}_9\text{H}_{12}\text{O}_2\text{N}$, 166.08626; found, 166.08622.



2-(2-(pyridin-3-yl)ethoxy)ethan-1-ol:

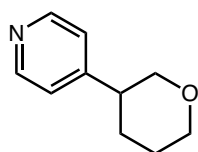
Prepared according to the General Procedure B using 3-iodopyridine (205 mg, 1 mmol, 1 equiv), and 2-(vinylloxy)ethan-1-ol (311 μ L, 306 mg, 3 mmol, 3 equiv), Hantzsch ester (329 mg, 1.3 mmol, 1.3 equiv), cyclohexanethiol (6 μ L, 0.05 mmol, 5 mol%), Ir[ppy]₂dtbbpy•PF₆ (9.1 mg, 0.01 mmol, 1 mol%), and NH₄Cl (106 mg, 2 mmol, 2 equiv). After 18 h, the reaction was purified according to the General Procedure B (silica gel, 30 – 100% EtOAc/hexanes, then 0 – 10% DCM/MeOH) to provide the desired product as a yellow oil (109 mg, 65% yield).

¹H NMR (400 MHz, CDCl₃) δ 8.44 (d, J = 1.5 Hz, 1H), 8.41 (dd, J = 4.9, 1.6 Hz, 1H), 7.54 (ddd, J = 7.8, 2.3, 1.7 Hz, 1H), 7.19 (ddd, J = 7.8, 4.8, 0.9 Hz, 1H), 3.71 – 3.65 (m, 4H), 3.55 – 3.50 (m, 2H), 2.87 (t, J = 6.7 Hz, 2H), 2.72 (br. s, 1H).

¹³C NMR (101 MHz, CDCl₃) δ 150.1, 147.6, 136.6, 134.6, 123.4, 72.2, 71.4, 61.7, 33.4.

FTIR (neat) ν_{max} : 3271, 2864, 1595, 1479, 1425, 1115 cm⁻¹.

HRMS (APCI) m/z : [M+H]⁺ calcd. for C₉H₁₄O₂N, 168.10191; found, 168.10187.



4-(tetrahydro-2H-pyran-3-yl)pyridine:

Prepared according to the General Procedure B using 4-bromopyridine hydrochloride (194 mg, 1 mmol, 1 equiv), and 3,4-dihydro-2H-pyran (254 μ L, 252 mg, 3 mmol, 3 equiv), Hantzsch ester (329 mg, 1.3 mmol, 1.3 equiv), cyclohexanethiol (6 μ L, 0.05 mmol, 5 mol%), Ir[ppy]₂dtbbpy•PF₆ (9.1 mg, 0.01 mmol, 1 mol%), and NH₄Cl (106 mg, 2 mmol, 2 equiv). After 18 h, the reaction was purified according to the General Procedure B (silica gel, 40 –

80% EtOAc/hexanes, 1% Et₃N modifier) to provide the desired product as a colorless oil (124 mg, 76% yield).

¹H NMR (400 MHz, CDCl₃) δ 8.51 – 8.49 (m, 2H), 7.14 – 7.12 (m, 2H), 4.04 – 3.91 (m, 2H), 3.50 – 3.43 (m, 1H), 3.40 (dd, *J* = 11.3, 10.4 Hz, 1H), 2.88 – 2.79 (m, 1H), 2.09 – 1.99 (m, 1H), 1.77 – 1.67 (m, 3H).

¹³C NMR (101 MHz, CDCl₃) δ 151.5, 150.0, 122.9, 72.8, 68.3, 42.2, 29.7, 25.6.

FTIR (neat) ν_{max} : 2935, 2848, 1665, 1598, 1593, 1507, 1443, 1412 cm⁻¹.

HRMS (APCI) *m/z*: [M+H]⁺ calcd. for C₁₀H₁₄O₄N₂, 164.10699; found, 164.10782.



2-(pyridin-4-yl)ethan-1-ol:

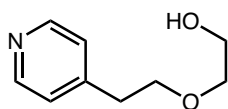
Prepared according to the General Procedure B using 4-bromopyridine hydrochloride (194 mg, 1 mmol, 1 equiv), and vinyl acetate (276 μ L, 258 mg, 3 mmol, 3 equiv), Hantzsch ester (329 mg, 1.3 mmol, 1.3 equiv), cyclohexanethiol (6 μ L, 0.05 mmol, 5 mol%), Ir[ppy]₂dtbbpy•PF₆ (9.1 mg, 0.01 mmol, 1 mol%), and NH₄Cl (106 mg, 2 mmol, 2 equiv). After 18 h, the reaction was purified according to the General Procedure B (silica gel, 40 – 100% EtOAc/hexanes, 1% Et₃N modifier then 10% MeOH/CH₂Cl₂) to provide the desired product as a yellow oil (76 mg, 62% yield).

¹H NMR (500 MHz, CDCl₃) δ 8.35 – 8.31 (m, 2H), 7.15 – 7.10 (m, 2H), 3.84 (t, *J* = 6.5 Hz, 2H), 3.55 (br. s, 1H), 2.81 (t, *J* = 6.4 Hz, 2H).

¹³C NMR (126 MHz, CDCl₃) δ 149.3, 148.9, 124.7, 62.1, 38.6.

FTIR (neat) ν_{max} : 3232, 2928, 1604, 1440, 1415, 1219 cm⁻¹.

HRMS (APCI) *m/z*: [M+H]⁺ calcd. for C₇H₁₀ON, 124.07569; found, 124.07564.



2-(2-(pyridin-4-yl)ethoxy)ethan-1-ol:

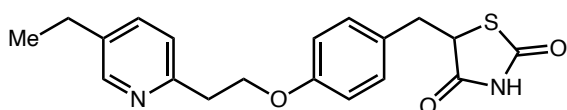
Prepared according to the General Procedure B using 4-bromopyridine hydrochloride (194 mg, 1 mmol, 1 equiv), and 2-(vinylloxy)ethan-1-ol (306 mg, 311 μ L, 3 mmol, 3 equiv), Hantzsch ester (329 mg, 1.3 mmol, 1.3 equiv), cyclohexanethiol (6 μ L, 0.05 mmol, 5 mol%), Ir[ppy]₂dtbbpy•PF₆ (9.1 mg, 0.01 mmol, 1 mol%), and NH₄Cl (106 mg, 2 mmol, 2 equiv). After 18 h, the reaction was purified according to the General Procedure B (silica gel, 40 – 100% EtOAc/hexanes, 1% Et₃N modifier then 10% MeOH/CH₂Cl₂) to provide the desired product as a yellow oil (75 mg, 45% yield).

¹H NMR (400 MHz, CDCl₃) δ 8.40 (d, *J* = 5.1 Hz, 2H), 7.12 (d, *J* = 5.1 Hz, 2H), 3.73 – 3.62 (m, 4H), 3.51 (t, *J* = 4.6 Hz, 2H), 3.25 (br. s, 1H), 2.84 (t, *J* = 6.6 Hz, 2H).

¹³C NMR (151 MHz, CDCl₃) δ 149.4, 148.3, 124.2, 72.1, 70.4, 61.5, 35.4.

FTIR (neat) ν_{max} : 3269, 2865, 1605, 1441, 1357, 1117 cm⁻¹.

HRMS (APCI) *m/z*: [M+H]⁺ calcd. for C₉H₁₄O₂N, 168.10191; found, 168.10187.



5-(4-(2-(5-ethylpyridin-2-yl)ethoxy)benzyl)thiazolidine-2,4-dione:

Prepared according to the General Procedure A using 2-bromo-5-ethylpyridine (93 mg, 0.5 mmol, 1 equiv), 5-(4-(vinylloxy)benzyl)thiazolidine-2,4-dione (375 mg, 1.5 mmol, 3 equiv), Hantzsch ester (164 mg, 0.65 mmol, 1.3 equiv), cyclohexanethiol (3 μ L, 0.025 mmol, 5 mol%), Ir[ppy]₂dtbbpy•PF₆ (4.5 mg, 0.005 mmol, 1 mol%), NH₄Cl (53 mg, 2 mmol, 2 equiv) and 2,2,2-trifluoroethanol (10 mL, 0.05 M). After all reagents and solvents were added, the reaction mixture was gently warmed until complete dissolution of all reagents. The reaction was then

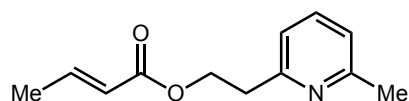
stirred at 1400 rpm at 30 °C for 18 h. After this time, the reaction was purified according to the General Procedure A (silica gel 30 – 80% EtOAc/hexanes) to provide the desired product as an amorphous white solid (114 mg, 64%).

¹H NMR (600 MHz, THF-*d*₈) δ 10.74 (br. s, 1H), 8.36 (d, *J* = 2.3 Hz, 1H), 7.47 (dd, *J* = 8.0, 2.3 Hz, 1H), 7.19 (d, *J* = 7.9 Hz, 1H), 7.13 (d, *J* = 8.3 Hz, 2H), 6.84 (d, *J* = 8.2 Hz, 2H), 4.60 (dd, *J* = 9.7, 4.0 Hz, 1H), 4.31 (t, *J* = 6.8 Hz, 2H), 3.39 (dd, *J* = 14.1, 4.0 Hz, 1H), 3.16 (t, *J* = 6.8 Hz, 2H), 3.01 (dd, *J* = 14.1, 9.7 Hz, 1H), 2.61 (d, *J* = 7.6 Hz, 2H), 1.22 (t, *J* = 7.6 Hz, 3H).

¹³C NMR (151 MHz, THF-*d*₈) δ 175.8, 171.3, 159.5, 157.0, 149.9, 137.8, 136.3, 131.2, 129.9, 123.9, 115.4, 68.1, 54.7, 38.6, 38.4, 26.6, 16.0.

FTIR (neat) ν_{\max} : 2924, 1691, 1665, 1605, 1331, 1250, 1137 cm⁻¹.

HRMS (APCI) *m/z*: [M+H]⁺ calcd. for C₁₉H₂₁O₃N₂S 357.12674; found, 357.12680.



2-(6-methylpyridin-2-yl)ethyl (E)-but-2-enoate:

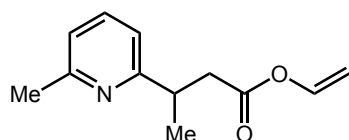
Prepared according to the General Procedure A using 2-bromo-6-methylpyridine (114 μL, 172 mg, 1 mmol, 1 equiv), and vinyl crotonate (364 μL, 336 mg, 3 mmol, 3 equiv), Hantzsch ester (329 mg, 1.3 mmol, 1.3 equiv), cyclohexanethiol (6 μL, 0.05 mmol, 5 mol%), Ir[ppy]₂dtbbpy•PF₆ (9.1 mg, 0.01 mmol, 1 mol%), and NH₄Cl (106 mg, 2 mmol, 2 equiv). After 18 h, the reaction was purified according to the General Procedure A (silica gel, 10 – 50% EtOAc/hexanes) to provide the desired product as a pale yellow oil (147 mg, 72% yield).

¹H NMR (600 MHz, CDCl₃) δ 7.49 (t, *J* = 7.7 Hz, 1H), 6.99 (t, *J* = 7.4 Hz, 2H), 6.94 (dq, *J* = 15.6, 7.0 Hz, 1H), 5.81 (dd, *J* = 15.5, 1.8 Hz, 1H), 4.48 (t, *J* = 6.8 Hz, 2H), 3.10 (t, *J* = 6.8 Hz, 2H), 2.53 (s, 3H), 1.85 (dd, *J* = 6.9, 1.8 Hz, 3H).

^{13}C NMR (151 MHz, CDCl_3) δ 166.6, 158.2, 157.6, 144.8, 136.8, 122.8, 121.3, 120.5, 63.7, 37.6, 24.6, 18.1.

FTIR (neat) ν_{max} : 2923, 2853, 1717, 1635, 1457, 1179 cm^{-1} .

HRMS (APCI) m/z : $[\text{M}+\text{H}]^+$ calcd. for $\text{C}_{12}\text{H}_{16}\text{O}_2\text{N}$, 206.11756; found, 206.11753



vinyl 3-(6-methylpyridin-2-yl)butanoate:

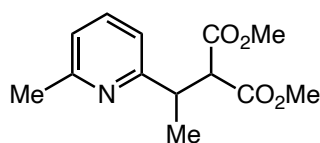
Prepared according to the General Procedure A using 2-bromo-6-methylpyridine (114 μL , 172 mg, 1 mmol, 1 equiv), and vinyl crotonate (364 μL , 336 mg, 3 mmol, 3 equiv), Hantzsch ester (329 mg, 1.3 mmol, 1.3 equiv), $\text{Ir}[\text{ppy}]_2\text{dtbbpy}\cdot\text{PF}_6$ (9.1 mg, 0.01 mmol, 1 mol%) in 10 mL $\text{DMSO}:\text{H}_2\text{O}$ 3:1(0.1 M). After 18 h, the reaction was purified according to the General Procedure A (silica gel, 10 – 50% $\text{EtOAc}/\text{hexanes}$) to provide the desired product as a pale yellow oil (115 mg, 56% yield).

^1H NMR (600 MHz, CDCl_3) δ 7.48 (t, $J = 7.7$ Hz, 1H), 7.25 – 7.22 (m, 1H), 6.97 (t, $J = 8.6$ Hz, 2H), 4.84 (d, $J = 14.0$ Hz, 1H), 4.53 (d, $J = 6.2$ Hz, 1H), 2.97 (dd, $J = 16.0, 7.3$ Hz, 1H), 2.66 (dd, $J = 16.0, 7.3$ Hz, 1H), 2.50 (s, 3H), 1.34 (d, $J = 7.0$ Hz, 3H).

^{13}C NMR (151 MHz, CDCl_3) δ 170.0, 163.4, 158.0, 141.3, 136.7, 121.1, 118.4, 97.6, 40.6, 37.9, 24.7, 20.8.

FTIR (neat) ν_{max} : 2964, 2923, 1722, 1572, 1443, 1370 1177 cm^{-1} .

HRMS (APCI) m/z : $[\text{M}+\text{H}]^+$ calcd. for $\text{C}_{12}\text{H}_{16}\text{O}_2\text{N}$, 206.11756; found, 206.11753



dimethyl 2-(1-(6-methylpyridin-2-yl)ethyl)malonate:

Prepared according to the General Procedure A using 2-bromo-6-methylpyridine (114 μ L, 172 mg, 1 mmol, 1 equiv), and dimethyl ethylidenemalonate (474 mg, 3 mmol, 3 equiv), Hantzsch ester (329 mg, 1.3 mmol, 1.3 equiv), Ir[ppy]₂dtbbpy•PF₆ (9.1 mg, 0.01 mmol, 1 mol%) in 10 mL DMSO:H₂O 3:1(0.1 M). After 18 h, the reaction was purified according to the General Procedure A (silica gel, 10 – 50% EtOAc/hexanes) to provide the desired product as a pale yellow oil (180 mg, 72% yield).

¹H NMR (500 MHz, CDCl₃) δ 7.46 (t, J = 7.7 Hz, 1H), 6.99 (d, J = 7.7 Hz, 1H), 6.97 – 6.91 (m, 1H), 4.10 (d, J = 10.1 Hz, 1H), 3.76 (s, 3H), 3.63 (dtd, J = 10.1, 8.2, 7.6, 6.3 Hz, 1H), 3.56 (s, 3H), 2.46 (s, 3H), 1.29 (d, J = 7.0 Hz, 3H).

¹³C NMR (126 MHz, CDCl₃) δ 169.5, 169.0, 161.8, 157.6, 136.5, 121.0, 119.3, 56.6, 52.4, 52.2, 41.1, 24.4, 19.0.

FTIR (neat) ν_{\max} : 2953, 1752, 1731, 1592, 1575, 1460, 1434, 1137 cm⁻¹.

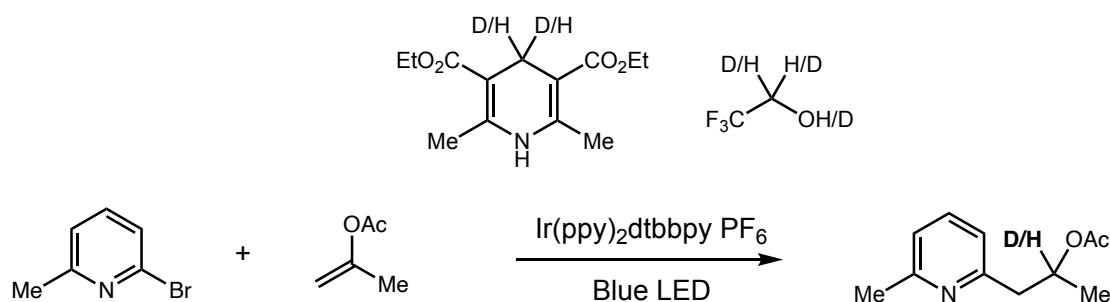
HRMS (APCI) m/z : [M+H]⁺ calcd. for C₁₃H₁₈O₄N, 252.12303; found, 252.12326.

A 50 mL round bottomed flask was charged with Ir(ppy)₂dtbbpy•PF₆ (18.2 mg, 0.02 mmol, 1 mol%), Hantzsch ester (660 mg, 2.6 mmol, 1.3 equiv). The tube was sealed with a rubber septum and the atmosphere was exchanged by applying vacuum and backfilling with N₂ (this process was conducted a total of three times). Under N₂ atmosphere, the tube was charged with prop-1-en-2-yl acetate (650 μL, 600 mg, 6 mmol, 3 equiv), 2-bromo-6-methylpyridine (228 μL, 344 mg, 2 mmol, 1 equiv), and separately degassed 2,2,2-trifluoroethanol (20 mL, 0.1 M) via syringe. The solution was stirred until complete dissolution of the solids. The reaction solution was removed by syringe, placed into a syringe pump shielded from extraneous light, and attached to the inlet of the flow reactor.

The flow reactor, which had been pre-equilibrated with 20 mL of 2,2,2-trifluoroethanol, was switched on and the reaction solution was pumped through at 1 mL/min with the outlet draining into a 250 mL round bottomed flask. After complete addition of the reaction solution, a second syringe of 20 mL of 2,2,2-trifluoroethanol was pumped through the flow reactor at 1 mL/min. The resulting solution was concentrated at reduced pressure and purified by flash column chromatography (silica gel, 20 – 50% EtOAc/hexanes) to provide the desired product as a yellow oil (288 mg, 75% yield).

3.4.7 Mechanistic Investigation

Deuterium Labeling Study



General procedure:

An oven-dried screw-top test tube equipped with a stir bar was sealed with a PTFE-faced silicon septa and cooled to room temperature under N_2 atmosphere. The tube was charged with $\text{Ir(ppy)}_2\text{dtbbpy}\cdot\text{PF}_6$ (0.9 mg, 1 mol%, 0.001 mmol) and Hantzsch ester (33 mg, 1.3 equiv, 0.13 mmol). The atmosphere was exchanged by applying vacuum and backfilling with N_2 (this process was conducted a total of three times). Under N_2 atmosphere, the tube was charged with prop-1-en-2-yl acetate (33 μL , 30 mg, 3 equiv, 0.3 mmol), 2-bromo-6-methylpyridine (11 μL , 17 mg, 1 equiv, 0.1 mmol), and separately degassed 2,2,2-trifluoroethanol (1 mL, 0.1 M) via syringe. The resulting mixture was stirred at 1200 RPM for 16 hours under irradiation with a blue LED. The crude reaction mixture was quenched with saturated sodium bicarbonate and extracted with dichloromethane (3 x 20 mL). The extracts were combined, dried over sodium sulfate, filtered, and concentrated under reduced pressure. The crude mixture was analyzed by ^1H NMR before purification. The crude residue was then purified by preparatory TLC (silica gel, 40% EtOAc/Hexanes) to provide the desired product. ^1H NMR analysis was used to determine the % D incorporation.

Experiment 1 – HEH- D_2 :

Prepared according to the general procedure using Hantzsch ester- D_2 (33 mg, 1.3 equiv, 0.13 mmol). ^1H NMR analysis showed 83% deuterium incorporation.

Experiment 2 – HEH- D_2 + CySH:

Prepared according to the general procedure using Hantzsch ester-D₂ (33 mg, 1.3 equiv, 0.13 mmol) and cyclohexane thiol (0.6 μL, 5 mol%, 0.005 mmol). ¹H NMR analysis showed 21% deuterium incorporation.

Experiment 3 – CF₃CH₂OD:

Prepared according to the general procedure using CF₃CH₂OD (1 mL). ¹H NMR analysis showed <5% deuterium incorporation.

Experiment 4 – CF₃CD₂OH:

Prepared according to the general procedure using CF₃CD₂OH (1 mL). ¹H NMR analysis showed 0% deuterium incorporation.

Stern—Volmer Quenching

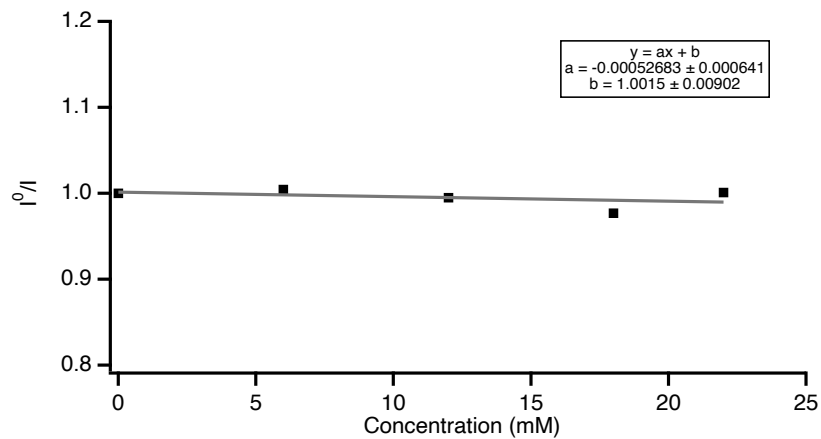
Quenching studies performed according to the procedure of MacMillan.¹⁰⁵

Photocatalyst (1.2 μmol) was dissolved in 2,2,2-trifluoroethanol (or isopropanol) (5.0 mL) to prepare a 0.24 mM solution. This solution (0.95 mL) was then diluted to a volume of 46 mL by adding further 2,2,2-trifluoroethanol (or isopropanol). The resulting 5.0 μM solution (1.6 mL) was added to each of a set of 4 mL reaction vials fitted with PTFE-faced silicon septa. A stock solution of quencher (0.25 mmol) in 2,2,2-trifluoroethanol (or isopropanol) (5.0 mL, 50 mM in quencher) was added in increasing amounts (0, 0.40, 0.80, 1.20, and 1.6 mL) to the vials containing the photocatalyst solution, and the volume for each vessel was adjusted to 3.2 mL by adding the necessary amount of 2,2,2-trifluoroethanol (or isopropanol) (1.6, 1.2, 0.80, 0.40, and 0.0 mL). The resulting mixtures were sparged with nitrogen for 15 minutes, then irradiated at 450 nm. The fluorescence emission spectra (3 trials per sample) were recorded. The ratio of the maximum fluorescence emission intensities maximum between samples without and with

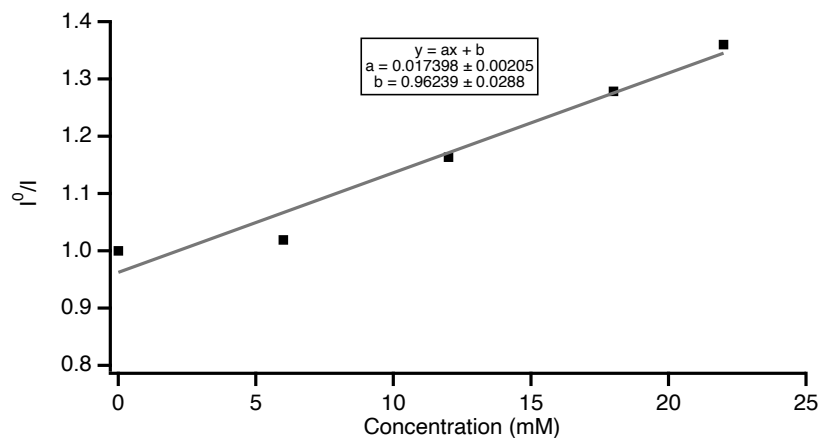
¹⁰⁵ Nacsa, E. D.; MacMillan, D. W. C. Spin-Center Shift-Enabled Direct Enantioselective α-Benzylolation of Aldehydes with Alcohols. *J. Am. Chem. Soc.* **2018**, *140* (9), 3322–3330

quencher were plotted against the quencher concentration to generate the Stern-Volmer plots below.

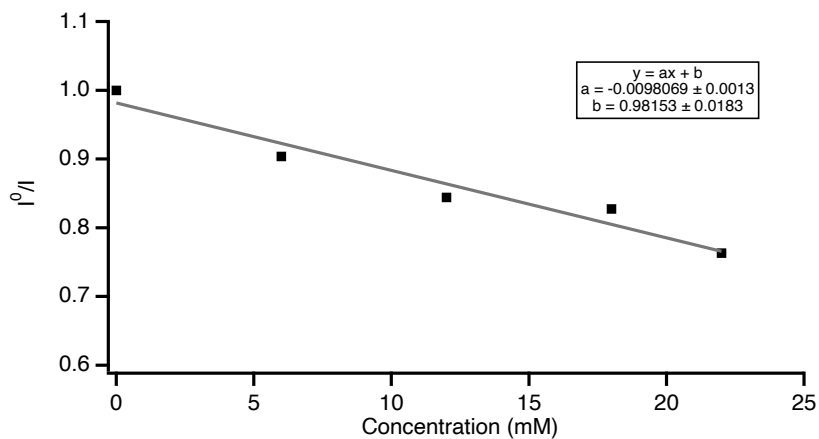
2-Bromo-6-methylpyridine in isopropyl alcohol:



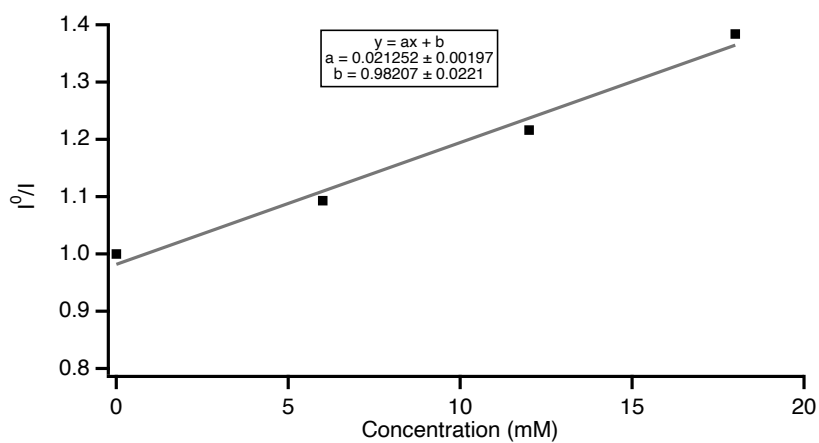
2-bromo-6-methylpyridine in 2,2,2-trifluoroethanol:



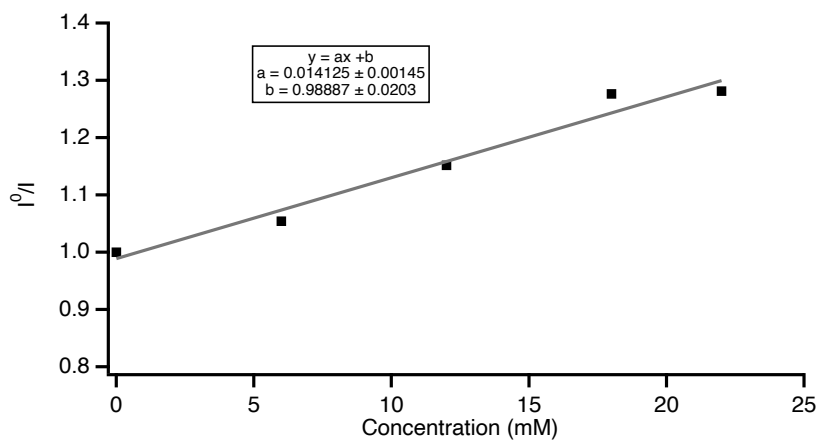
Prop-1-en-2-yl acetate in 2,2,2-trifluoroethanol:



Hantzsch ester in 2,2,2-trifluoroethanol:

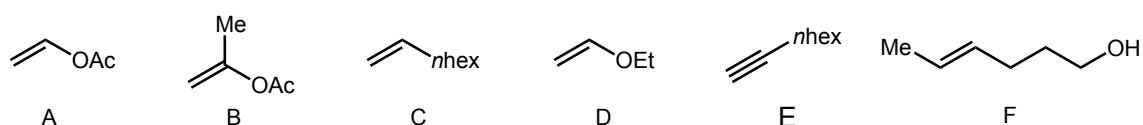


4-Bromopyridine hydrochloride in 2,2,2-trifluoroethanol:



Competition Experiments

A wide range of electronically differentiated alkenes were effective in this reaction manifold, however, small steric contributions (1,2 trans alkenes) were not well tolerated, apart from in the most simple cases (see below). Since radical-olefin addition is often highly tolerant of steric effects, based on an early transition state, we decided to investigate the effect that olefin stereo-electronics had on the reaction outcome. A small set of 1:1 competition reactions were undertaken to access the primary contributors to reaction success.



Primary neutral alkene C, which has minimal steric contributions, was reacted in the presence of alkenes A, and D, which share a similar steric profile, yet differ electronically. Octene alkylation provided the major product in both cases, consistent with a more stable radical formed upon addition (alkyl vs. α -oxy). More electron rich ethoxyethene was more competitive than vinyl acetate, consistent with a greater stabilization of the resulting C-centred radical through the neighboring lone pair on oxygen. Comparison of vinyl acetate and isopropenyl acetate (1-, vs 1,1-di substitution) demonstrated the effect of increasing radical stability in otherwise similar systems, with the 1,1-disubstituted alkene providing low levels of chemoselectivity versus primary alkene A. Our scoping exercise in the alkene component showed that internal acyclic olefins were poorly tolerated. This was observed across a range of alkenes although the simplest example, Alkene F above did work effectively. Chemoselectivity experiments using this alkene showed it to be outcompeted by 1-octene but give a 50:50 mixture with isopropenyl acetate.

In line with these observations, a cyclic 1,2-disubstituted alkene was outcompeted by primary olefin D. These data suggest that both steric and electronic factors influence the reaction course.

In systems where the steric barrier is low, alkene electronics play a significant, observable role; consistent with a mid to late transition state.

To determine information about which properties of the alkene-coupling partner (steric or electronic) most influence the fate of the reaction a number of competition experiments were performed.

Alkenes of similar steric properties, but different electronic properties (and vice versa) were compared to define the impact of alkene stereoelectronics on reaction efficiency. An excess of both alkenes was used to minimize any developing concentration gradient.

General procedure:

An oven-dried screw-top test tube equipped with a stir bar was sealed with a PTFE-faced silicon septa and cooled to room temperature under N₂ atmosphere. The tube was charged with Ir(ppy)₂dtbbpy•PF₆ (0.9 mg, 1 mol%, 0.001 mmol) and Hantzsch ester (33 mg, 1.3 equiv, 0.13 mmol). The atmosphere was exchanged by applying vacuum and backfilling with N₂ (this process was conducted a total of three times). Under N₂ atmosphere, the tube was charged with alkene 1 (3 equiv, 0.3 mmol), alkene 2 (3 equiv, 0.3 mmol), 2-bromo-6-methylpyridine (11 μL, 17 mg, 1 equiv, 0.1 mmol), and separately degassed 2,2,2-trifluoroethanol (1 mL, 0.1 M) via syringe. The resulting mixture was stirred at 1200 RPM for 16 hours under irradiation with a blue LED. The crude reaction mixture was quenched with saturated sodium bicarbonate and extracted with dichloromethane (3 x 20 mL). The extracts were combined, dried over sodium sulfate, filtered, and concentrated under reduced pressure. The crude mixture was analyzed by ¹H NMR to determine the ratio of products.

Octene vs vinyl acetate

Prepared according to the general procedure using 1-octene (47 μL , 34 mg, 3 equiv, 0.3 mmol) and vinyl acetate (28 μL , 26 mg, 3 equiv, 0.3 mmol). ^1H NMR analysis showed a ratio of 75:25 in favor of the 1-octene addition product.

Octene vs ethoxyethene

Prepared according to the general procedure using 1-octene (47 μL , 34 mg, 3 equiv, 0.3 mmol) and ethoxyethene (29 μL , 22 mg, 3 equiv, 0.3 mmol). ^1H NMR analysis showed a ratio of 60:40 in favor of the 1-octene addition product.

Vinyl acetate vs prop-1-en-2-yl acetate

Prepared according to the general procedure using vinyl acetate (28 μL , 26 mg, 3 equiv, 0.3 mmol) and prop-1-en-2-yl acetate (33 μL , 30 mg, 3 equiv, 0.3 mmol). ^1H NMR analysis showed a ratio of 59:41 in favor of the prop-1-en-2-yl acetate addition product.

Ethoxyethene vs 3,4-dihydro-2*H*-pyran

Prepared according to the general procedure using ethoxyethene (29 μL , 22 mg, 3 equiv, 0.3 mmol) and 3,4-dihydro-2*H*-pyran (26 μL , 25 mg, 3 equiv, 0.3 mmol). ^1H NMR analysis showed a ratio of 63:37 in favor of the ethoxyethene addition product.

Octene vs octyne

Prepared according to the general procedure using 1-octene (47 μL , 34 mg, 3 equiv, 0.3 mmol) and 1-octyne (44 μL , 33 mg, 3 equiv, 0.3 mmol). ^1H NMR analysis showed a ratio of 71:29 in favor of the 1-octene addition product.

(*E*)-Hex-4-en-1-ol vs prop-1-en-2-yl acetate

Prepared according to the general procedure using prop-1-en-2-yl acetate (33 μL , 30 mg, 3 equiv, 0.3 mmol) and (*E*)-hex-4-en-1-ol (35 μL , 30 mg, 3 equiv, 0.3 mmol). ^1H NMR analysis showed a ratio of 50:50.

(*E*)-Hex-4-en-1-ol vs 1-octene

Prepared according to the general procedure using 1-octene (47 μL , 34 mg, 3 equiv, 0.3 mmol) and (*E*)-hex-4-en-1-ol (35 μL , 30 mg, 3 equiv, 0.3 mmol). ^1H NMR analysis showed a ratio of 86:14 in favor of the 1-octene addition product.

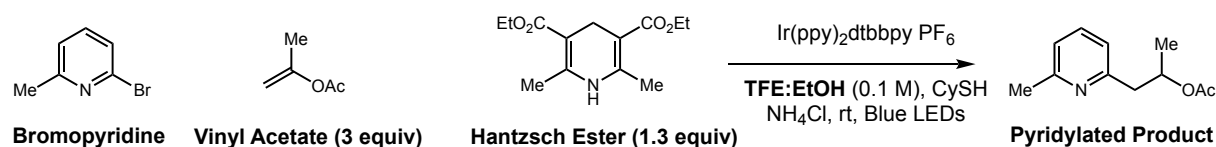
Effect of Reaction Medium

A number of changes to the reaction medium were assessed to develop an understanding of the effect that 2,2,2-trifluoroethanol has on the reaction. Moving to other protic solvents resulted in a loss of activity. 2,2,2-Trifluoroethanol has a very low dielectric constant ($\epsilon = 8.55$), is more H-bond donating, and higher acidity ($pK_a = 12.4$), in comparison to common protic solvents, which may explain the difference in reactivity.

Table 3.5 Solvent Screen

Entry	Solvent	Dielectric constant	pK_a	Yield (%)
1	MeOH	33	15.5	6%
2	EtOH	24.3	15	4%
3	<i>n</i> BuOH	17.8	15	7%
4	1,2 - Ethanediol	40.2	14	2%
5	Acetone	20.7	26	0%
6	MeNO ₂	35.9	10	0%

Table 3.6 Effect of EtOH additive. Use of TFE:EtOH mixtures resulted in a uniform decrease in yield.



Entry	TFE:EtOH ratio	Yield (%)
1	9:1	30%
2	5:1	42%
3	7:3	27%
4	3:2	36%
5	1:1	10%

Table 3.7 Effect of HFIP additive. Use of TFE:HFIP mixtures led to similar yields to the optimal system (71% isolated).

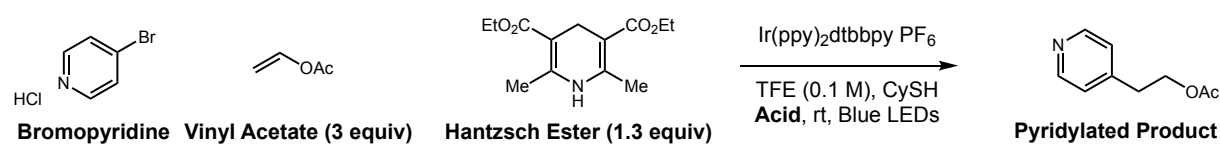


Entry	TFE:HFIP ratio	Yield (%)
1	9:1	68%
2	5:1	63%
3	7:3	71%
4	3:2	71%
5	1:1	68%

Table 3.8 Effect of acidic additives. In this system, use of different acidic additives provided lower yields than with NH_4Cl . Use of stronger acids led to a more dramatic reduction in yield.



Entry	Acidic additive	pK_a	Yield (%)
1	AcOH	4.76	65%
2	BzOH	4.19	57%
3	Formic acid	3.75	66%
4	Trifluoroacetic acid	0.23	35%
5	PTSA	-2.8	19%
6	Pthalimide	8.3	0%

Table 3.9 Effect of acidic additives on reaction with 4-bromopyridine.

Entry	Acidic additive	pK _a	Yield (%)
1	NH ₄ Cl	9	62%
2	NaH ₂ PO ₄	7	63%
3	AcOH	5	62%
4	H ₃ PO ₄	2	15%
5	HF ₄	1	0%
6	TFA	0	0%

Further evaluation with acidic additives was assessed using a more sensitive substrate pair, 4-bromopyridine hydrochloride with vinyl acetate. We noted this system reacted differently to the 2-bromo-6-methylpyridine/prop-1-en-2-yl acetate substrate pair, and was less tolerant to changes in the system. In this system, the weaker acids (entries 1-3) all provided comparable yields where the stronger acids (entries 4-6) all led to a significant reduction in product.

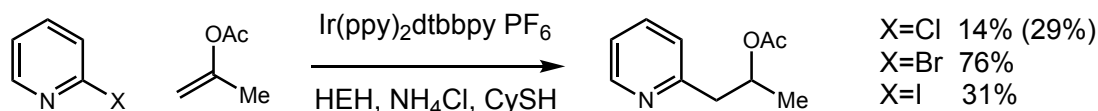
Effect of Reaction Medium on Chemoselectivity

Titration of water into the reaction medium led to a linear decrease in product formation, with the remainder of the mass balance consisting of hydrodehalogenated bromopyridine.

Table 3.10 Effect of water on reaction efficiency.

Entry	H ₂ O (equiv)	Yield (%)
1	1	77%
2	5	72%
3	10	68%
4	20	65%
5	50	53%
6	75	45%
7	100	38%

Effect of Halide Identity on Reaction Efficiency



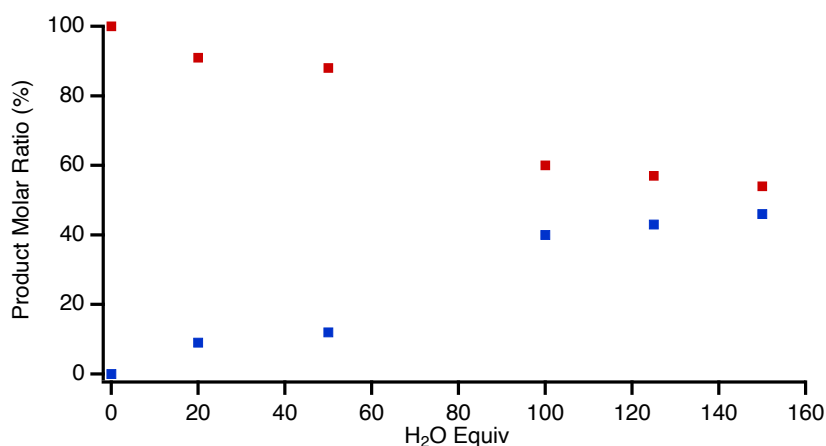
Moving from Br to I or Cl led to a reduction in reaction efficiency. The conversion in the Cl example was increased using the more reducing photocatalyst *fac*-Ir(ppy)₃ (yield in parentheses).

Effect of water concentration on chemoselectivity

Table 3.11

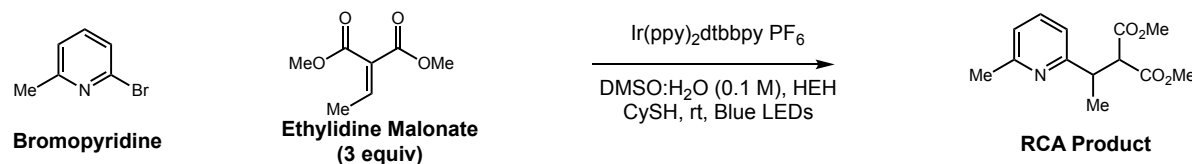
Entry	H ₂ O (equiv)	Molar Ratio	Molar Ratio
1	0	100%	0%
2	20	91%	9%
3	50	88%	12%
4	100	60%	40%
5	125	57%	43%
6	150	54%	46%

Figure 3.6 Effect of water addition on chemoselectivity. Blue Squares represent RCA product. Red diamonds represent hydroarylation product.



Effect of acidic additives on radical conjugate addition

Table 3.12 Effect of acidic additives on radical conjugate addition efficiency. Addition of stoichiometric amounts (2 equiv) of strong acid does not have any deleterious effect on the reaction yield in the RCA system.



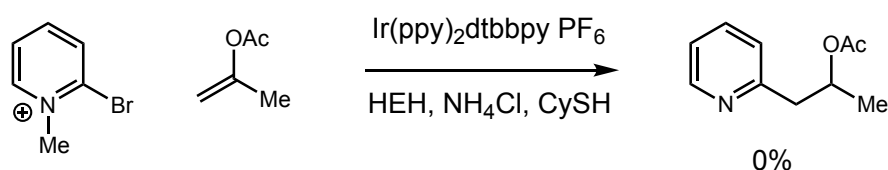
Entry	Acidic additive	Yield (%)
1	AcOH	89%
2	TFA	100%
3	HCl (12 N)	100%
4	TfOH	100%

Effect of acidic additives on radical conjugate addition chemoselectivity.

Addition of octene (3 equiv) to the above reactions led to the same yields of RCA product, with no observed hydroarylation product.

Reaction of Methyl Pyridinium Bromide

Use of methyl pyridinium salt resulted in no product being formed under the reaction conditions.

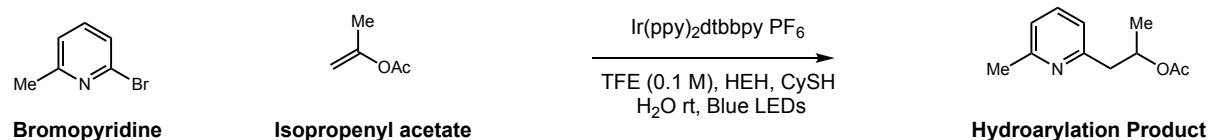


Effect of Basic Additives on Hydroarylation

As part of our previous work we observed product inhibition with some substrates. We found that addition of 2,6-lutidine shut down reactivity; we proposed a mechanism where protonation of the pyridine substrate is vital for reaction efficiency and adding stoichiometric base is

counter productive. Through the below experiment we find that pK_a of the additive is not related to performance. A more likely source of product inhibition is through a disruption of the TFE solvent cage.

Table 3.13 Effect of basic additives on hydroarylation.

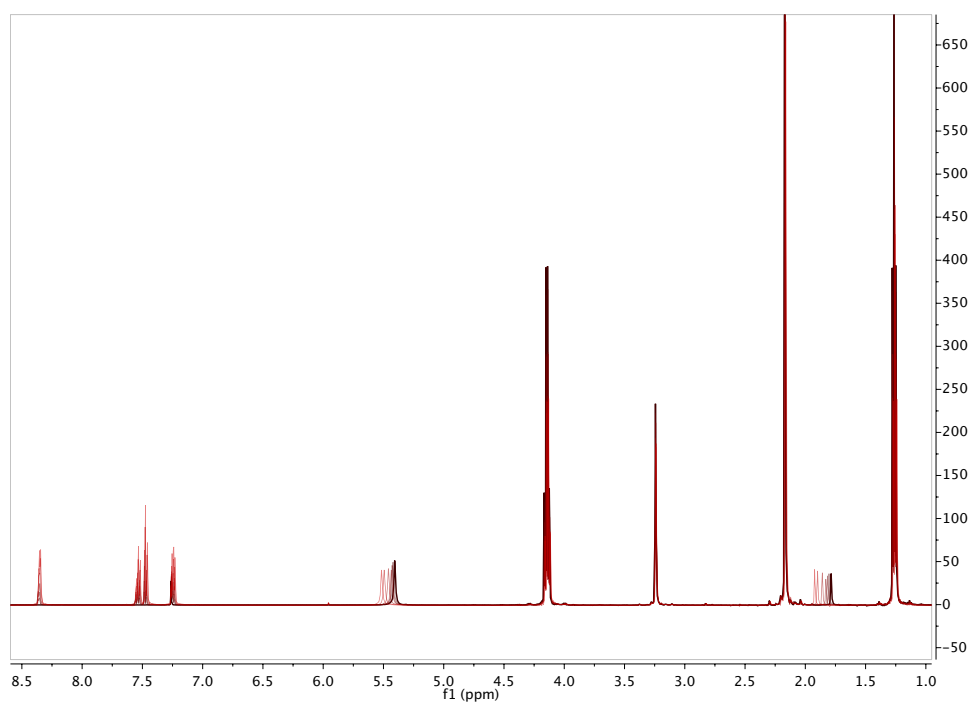


Entry	Basic additive (equiv)	pK_a	Yield (%)
1	Lutidine (0.1)	6.6	61%
2	Lutidine (0.2)	6.6	43%
3	Lutidine (0.5)	6.6	17%
4	Lutidine (1)	6.6	0%
5	NaHCO ₃ (0.1)	6.4	77%
6	NaHCO ₃ (0.2)	6.4	80%
7	NaHCO ₃ (0.5)	6.4	74%
8	NaHCO ₃ (0.1)	6.4	77%

UV/Vis and ¹H NMR titrations to observe possible charge transfer complexes

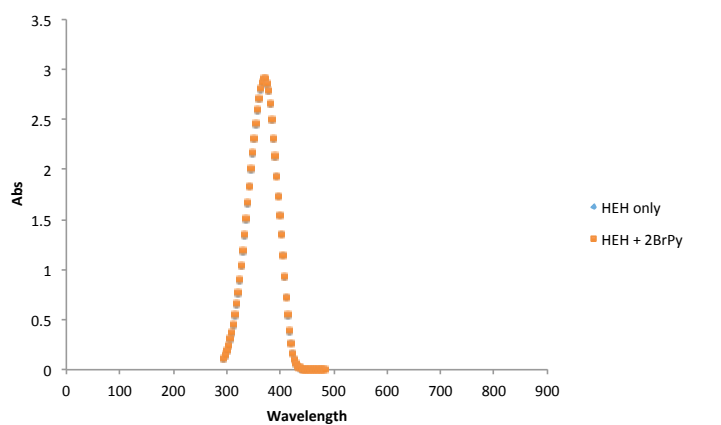
¹H NMR Procedure: A solution of 25 mg Hantzsch ester in 0.7 mL CDCl₃ was transferred to an NMR tube. The solution was analyzed by ¹H NMR. 2-Bromopyridine was added to the solution in 1 μL aliquots, and the mixture was analysed after every subsequent addition. No significant change was observed to the signal upon addition.

Figure 3.7 Superimposed NMR spectra for titration of 2-Bromopyridine into a HEH solution.



UV/Vis Analysis: Upon measurement of the absorbance spectra for solutions of Hantzsch ester with varied concentrations of 2-bromopyridine no change was observed.

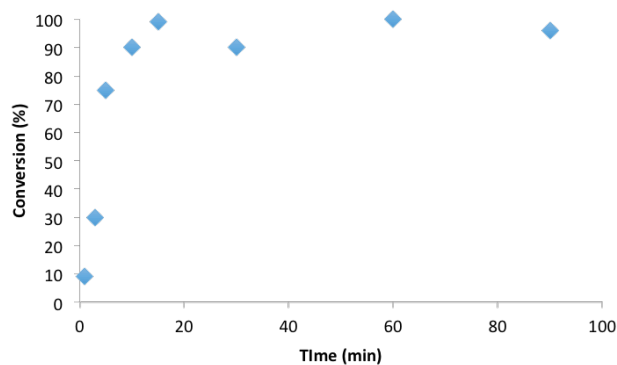
Figure 3.8 Absorption spectrum for HEH and HEH + 2-bromopyridine.



Temporal analysis

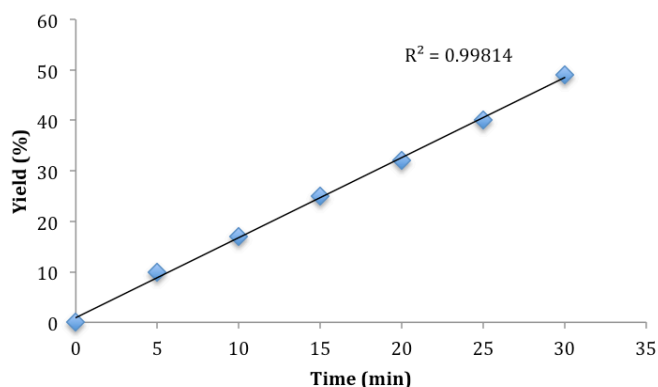
Time studies were undertaken to determine the approximate rate of the reaction. When using the standard blue LED lamp set up that was used during optimization and scope, the reaction was rapid (Figure 3.9).

Figure 3.9 Temporal profile of hydroarylation reaction using blue LED array.

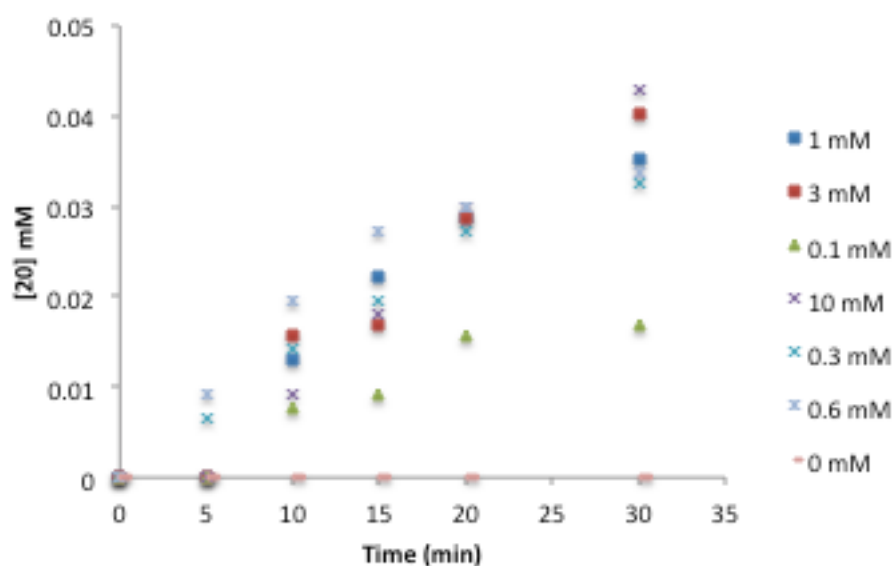


However, to avoid unnecessary exposure to the high-powered blue LED lamp, reactions were performed overnight. No reduction in yield was observed from the extra irradiation time.

Additional rate information was obtained using UV/vis absorbance spectroscopy in combination with ^1H NMR. Aliquots taken from a reaction every 5 minutes were analyzed by UV/Vis spectroscopy and ^1H NMR for a 30 minute time course. The 90.9 mW 455nm LED used in this time study was less powerful, allowing for a slower rate and a clearer picture of the temporal profile of the reaction. (Figure 3.10)

Figure 3.10 Temporal profile using a single focused Blue LED***Effect of catalyst concentration***

The effect the light source has on the rate of the reaction suggests that excitation of the Ir-sensitizer is turnover limiting. Based on Beers law, a catalyst concentration of 0.0000924 M (~0.1 mol% catalyst equiv.) will provide 99.9% absorbance in the 1 cm cuvette used for time course experiments. We anticipate 1st order rate dependence below this concentration but zero order above this level. A series of temporal profiles of the reaction at different catalyst concentrations were measured to assess this reactivity.

Figure 3.11 Temporal profile of reaction at various catalyst loadings

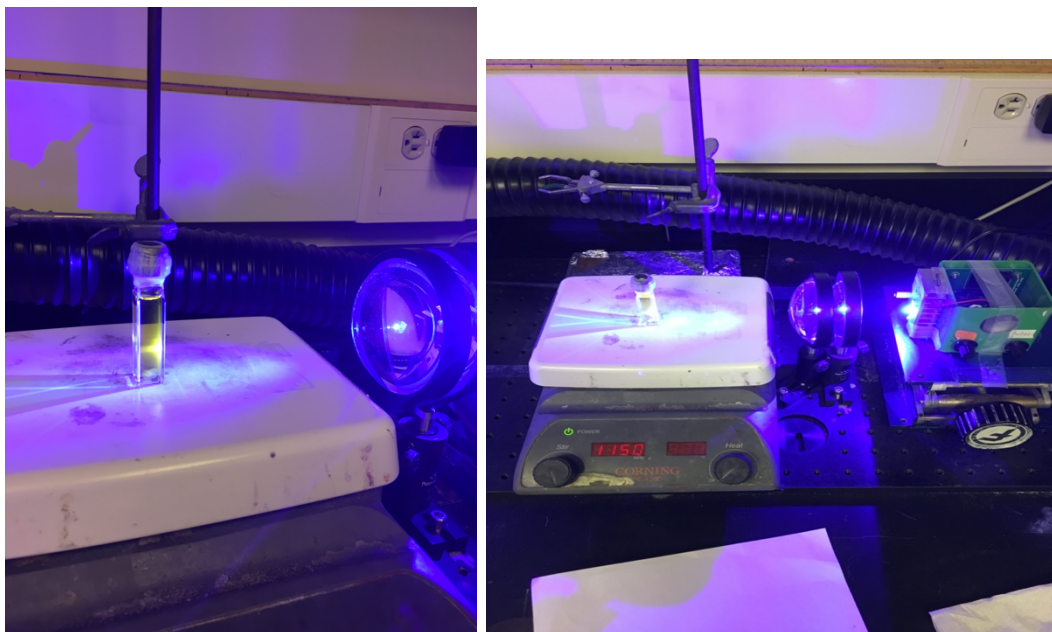
As shown above concentrations above 0.3 mM gave no rate increase, although moving to 0.1 mM showed a significant decrease, in line with the Beers law calculations.

Quantum Yield

In an Ar filled glovebox, a reaction vial was charged with Ir(ppy)₂dtbbpy•PF₆ (9.1 mg, 1 mol%, 0.01 mmol), Hantzsch ester (329 mg, 1.3 equiv, 1.3 mmol), prop-1-en-2-yl acetate (325 μL, 300 mg, 3 equiv, 3 mmol), 2-bromo-6-methylpyridine (114 μL, 172 mg, 1 equiv, 1 mmol), and separately degassed 2,2,2-trifluoroethanol (10 mL, 0.1 M). The mixture was agitated until fully homogenized, and 3.5 mL of the solution was transferred to a 3.5 mL screw-top quartz cuvette fitted with a stir bar. The cuvette was sealed with a screw top fitted with a PTFE-faced silicon septa and removed from the glovebox.

Evaluation of the quantum yield was performed using a blue 455 nm LED that was focused on the quartz cuvette using Thorlabs optics (see picture below). 100 μL aliquots were removed via syringe every 5 minutes (0, 5, 10, 15, 20, 25, 30 mins). 10 μL of each aliquot was diluted with 2,2,2-trifluoroethanol (5 mL) and the UV/Vis spectra were recorded (Figure 3.14). The consumption of Hantzsch ester was readily monitored with this method, and product formation could be monitored by ¹H NMR analysis of the same aliquots. After an initial burst phase, steady state, linear kinetics were observed. The quantum yield was determined from the steady state portion of the reaction.

Figure 3.12 Typical set up for quantum yield measurement



The quantum yield (QY) was defined as the ratio between the amount of electrons consumed during the reaction and the total number of photons absorbed by the photosensitizer. QY can be determined through the following equations.

The photon flux was calculated based on the LED illumination power at the focal point of the LED right before the sample with a Ophir Starlite power meter with a 3A thermal sensor.

First, the number of photons, n , arrived onto the sample per second from the 455nm LED per second could be calculated as:

$$n = E/h\nu$$

Where $E = 90.9\text{mW}$ (455nm LED power before the sample)

$$h = \text{Planck constant} = 6.626 \times 10^{-34} \text{ Js}$$

$$\nu = \text{frequency of the 455nm photon}$$

$$\nu = c/\lambda$$

Where $c = \text{speed of light} = 2.998 \times 10^8 \text{ ms}^{-1}$

$$\lambda = \text{wavelength (455 nm} = 455 \times 10^{-9} \text{ m)}$$

$$\nu = \frac{2.998 \times 10^{-8}}{455 \times 10^{-9}}$$

$$\nu = 6.589 \times 10^{14}$$

So number of photons =

$$n = \frac{0.0909}{6.626 \times 10^{-34} \times 6.589 \times 10^{14}}$$

$$n = 2.082 \times 10^{17} \text{ photons per sec}$$

The amount of photons absorbed by the sample per minute n^* can be calculated based on the absorbance of the sample at 455nm A_{455} from Beer-Lambert law.

$A_{455}=0.866$ (taken from UV/Vis spectra—relative to Ir conc at $t=0$ should not change during the reaction, this tells us the amount of light Ir absorbs)

$$n^* = 60n(1 - 10^{-A_{455}})$$

$$n^* = 1.079 \times 10^{19} \text{ photons absorbed per minute}$$

The gradient of the slope derived from ^1H NMR analysis is equal to conc per min * vol = mol%/min

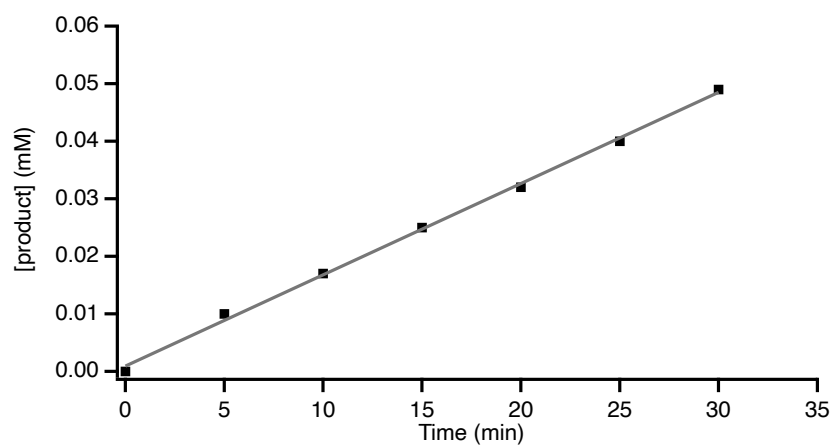
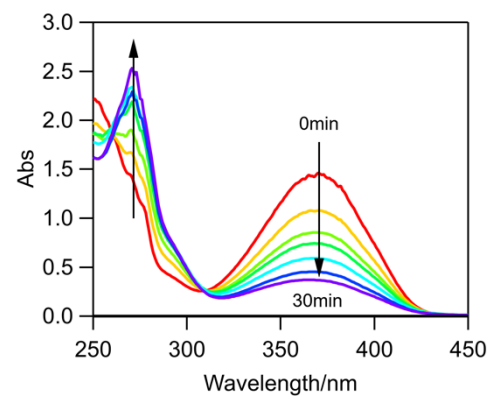
$$0.0016 \text{ mol/min} = \text{slope}$$

$$(\text{slope}) \times (3.5/1000) = 5.6 \times 10^{-6} \text{ M} \times \text{Avogadro gives no. electrons}$$

$$= 3.372 \times 10^{17}$$

As defined, the QY can be calculated as

$$QY = \frac{ne}{n_*} \times 100\% = 31\%$$

Figure 3.13 Temporal Profile**Figure 3.14** UV/Vis spectra

3.4.8 Computational Details

General Computational Details

DFT calculations were carried out using the Gaussian 16 software package.¹⁰⁶

All 3D images were generated using Chemcraft Version 1.8 (build 536a)

Calculation of Gibbs free energy for electron transfer

Energies for electron transfer within the reaction were calculated according to the method of Nicewicz et al.¹⁰⁷

$$\Delta G^0 = \frac{E_{reduced}^0 - E_{oxidized}^0}{n_e \mathcal{F}}$$

Where n_e = the number of electrons

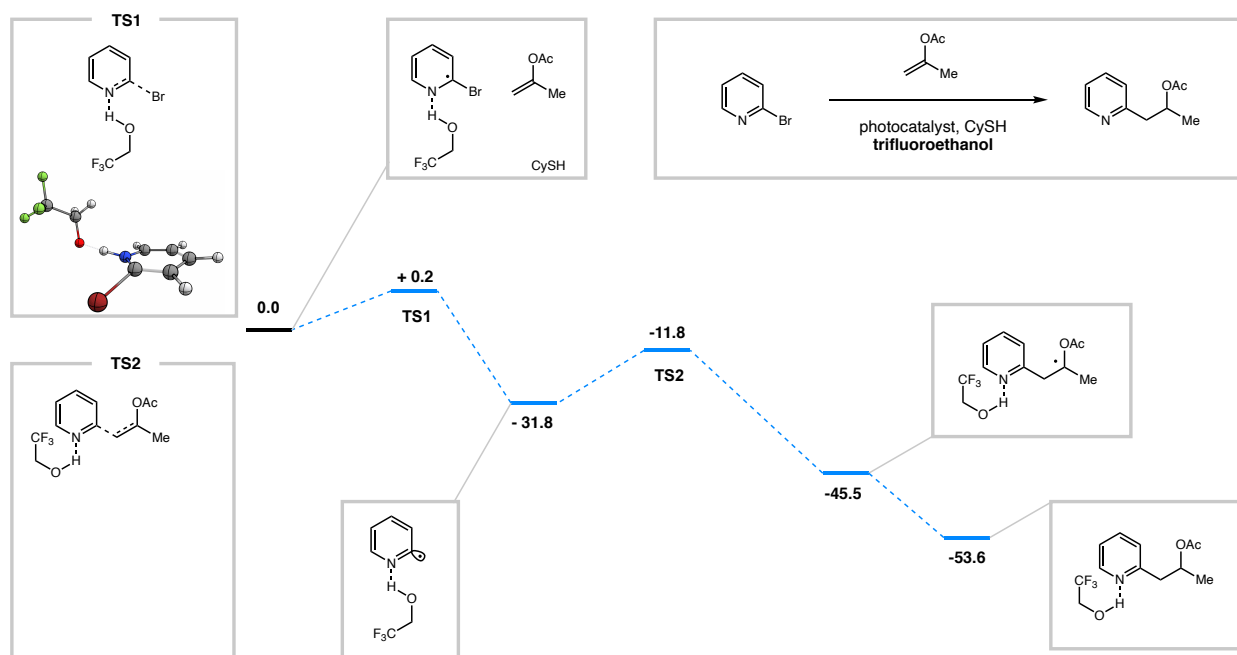
And \mathcal{F} = Faraday's constant = 23.061 kcal mol⁻¹ V⁻¹

Computationally Derived Reaction Coordinate

Described is the computationally derived reaction coordinate, post reduction. A very low barrier was observed for heterolytic cleavage, in line with previous reports from Saveant. Alkene addition was exergonic by almost 15 kcal/mol with a barrier of 20 kcal/mol. HAT was barrier less and exergonic to deliver the product.

¹⁰⁶ Frisch, M. J.; Trucks, G. W.; Schlegel, H. B.; Scuseria, G. E.; Robb, M. A.; Cheeseman, J. R.; Scalmani, G.; Barone, V.; Petersson, G. A.; Nakatsuji, H.; Li, X.; Caricato, M.; Marenich, A. V.; Bloino, J.; Janesko, B. G.; Gomperts, R.; Mennucci, B.; Hratchian, H. P.; Ortiz, J. V.; Izmaylov, A. F.; Sonnenberg, J. L.; Williams-Young, D.; Ding, F.; Lipparini, F.; Egidi, F.; Goings, J.; Peng, B.; Petrone, A.; Henderson, T.; Ranasinghe, D.; Zakrzewski, V. G.; Gao, J.; Rega, N.; Zheng, G.; Liang, W.; Hada, M.; Ehara, M.; Toyota, K.; Fukuda, R.; Hasegawa, J.; Ishida, M.; Nakajima, T.; Honda, Y.; Kitao, O.; Nakai, H.; Vreven, T.; Throssell, K.; Montgomery, J. A., Jr.; Peralta, J. E.; Ogliaro, F.; Bearpark, M. J.; Heyd, J. J.; Brothers, E. N.; Kudin, K. N.; Staroverov, V. N.; Keith, T. A.; Kobayashi, R.; Normand, J.; Raghavachari, K.; Rendell, A. P.; Burant, J. C.; Iyengar, S. S.; Tomasi, J.; Cossi, M.; Millam, J. M.; Klene, M.; Adamo, C.; Cammi, R.; Ochterski, J. W.; Martin, R. L.; Morokuma, K.; Farkas, O.; Foresman, J. B.; Fox, D. J. Gaussian Inc 16, Revision B.01. *Gaussian Inc., Wallingford CT*. 2016

¹⁰⁷ Roth, H. G.; Romero, N. A.; Nicewicz, D. A. Experimental and Calculated Electrochemical Potentials of Common Organic Molecules for Applications to Single-Electron Redox Chemistry. *Synlett* **2016**, 27 (05), 714–723

Scheme 3.4 Computationally derived reaction coordinate. All values in kcal/mol.**Table 3.14** Reduction potentials for 2-bromopyridine with different levels of theory and solvation

Substrate/Parameters	G(298) Oxidized (hartree)	G(298) Reduced (hartree)	dG1/2 (hartree)	dG1/2 (kcal/mol)	E (V vs SCE)
um06 implicit solvation (CPCM) DMSO	-2821.533958	-2821.609043	-0.075085	-47.1158375	-2.52
um06 tight convergence					
um06-2x implicit solvation (CPCM) DMSO	-2821.770246	-2821.843579	-0.073333	-46.0164575	-2.56
um06-2x tight convergence					
um06 implicit solvation (CPCM) DMF	-2821.533915	-2821.608569	-0.074654	-46.845385	-2.35
um06 tight convergence					
um06-2x implicit solvation (CPCM) DMF	-2821.770199	-2821.843098	-0.072899	-45.7441225	-2.40
um06-2x tight convergence					

Investigating PCET Energetics

The following data was obtained from 10 discrete optimizations (2 for each entry 1 – 5) with redundant coordinates defining the N-H bond length to equal the tabulated values and a fixed distance of 2.84439 Å between the N of the pyridine and O of the TFE. Structures were

optimized at the uB3LYP¹⁰⁸ level of theory using the 6-311G(d,p) basis set.¹⁰⁹ The CPCM formalism for the Self Consistent Reaction Field (SCRF) model of solvation was employed in all calculations to account for solvation in DMSO. Optimized structures were confirmed by ensuring no negative frequencies existed. The outputs of these optimizations provided Gibbs Free energies for each species, which are listed in Table 3.15 as “G(298) Neutral” and “G(298) Reduced” for the neutral and reduced (doublet) species respectively.

The equation below was used to calculate the reduction potentials where n_e is the number of electrons transferred ($n_e = 1$ for all calculations here), \mathcal{F} is the Faraday constant (value 23.061 kcal mol⁻¹ V⁻¹), $E_{1/2}^{0,SHE}$ is the absolute value for the standard hydrogen electrode (SHE, value = 4.281 V)¹¹ and $E_{1/2}^{0,SCE}$ is the potential of the saturated calomel electrode (SCE) relative to the SHE in DMSO (value = -0.279V)¹¹⁰, and $G_{298}[\text{oxidized}]$ and $G_{298}[\text{reduced}]$ are the Gibbs free energies in DMSO obtained from DFT calculations.

“ ΔG Protonation” equals the difference in free energy from the freely optimized neutral structure (no defined bond lengths), which here is defined as entry 5: neutral. This value represents the free energy required to move against the pK_a gradient to further protonate the pyridine (entry 5→1). “ ΔG Reduction” equals the free energy difference between the reduced and neutral species in each entry.

¹⁰⁸ (a) Lee, C.; Yang, W.; Parr, R. G. Development of the Colle-Salvetti Correlation-Energy Formula into a Functional of the Electron Density. *Phys. Rev. B* **1988**, *37* (2), 785–789; (b) Beckers, T.; Bernd, M.; Kutscher, B.; Kühne, R.; Hoffmann, S.; Reissmann, T. Structure–Function Studies of Linear and Cyclized Peptide Antagonists of the GnRH Receptor. *Biochem. Biophys. Res. Commun.* **2001**, *289* (3), 653–663

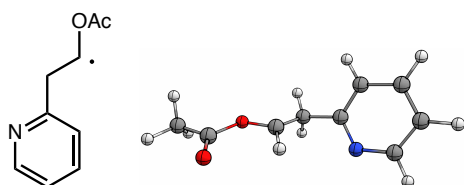
¹⁰⁹ McLean, A. D.; Chandler, G. S. Contracted Gaussian Basis Sets for Molecular Calculations. I. Second Row Atoms, Z=11–18. *J. Chem. Phys.* **1980**, *72* (10), 5639–5648

¹¹⁰ Isse, A. A.; Gennaro, A. Absolute Potential of the Standard Hydrogen Electrode and the Problem of Interconversion of Potentials in Different Solvents. *J. Phys. Chem. B* **2010**, *114* (23), 7894–7899

$$E_{1/2}^{0,calc} = -\frac{(G_{298}[reduced]-G_{298}[oxidized])}{n_e\mathcal{F}} - E_{1/2}^{0,SHE} + E_{1/2}^{0,SCE}$$

Table 3.15

Entry	N-H Bond	G(298)		E in DMSO	ΔG Protonation	ΔG Reduction
	Length (Å)	Neutral	Reduced	(V vs SCE)	(kcal/mol)	(kcal/mol)
1	1.01677	-3274.702368	-3274.821257	-1.324931378	26.9759844	-4.267867501
2	1.2285075	-3274.708337	-3274.817118	-1.599978469	23.23038318	2.074993471
3	1.440245	-3274.712113	-3274.809759	-1.902971085	20.8609092	9.062306186
4	1.6519825	-3274.731278	-3274.819415	-2.161718888	8.834699211	15.02928927
5	1.86372	-3274.745357	-3274.828614	-2.294507748	0	18.09153319

Molecular Coordinates and Energies of**Optimized Structures**

Charge: 0

Spin Multiplicity: 2

Number of Imaginary Frequencies: 0

Solvation: DMSO

Gibbs Free Energy at 298.150 K (Hartree):

-554.168195

H	-0.874641	1.002061	-0.34002
O	-2.275978	-0.438107	0.268285
C	-3.328155	0.263349	-0.254507
C	-4.629273	-0.41063	0.064785
H	-4.66729	-1.385698	-0.42786
H	-4.714404	-0.580758	1.139852
H	-5.455812	0.205384	-0.282349
O	-3.179758	1.280257	-0.890516

C	1.446391	-0.341727	0.379067	
C	2.217804	-1.202931	-0.406134	
C	3.49098	-0.801714	-0.800585	
C	3.953135	0.44986	-0.403082	
C	3.114361	1.242929	0.37574	
N	1.890237	0.864808	0.764304	
H	4.1093	-1.454234	-1.406236	
H	1.825429	-2.169588	-0.698566	
H	4.936654	0.805512	-0.684366	
H	3.439843	2.224836	0.70686	

C	1.441725	-0.42695	0.34339
C	2.342715	-1.248553	-0.330413
C	3.558223	-0.701049	-0.735408
C	3.817711	0.638552	-0.463371
C	2.845915	1.379542	0.205637

Charge: +1

Spin Multiplicity: 1

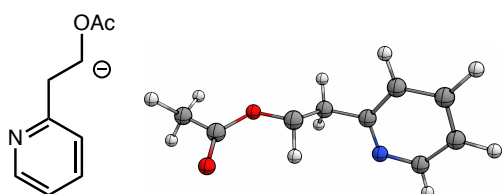
Number of Imaginary Frequencies: 0

Solvation: DMSO

Gibbs Free Energy at 298.150 K (Hartree):

-553.992877

N	1.679199	0.861721	0.606078	Number of Imaginary Frequencies: 0			
H	4.285541	-1.311824	-1.256849	Solvation: DMSO			
H	2.102975	-2.285578	-0.529327	Gibbs Free Energy at 298.150 K (Hartree):			
H	4.74807	1.104516	-0.762615	-554.273608			
H	3.008543	2.428587	0.43117	C	1.441063	-0.259557	0.400511
C	0.110839	-0.973684	0.838141	C	2.208073	-1.192024	-0.314146
H	-0.058212	-2.018874	0.580137	C	3.506795	-0.870424	-0.690344
H	0.094846	-0.904773	1.939828	C	4.011157	0.385739	-0.354064
C	-1.026175	-0.142154	0.41044	C	3.183341	1.254207	0.34902
H	-0.894574	0.939119	0.296063	N	1.931166	0.949933	0.723933
O	-2.146711	-0.64035	0.195968	H	4.115786	-1.583639	-1.234866
C	-3.370694	0.413283	-0.251434	H	1.781641	-2.157695	-0.559009
C	-4.538109	-0.450215	-0.440966	H	5.016921	0.68416	-0.624328
H	-4.307101	-1.195796	-1.20537	H	3.53991	2.241153	0.631603
H	-4.742351	-0.979288	0.492897	C	0.019266	-0.561452	0.796665
H	-5.387026	0.162957	-0.736536	H	-0.065266	-1.631723	1.022193
O	-3.06554	1.527384	-0.314473	H	-0.1881	-0.018887	1.736938
				C	-0.926203	-0.188778	-0.350042
				H	-0.874052	0.897422	-0.500255
				O	-2.288565	-0.445137	0.214837
				C	-3.338263	0.205439	-0.228092
				C	-4.641408	-0.30857	0.345487
				H	-5.214828	-0.795782	-0.449701
				H	-4.479392	-1.022687	1.152091
				H	-5.237746	0.530046	0.711339



Charge: -1

Spin Multiplicity: 1

O -3.298429 1.122715 -1.050275

C 1.908915 1.192671 0.355799

H 2.948429 1.060638 0.625945

Structures for Scheme 3.4:

H 1.458641 2.166901 0.498165

Structures were optimized at the uB3LYP

C 1.214431 0.178421 -0.143433

level of theory using the 6-311G(d,p) basis

C 1.696442 -1.207485 -0.425085

set. The CPCM formalism for the Self

H 1.10804 -1.944974 0.126678

Consistent Reaction Field (SCRF) model of

H 1.597214 -1.433609 -1.491289

solvation was employed in all calculations

H 2.743762 -1.311039 -0.140722

to account for solvation of the listed

O -0.11414 0.427528 -0.565842

solvent. Optimized structures were

C -1.143394 -0.049271 0.183404

confirmed by ensuring no negative

O -0.985085 -0.621167 1.236261

frequencies existed. Transition states were

C -2.462541 0.235472 -0.476233

obtained using a Berny (TS) optimization

H -2.532555 -0.331592 -1.407838

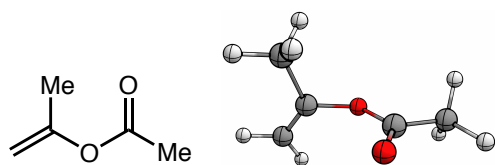
and confirmed by ensuring a single

H -3.275301 -0.050785 0.187509

negative frequency existed that represented

H -2.537555 1.294727 -0.728506

the reaction coordinate.



Charge: 0

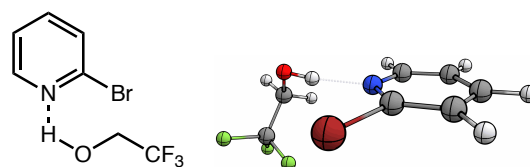
Spin Multiplicity: 1

Number of Imaginary Frequencies: 0

Solvation: 2,2,2-trifluoroethanol

Gibbs Free Energy at 298.150 K (Hartree):

-345.813640



Charge: 0

Spin Multiplicity: 1

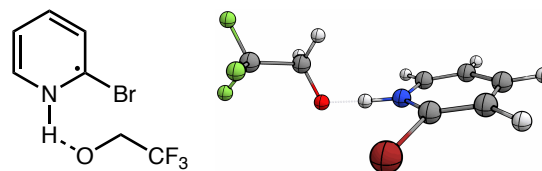
Number of Imaginary Frequencies: 0

Solvation: 2,2,2-trifluoroethanol

Gibbs Free Energy at 298.150 K (Hartree):

-3274.745103

C	-1.893792	-0.064511	0.013413
C	-3.178931	0.170444	0.494909
C	-3.60436	1.493607	0.550371
C	-2.743896	2.506109	0.128651
C	-1.483249	2.152822	-0.332498
N	-1.058645	0.877222	-0.388976
H	-4.59651	1.726775	0.917857
H	-3.81445	-0.645096	0.809767
H	-3.041152	3.546241	0.155725
H	-0.77946	2.904116	-0.672204
H	0.64937	0.584482	-1.074854
Br	-1.262985	-1.882313	-0.091309
O	1.516846	0.481207	-1.529389
C	2.527094	1.127223	-0.801167
H	2.187245	2.049495	-0.318933
H	3.348386	1.374407	-1.477333
C	3.105207	0.237362	0.29093
F	4.105411	0.872729	0.950206
F	3.62075	-0.914561	-0.195532
F	2.180322	-0.112391	1.217114



Charge: -1

Spin Multiplicity: 2

Number of Imaginary Frequencies: 0

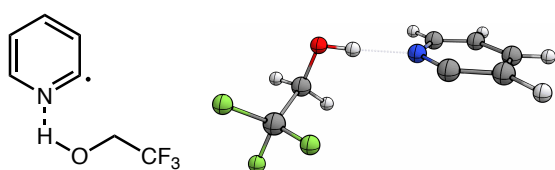
Solvation: 2,2,2-trifluoroethanol

Gibbs Free Energy at 298.150 K (Hartree):

-3274.824776

C	-1.97209	-0.143118	-0.033931
C	-3.254872	0.022456	-0.466383
C	-3.811374	1.334045	-0.531202
C	-2.983015	2.411325	-0.107362
C	-1.707329	2.182551	0.323037
N	-1.158817	0.897469	0.364479
H	-4.821054	1.491707	-0.884072
H	-3.837443	-0.844077	-0.751621
H	-3.353092	3.430383	-0.117656
H	-1.045046	2.970592	0.656612
H	-0.097495	0.797736	0.658597
Br	-1.19956	-1.899403	0.107133
O	1.303611	0.858202	1.083269
C	2.145102	1.265556	0.089025
H	2.685203	2.210213	0.304639
H	1.650032	1.4171	-0.893324

C	3.25766	0.260727	-0.203347	H	-2.176789	2.231252	0.303325
F	4.091884	0.696805	-1.194318	H	0.15897	0.918508	-0.60684
F	2.794538	-0.951493	-0.608458	O	1.035581	1.320397	-0.803016
F	4.051557	0.0165	0.873961	C	1.902803	1.107996	0.27987
				H	1.382318	1.075396	1.242297
				H	2.640984	1.912436	0.312475
				C	2.673956	-0.19725	0.139471
				F	3.523086	-0.370292	1.182257
				F	3.419009	-0.240768	-0.988964
				F	1.859131	-1.278797	0.107523



Charge: 0

Spin Multiplicity: 2

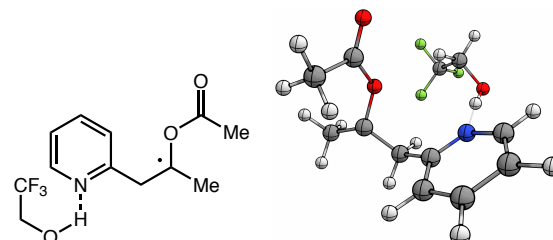
Number of Imaginary Frequencies: 0

Solvation: 2,2,2-trifluoroethanol

Gibbs Free Energy at 298.150 K (Hartree):

-700.52110

C	-1.905881	-0.912717	-0.410838
C	-3.167027	-1.45536	-0.216154
C	-4.139001	-0.54816	0.207785
C	-3.79744	0.795008	0.40207
C	-2.493115	1.203826	0.16893
N	-1.553065	0.317304	-0.242439
H	-5.154339	-0.885596	0.385034
H	-3.384497	-2.502191	-0.379578
H	-4.536642	1.514535	0.730345



Charge: 0

Spin Multiplicity: 2

Number of Imaginary Frequencies: 0

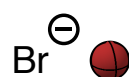
Solvation: 2,2,2-trifluoroethanol

Gibbs Free Energy at 298.150 K (Hartree):

-1046.356529

C	-1.735129	0.808394	0.830872
C	-3.132002	0.779016	0.890246

C	-3.867214	1.667411	0.114389	O	-0.263252	-1.527765	-0.234995
C	-3.188663	2.565515	-0.707053	C	-0.83573	-2.18407	-1.288026
C	-1.800278	2.53216	-0.7081	O	-0.218734	-2.223277	-2.325412
N	-1.085242	1.678379	0.041201	C	-2.19911	-2.785397	-1.080758
H	-4.950341	1.661824	0.151378	H	-2.130441	-3.665464	-0.437018
H	-3.628088	0.069725	1.541905	H	-2.869157	-2.073974	-0.595446
H	-3.718132	3.276453	-1.328495	H	-2.59979	-3.085217	-2.046647
H	-1.229035	3.214837	-1.328861				
H	0.676377	1.903084	-0.138406				
O	1.623578	2.126343	-0.332479				
C	2.249337	1.019828	-0.9285				
H	2.796365	1.323498	-1.826556				
H	1.541269	0.231184	-1.198739				
C	3.268211	0.399738	0.014706				
F	3.886792	-0.65679	-0.56938				
F	2.710561	-0.053769	1.162954				
F	4.238881	1.272214	0.377143				
C	-0.903796	-0.156609	1.651428				
H	0.103805	0.264833	1.774905				
H	-1.333667	-0.251314	2.651532				
C	-0.807747	-1.531618	1.058518				
C	-0.477314	-2.715467	1.902859				
H	-0.610229	-3.655794	1.363654				
H	0.571852	-2.677835	2.236508				
H	-1.106328	-2.735216	2.795036				



Charge: -1

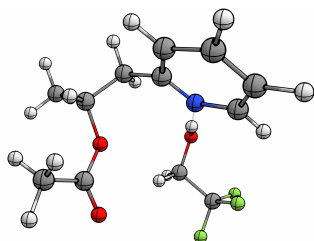
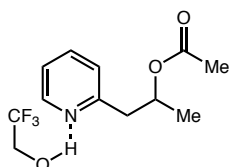
Spin Multiplicity: 0

Number of Imaginary Frequencies: 0

Solvation: 2,2,2-trifluoroethanol

Gibbs Free Energy at 298.150 K (Hartree):

-2574.354345



Charge: 0

Spin Multiplicity: 1

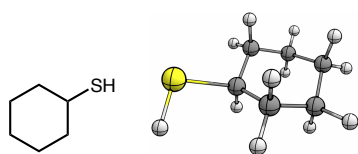
Number of Imaginary Frequencies: 0

Solvation: 2,2,2-trifluoroethanol

Gibbs Free Energy at 298.150 K (Hartree):

-1047.003245

C	-2.243696	-0.748057	0.844463
H	-2.657957	-1.552673	1.457936
H	-1.493554	-1.175415	0.171541
C	-3.383121	-0.224598	-0.016873
F	-3.890779	-1.208682	-0.800811
F	-2.991696	0.776108	-0.844379
F	-4.412013	0.26429	0.715729
C	2.03623	0.187827	1.517123
H	2.904719	0.464912	2.120731
H	1.208954	-0.016794	2.199795
C	2.394326	-1.105038	0.771827
C	2.852353	-2.209905	1.713893
H	3.070667	-3.129146	1.166488
H	3.76184	-1.901218	2.234615
H	2.08075	-2.423717	2.457381
O	1.177337	-1.532961	0.085484
C	1.162146	-2.111638	-1.132283
O	0.086917	-2.4585	-1.575549
C	2.457663	-2.283914	-1.885996
H	2.885552	-1.311257	-2.14125
H	3.196818	-2.830856	-1.297856
H	2.250416	-2.83062	-2.802858
H	3.164097	-0.891773	0.029584
H	0.597564	4.205146	-1.700199
H	-1.052983	2.779066	-0.498114
H	-0.968996	0.709809	1.216785
O	-1.72102	0.253285	1.677596
C	1.670357	1.337637	0.60829
C	2.659875	2.095216	-0.027397
C	2.289073	3.137191	-0.869521
C	0.934365	3.402505	-1.056494
C	0.012594	2.608274	-0.385879
N	0.364883	1.60079	0.426508
H	3.043605	3.735265	-1.36715
H	3.705877	1.870696	0.145003



Charge: 0

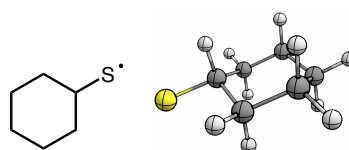
Spin Multiplicity: 1

Number of Imaginary Frequencies: 0

Solvation: 2,2,2-trifluoroethanol

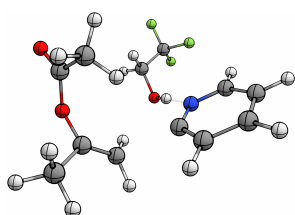
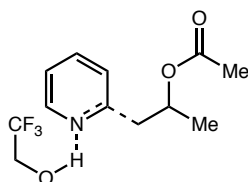
Gibbs Free Energy at 298.150 K (Hartree):

-634.027018

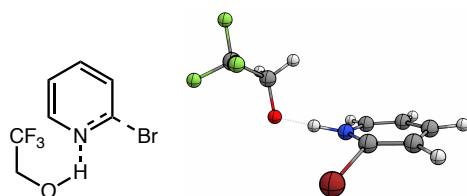


C	1.571578	-1.261604	0.214623	Charge: 0			
C	0.07429	-1.267621	-0.135589	Spin Multiplicity: 2			
C	-0.610943	0.008616	0.370141	Number of Imaginary Frequencies: 0			
C	0.076367	1.267576	-0.169402	Solvation: 2,2,2-trifluoroethanol			
C	1.573103	1.271986	0.185764	Gibbs Free Energy at 298.150 K (Hartree):			
C	2.272404	-0.001027	-0.309855	-633.393209			
H	-0.044337	-1.331704	-1.224502	C	1.529157	-1.265845	0.208465
H	-0.409964	-2.150334	0.29261	C	0.038626	-1.275704	-0.170203
H	1.687184	-1.314866	1.304439	C	-0.668733	0.000008	0.319192
H	2.044422	-2.159924	-0.194293	C	0.038635	1.275696	-0.170243
H	-0.043917	1.299056	-1.258773	C	1.529141	1.265841	0.208507
H	-0.409781	2.162122	0.2318	C	2.235529	0.000012	-0.293545
H	2.047325	2.160484	-0.242785	H	-0.060216	-1.338478	-1.260441
H	1.687856	1.349888	1.274289	H	-0.456605	-2.15603	0.247405
H	2.265337	-0.013299	-1.407329	H	1.623184	-1.324987	1.300331

H	2.012966	-2.160335	-0.196327	C	1.187429	1.642624	-0.479065
H	-0.060139	1.338388	-1.260492	C	2.083063	2.606332	-0.035151
H	-0.456623	2.15605	0.24727	C	1.535076	3.688685	0.652106
H	2.012971	2.16036	-0.196196	C	0.152737	3.74387	0.855112
H	1.623105	1.324907	1.300383	C	-0.640361	2.717838	0.362741
H	2.242844	0.000032	-1.391127	N	-0.105909	1.669417	-0.306434
H	3.282123	0.00001	0.027163	H	2.176013	4.48012	1.025353
H	-0.667329	0.000023	1.421118	H	3.147405	2.522603	-0.214138
S	-2.456901	0.000001	-0.053258	H	-0.301333	4.570671	1.386504
				H	-1.716343	2.713991	0.493961
				O	-1.71676	-0.281918	-1.490605
				C	-2.248413	-1.157191	-0.532394
TS2				H	-1.583398	-1.306796	0.324633
				H	-2.437294	-2.128002	-0.996182
				C	-3.579442	-0.659041	0.013753
				F	-4.086495	-1.528467	0.921723
				F	-4.513847	-0.505582	-0.952122
				F	-3.465539	0.540852	0.63546
				C	2.034795	-0.202225	-1.732477
				H	1.001417	-0.455017	-1.928523
				H	2.509816	0.531941	-2.368509
				C	2.804472	-1.022697	-0.985053
				C	4.284154	-0.946744	-0.803333
				H	4.567628	-0.786768	0.241368
				H	4.751175	-1.883442	-1.124935
Charge: 0							
Spin Multiplicity: 2							
Number of Imaginary Frequencies: 1							
Solvation: 2,2,2-trifluoroethanol							
Gibbs Free Energy at 298.150 K (Hartree):							
-1046.302799							



H	4.695749	-0.129501	-1.39582	C	2.757514	2.529788	-0.01029
O	2.180033	-2.141386	-0.400775	C	1.606644	2.153804	-0.638195
C	1.947366	-2.286094	0.93683	N	1.069324	0.882987	-0.492788
O	1.482479	-3.336686	1.309358	H	4.348625	1.878334	1.359858
C	2.276835	-1.140579	1.855948	H	3.57745	-0.524316	1.292507
H	3.304549	-1.256792	2.210983	H	3.127588	3.539173	-0.145452
H	2.185999	-0.171614	1.368228	H	1.041262	2.821355	-1.277198
H	1.615691	-1.190602	2.719399	H	0.011812	0.7231	-0.802485
H	-1.175068	0.413327	-1.040762	Br	1.380118	-1.935877	-0.16269
				O	-1.365437	0.665751	-1.247803
				C	-2.232044	1.225272	-0.35283
				H	-2.8874	2.008673	-0.783437
TS1				H	-1.739533	1.690037	0.52682
				C	-3.203763	0.214314	0.25307
				F	-4.063053	0.800193	1.139553
				F	-2.581578	-0.783441	0.935302
				F	-3.984636	-0.398577	-0.676619



Charge: -1

Spin Multiplicity: 2

Number of Imaginary Frequencies: 1

Solvation: 2,2,2-trifluoroethanol

Gibbs Free Energy at 298.150 K (Hartree):

-3274.824506

C	1.81243	-0.048744	0.202766
C	3.007624	0.261314	0.810817
C	3.471211	1.58906	0.796551

3.4.9 Troubleshooting and Reaction Limitations

Troubleshooting

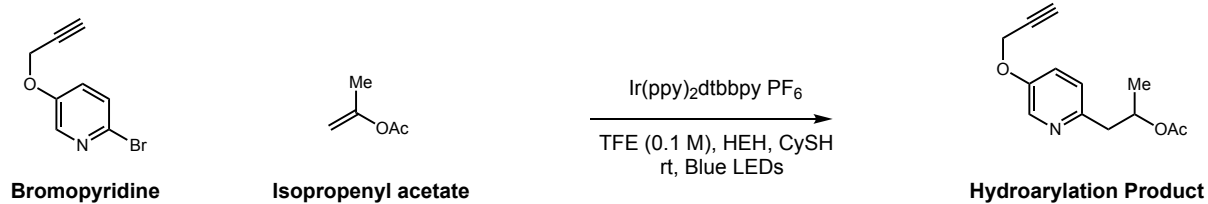
For low yielding substrates a number of simple experiments can be performed that may improve performance. For example, if alkene oligomerization is present, moving to a more electrophilic thiol (such as thiophenol) can increase yield and clean up the reaction profile.

If conversion of the starting material is low, the solvent/purging cycle is the problem. If the problem persists, moving to a more reducing photocatalyst or the addition of more HEH may promote further reduction.

This reaction manifold is highly dependent on the $\Delta\Delta G$ for the reaction of the pyridyl radical with either HEH or alkene addition. Small, seemingly innocuous, alterations to pyridine or alkene structure can dramatically affect yield. Additionally, donating groups attached to the pyridine core will alter the reduction potential, which can affect the conversion of starting material.

A short, unsuccessful, optimization of substrate **30** is shown in Table 3.16. The mass balance of the reaction under standard conditions consisted of 29% product, 22% starting material, and 16% hydrodehalogenation – the remaining material is unaccounted for by ^1H NMR assay. Although marginal, addition of PhSH was the most beneficial change.

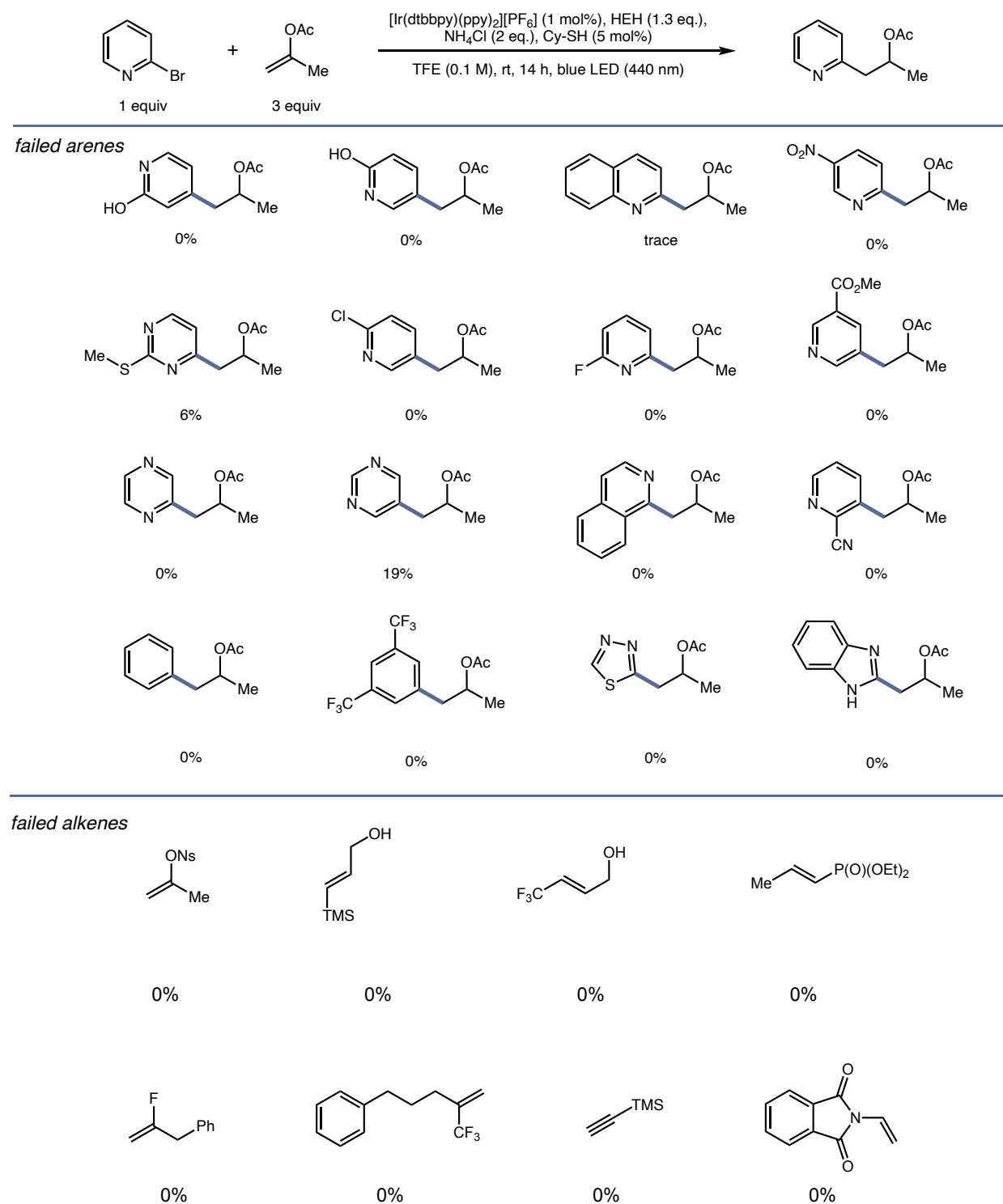
Table 3.16



Entry	Deviation from Standard Conditions	Yield (%)
1	2 eq HEH	25%
2	2.5 eq HEH	17%
3	Ir(ppy) ₃	28%
4	AcOH instead of NH ₄ Cl	29%
5	PhSH instead of CySH	36%
6	50 °C	20%

Reaction Limitations

The reaction scope, while broad, has many limitations. A representative portion of the (het)arenes and alkenes that were not tolerated under the reaction conditions are shown in Table 3.17.

Table 3.17 Failed and limited substrate scope.

Chapter 4:

**Selective C–F Functionalization of Unactivated
Trifluoromethylarenes**

Adapted and reprinted in part with permission from *J. Am. Chem. Soc.* **2019**, 13203-13211
Copyright 2019 American Chemical Society

<https://pubs.acs.org/doi/10.1021/jacs.9b06004>

Abstract: Fluorinated organic molecules are pervasive within the pharmaceutical and agrochemical industries due to the range of structural and physicochemical properties that fluorine imparts. Currently, the most abundant methods for the synthesis of the aryl-CF₂ functionality have relied on the deoxyfluorination of ketones and aldehydes using expensive and poorly atom economical reagents. Here, we report a general method for the synthesis of aryl-CF₂R and aryl-CF₂H compounds through activation of the corresponding trifluoromethyl arene precursors. This strategy is enabled by an endergonic electron transfer event that provides access to arene radical anions that lie outside of the catalyst reduction potential. Fragmentation of these reactive intermediates delivers difluorobenzyl radicals that can be intercepted by abundant alkene feedstocks or a hydrogen atom to provide a diverse array of difluoroalkylaromatics.

4.1 Introduction

4.1.1 A Different Mode of Activation

In the previous chapters a number of means have been used to generate radicals, some of which have been specifically characterized. PCET, for example, is a useful means of redox activation where high potentials would otherwise be required, but only finds relevance with certain classes of molecules (namely those with acidic or basic sites). However, each method shares the requirement for a subsequent, irreversible reaction to take place for the reaction to move forward. For halopyridine alkylation, the entropically-biased rearomatization and concerted C-X bond cleavage drive reactivity forward.

The Curtin Hammett principle outlines that before an irreversible step in any given mechanism, that all the discrete intermediates exist in equilibrium. When developing new reactions, this is a particularly intriguing concept because, in principle, reactivity can be

thermodynamically uphill (even significantly) so long as it's followed by an irreversible step. For the photoredox reactions described in the previous chapters, this indeed means that single electron transfer from the catalyst is reversible (Ir^{II} and Ir^{III} are in equilibrium with the arene and its radical anion). The equilibrium is then shifted as the radical anion undergoes carbon-halogen cleavage to restore aromaticity.

We envisioned employing this principle to drastically expand the scope of a defluoroalkylation reaction developed by the Jui group in 2018.¹¹¹ With this chemistry, we aimed to utilize a very exothermic C–F bond cleavage to overcome a highly endergonic electron transfer. This would result in a powerful method for the activation and modification of fluorinated molecules which are typically thought of as inert.

4.1.2 Modification of Trifluoromethylaromatics

The trifluoromethylaromatic ($\text{Ar}-\text{CF}_3$) motif is routinely utilized in drug and agrochemical design, because its incorporation can significantly alter the properties of a given biologically active small molecule.¹¹² Accordingly, a number of methods have been reported over the past decade that enable the efficient construction of $\text{Ar}-\text{CF}_3$ compounds.¹¹³ Although trifluoromethyl units are

¹¹¹ Wang, H.; Jui, N. T. Catalytic Defluoroalkylation of Trifluoromethylaromatics with Unactivated Alkenes. *J. Am. Chem. Soc.* **2018**, *140* (1), 163–166

¹¹² (a) Gillis, E. P.; Eastman, K. J.; Hill, M. D.; Donnelly, D. J.; Meanwell, N. A. Applications of Fluorine in Medicinal Chemistry. *J. Med. Chem.* **2015**, *58* (21), 8315–8359; (b) Purser, S.; Moore, P. R.; Swallow, S.; Gouverneur, V. Fluorine in Medicinal Chemistry. *Chem. Soc. Rev.* **2008**, *37* (2), 320–330; (c) Hagmann, W. K. The Many Roles for Fluorine in Medicinal Chemistry. *J. Med. Chem.* **2008**, *51* (15), 4359–4369; (d) Zhou, Y.; Wang, J.; Gu, Z.; Wang, S.; Zhu, W.; Aceña, J. L.; Soloshonok, V. A.; Izawa, K.; Liu, H. Next Generation of Fluorine-Containing Pharmaceuticals, Compounds Currently in Phase II–III Clinical Trials of Major Pharmaceutical Companies: New Structural Trends and Therapeutic Areas. *Chem. Rev.* **2016**, *116* (2), 422–518

¹¹³ (a) Le, C.; Chen, T. Q.; Liang, T.; Zhang, P.; MacMillan, D. W. C. A Radical Approach to the Copper Oxidative Addition Problem: Trifluoromethylation of Bromoarenes. *Science*. **2018**, *360* (6392), 1010 – 1014; (b) Nagib, D. A.; MacMillan, D. W. C. Trifluoromethylation of Arenes and Heteroarenes by Means of Photoredox Catalysis. *Nature* **2011**, *480*, 224; (c) Zhu, W.; Wang, J.; Wang, S.; Gu, Z.; Aceña, J. L.; Izawa, K.; Liu, H.; Soloshonok, V. A. Recent Advances in the Trifluoromethylation Methodology and New CF_3 -Containing Drugs. *J. Fluor. Chem.* **2014**, *167*, 37–54; (d) Morimoto, H.; Tsubogo, T.; Litvinas, N. D.; Hartwig, J. F. A Broadly Applicable Copper Reagent for Trifluoromethylations and Perfluoroalkylations of Aryl Iodides and Bromides. *Angew. Chemie Int. Ed.* **2011**, *50* (16),

traditionally unreactive, we recently became interested in selective manipulation of these compounds through a radical anion-based mechanism for carbon–fluorine (C–F) bond cleavage. We envisioned that the resulting radical intermediates could serve as precursors to a number of valuable fluorinated scaffolds, including difluoroalkyl aromatics (isosteres for aryl ethers and aryl ketones)¹¹⁴ and difluoromethyl arenes (lipophilic hydrogen bond donors).¹¹⁵ These difluorobenzyl arrays have emerged as important components of bioactive small molecules (two of which are shown in Figure 4.1). The direct molecular editing of trifluoromethylaromatics in this way would offer a valuable complement to technologies that grant access to these difluorinated motifs through construction of the $C_{\text{Aryl}}\text{--CF}_2\text{R/H}$ bond.¹¹⁶

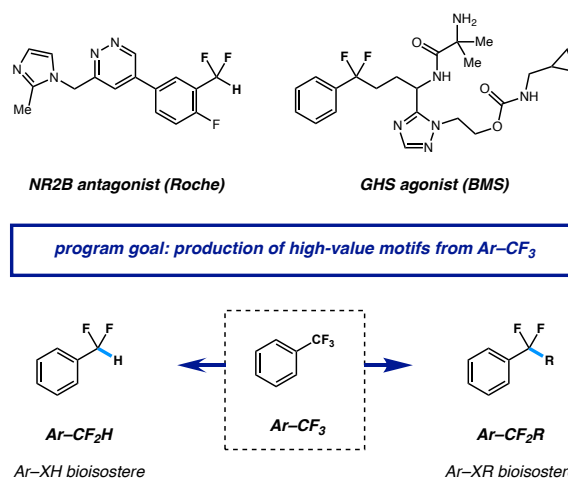


Figure 4.1 Molecular editing of Ar-CF_3 groups via catalytic C–F

3793–3798; (e) Ji, Y.; Brueckl, T.; Baxter, R. D.; Fujiwara, Y.; Seiple, I. B.; Su, S.; Blackmond, D. G.; Baran, P. S. Innate C–H Trifluoromethylation of Heterocycles. *Proc. Natl. Acad. Sci.* **2011**, *108* (35), 14411 – 14415 (f) Cho, E. J.; Senecal, T. D.; Kinzel, T.; Zhang, Y.; Watson, D. A.; Buchwald, S. L. The Palladium-Catalyzed Trifluoromethylation of Aryl Chlorides. *Science*. **2010**, *328* (5986), 1679 – 1681

¹¹⁴ Müller, K.; Faeh, C.; Diederich, F. Fluorine in Pharmaceuticals: Looking Beyond Intuition. *Science*. **2007**, *317* (5846), 1881 – 1886

¹¹⁵ (a) Erickson, J. A.; McLoughlin, J. I. Hydrogen Bond Donor Properties of the Difluoromethyl Group. *J. Org. Chem.* **1995**, *60* (6), 1626–1631; (b) Sessler, C. D.; Rahm, M.; Becker, S.; Goldberg, J. M.; Wang, F.; Lippard, S. J. CF_2H , a Hydrogen Bond Donor. *J. Am. Chem. Soc.* **2017**, *139* (27), 9325–9332; (c) Zafrani, Y.; Yeffet, D.; Sod-Moriah, G.; Berliner, A.; Amir, D.; Marciano, D.; Gershonov, E.; Saphier, S. Difluoromethyl Bioisostere: Examining the “Lipophilic Hydrogen Bond Donor” Concept. *J. Med. Chem.* **2017**, *60* (2), 797–804; (d) Meanwell, N. A. Fluorine and Fluorinated Motifs in the Design and Application of Bioisosteres for Drug Design. *J. Med. Chem.* **2018**, *61* (14), 5822–5880; (e) Meanwell, N. A. Synopsis of Some Recent Tactical Application of Bioisosteres in Drug Design. *J. Med. Chem.* **2011**, *54* (8), 2529–2591

¹¹⁶ (a) Merchant, R. R.; Edwards, J. T.; Qin, T.; Kruszyk, M. M.; Bi, C.; Che, G.; Bao, D.-H.; Qiao, W.; Sun, L.; Collins, M. R.; Fadeyi, O. O.; Gallego, G. M.; Mousseau, J. J.; Nuhant, P.; Baran, P. S. Modular Radical Cross-Coupling with Sulfones Enables Access to $\text{Sp}^3\text{-Rich}$ (Fluoro)Alkylated Scaffolds. *Science*. **2018**, *360* (6384), 75 – 80; (b) Fujiwara, Y.; Dixon, J. A.; Rodriguez, R. A.; Baxter, R. D.; Dixon, D. D.; Collins, M. R.; Blackmond, D. G.; Baran, P. S. A New Reagent for Direct Difluoromethylation. *J. Am. Chem. Soc.* **2012**, *134* (3), 1494–1497; (c) Bacauanu, V.; Cardinal, S.; Yamauchi, M.; Kondo, M.; Fernández, D. F.; Remy, R.; MacMillan, D. W. C. Metallaphotoredox Difluoromethylation of Aryl Bromides. *Angew. Chemie Int. Ed.* **2018**, *57* (38), 12543–12548; (d) Xiao, Y.-L.; Min, Q.-Q.; Xu, C.; Wang, R.-W.; Zhang, X. Nickel-Catalyzed Difluoroalkylation of (Hetero)Arylborons with Unactivated 1-Bromo-1,1-Difluoroalkanes. *Angew. Chemie Int. Ed.* **2016**, *55* (19), 5837–

Although reductive activation of the C–F bonds in this substrate class can be accomplished using a range of approaches (e.g., electrochemical reduction,¹¹⁷ low-valent metals,¹¹⁸ or frustrated Lewis pairs¹¹⁹), preventing exhaustive defluorination (thereby bypassing valuable di- and monofluorinated intermediates) remains a significant synthetic problem. This is because, in part, C–F bond strength decreases as defluorination proceeds.¹²⁰ Troupel¹²¹ and Lalic¹²² reported two different systems for interception of anionic difluorobenzyl species through trapping with carbonyl-based electrophiles. In addition, Prakash reported a Mg⁰-based system for hydrodefluorination (HDF) of bis(trifluoromethyl)-benzene derivatives.^{118a} Yoshida and Hosoya recently described an intermolecular coupling of trifluoromethyl arenes that contain ortho-silyl groups with allyl silanes, which operates through a cationic mechanism.¹²³ While these systems

5841; (e) Zhou, Q.; Ruffoni, A.; Gianatassio, R.; Fujiwara, Y.; Sella, E.; Shabat, D.; Baran, P. S. Direct Synthesis of Fluorinated Heteroarylether Bioisosteres. *Angew. Chemie Int. Ed.* **2013**, 52 (14), 3949–3952; (f) Fier, P. S.; Hartwig, J. F. Copper-Mediated Difluoromethylation of Aryl and Vinyl Iodides. *J. Am. Chem. Soc.* **2012**, 134 (12), 5524–5527; (g) Prakash, G. K. S.; Ganesh, S. K.; Jones, J.-P.; Kulkarni, A.; Masood, K.; Swabeck, J. K.; Olah, G. A. Copper-Mediated Difluoromethylation of (Hetero)Aryl Iodides and β -Styryl Halides with Tributyl(Difluoromethyl)Stannane. *Angew. Chemie Int. Ed.* **2012**, 51 (48), 12090–12094

¹¹⁷ (a) Yamauchi, Y.; Fukuhara, T.; Hara, S.; Senboku, H. Electrochemical Carboxylation of α,α -Difluorotoluene Derivatives and Its Application to the Synthesis of α -Fluorinated Nonsteroidal Anti-Inflammatory Drugs. *Synlett* **2008**, 2008 (03), 438–442; (b) Lund, Henning; Jensen, N. J. Electroorganic Preparations. XXXVI. Stepwise Reduction of Benzotrifluoride. *Acta Chem. Scand.* **1974**, 28B (2), 263–265

¹¹⁸ (a) Munoz, S. B.; Ni, C.; Zhang, Z.; Wang, F.; Shao, N.; Mathew, T.; Olah, G. A.; Prakash, G. K. S. Selective Late-Stage Hydrodefluorination of Trifluoromethylarenes: A Facile Access to Difluoromethylarenes. *European J. Org. Chem.* **2017** (16), 2322–2326; (b) Fuchibe, K.; Ohshima, Y.; Mitomi, K.; Akiyama, T. Low-Valent Niobium-Catalyzed Reduction of α,α,α -Trifluorotoluenes. *Org. Lett.* **2007**, 9 (8), 1497–1499; (c) Amii, H.; Hatamoto, Y.; Seo, M.; Uneyama, K. A New C–F Bond-Cleavage Route for the Synthesis of Octafluoro[2.2]Paracyclophane. *J. Org. Chem.* **2001**, 66 (21), 7216–7218

¹¹⁹ (a) Stahl, T.; Klare, H. F. T.; Oestreich, M. Main-Group Lewis Acids for C–F Bond Activation. *ACS Catal.* **2013**, 3 (7), 1578–1587; (b) Forster, F.; Metsänen, T. T.; Irran, E.; Hrobárik, P.; Oestreich, M. Cooperative Al–H Bond Activation in DIBAL-H: Catalytic Generation of an Aluminum-Ion-Like Lewis Acid for Hydrodefluorinative Friedel–Crafts Alkylation. *J. Am. Chem. Soc.* **2017**, 139 (45), 16334–16342

¹²⁰ Radom, L.; Hehre, W. J.; Pople, J. A. Molecular Orbital Theory of the Electronic Structure of Organic Compounds. VII. A Systematic Study of Energies, Conformations, and Bond Interactions. *J. Am. Chem. Soc.* **1971**, 93 (2), 289–300

¹²¹ Saboureau, C.; Troupel, M.; Sibille, S.; Perichon, J. Electroreductive Coupling of Trifluoromethylarenes with Electrophiles: Synthetic Applications. *J. Chem. Soc., Chem. Commun.* **1989**, 1138–1139

¹²² Dang, H.; Whittaker, A. M.; Lalic, G. Catalytic Activation of a Single C–F Bond in Trifluoromethyl Arenes. *Chem. Sci.* **2016**, 7 (1), 505–509

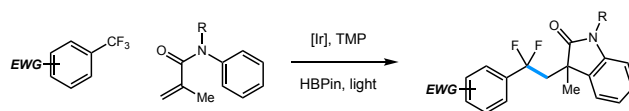
¹²³ Yoshida, S.; Shimomori, K.; Kim, Y.; Hosoya, T. Single C–F Bond Cleavage of Trifluoromethylarenes with an Ortho-Silyl Group. *Angew. Chemie - Int. Ed.* **2016**, 55 (35), 10406–10409

allow for selective defluorofunctionalization of specific substrate classes, a general approach to Ar–CF₃ functionalization remains elusive.

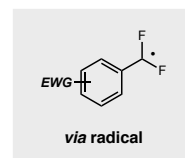
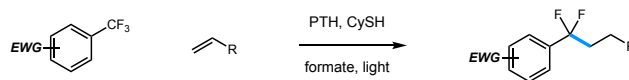
Our strategy is mechanistically founded on recent work from our group¹¹¹ and König's,¹²⁴ where the use of highly reducing photoredox catalysts resulted in partial defluorination of activated trifluoromethylaromatic substrates (Figure

4.2), under irradiation with visible light. In our method, single electron transfer (SET) from an organic photoredox catalyst to the aryl substrate is followed by C–F cleavage to deliver difluorobenzylic radicals that display unique reactivity profiles. This system, ultimately propelled by oxidation of formate to CO₂, effectively performs monodefluoroalkylation reactions with a wide range of unactivated olefins as alkyl sources. However, the utility of both of these systems is limited by the requirement for electronic activation of the substrates. More specifically, successful reaction has only been demonstrated for trifluoromethylaromatics that contain auxiliary electron-withdrawing groups (e.g., –CF₃, –CN, –SO₂NH₂). Here, we describe the development of conditions that overcome this limitation, thus enabling controlled C–F functionalization of unactivated trifluoromethylaromatics. We show that these difluorobenzylic radical intermediates can be utilized selectively in both alkylation and reduction processes.

König: Cascade Radical Addition/Cyclization with Methacrylamides



Jui: Dual Catalytic Defluoroalkylation with Simple Alkenes



Previous Work: Auxiliary EWG is required

This Work: Unactivated Ar–CF₃ substrates;

HAT to radical intermediate for Ar–CF₂H

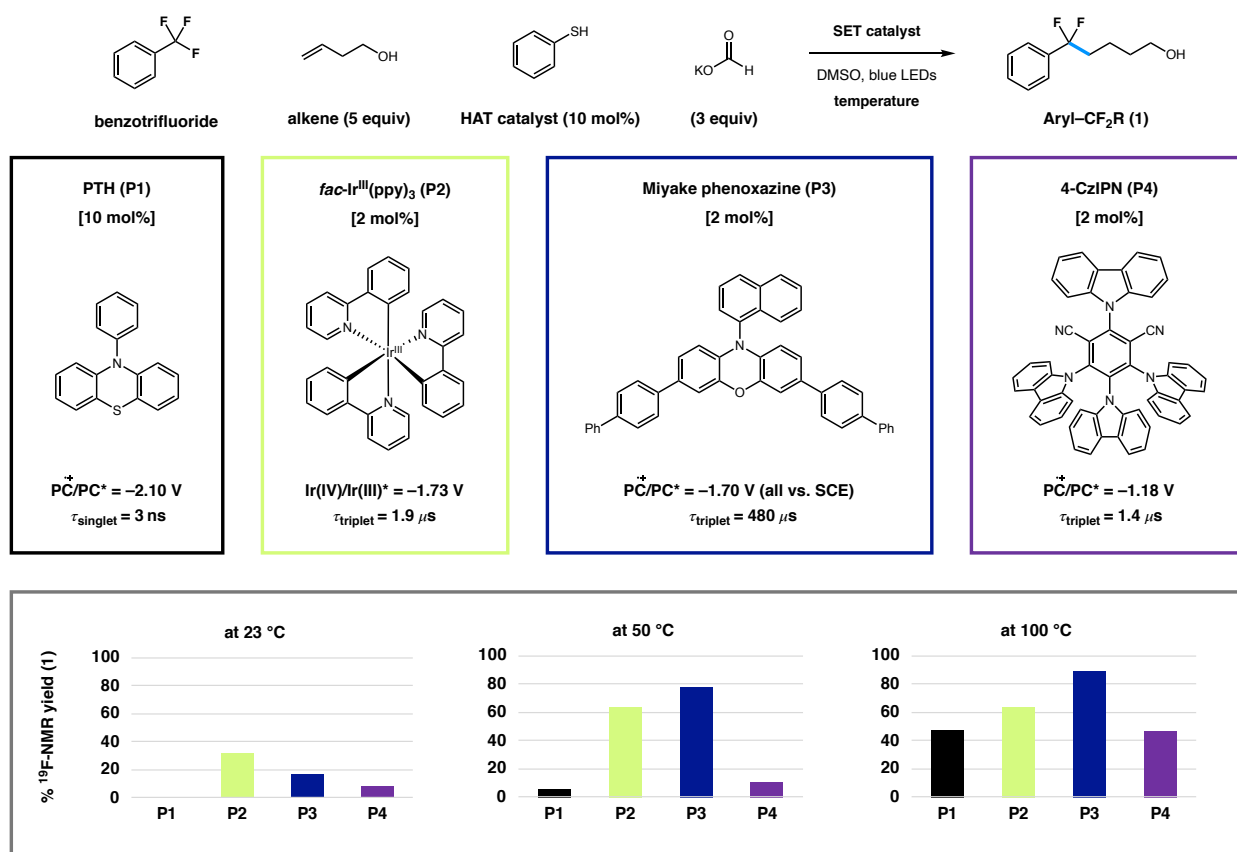
Figure 4.2 Radical C–F functionalization of Ar–CF₃ substrates via photoredox catalysis

¹²⁴ Chen, K.; Berg, N.; Gschwind, R.; König, B. Selective Single C(Sp³)–F Bond Cleavage in Trifluoromethylarenes: Merging Visible-Light Catalysis with Lewis Acid Activation. *J. Am. Chem. Soc.* **2017**, *139* (51), 18444–18447

4.2 Results and Discussion

We began our study by examining the reaction of benzotrifluoride (Ph-CF₃) with 3-buten-1-ol to afford the defluoroalkylation (DFA) product **1** (shown in Scheme 4.1). After slight modification of our initially reported conditions, we evaluated a series of photoredox catalysts, a selection of which is shown in Scheme 4.1. While N-phenylphenothiazine (PTH, P1) was ineffective at room temperature, the use of P2–P4 afforded the desired product to varying degrees (up to 31% yield after 24 h). Increasing reaction temperature resulted in significantly improved yields of the desired linear alkylation product. The most effective catalyst (P3, developed by

Scheme 4.1 Activation of Stable C–F Bonds by Single-Electron Transfer using Photoredox Catalysis^a



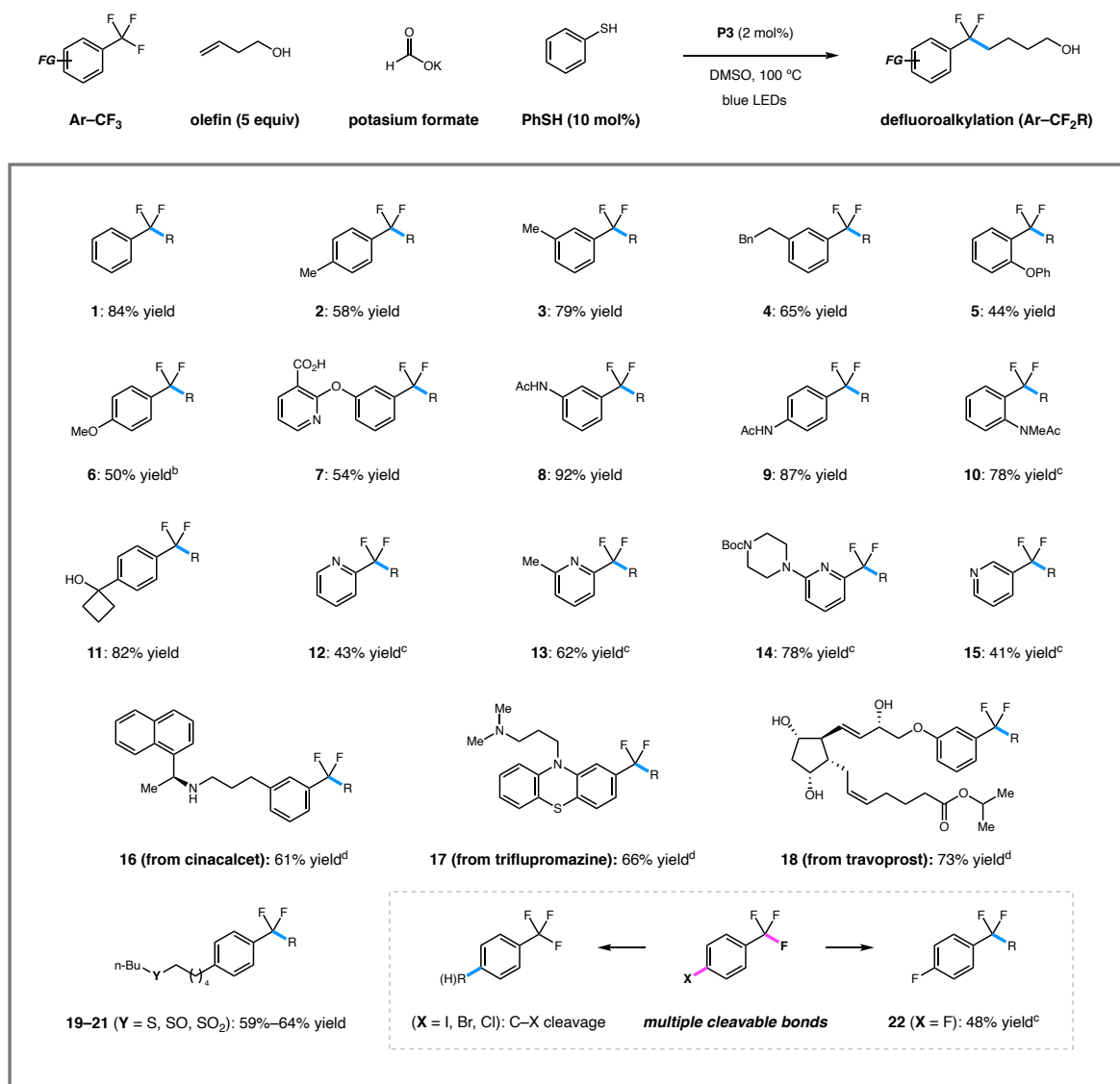
^aReaction conditions: benzotrifluoride (0.25 mmol), 3-buten-1-ol (1.25 mmol), photoredox catalyst (P1: 10 mol%; P2–P4: 2 mol%), potassium formate (0.75 mmol), thiophenol (10 mol%), DMSO (2.5 mL), blue light, 24 h. Yields determined by ¹⁹F NMR analysis with internal standard.

Miyake for organic atom-transfer radical polymerization)¹²⁵ has been reported to be highly absorbent in the visible spectrum ($\lambda_{\text{max}} = 388 \text{ nm}$, $\epsilon_{\text{max}} = 26\,635 \text{ M}^{-1} \text{ cm}^{-1}$) with a 98% intersystem crossing (ISC) efficiency to a long-lived triplet excited state that is strongly reducing ($E_{1/2}^* = -1.70 \text{ V}$ vs standard calomel electrode (SCE)).¹²⁶ The use of P3 (2 mol %) at 100 °C resulted in 89% yield of 1, as determined by NMR. Interestingly, for the organic SET catalysts (P1, P3, P4), reaction progress is not strongly correlated with reduction potential of the catalyst. Rather, conversion at higher temperatures is more closely related to excited-state lifetime. This effect is most pronounced through the use of P4 in this process, because it is significantly less reducing than P1 but equally effective at high temperature.

As shown in Table 4.1, a collection of unactivated trifluoromethylaromatics could be engaged under these conditions. In addition to carbon and oxygen-substituted substrates, arylamine derivatives reacted smoothly to afford the desired products 2–10 in 44–92% yield. The benzylic carbinol was cleanly retained, giving alkylation product 11 in 82% yield. Pyridine substrates with trifluoromethyl groups at the 2- and 3- positions gave rise to 12–15 in 41–78% yield. These reactions were most effectively performed at room temperature, because the difluoroalkylpyridine products can be further reductively defluorinated. In fact, 4-trifluoromethylpyridine currently remains outside the scope of these processes; attempted alkylation reactions largely resulted in picoline production with only trace amounts of the desired product. Likewise, while this protocol is effective in activating electron-deficient aromatics (such as those described in our previous report),¹¹¹ the elevated temperature and more effective catalyst typically resulted in further

¹²⁵ Pearson, R. M.; Lim, C.-H.; McCarthy, B. G.; Musgrave, C. B.; Miyake, G. M. Organocatalyzed Atom Transfer Radical Polymerization Using N-Aryl Phenoxazines as Photoredox Catalysts. *J. Am. Chem. Soc.* **2016**, *138* (35), 11399–11407

¹²⁶ Du, Y.; Pearson, R. M.; Lim, C.-H.; Sartor, S. M.; Ryan, M. D.; Yang, H.; Damrauer, N. H.; Miyake, G. M. Strongly Reducing, Visible-Light Organic Photoredox Catalysts as Sustainable Alternatives to Precious Metals. *Chem. – A Eur. J.* **2017**, *23* (46), 10962–10968

Table 4.1 Catalytic Defluoroalkylation: Scope of Unactivated Trifluoromethylaromatic Substrates^a

^aReaction conditions: Ar-CF_3 substrate (0.5 mmol), 3-buten-1-ol (2.5 mmol), P3 (2 mol%), potassium formate (1.5 mmol), thio-phenol (10 mol%), DMSO (5.0 mL), blue light, 100 °C, 24 h, isolated yields given. ^bReaction conducted with 2.5 mmol of potassium formate. ^cReaction conducted at 23 °C. ^dReaction conducted with 0.5 mmol of olefin.

defluorination of these substrates. The functionalization of marketed pharmaceuticals could also be performed under these conditions to afford derivatives 16–18 in 61%–73% yield, demonstrating that basic functions, alcohols, and internal alkenes are well-tolerated.

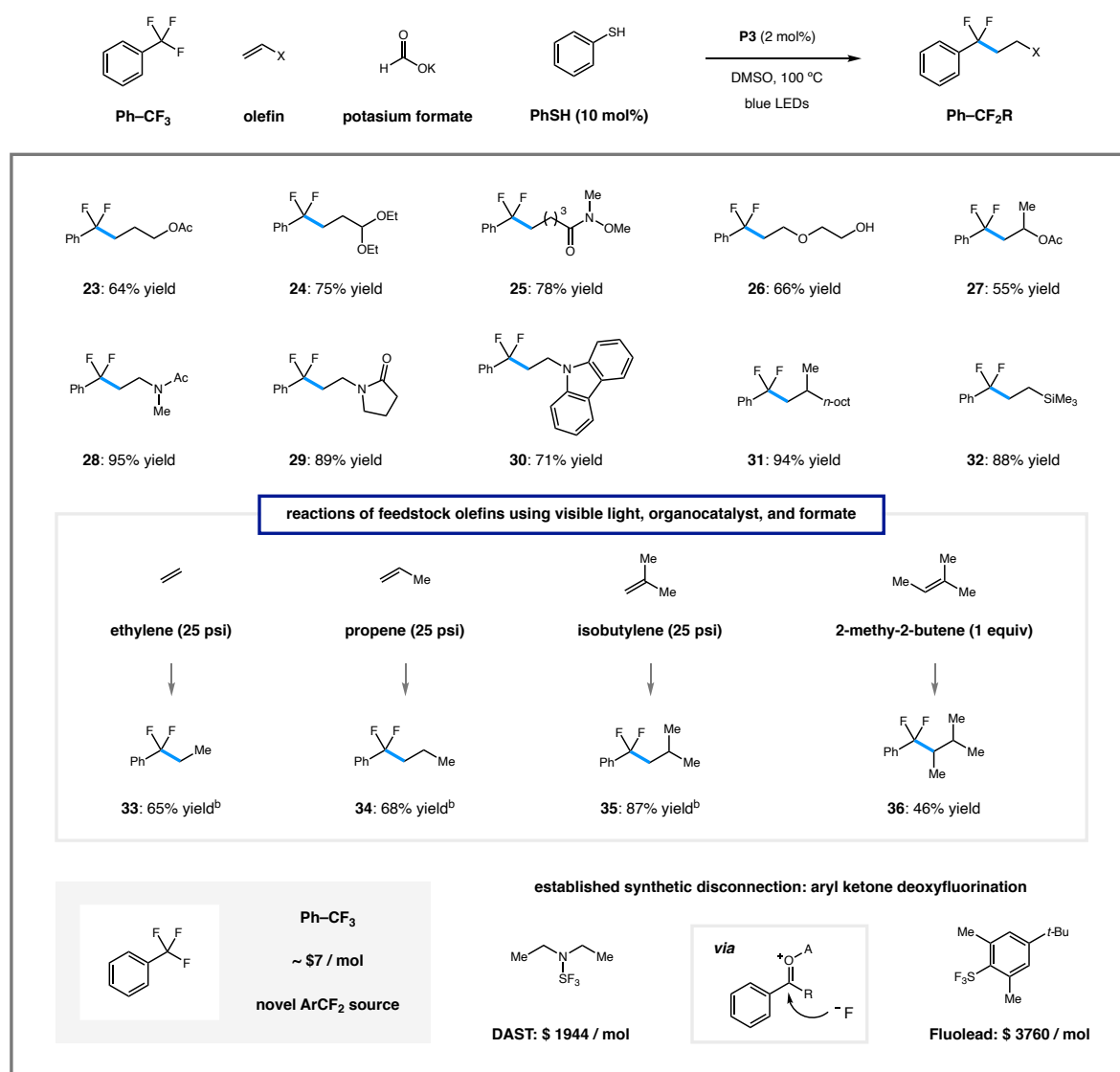
Although these conditions are able to accomplish challenging redox events, we found that thioethers, sulfoxides, and sulfones alike were preserved throughout the course of the reaction without any observable alteration of the sulfur oxidation states (19–21, 59–64% yield). To probe

the chemoselective nature of heterolytic C–X cleavage within a single π -system, we examined the reactivity of a series of 4- halogenated benzotrifluorides. From the corresponding radical anions, cleavage of the aryl C–I, C–Br, and C–Cl bonds (bond dissociation energy (BDE) = 71.6, 80.3, and 95.5 kcal/ mol, respectively; see 4.4.6 Computational Details for further details, pg. 282) occurred in preference to the stronger benzylic C(sp₃)–F bond (BDE = 118.1 kcal/mol), resulting in mixtures of protodehalogenation and aryl radical alkylation products.¹²⁷ In contrast, the aryl C–F bond (BDE = 127.5 kcal/mol) was completely preserved, affording 22 in 48% yield (where the mass balance was comprised of unreacted starting material). In addition to aryl halides, alkyl halides currently lie outside the scope of this process, where either reductive dehalogenation or substitution with formate are primary pathways of these substrates.

In line with our previous report, the olefin scope for coupling with unactivated trifluoromethylaromatics is broad, giving a range of difluoroalkylated benzene derivatives from benzotrifluoride. The use of benzotrifluoride as a precursor to difluoroalkyl benzene derivatives is attractive, because it is abundantly available at low cost (~\$7/mol) when compared to conventional reagents that accomplish deoxyfluorination of aryl ketones (e.g., diethylaminosulfur trifluoride (DAST) or Fluolead).¹²⁸ While the standard conditions (5 equiv of olefin with limiting Ar–CF₃ substrate) were effective here (see Table 4.1 and 4.4.5 Procedures and Characterization Data, pg. 261), we found that using a cosolvent quantity (50 equiv) of benzotrifluoride could be conveniently employed for coupling of simple olefins with acetate, acetal, or Weinreb amide groups (Table 4.2:

¹²⁷ Boyington, A. J.; Seath, C. P.; Zearfoss, A. M.; Xu, Z.; Jui, N. T. Catalytic Strategy for Regioselective Arylethylamine Synthesis. *J. Am. Chem. Soc.* **2019**, *141* (9), 4147–4153

¹²⁸ For an alternative strategy to Ar–CF₂R synthesis via deprotonation of difluoromethylaromatics, see: Geri, J. B.; Wade Wolfe, M. M.; Szymczak, N. K. The Difluoromethyl Group as a Masked Nucleophile: A Lewis Acid/Base Approach. *J. Am. Chem. Soc.* **2018**, *140* (30), 9404–9408

Table 4.2 Scope of Olefinic Coupling Partner for Photocatalytic Difluoroalkylaromatic Synthesis^a

^aReaction conditions: benzotrifluoride (3 mL), alkene (0.5 mmol), P3 (2 mol %), potassium formate (2.5 mmol), thiophenol (10 mol %), DMSO (5.0 mL), blue light, 100 °C, 24 h; isolated yields given. ^bReaction conducted with potassium formate as limiting reagent, yields determined by ¹⁹F NMR analysis with an internal standard.

23–25, 64–78% yield). Other nucleophilic olefins including the vinyl ether, acetate, amides, and vinyl carbazole were also effective coupling partners under this protocol (26–30, 55–95%). β -Substitution of aliphatic olefins was also well-tolerated (31, 94% yield). Although these conditions operate at elevated temperature, decomposition through saponification or hydrolysis pathways was not observed. Ethylene, propylene, isobutylene, and 2-methyl-2-butene) are attractive two-, three-

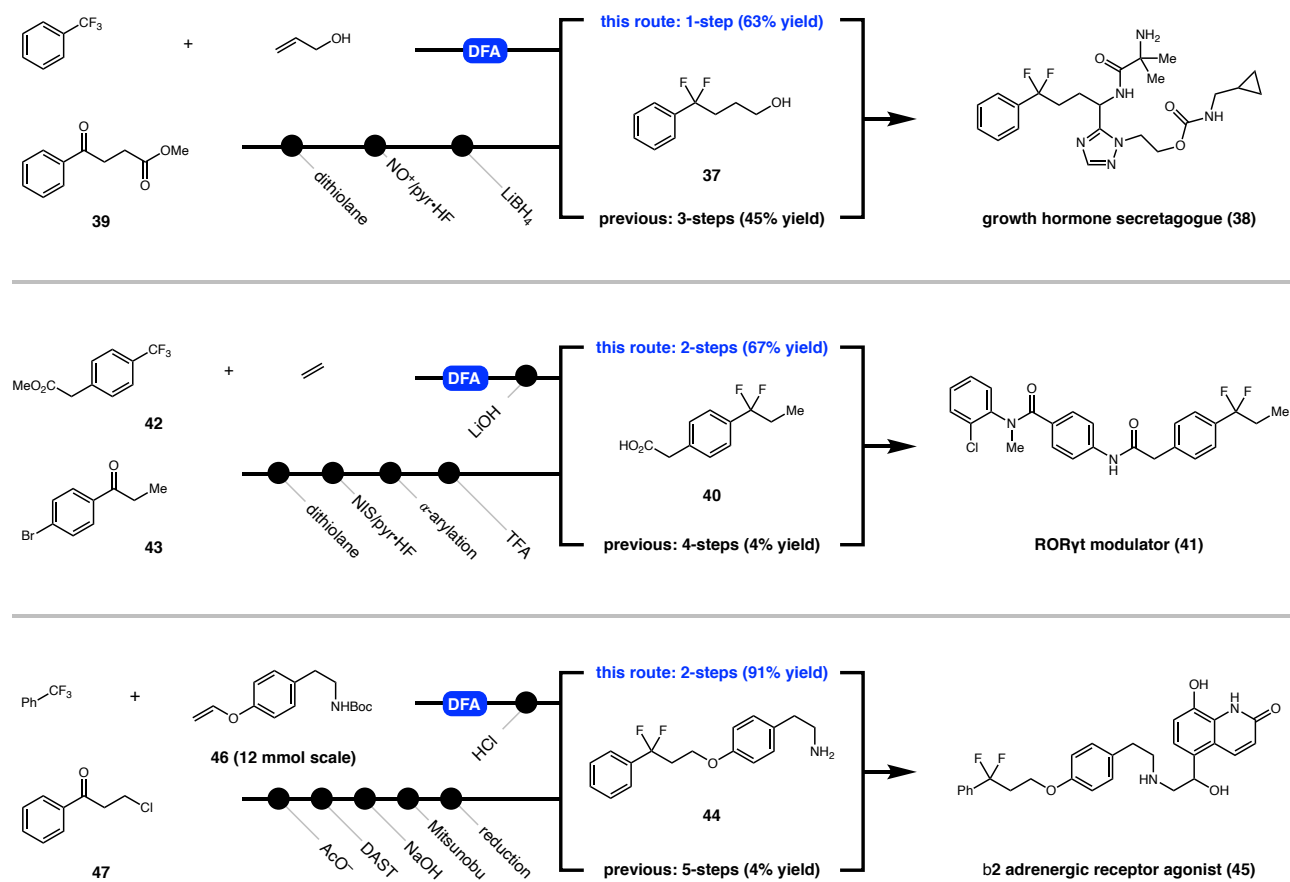
, four-, and five-carbon synthons that are produced on large scale from hydrocarbon cracking. Performing our reductive DFA method on Ph-CF₃ under 25 psi of ethylene provided the desired product (33) in 65% yield (based on formate as limiting reagent). This result was replicated with propylene (34, 68% yield), isobutylene (35, 87% yield), and 2- methyl-2-butene (36, 46% yield).

To further illustrate the value of this photocatalytic DFA in medicinal chemistry, we applied it in the formal syntheses of bioactive difluoroalkylaromatic molecules (as indicated in Scheme 2). The patent routes proceed through difluorobenzyl arene intermediates 37, 40, and 44, all of which were synthesized via deoxyfluorination of the corresponding carbonyl compounds. The reported preparation of growth hormone secretagogue 38 involves construction of a 1,3-dithiolane intermediate from 39 and 1,2-ethanedithiol. Subsequent desulfurative fluorination with nitrosonium cation and Olah's reagent delivered the geminal difluoride motif. Ester reduction provided primary alcohol 37 in 45% yield over three steps.¹²⁹ With this catalytic approach, reaction of Ph-CF₃ (50 equiv) with allyl alcohol provided the same intermediate in a single step (63% yield). The reported synthesis of 41, a Retinoid related orphan receptor gamma (ROR γ T) modulator, also involves a dithiolation/desulfurative fluorination sequence using ketone 43 as starting material. Palladium-catalyzed enolate coupling and carboxylic acid deprotection afforded 40 in 4% yield over four steps.¹³⁰ Under our conditions, commercial trifluoromethyl arene 42 reacted with ethylene gas (25 psi) to afford the same intermediate, after ester saponification, in

¹²⁹ Ewing, William R.; Li, Jun; Sulsky, Richard B.; Hernandez, A. S. Preparation of Azoles as Growth Hormone Secretagogues. US 20060079562, 2006

¹³⁰ Das, Sanjib; Gharat, Laxmikant Atmaram; Harde, Rajendra Laxman; Shelke, Dnyaneshwar Eknath; Pardeshi, Shailesh Ramesh; Thomas, Abraham; Khairatkar-Joshi, Neelima; Shah, Daisy Manish; Bajpai, M. Preparation of Carbocyclic Compounds as ROR Gamma Modulators. WO 2017037595, 2017

Scheme 4.2 Catalytic Defluoroalkylation in the Synthesis of Medicinal Building Blocks



63% overall yield. In the reported synthesis of amine 44, a precursor to β₂ adrenergic receptor agonist 45, DAST was employed for direct deoxyfluorination of benzylic ketone 47. Phenethylamine 44 was then delivered via sequential alcohol deprotection, Mitsunobu etherification, and reduction (4% yield over five steps).¹³¹ Our alternative route to this intermediate involves reacting trifluorotoluene (50 equiv) with vinyl ether 46 on 12 mmol scale (1 mol % P3) to give the corresponding defluoroalkylation product in 92% yield (4 g). Acidic cleavage of the tert-butyloxycarbonyl (Boc) group gave 44 in 91% over two steps. While deoxyfluorination remains an effective tool for difluoroalkylaromatic production, these examples illustrate the

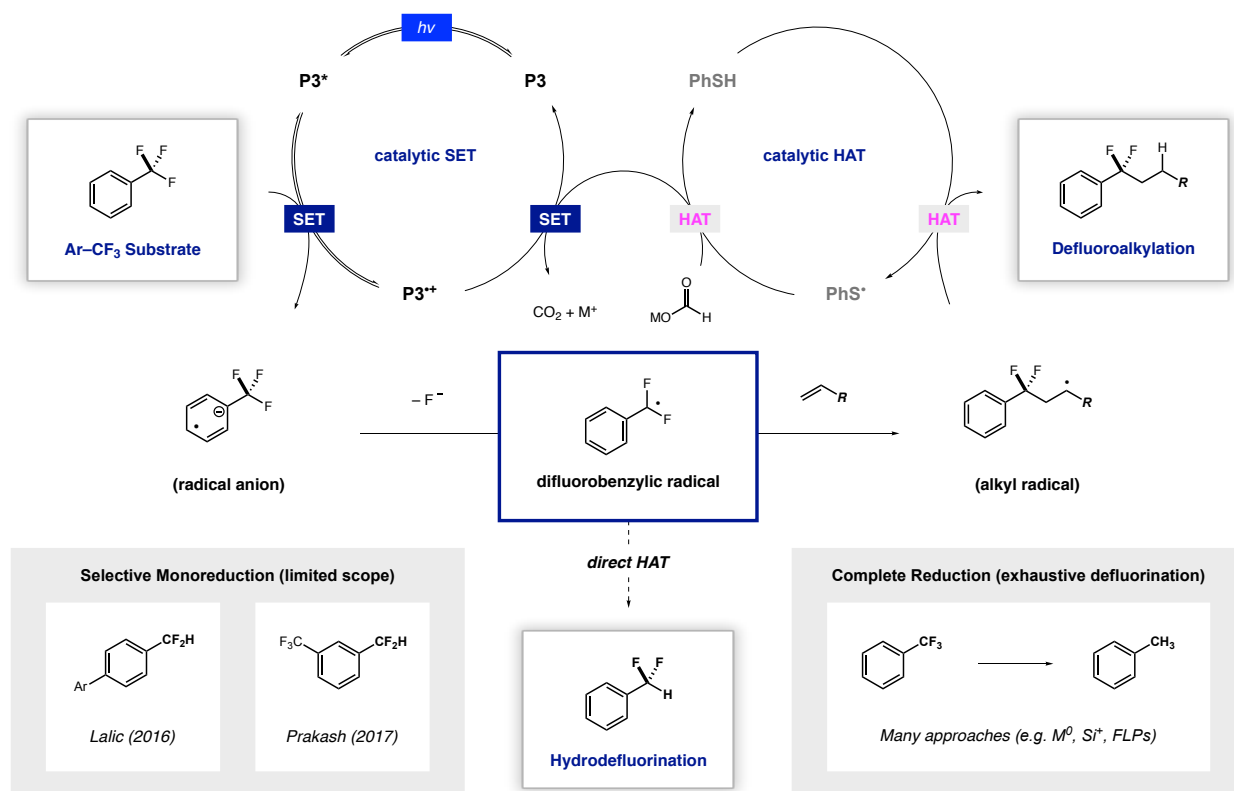
¹³¹ Bach Tana, Jordi; Crespo Crespo, Maria Isabel; Puig Duran, Carlos; Gual Roig, Silvia; Ortega Munoz, A. Derivatives of 4-(2-Amino-1-Hydroxyethyl)Phenol as Agonists of the B₂ Adrenergic Receptor. WO 2008046598, 2008

potential of this catalytic protocol to streamline the preparation of medicinally relevant Ar–CF₂R building blocks.

Scheme 3 shows our proposed mechanism for this transformation, where excitation of P3 with visible light (through irradiation with commercial blue light-emitting diodes (LEDs)) delivers the excited-state reductant P3*. Reversible single-electron transfer to the trifluoromethylarene substrate gives rise to the corresponding radical anion and the ground-state catalyst radical cation. Formation of the key difluorobenzyl radical intermediate is then accomplished via thermodynamically driven mesolytic C–F cleavage event. Regioselective intermolecular addition to the olefin substrate provides an alkyl radical adduct that undergoes polarity matched hydrogen atom transfer (HAT) with thiophenol to furnish the defluoroalkylation products. Regeneration of both the thiol and photoredox catalysts occurs with formate as stoichiometric reductant producing a metal fluoride salt and CO₂ as byproducts.

The findings that are described in this paper were enabled by the discovery that P3 has the ability to engage unactivated trifluoromethylaromatics. This is mechanistically interesting because, in comparison to our initial report in this area (using P1 and activated Ar–CF₃ substrates), this substrate set is more difficult to reduce, and the most effective catalyst (P3) is not as strongly reducing. Within this context, we propose that the reversible SET events that are operational here are endergonic in the forward direction. Consistent with this proposal are Stern–Volmer excited-state quenching studies, which revealed that quenching of P3* with benzotrifluoride occurs to a minute extent ($K_{sv} = 0.02$; none of the other reaction components quench the excited state). Although the concentration of radical anion intermediate is low under these conditions, fluoride expulsion provides a thermodynamic driving force for radical formation. Indeed, the calculated

Scheme 4.3 Catalytic or Direct HAT Mechanisms for Defluorofunctionalization of Trifluoromethyl Arenes



thermodynamic profile (details given in 4.4.6 Computational Details, pg. 282) indicates that C–F bond elongation from benzotrifluoride radical anion is essentially barrierless (<3 kcal/mol). Taken together, these results indicate that, although substrate reduction is a critical step within this pathway, mesolytic cleavage acts as the primary determinant in radical formation.

We questioned whether the radical intermediates that are accessible under this paradigm could be generally utilized in the formation of other bonds. Of particular interest to us was the idea that interception of this species with a hydrogen atom would grant access to the corresponding difluoromethyl arene (Ar–CF₂H). Selective HDF of trifluoromethylaromatics in this manner would offer a novel approach to this high-value motif.

Summarized in Scheme 4.3 are existing strategies for trifluoromethylaromatic HDF. In 2016, Lalic reported a system that utilizes catalytic amounts of both palladium and copper in

conjunction with triphenylsilane and potassium tert-butoxide to defluorinate a series of 4-trifluoromethyl biaryl compounds, generating presumed nucleophilic addition products to dimethylformamide (DMF).¹²² Reaction of these intermediates with tert-butanol resulted in selective production of the corresponding difluoromethylaromatics. Prakash described that Mg^0 can be utilized in HDF processes of various bis(trifluoromethyl)benzene derivatives with varying selectivity for the corresponding reduction products.^{118a} While appealing for its operational simplicity, this protocol is limited to bis(trifluoromethyl)benzene substrates, as benzotrifluoride was reported to be unreactive, and more electron-poor systems underwent exhaustive defluorination (complete reduction of trifluoromethylaromatics to the corresponding toluene derivatives). Exhaustive defluorination is the major outcome within the trifluoromethylaromatic HDF literature, where electrochemical reduction,^{117b} alkali metal reduction,¹¹⁸ or Lewis acids¹¹⁹ have been reported to activate these strong C–F bonds.

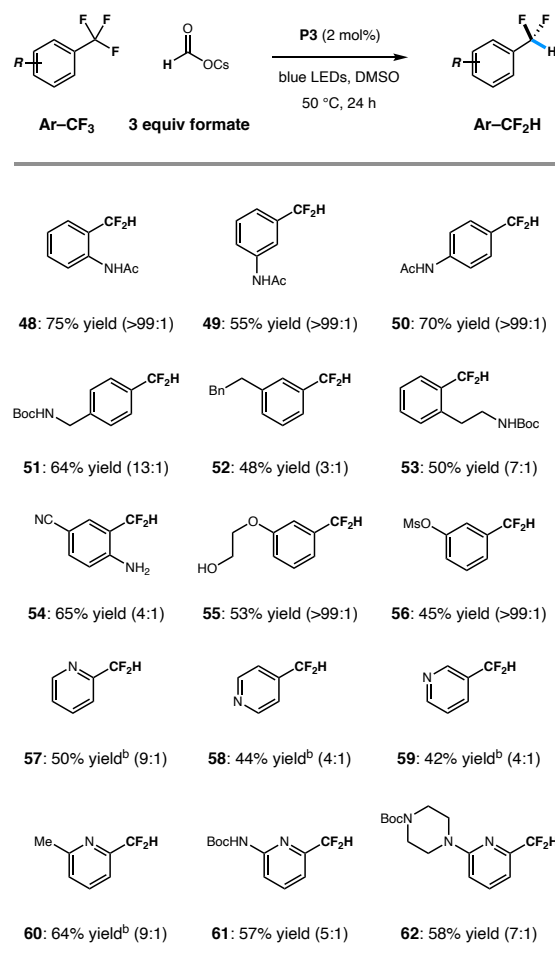
To evaluate the feasibility of the proposed HDF pathway, we reacted 2-trifluoromethylacetanilide with P3 and a range of reductants in dimethyl sulfoxide (DMSO) under irradiation with blue LEDs. These studies (optimization details are given in 4.4.3 Optimization Details, pg. 217) revealed that formate reductants are uniquely effective for HDF and that there is a pronounced effect of the formate counterion on reactivity. The optimized conditions (indicated in Table 4.3) again involve the use of P3 (2 mol %) along with cesium formate (3 equiv) at 50 °C,

which delivered the desired difluoromethylaromatic 48 in 75% isolated yield without detectable overreduction products. Similarly, the isomeric trifluoromethyl-bearing acetanilides were good substrates for this transformation, affording the corresponding products 49 and 50 in 55–70% yield. Additionally, the outlined conditions efficiently engaged compounds bearing only alkyl substituents in the para- (51, 64% yield), meta- (52, 48% yield), and ortho- (53, 50% yield), a significant advance over previously reported technologies. Other oxygen- or nitrogen-substituted substrates could be reductively defluorinated with high selectivity for the Ar–CF₂H products (54–56, 45–65% yield).

Hydrodefluorination of 2-, 3-, and 4-trifluoromethyl substituted pyridines 57–59 was

also successful under this protocol, giving the desired products in acceptable (42–50%) yield. Much like we observed under DFA conditions, yields of pyridine-based substrates were bolstered by substitution of electron-donating groups at the 2-position (60–62, 57–64% yield). Although this substrate set underwent HDF in moderate yield, these results demonstrate that significant structural diversity is tolerated by this protocol including acidic protons, heterocycles, and other reducible groups.

Table 4.3 Substrate Scope for Hydrodefluorination^a



^aReaction conditions: Ar–CF₃ substrate (0.5 mmol), cesium formate (1.5 mmol), Miyake phenoxazine P3 (2 mol %), DMSO (5.0 mL), blue light, 50 °C, 24 h; isolated yields given; parentheses indicate the ratios of Ar–CF₂H to Ar–CFH₂ products, as determined by NMR analysis of the crude reaction mixtures. ^bReaction run at 23 °C ^cYield determined by ¹⁹F NMR with an internal standard.

4.3 Conclusions

In summary, we have developed a robust method for the defluoroalkylation and hydrodefluorination of unactivated trifluorotoluene derivatives using the combination of two organocatalysts (no metal is required), inexpensive formate salts, and visible light. The use of Miyake's phenoxazine, P3, was key in the development and generality of these methods. The reductive radical process, driven by the selective cleavage of a single benzylic C–F bond, can be employed to access a diverse range of Ar–CF₂R and Ar–CF₂H substrates. Mechanistic studies and the development of additional applications of difluorobenzylic radicals are underway in our laboratory.

4.4 Supporting Information

4.4.1 General Information

General Reagent Information

All reactions were set up on the bench top and conducted under nitrogen atmosphere while subject to irradiation from blue LEDs (LEDwholesalers PAR38 Indoor Outdoor 16-Watt LED Flood Light Bulb, Blue; or Hydrofarm® PPB1002 PowerPAR LED Bulb-Blue 15W/E27 (available from Amazon). Flash chromatography was carried out using Siliaflash® P60 silica gel obtained from Silicycle. Preparative HPLC was carried out using an Agilent Technologies 1260 Infinity HPLC with a 21.2 x 250 mm, 7µm pore size, ZORBAX Eclipse XDB-C18 Column. Eluents used were unmodified unless otherwise stated. Photoredox catalyst P1 and P3 were all prepared according to literature procedures.^{30e,125} Metal formates were purchased from Sigma-Aldrich chemicals co. Trifluoromethyl arenes were purchased from Alfa Aesar, Acros Organics, Combi-Blocks, Oakwood Chemicals, Astatech, and Toronto Research Chemicals, and were used as received. Non-commercial trifluoromethyl arenes were prepared according to the designated procedures in 4.4.4 Preparation of Trifluoromethylarenes (pg. 219).

General Analytical Information

Unless otherwise noted, all yields refer to isolated yields. New compounds were characterized by NMR, IR spectroscopy, and high-resolution mass spectrometry (HRMS). NMR data were recorded on one of six spectrometers: Bruker 600 MHz, INOVA 600 MHz, INOVA 500 MHz, VNMR 400 MHz, INOVA 400 MHz, or Mercury 300 MHz. Chemical shifts (δ) are internally referenced to residual protio solvent (CDCl_3 : δ 7.26 ppm for ^1H NMR and 77.2 ppm for ^{13}C NMR; CD_3OD : δ 3.31 ppm for ^1H NMR and 49.1 ppm for ^{13}C NMR; THF-d_8 : δ 3.58 ppm for ^1H NMR and 67.6 ppm for ^{13}C NMR; $(\text{CD}_3)_2\text{CO}$: δ 2.05 ppm for ^1H NMR and 29.84 ppm for ^{13}C NMR; C_6D_6 : δ 7.16

ppm for ^1H NMR and 128.06 ppm for ^{13}C NMR). IR spectra were obtained with a Thermo Scientific Nicolet iS10 Fourier transform infrared spectrophotometer. Mass spectrometry data were obtained from the Emory Mass Spectrometry Center using a Thermo LTQ-FTMS high-resolution mass spectrometer.

4.4.2 General Procedures

General Procedure A: Defluoroalkylation with excess alkene

An oven-dried screw-top test tube equipped with a stir bar was sealed with a PTFE/silicon septa and cooled to room temperature under N_2 atmosphere. The tube was charged with photocatalyst **P3** (2 mol%), potassium formate (3 or 5 equiv, as indicated), and trifluoromethyl arene (if solid, 1 equiv). The atmosphere was exchanged by applying vacuum and backfilling with N_2 (this process was conducted a total of three times). Under N_2 atmosphere, the tube was charged with 3-buten-1-ol (5 equiv or 10 equiv for drug molecules), trifluoromethyl arene (if liquid, 1 equiv), thiophenol (10 mol%), and separately degassed, freshly distilled dimethylsulfoxide (0.1 M) via syringe. The nitrogen line was removed, and the resulting mixture was stirred at 1200 RPM for 24 hours under irradiation with a blue LED either in a shallow oil bath heated to 100 °C, or maintained at 23 °C with air cooling (as indicated). The crude reaction mixture was quenched with saturated sodium bicarbonate and extracted with EtOAc (3 x 100 mL). The extracts were combined, washed with brine (3 x 50 mL), dried over sodium sulfate, filtered, and concentrated under reduced pressure. The residue was purified by flash column chromatography using the indicated solvent mixture to afford the title compound.

General Procedure B: Defluoroalkylation with excess benzotrifluoride

An oven-dried screw-top test tube equipped with a stir bar was sealed with a PTFE/silicon septa and cooled to room temperature under N_2 atmosphere. The tube was charged with photocatalyst

P3 (2 mol%), potassium formate (5 equiv), and alkene (if solid, 1 equiv). The atmosphere was exchanged by applying vacuum and backfilling with N₂ (this process was conducted a total of three times). Under N₂ atmosphere, the tube was charged with alkene (if liquid, 1 equiv), thiophenol (10 mol%), and separately degassed, freshly distilled dimethylsulfoxide (5 mL), and benzotrifluoride (3 mL) via syringe. The nitrogen line was removed, and the resulting mixture was stirred at 1200 RPM for 24 hours under irradiation with a blue LED in a shallow oil bath heated to 100 °C. The crude reaction mixture was quenched with saturated sodium bicarbonate and extracted with EtOAc (3 x 100 mL). The extracts were combined, washed with brine (3 x 50 mL), dried over sodium sulfate, filtered, and concentrated under reduced pressure. The residue was purified by flash column chromatography using the indicated solvent mixture to afford the title compound.

General Procedure C: Defluoroalkylation with gaseous alkenes

A pressure rated Schleck reaction tube with a side arm was equipped with a stir bar, connected to high vacuum, flame dried, and cooled to room temperature under N₂ atmosphere. The tube was charged with photocatalyst **P3** (2 mol%) and potassium formate (5 equiv). The atmosphere was exchanged by applying vacuum and backfilling with N₂ (this process was conducted a total of three times). Under N₂ atmosphere, the tube was charged with thiophenol (10 mol%), and separately degassed, freshly distilled dimethylsulfoxide (10 mL), and benzotrifluoride (6 mL) via syringe. The nitrogen line was removed, and the resulting mixture was attached to a pressure manifold and the atmosphere was exchanged by applying mild vacuum and backfilling with the gaseous alkene (regulated at 25 psi). This process was conducted a total of 5 times. The reaction was stirred at 1200 RPM for 24 hours under irradiation with a blue LED in an oil bath heated to 100 °C. The 25 psi atmosphere of alkene was regulated for the entire duration of the reaction. The crude reaction mixture was quenched with saturated sodium bicarbonate and extracted with

pentane (3 x 50 mL). The extracts were combined, washed with brine (3 x 100 mL), dried over sodium sulfate, filtered, and concentrated under reduced pressure. The residue was purified by flash column chromatography using the indicated solvent mixture to afford the title compound.

General Procedure D: Hydrodefluorination

To a screw top test tube equipped with a stir bar was added **P3** (0.02 equiv), trifluoromethylarene (1 equiv, if solid) and cesium formate (3 equiv). The tube was sealed with a cap and PTFE/silicon septum. The sealed tube was connected to a Schlenk line via a needle, and the atmosphere was exchanged by applying vacuum and backfilling with dry N₂ (this process was conducted five times total). Under N₂ atmosphere, the tube was charged with trifluoromethylarene (1 equiv, if liquid). DMSO (10 mL/mmol, as prepared above) was added by syringe. The nitrogen line was removed, the resulting mixture was stirred at 1200 RPM for 24 hours under irradiation with a blue LED in a shallow oil bath heated to 100 °C or maintained at 23 °C with air cooling (as indicated). The reaction mixture was diluted with brine and extracted three times with ethyl acetate. The combined organic layers were dried with sodium sulfate, filtered and concentrated by rotary evaporation. The crude residue was purified by flash chromatography or preparative HPLC (under the indicated conditions) to afford the title compounds.

4.4.3 Optimization Details

Defluoroalkylation Optimization: Reaction setup

An oven-dried screw-top test tube equipped with a stir bar was sealed with a PTFE/silicon septa and cooled to room temperature under N₂ atmosphere. The tube was charged with photocatalyst (10 mol% for **P1**, 2 mol% for **P2–P8**.) and formate salt (0.75 mmol, 3 equiv). The atmosphere was exchanged by applying vacuum and backfilling with N₂ (this process was conducted a total of

three times). The tube was charged with 3-buten-1-ol (107 μL , 1.25 mmol, 5 equiv), trifluorotoluene (31 μL , 0.25 mmol, 1 equiv), thiophenol (2.5 μL , 10 mol%), and separately degassed, freshly distilled dimethylsulfoxide (2.5 mL, 0.1 M) via syringe. The resulting mixture was stirred at 1200 RPM for 24 hours under irradiation with a blue LED in a shallow oil bath heated to 100 $^{\circ}\text{C}$. The crude reaction mixture diluted with EtOAc (5 mL) before the addition of fluorobenzene as an internal standard (94 μL). Analysis by ^{19}F NMR provided the yield of the defluoroalkylated product **1**.

Figure 4.3 Optimization of the defluoroalkylation conditions

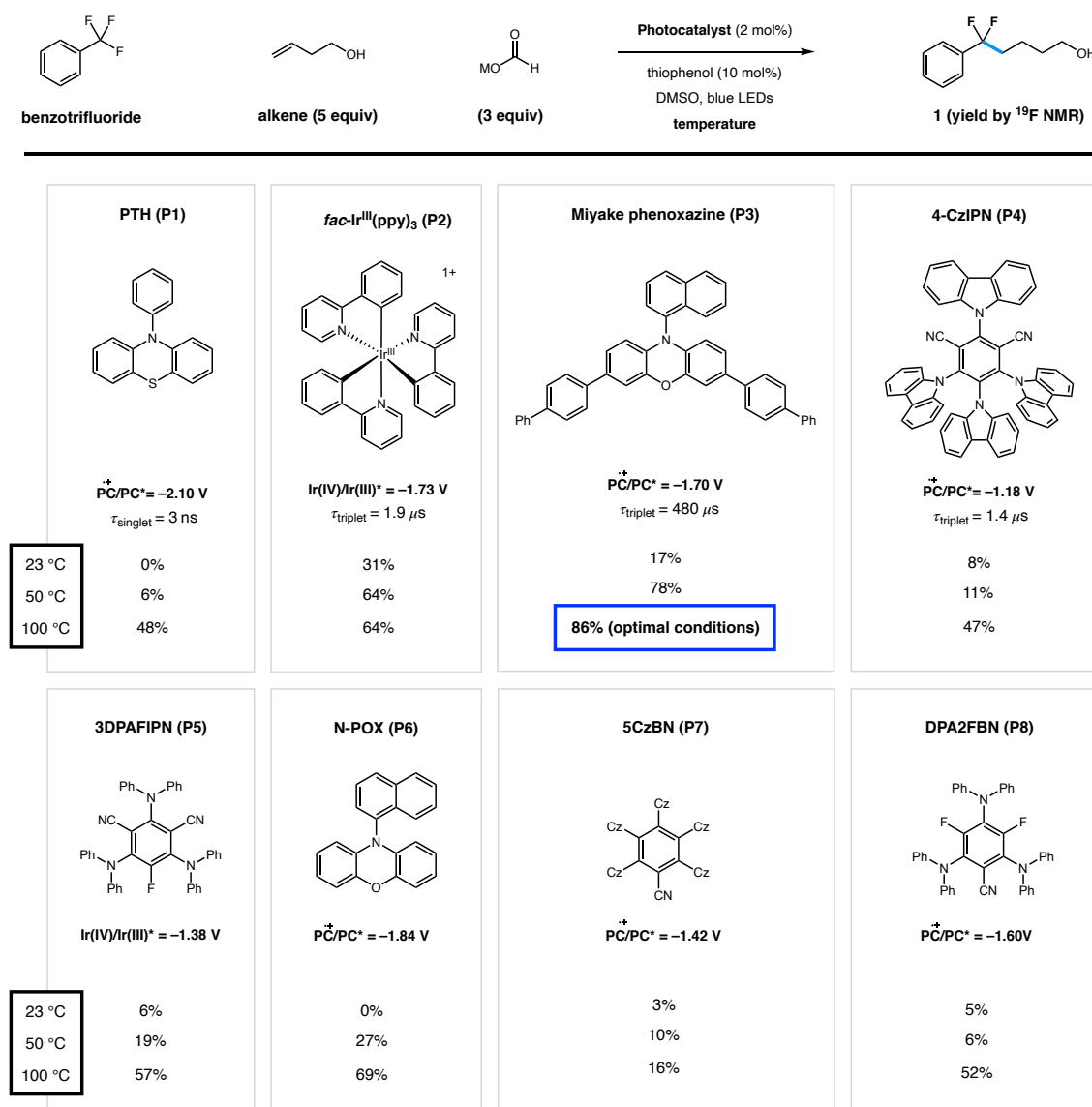


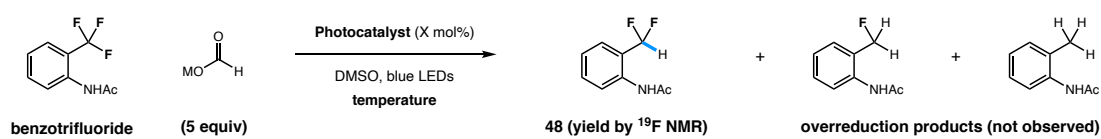
Figure 4.4 Deviation from the optimal conditions for defluoroalkylation


deviation from optimal conditions	% yield	control experiments	% yield	catalyst loading (P3)	% yield
NaCHO ₂	62	no catalyst	0	2 mol%	89
CsCHO ₂	42	no light	0	0.2 mol%	61
under air	67	no formate	0	0.02 mol%	45
any other solvent	0	no HAT catalyst	21	0.002 mol%	26
different solvents	% yield	different solvents cont.	% yield	Summary	
DMF	12	EtOAc	0	DMSO uniquely effective solvent light, catalysts, formate required	
DMA	21	DCE	0		
MeCN	0	Toluene	0		
Dioxane	0	tBuOH	0		

Hydrodefluorination Optimization: Reaction Setup

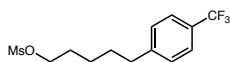
Initial optimization studies were performed on N-(2-(trifluoromethyl)phenyl)acetamide. In the table below the remaining mass balance was uniformly unreacted starting material.

An oven-dried screw-top test tube equipped with a stir bar was sealed with a PTFE/silicon septa and cooled to room temperature under N₂ atmosphere. The tube was charged with photocatalyst (10 mol% for P1; 1 mol% for P2, 2 mol% for P3), formate salt (0.75 mmol, 5 equiv), and N-(2-(trifluoromethyl)phenyl)acetamide (51 mg, 0.25 mmol, 1 equiv). The atmosphere was exchanged by applying vacuum and backfilling with N₂ (this process was conducted a total of three times). The tube was charged with separately degassed, freshly distilled dimethylsulfoxide (2.5 mL, 0.1 M) via syringe. The resulting mixture was stirred at 1200 RPM for 24 hours under irradiation with a blue LED at the indicated temperatures. Product yields were obtained via ¹⁹F NMR of the crude reaction mixture with a Mercury 300 MHz NMR using 1,1,1,3,3,3-hexafluoro-2-propanol (4 equiv) as an internal standard, with relaxation delay set to 10 seconds.

Table 4.4 Optimization with N-(2-(trifluoromethyl)phenyl)acetamide

Entry	formate	Photocatalyst	Temperature	Solvent	% yield (48)
1	NaCO ₂ H	P1 (10 mol%)	23 °C	DMSO	1%
2	NaCO ₂ H	P2 (1 mol%)	23 °C	DMSO	0%
3	NaCO ₂ H	P3 (10 mol%)	23 °C	DMSO	20%
4	NaCO ₂ H	P3 (2 mol%)	23 °C	DMSO	18%
5	LiCO ₂ H	P3 (2 mol%)	23 °C	DMSO	15%
6	KCO ₂ H	P3 (2 mol%)	23 °C	DMSO	46%
7	CsCO ₂ H	P3 (2 mol%)	23 °C	DMSO	57%
8	CsCO ₂ H	P3 (2 mol%)	50 °C	DMSO	83%
9	CsCO ₂ H	P3 (2 mol%)	50 °C	DMF	10%
10	CsCO ₂ H	P3 (2 mol%)	50 °C	NMP	2%
11	CsCO ₂ H	P3 (2 mol%)	50 °C	THF	0%
P1 = PTH		P2 = <i>fac</i> -Ir ^{III} (ppy) ₃		P3 = Miyake phenoxazine	

4.4.4 Preparation of Trifluoromethylarenes



5-(4-(Trifluoromethyl)phenyl)pentyl methanesulfonate (S1)

To an oven dried 250 mL round bottomed flask charged with 5-(4-(trifluoromethyl)phenyl)pentan-1-ol¹³² (4.4 g, 19 mmol, 1 equiv) was added CH₂Cl₂ (50 mL) and Et₃N (5 mL, 38 mmol, 2 equiv) before being cooled to 0 °C. To the cooled reaction mixture was added methanesulfonyl chloride (2 mL, 25 mmol, 1.3 equiv) dropwise. The reaction mixture was slowly brought to room temperature and stirred for 30 minutes before being quenched through the addition of 1 M HCl (50 mL). The organics were separated and washed with 1 M HCl (2 x 50 mL) and brine (50 mL) before being dried over Na₂SO₄ and concentrated under reduced pressure. The crude oil was dissolved in CH₂Cl₂ (50 mL) and passed rapidly through a short pad of silica. The eluted product was concentrated to provide the desired product as a clear oil (5.9 g, 99%). This material was carried directly into the following step.

Rf: 0.75 (50% ethyl acetate/hexanes)

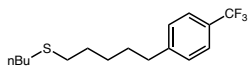
¹H NMR (500 MHz, Chloroform-*d*) δ 7.52 (d, *J* = 7.9 Hz, 2H), 7.27 (d, *J* = 8.5 Hz, 2H), 4.21 (t, *J* = 6.5 Hz, 2H), 2.97 (s, 3H), 2.71 – 2.64 (m, 2H), 1.81 – 1.73 (m, 2H), 1.71 – 1.62 (m, 2H), 1.49 – 1.41 (m, 2H).

¹³C NMR (126 MHz, Chloroform-*d*) δ 146.4, 128.7, 128.2 (q, *J* = 32.1 Hz), 125.3 (q, *J* = 3.8 Hz), 124.5 (q, *J* = 271.7 Hz), 70.0, 37.3, 35.5, 30.5, 29.0, 25.0.

¹⁹F NMR (376 MHz, Chloroform-*d*) δ -62.25.

¹³² For synthesis see: (a) Nagendiran, A.; Verho, O.; Haller, C.; Johnston, E. V; Bäckvall, J.-E. Cycloisomerization of Acetylenic Acids to γ -Alkylidene Lactones Using a Palladium(II) Catalyst Supported on Amino-Functionalized Siliceous Mesocellular Foam. *J. Org. Chem.* **2014**, *79* (3), 1399–1405; (b) Evindar, Ghotas; Deng, Hongfeng; Bernier, Sylvie; Yao, Gang; Coffin, Aaron; Yang, H. Aminoalcohols and Related Derivatives as Selective Agonists for S1P-1, Their Preparation, Pharmaceutical Compositions, and Their Use as Immunosuppressants. WO2008016692, 2008

FTIR (neat) ν_{\max} : 2941, 2863, 1617, 1417, 1352, 1321, 1161, 1112, 1065, 1018, 971, 941, 906, 818, 733, 631, 613, and 595 cm^{-1} .



Butyl(5-(4-(trifluoromethyl)phenyl)pentyl)sulfane:

A 250 mL round bottomed flask charged with butane thiol (2.6 mL, 25 mmol, 1.3 equiv) in THF (50 mL) was cooled to 0 °C before the portion wise addition of NaH (60% in mineral oil) (1.2 g, 25 mmol, 1.3 equiv). The resulting solution warmed to room temperature over 30 minutes before being added dropwise to a solution of 5-(4-(Trifluoromethyl)phenyl)pentyl methanesulfonate (5.9 g, 19 mmol, 1 equiv) in THF (20 mL) at 0 °C. The reaction mixture was slowly warmed to room temperature and stirred for 14 h. The reaction mixture was quenched with H₂O (50 mL), diluted with EtOAc (100 mL) and washed with 1 M NaOH (50 mL x 2) and brine (50 mL) before being dried over Na₂SO₄ and concentrated under reduced pressure. The resulting oil was purified by flash column chromatography (silica gel, 0 – 15% EtOAc/hexanes) to provide the desired product as a colorless oil (3 g, 51%).

R_f: 0.32 (30% ethyl acetate/hexanes)

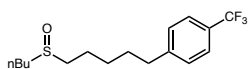
¹H NMR (500 MHz, CDCl₃) δ 7.52 (d, J = 7.6 Hz, 2H), 7.27 (d, J = 7.4 Hz, 2H), 2.76 – 2.62 (m, 2H), 2.50 (td, J = 7.4, 1.4 Hz, 4H), 1.70 – 1.51 (m, 6H), 1.48 – 1.36 (m, 4H), 0.91 (t, J = 7.4 Hz, 3H).

¹³C NMR (126 MHz, CDCl₃) δ 146.8 (q, J_{C-F} = 1.4 Hz), 128.8, 128.1 (q, $^2J_{C-F}$ = 32.2 Hz), 124.5 (d, $^1J_{C-F}$ = 271.6 Hz), 125.3 (q, $^3J_{C-F}$ = 3.8 Hz), 35.7, 32.1, 32.0, 31.9, 30.9, 29.6, 28.5, 22.1, 13.8.

¹⁹F NMR (376 MHz, CDCl₃) δ -60.15 – -68.20 (m).

FTIR (neat) ν_{\max} : 2930, 2858, 1464, 1323, 1161, 1120 cm^{-1} .

HRMS (APCI) m/z : $[M+H]^+$ calcd. for $C_{16}H_{24}F_3S$, 305.1545; found, 305.1545.



1-(5-(Butylsulfinyl)pentyl)-4-(trifluoromethyl)benzene:

To a 20 mL reaction vial charged with Butyl(5-(4-(trifluoromethyl)phenyl)pentyl)sulfane (152 mg, 0.5 mmol, 1 equiv) was added CH_2Cl_2 (1 mL). The reaction mixture was cooled to 0 °C before the addition of *meta*-chloroperoxybenzoic acid (86 mg, 0.5 mmol, 1 equiv). The reaction was slowly brought to room temperature and stirred for 4 h. Upon completion, the reaction was diluted with CH_2Cl_2 (5 mL) and quenched with H_2O (5 mL), the organics were separated and washed with brine (5 mL), dried over Na_2SO_4 and concentrated under reduced pressure. The crude residue was purified by flash column chromatography (silica gel, 10 – 60% EtOAc/hexanes) to provide the desired product as an amorphous white solid (100 mg, 63%).

R_f: 0.20 (30% ethyl acetate/hexanes)

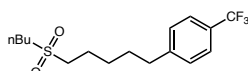
¹H NMR (500 MHz, $CDCl_3$) δ 7.52 (d, $J = 8.3$ Hz, 2H), 7.27 (d, $J = 7.3$ Hz, 2H), 2.76 – 2.51 (m, 6H), 1.92 – 1.61 (m, 6H), 1.59 – 1.35 (m, 4H), 0.96 (t, $J = 7.4$ Hz, 3H).

¹³C NMR (126 MHz, $CDCl_3$) δ 146.4, 128.8, 128.3 (q, $^3J_{C-F} = 32.2$ Hz), 125.4 (q, $^3J_{C-F} = 3.8$ Hz), 124.5 (q, $^3J_{C-F} = 271.8$ Hz), 52.4, 52.3, 35.6, 30.9, 28.5, 24.7, 22.6, 22.2, 13.8.

¹⁹F NMR (376 MHz, $CDCl_3$) δ -62.33.

FTIR (neat) ν_{max} : 2925, 2859, 1467, 1330, 1155, 1118, 1015 cm^{-1} .

HRMS (APCI) m/z : $[M-H]^-$ calcd. for $C_{16}H_{24}F_3SO$, 321.1495; found, 321.1494.



1-(5-(Butylsulfonyl)pentyl)-4-(trifluoromethyl)benzene:

To a 20 mL reaction vial charged with 1-(5-(Butylsulfinyl)pentyl)-4-(trifluoromethyl)benzene (600 mg, 2 mmol, 1 equiv) was added CH₂Cl₂ (5 mL). The reaction mixture was cooled to 0 °C before the addition of *meta*-chloroperoxybenzoic acid (1 g, 6 mmol, 3 equiv). The reaction was slowly brought to room temperature and stirred for 4 h. Upon completion, the reaction was quenched with H₂O (5 mL), the organics were separated and washed with brine (5 mL), dried over Na₂SO₄ and concentrated under reduced pressure. The crude residue was purified by flash column chromatography (silica gel, 10 – 30% EtOAc/hexanes) to provide the desired product as an amorphous white solid (510 mg, 76%).

R_f: 0.51 (60% ethyl acetate/hexanes)

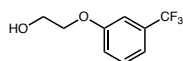
¹H NMR (600 MHz, CDCl₃) δ 7.50 (d, *J* = 7.8 Hz, 2H), 7.24 (d, *J* = 7.8 Hz, 2H), 2.91 (ddd, *J* = 9.9, 6.6, 2.0 Hz, 4H), 2.66 (t, *J* = 7.6 Hz, 2H), 1.96 – 1.74 (m, 4H), 1.71 – 1.59 (m, 2H), 1.50 – 1.40 (m, 4H), 0.93 (t, *J* = 7.3 Hz, 3H).

¹³C NMR (100 MHz, CDCl₃) δ 146.2, 128.7, 128.2 (d, ²*J*_{C-F} = 32.3 Hz), 125.3 (q, ³*J*_{C-F} = 3.8 Hz), 124.4 (q, ¹*J*_{C-F} = 271.7 Hz), 52.6, 52.5, 35.4, 30.6, 28.0, 24.0, 21.8, 21.7, 13.6.

¹⁹F NMR (376 MHz, CDCl₃) δ -62.29.

FTIR (neat) *v*_{max}: 2943, 1417, 1258, 1116, 1067 cm⁻¹.

HRMS (APCI) *m/z*: [M-H]⁻ calcd. for C₁₆H₂₂F₃SO₂, 335.1298; found, 335.1294.



2-(3-(Trifluoromethyl)phenoxy)ethan-1-ol:

To a round bottom flask charged with a stir bar was added 3-(trifluoromethyl)phenol (1.20 mL, 9.9 mmol, 1 equiv), 2-bromoethan-1-ol (1.05 mL, 14.8 mmol, 1.5 equiv), K₂CO₃ (2.22 g, 14.8 mmol, 1.5 equiv), and DMF (20 mL). The reaction was heated to 120 °C and stirred for 12 hours.

Once complete, the reaction was cooled to room temperature, diluted with 2 N aq. NaOH, then extracted 3 times with EtOAc. The combined organic extracts were washed 3 times with sat. aq. NaHCO₃ then dried over Na₂SO₄, filtered, and concentrated by rotary evaporation. The product was isolated as a colorless liquid (1.19 g, 58% yield) by column chromatography on silica using 30% – 40% EtOAc/hexanes.

R_f: 0.64 (30% ethyl acetate/hexanes)

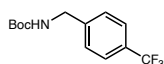
¹H NMR (600 MHz, Chloroform-*d*) δ 7.41 – 7.34 (m, 1H), 7.21 (s, 1H), 7.14 (s, 1H), 7.07 (s, 1H), 4.16 – 4.05 (m, 2H), 3.97 (s, 2H).

¹³C NMR (151 MHz, Chloroform-*d*) δ 158.9, 132.0 (q, *J* = 32.3 Hz), 130.2, 124.0 (q, *J* = 272.1 Hz), 118.1, 117.9, 111.5 (q, *J* = 3.4 Hz), 69.6, 61.3.

¹⁹F NMR (282 MHz, Chloroform-*d*) δ -62.76.

FTIR (neat) ν_{max} : 3352, 2938, 2878, 1591, 1492, 1448, 1326, 1240, 1118, 1064, 937, 885, 858, 784, 746, 696, 657, and 610

HRMS (ESI) *m/z*: [M+Cl]⁻ calcd. for C₉H₉O₂ClF₃, 241.0249; found, 241.0243.



***tert*-Butyl (4-(trifluoromethyl)benzyl)carbamate:**

To a round bottom flask charged with a stir bar was added (4-(trifluoromethyl)phenyl)methanamine (1 g, 5.7 mmol, 1 equiv), DMAP (69 mg, 0.57 mmol, 0.1 equiv), and MeCN (100 mL). The reaction was cooled to 0 °C in an ice bath then di-*tert*-butyl dicarbonate (1.37 g, 6.3 mmol, 1.1 equiv) was added. The reaction was stirred at 0 °C for a total of 30 minutes then warmed to room temperature and stirred for 18 hours. Once complete, the reaction mixture was concentrated by rotary evaporation, diluted with EtOAc. The reaction

mixture was washed once with saturated aqueous NH_4Cl then washed twice with brine. The combined organics were dried over Na_2SO_4 , filtered, and concentrated by rotary evaporation. The product was isolated as a white amorphous solid (1.42 g, 91%) by column chromatography on silica using 5% – 30% EtOAc/hexanes.

R_f: 0.63 (30% ethyl acetate/hexanes)

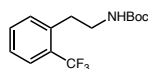
¹H NMR (600 MHz, Chloroform-*d*) δ 7.56 (d, $J = 7.9$ Hz, 2H), 7.38 (d, $J = 7.8$ Hz, 2H), 5.07 (s, 1H), 4.35 (s, 2H), 1.45 (s, 9H).

¹³C NMR (151 MHz, Chloroform-*d*) δ 156.1, 143.3, 129.6 (q, $J = 32.4$ Hz), 127.6, 125.6 (q, $J = 3.6$ Hz), 124.3 (q, $J = 271.9$ Hz), 79.9, 44.3, 28.5.

¹⁹F NMR (282 MHz, Chloroform-*d*) δ -62.81.

FTIR (neat) ν_{max} : 3347, 3304, 2984, 2932, 1716, 1674, 1542, 1368, 1298, 1153, 1110, 1066, 1019, 934, 854, 819, 693, 633, and 592.

HRMS (ESI) m/z : $[\text{M}-\text{H}]^-$ calcd. for $\text{C}_{13}\text{H}_{15}\text{O}_2\text{NF}_3$, 274.1060; found, 274.1059.



***tert*-Butyl (2-(trifluoromethyl)phenethyl)carbamate:**

An oven-dried 30 mL screw-top test tube equipped with a stir bar was sealed with a PTFE/silicon septa and cooled to room temperature under Ar atmosphere. The tube was charged with **P1** (21.0 mg, 0.075 mmol, 5 mol%), sodium formate (0.306 g, 4.5 mmol 3 equiv), *t*-butylvinyl carbamate (0.536 g, 3.75 mmol, 2.5 equiv). The atmosphere was exchanged by applying vacuum and backfilling with Ar (this process was conducted a total of three times). Under Ar atmosphere, the tube was charged with 2-bromobenzotrifluoride (0.204 mL, 1.5 mmol, 1 equiv) and cyclohexanethiol (9 μL , 0.075 mmol, 5 mol%) and separately degassed 20:1 DMSO:H₂O (15 mL,

0.1 M) via syringe. The resulting mixture was stirred at 1200 RPM for 18 hours under irradiation with a blue LED with cooling from house air. The reaction was quenched with sat. aq. sodium bicarbonate solution (30 mL) and extracted with ethyl acetate (3 x 30 mL). The organic extracts were combined, dried over magnesium sulfate, filtered, and concentrated by rotary evaporation. The crude residue was purified by flash column chromatography (silica gel, 2 – 30% EtOAc:hexanes) to afford the title compound as an amorphous white solid (0.235 g, 81% yield).

R_f: 0.64 (30% ethyl acetate/hexanes)

¹H NMR (600 MHz, Chloroform-*d*) δ 7.63 (d, J = 7.8 Hz, 1H), 7.48 (t, J = 7.5 Hz, 1H), 7.37 (d, J = 6.9 Hz, 1H), 7.31 (t, J = 7.6 Hz, 1H), 4.65 (s, 1H), 3.44 – 3.31 (m, 2H), 2.98 (t, J = 6.6 Hz, 2H), 1.43 (s, 9H).

¹³C NMR (151 MHz, Chloroform-*d*) δ 156.0, 137.8, 132.0, 131.7, 129.0 (q, J = 29.7 Hz), 126.6, 126.2, 124.7 (q, J = 274.0 Hz), 79.4, 41.8, 33.2, 28.5.

¹⁹F NMR (282 MHz, Chloroform-*d*) δ -59.48.

FTIR (neat) ν_{max} : 3345, 2978, 2933, 1695, 1520, 1455, 1392, 1366, 1314, 1250, 1162, 1117, 1059, 1038, 963, 868, 768, 652, and 598.

HRMS (NSI) m/z : $[M+H]^+$ calcd. for C₁₄H₁₉O₂NF₃, 290.1362; found, 290.1373.



***N*-(3-(Trifluoromethyl)phenyl)acetamide:**

To a round bottom flask charged with a stir bar was added 3-(trifluoromethyl)aniline (1.55 mL, 12.4 mmol, 1 equiv), acetic anhydride (1.29 mL, 13.6 mmol, 1.1 equiv), DMAP (151 mg, 1.24 mmol, 0.1 equiv), Et₃N (1.73 mL, 12.4 mmol, 1 equiv), and DCM (100 mL). The reaction was stirred at room temperature for 12 hours. Once complete, the reaction was washed with sat. aq.

NH₄Cl then concentrated to yield a white solid. The solid was triturated in a minimal amount of hexanes then filtered and washed with cold hexanes to provide the product as an amorphous white solid (2.28 g, 86% yield)

R_f: 0.20 (30% ethyl acetate/hexanes)

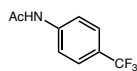
¹H NMR (600 MHz, Chloroform-*d*) δ 7.78 (s, 1H), 7.72 (d, *J* = 8.0 Hz, 1H), 7.53 (s, 1H), 7.42 (t, *J* = 7.9 Hz, 1H), 7.35 (d, *J* = 7.7 Hz, 1H), 2.20 (s, 3H).

¹³C NMR (151 MHz, Chloroform-*d*) δ 168.7, 138.5, 131.5 (q, *J* = 32.6 Hz), 129.7, 124.0 (q, *J* = 272.3 Hz), 123.0, 121.05 – 120.95 (m), 116.7, 24.7.

¹⁹F NMR (282 MHz, Chloroform-*d*) δ -62.81.

FTIR (neat) ν_{max} : 3306, 3276, 3218, 3164, 3102, 1668, 1621, 1600, 1560, 1483, 1442, 1336, 1317, 1289, 1267, 1215, 1159, 1116, 1066, 910, 889, 794, 743, 694, 675, 655, 597, and 537.

HRMS (NSI) *m/z*: [M+H]⁺ calcd. for C₉H₉O₂NF₃, 204.0631; found, 204.0633.



***N*-(4-(Trifluoromethyl)phenyl)acetamide:**

To a round bottom flask charged with a stir bar was added 4-(trifluoromethyl)aniline (1.55 mL, 12.4 mmol, 1 equiv), acetic anhydride (1.29 mL, 13.6 mmol, 1.1 equiv), DMAP (151 mg, 1.24 mmol, 0.1 equiv), Et₃N (1.73 mL, 12.4 mmol, 1 equiv), and DCM (100 mL). The reaction was stirred at room temperature for 12 hours. Once complete, the reaction was washed with sat. aq. NH₄Cl then concentrated to yield a white solid. The solid was triturated in a minimal amount of hexanes then filtered and washed with cold hexanes to provide the product as an amorphous white solid (2.28 g, 90% yield)

R_f: 0.23 (30% ethyl acetate/hexanes)

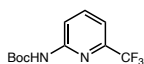
¹H NMR (600 MHz, Chloroform-*d*) δ 7.65 (d, J = 8.3 Hz, 2H), 7.59 (d, J = 8.5 Hz, 2H), 7.53 (s, 1H), 2.23 (s, 3H).

¹³C NMR (151 MHz, Chloroform-*d*) δ 168.7, 141.0, 126.4 (q, J = 3.6 Hz), 126.2 (q, J = 31.9 Hz), 124.2 (q, J = 271.5 Hz), 119.5, 24.8.

¹⁹F NMR (282 MHz, Chloroform-*d*) δ -62.17.

FTIR (neat) ν_{max} : 3310, 3268, 3205, 3138, 3081, 1671, 1606, 1543, 1518, 1410, 1372, 1320, 1269, 1185, 1156, 1095, 1066, 1015, 968, 834, 756, 732, 679, and 586.

HRMS (NSI) m/z : $[M+H]^+$ calcd. for C₉H₉O₂NF₃, 204.0631; found, 204.0633.



***tert*-Butyl (6-(trifluoromethyl)pyridin-2-yl)carbamate:**

To a previously flame dried round bottom Schlenk flask (flask A) was added 2-amino-6-(trifluoromethyl)pyridine (1 g, 6.1 mmol, 1 equiv). The atmosphere was exchanged by applying vacuum and backfilling with N₂ (this process was conducted a total of three times). To the flask was then added THF (20 mL). In a glovebox, a separate Schlenk flask (flask B) was charged with NaHMDS (1.8 g, 9.8 mmol, 1.6 equiv) and THF (10 mL) then taken out of the glovebox and placed under positive pressure with N₂. A third flame dried Schlenk flask (flask C) was charged with Boc₂O (1.33 g, 6.1 mmol, 1 equiv). The atmosphere was exchanged by applying vacuum and backfilling with N₂ (this process was conducted a total of three times). To the flask was then added THF (20 mL). The reaction flask (flask A) was cooled to 0 °C in an ice bath and the stirred while the solution of NaHMDS (flask B) was added dropwise via cannula. After the addition was complete, the solution of Boc₂O (flask C) was added to the reaction (flask A) dropwise via cannula. The solution was stirred for an additional 30 minutes at 0 °C after the addition was complete then

warmed to room temperature and stirred for 12 hours. The reaction was quenched with water, diluted with sat. aq. NH_4Cl , and extracted 3 times with EtOAc. The combined extracts were dried over Na_2SO_4 , filtered, and concentrated. The product was isolated as a colorless oil (1.4 g, 88% yield) by column chromatography on silica using 10% – 30% EtOAc/hexanes.

R_f: 0.81 (60% ethyl acetate/hexanes)

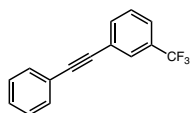
¹H NMR (600 MHz, Chloroform-*d*) δ 8.14 (d, $J = 8.5$ Hz, 1H), 7.80 (d, $J = 7.6$ Hz, 1H), 7.54 – 7.36 (m, 1H), 7.35 – 7.26 (m, 1H), 1.51 (s, 9H).

¹³C NMR (151 MHz, Chloroform-*d*) δ 152.3, 152.2, 146.4 (q, $J = 34.9$ Hz), 139.5, 121.3 (q, $J = 274.0$ Hz), 115.3, 114.9, 81.7, 28.3.

¹⁹F NMR (282 MHz, Chloroform-*d*) δ -68.51.

FTIR (neat) ν_{max} : 3438, 3309, 2982, 1733, 1609, 1586, 1518, 1468, 1411, 1369, 1308, 1222, 1186, 1148, 1124, 1085, 1066, 989, 866, 738, 683, 659, 613, and 530.

HRMS (NSI) m/z : $[\text{M}+\text{H}]^+$ calcd. for $\text{C}_{11}\text{H}_{14}\text{O}_2\text{N}_2\text{F}_3$, 263.1002; found, 263.1003.



1-(Phenylethynyl)-3-(trifluoromethyl)benzene:

To an oven dried round bottom flask charged with a stir bar was added bis(triphenylphosphine)palladium dichloride (124.9 mg, 0.18 mmol, 0.02 equiv) and copper (I) iodide (67.8 mg, 0.36 mmol, 0.04 equiv). The atmosphere was exchanged by applying vacuum and backfilling with N_2 (this process was conducted a total of three times). Triethylamine (10 mL), 1-bromo-3-(trifluoromethyl)benzene (1.24 mL, 8.9 mmol, 1.0 equiv), and ethynylbenzene (1.1 mL, 9.9 mmol, 1.1 equiv) were added to the flask via syringe and the reaction was stirred for 16

hours at 60 °C. Once complete, the reaction was removed from heat and cooled to room temperature. The reaction mixture was pushed through a pad of silica which was flushed with 30% EtOAc/hexanes and the eluent was concentrated via rotary evaporation. The product was isolated as a light yellow oil (2.08 g, 95% yield) by column chromatography on silica using 100% hexanes.

R_f: 0.58 (100% hexanes)

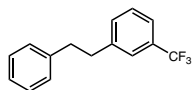
¹H NMR (600 MHz, Chloroform-*d*) δ 7.82 (s, 1H), 7.71 (s, 1H), 7.58 (d, *J* = 16.5 Hz, 3H), 7.49 (d, *J* = 7.3 Hz, 1H), 7.38 (s, 3H).

¹³C NMR (151 MHz, Chloroform-*d*) δ 134.8, 131.9, 131.1 (q, *J* = 32.6 Hz), 129.0, 128.9, 128.6, 128.5 (d, *J* = 3.8 Hz), 124.9 (d, *J* = 3.6 Hz), 124.4, 123.9 (q, *J* = 272.5 Hz), 122.8, 91.1, 87.9.

¹⁹F NMR (282 MHz, Chloroform-*d*) δ -62.58.

FTIR (neat) ν_{max} : 3062, 1597, 1493, 1429, 1335, 1290, 1269, 1121, 1092, 1068, 889, 798, 753, 707, 687, 656, and 538 cm⁻¹.

HRMS (NSI) *m/z*: [M]⁺ calcd. for C₁₅H₉F₃, 246.0651; found, 246.0651.



1-Phenethyl-3-(trifluoromethyl)benzene:

To a round bottom flask charged with a stir bar was added 1-(phenylethynyl)-3-(trifluoromethyl)benzene (2.08 g, 8.4 mmol, 1.0 equiv) and methanol (100 mL). 5% Palladium on carbon (1 g) was added to the reaction. The atmosphere was exchanged by applying vacuum and backfilling with H₂ (this process was conducted a total of three times). Using a balloon, the reaction was stirred under positive pressure of H₂ overnight at room temperature. Once complete, the reaction mixture was pushed through a pad of celite and flushed with hexanes. The eluent was

concentrated by rotary evaporation to afford the product as a colorless liquid which was used without further purification.

R_f: 0.50 (100% hexanes)

¹H NMR (600 MHz, Chloroform-*d*) δ 7.48 (d, $J = 7.6$ Hz, 1H), 7.44 (s, 1H), 7.40 (t, $J = 7.6$ Hz, 1H), 7.35 (d, $J = 7.6$ Hz, 1H), 7.31 (t, $J = 7.5$ Hz, 2H), 7.23 (t, $J = 7.3$ Hz, 1H), 7.19 (d, $J = 7.6$ Hz, 2H), 3.03 – 2.93 (m, 4H).

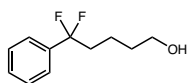
¹³C NMR (151 MHz, Chloroform-*d*) δ 141.2, 132.1, 130.8 (q, $J = 31.9$ Hz), 128.8, 128.6, 128.6, 126.3, 125.3 (d, $J = 3.6$ Hz), 124.1 (d, $J = 272.2$ Hz), 123.0 (q, $J = 3.8$ Hz), 37.8, 37.8.

¹⁹F NMR (282 MHz, Chloroform-*d*) δ -62.58.

FTIR (neat) ν_{max} : 3064, 3028, 2927, 2860, 1602, 1495, 1449, 1325, 1161, 1117, 1072, 901, 879, 795, 749, 696, and 660 cm^{-1} .

4.4.5 Procedures and Characterization Data

Products from Table 4.1: Defluoroalkylation Arene Scope



5,5-Difluoro-5-phenylpentan-1-ol (1):

Prepared according to the General Procedure A using trifluorotoluene (61.3 μL , 0.5 mmol, 1 equiv), and 3-buten-1-ol (215 μL , 2.5 mmol, 5 equiv), potassium formate (126 mg, 1.5 mmol, 3 equiv), thiophenol (5 μL , 0.05 mmol, 10 mol%) and photocatalyst **P3** (6 mg, 0.01 mmol, 2 mol%) at 100 $^{\circ}\text{C}$. After 24 h, the reaction was purified according to the General Procedure A (silica gel, 20 – 60% EtOAc/hexanes) to provide the desired product as a colorless oil (84 mg, 84% yield).

R_f: 0.71 (60% ethyl acetate/hexanes)

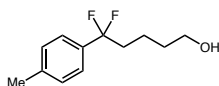
¹H NMR (600 MHz, CDCl_3) δ 7.46 (d, $J = 4.2$ Hz, 2H), 7.44 – 7.36 (m, 3H), 3.60 (t, $J = 6.4$ Hz, 2H), 2.15 (tt, $J = 16.0, 7.9$ Hz, 2H), 1.85 (s, 1H), 1.58 (p, $J = 6.6$ Hz, 2H), 1.51 (p, $J = 7.7, 6.8$ Hz, 2H).

¹³C NMR (151 MHz, CDCl_3) δ 137.4 (t, $^2J_{\text{C-F}} = 26.6$ Hz), 129.6, 128.4, 124.9 (t, $^3J_{\text{C-F}} = 6.3$ Hz), 123.0 (t, $^1J_{\text{C-F}} = 242.1$ Hz), 62.4, 38.9 (t, $^2J_{\text{C-F}} = 27.6$ Hz), 32.2, 19.0.

¹⁹F NMR (376 MHz, CDCl_3) δ -95.64 (t, $J = 16.2$ Hz).

FTIR (neat) ν_{max} : 3328, 2930, 2873, 1451, 1327, 1171 cm^{-1} .

HRMS (NSI) m/z : $[\text{M}+\text{Na}]^+$ calcd. for $\text{C}_{11}\text{H}_{14}\text{F}_2\text{ONa}$, 223.0905; found, 223.0904.



5,5-Difluoro-5-(*p*-tolyl)pentan-1-ol (2):

Prepared according to the General Procedure A using 1-methyl-4-(trifluoromethyl)benzene (70 μL , 0.5 mmol, 1 equiv), and 3-buten-1-ol (215 μL , 2.5 mmol, 5 equiv), potassium formate (126 mg, 1.5 mmol, 3 equiv), thiophenol (5 μL , 0.05 mmol, 10 mol%) and photocatalyst **P3** (6 mg, 0.01 mmol, 2 mol%) at 100 °C. After 24 h, the reaction was purified according to the General Procedure A (silica gel, 20 – 60% EtOAc/hexanes) to provide the desired product as a colorless oil (64 mg, 60 % yield).

R_f: 0.71 (60% ethyl acetate/hexanes)

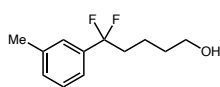
¹H NMR (600 MHz, CDCl₃) δ 7.35 (d, J = 7.8 Hz, 2H), 7.21 (d, J = 7.8 Hz, 2H), 3.60 (t, J = 6.4 Hz, 2H), 2.38 (s, 3H), 2.14 (dp, J = 16.0, 7.9 Hz, 2H), 1.82 (s, 1H), 1.58 (p, J = 6.7 Hz, 2H), 1.50 (p, J = 7.8, 6.9 Hz, 2H).

¹³C NMR (151 MHz, CDCl₃) δ 139.7, 134.6 (t, $^2J_{C-F}$ = 26.7 Hz), 129.1, 125.0 (t, $^3J_{C-F}$ = 6.1 Hz), 123.3 (t, $^1J_{C-F}$ = 241.8 Hz), 62.5, 38.9 (t, $^2J_{C-F}$ = 27.8 Hz), 32.3, 21.3, 19.1.

¹⁹F NMR (376 MHz, CDCl₃) δ -94.86 (t, J = 15.1 Hz).

FTIR (neat) ν_{max} : 3330, 2926, 2872, 1459, 1326, 1169 cm^{-1} .

HRMS (NSI) m/z : [M+Na]⁺ calcd. for C₁₂H₁₆F₂ONa, 237.1061; found, 237.1061.



5,5-Difluoro-5-(*m*-tolyl)pentan-1-ol (3):

Prepared according to the General Procedure A using 1-methyl-3-(trifluoromethyl)benzene (70 μL , 0.5 mmol, 1 equiv), and 3-buten-1-ol (215 μL , 2.5 mmol, 5 equiv), potassium formate (126 mg, 1.5 mmol, 3 equiv), thiophenol (5 μL , 0.05 mmol, 10 mol%) and photocatalyst **P3** (6 mg, 0.01 mmol, 2 mol%) at 100 °C. After 24 h, the reaction was purified according to the General Procedure

A (silica gel, 20 – 60% EtOAc/hexanes) to provide the desired product as a colorless oil (85 mg, 79 % yield).

R_f: 0.71 (60% ethyl acetate/hexanes)

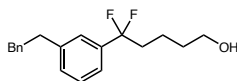
¹H NMR (600 MHz, CDCl₃) δ 7.31 (dq, *J* = 14.8, 7.5 Hz, 3H), 7.25 (d, *J* = 7.5 Hz, 1H), 3.63 (t, *J* = 6.4 Hz, 2H), 2.41 (s, 1H), 2.17 (dp, *J* = 16.1, 8.0 Hz, 2H), 1.78 (s, 1H), 1.61 (p, *J* = 6.6 Hz, 2H), 1.53 (p, *J* = 7.7, 7.0 Hz, 2H).

¹³C NMR (151 MHz, CDCl₃) δ 138.3, 137.4 (t, ²*J*_{C-F} = 26.4 Hz), 130.4, 128.4, 125.6 (t, ³*J*_{C-F} = 6.2 Hz), 123.2 (t, ¹*J*_{C-F} = 242.1 Hz), 122.1 (t, ³*J*_{C-F} = 6.2 Hz), 62.5, 39.0 (t, ²*J*_{C-F} = 27.7 Hz), 32.3, 21.5, 19.1.

¹⁹F NMR (376 MHz, CDCl₃) δ -95.43 (t, *J* = 15.5 Hz).

FTIR (neat) *v*_{max}: 3328, 2926, 2871, 1458, 1328, 1167, 1036 cm⁻¹.

HRMS (NSI) *m/z*: [M+Na]⁺ calcd. for C₁₂H₁₆F₂ONa, 237.1061; found, 237.1061.



5,5-Difluoro-5-(3-phenethylphenyl)pentan-1-ol (4):

Prepared according to the General Procedure A using 1-phenethyl-3-(trifluoromethyl)benzene (125 mg, 0.5 mmol, 1 equiv), and 3-buten-1-ol (215 μL, 2.5 mmol, 5 equiv), potassium formate (126 mg, 1.5 mmol, 3 equiv), thiophenol (5 μL, 0.05 mmol, 10 mol%) and photocatalyst **P3** (6 mg, 0.01 mmol, 2 mol%) at 100 °C. After 24 h, the reaction was purified according to the General Procedure A (silica gel, 20 – 60% EtOAc/hexanes) to provide the desired product as a colorless oil (99 mg, 65 % yield).

R_f: 0.45 (30% ethyl acetate/hexanes)

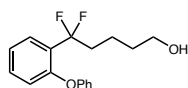
¹H NMR (600 MHz, CDCl₃) δ 7.34 (dt, *J* = 20.5, 7.4 Hz, 4H), 7.29 – 7.26 (m, 2H), 7.26 – 7.23 (m, 1H), 7.21 (d, *J* = 7.5 Hz, 2H), 3.66 (t, *J* = 6.4 Hz, 2H), 3.11 – 2.86 (m, 4H), 2.16 (tt, *J* = 16.2, 8.0 Hz, 2H), 1.76 (s, 1H), 1.63 (p, *J* = 6.8 Hz, 2H), 1.54 (p, *J* = 7.9, 7.3 Hz, 2H).

¹³C NMR (151 MHz, CDCl₃) δ 142.1, 141.4, 137.4 (t, ²*J*_{C-F} = 26.3 Hz), 129.9, 128.6, 128.5, 128.4, 126.1, 125.1 (t, ³*J*_{C-F} = 6.1 Hz), 122.6 (t, ³*J*_{C-F} = 6.2 Hz), 62.5, 38.9 (t, ²*J*_{C-F} = 27.6 Hz), 37.9, 37.8, 32.3, 19.1 (t, ³*J*_{C-F} = 4.1 Hz).

¹⁹F NMR (376 MHz, CDCl₃) δ -95.45 (t, *J* = 16.1 Hz).

FTIR (neat) *v*_{max}: 3328, 2926, 2860, 1453, 1327, 1167, 1029 cm⁻¹.

HRMS (NSI) *m/z*: [M+Na]⁺ calcd. for C₁₉H₂₂F₂ONa, 327.1531; found, 327.1532.



5,5-Difluoro-5-(2-phenoxyphenyl)pentan-1-ol (5):

Prepared according to the General Procedure A using 1-phenoxy-2-(trifluoromethyl)benzene (119 mg, 0.5 mmol, 1 equiv), and 3-buten-1-ol (215 μL, 2.5 mmol, 5 equiv), potassium formate (126 mg, 1.5 mmol, 3 equiv), thiophenol (5 μL, 0.05 mmol, 10 mol%) and photocatalyst **P3** (6 mg, 0.01 mmol, 2 mol%) at 100 °C. After 24 h, the reaction was purified according to the General Procedure A (silica gel, 20 – 60% EtOAc/hexanes) to provide the desired product as a colorless oil (64 mg, 44 % yield).

R_f: 0.77 (60% ethyl acetate/hexanes)

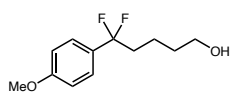
¹H NMR (600 MHz, CDCl₃) δ 7.61 (d, *J* = 7.8 Hz, 1H), 7.34 (t, *J* = 7.3 Hz, 3H), 7.14 (dt, *J* = 18.5, 7.5 Hz, 2H), 6.99 (d, *J* = 8.0 Hz, 2H), 6.90 (d, *J* = 8.2 Hz, 1H), 3.60 (t, *J* = 6.4 Hz, 2H), 2.39 (dp, *J* = 16.5, 7.9 Hz, 2H), 1.58 (p, *J* = 6.5 Hz, 2H), 1.51 (p, *J* = 8.1, 7.5 Hz, 2H).

^{13}C NMR (151 MHz, CDCl_3) δ 157.2, 154.3, 131.2, 129.8, 128.0 (t, $^2J_{\text{C-F}} = 26.2$ Hz), 127.2 (t, $^1J_{\text{C-F}} = 8.5$ Hz), 123.5, 123.2, 122.4 (t, $^1J_{\text{C-F}} = 242.9$ Hz), 119.8, 118.9, 62.5, 37.1 (t, $^2J_{\text{C-F}} = 26.4$ Hz), 32.2, 19.2 (t, $^3J_{\text{C-F}} = 4.2$ Hz).

^{19}F NMR (376 MHz, CDCl_3) δ -94.02 (t, $J = 16.8$ Hz).

FTIR (neat) ν_{max} : 3326, 2939, 2873, 1606, 1582, 1485, 1453, 1234 cm^{-1} .

HRMS (NSI) m/z : $[\text{M}+\text{Na}]^+$ calcd. for $\text{C}_{17}\text{H}_{18}\text{O}_2\text{F}_2\text{Na}$, 315.1167; found, 315.1169.



5,5-Difluoro-5-(4-methoxyphenyl)pentan-1-ol (6):

Prepared according to the General Procedure A using 1-methoxy-4-(trifluoromethyl)benzene (70 μL , 0.5 mmol, 1 equiv), and 3-buten-1-ol (107 μL , 2.5 mmol, 5 equiv), potassium formate (126 mg, 1.5 mmol, 5 equiv), thiophenol (5 μL , 0.05 mmol, 10 mol%) and photocatalyst **P3** (6 mg, 0.01 mmol, 2 mol%) at 100 $^\circ\text{C}$. After 24 h, the reaction was purified according to the General Procedure A (silica gel, 30 – 50% EtOAc/hexanes) to provide the desired product as a colorless oil (58 mg, 50 % yield).

R_f: 0.29 (30% ethyl acetate/hexanes)

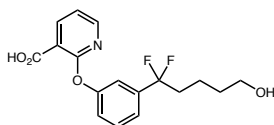
^1H NMR (600 MHz, CDCl_3) δ 7.38 (d, $J = 8.9$ Hz, 2H), 6.91 (d, $J = 7.9$ Hz, 2H), 3.81 (s, 3H), 3.60 (t, $J = 6.4$ Hz, 2H), 2.14 (dt, $J = 13.8, 8.1$ Hz, 2H), 1.88 (s, 1H), 1.57 (dt, $J = 12.7, 5.9$ Hz, 2H), 1.50 (td, $J = 9.2, 8.4, 5.1$ Hz, 2H).

^{13}C NMR (151 MHz, CDCl_3) δ 160.6, 129.7 (t, $^2J_{\text{C-F}} = 27.2$ Hz), 126.5 (t, $^3J_{\text{C-F}} = 6.2$ Hz), 123.2 (t, $^1J_{\text{C-F}} = 241.5$ Hz), 113.8, 62.5, 55.4, 38.9 (t, $^2J_{\text{C-F}} = 28.1$ Hz), 32.3, 19.2 (t, $^3J_{\text{C-F}} = 4.1$ Hz).

^{19}F NMR (282 MHz, CDCl_3) δ -93.72 (t, $J = 15.7$ Hz).

FTIR (neat) ν_{max} : 3329, 2931, 2862, 1615, 1517, 1463, 1326, 1249 cm^{-1} .

HRMS (NSI) m/z : $[M+Na]^+$ calcd. for $C_{12}H_{16}O_2F_2Na$, 253.1011; found, 253.1011.



2-(3-(1,1-Difluoro-5-hydroxypentyl)phenoxy)nicotinic acid (7):

Prepared according to the General Procedure A using 2-(3-(trifluoromethyl)phenoxy)nicotinic acid (141 mg, 0.5 mmol, 1 equiv), 3-buten-1-ol (107 μ L, 2.5 mmol, 5 equiv), potassium formate (126 mg, 1.5 mmol, 3 equiv), thiophenol (5 μ L, 0.05 mmol, 10 mol%) and photocatalyst **P3** (6 mg, 0.01 mmol, 2 mol%) at 100 °C. After 24 h, the reaction was purified by reverse phase preparative HPLC (30 – 99%, MeCN/H₂O) to provide the desired product as a colorless oil (91 mg, 54% yield).

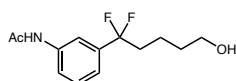
¹H NMR (400 MHz, CDCl₃) δ 8.44 (dd, $J = 7.6, 2.1$ Hz, 1H), 8.31 (dd, $J = 4.8, 2.0$ Hz, 1H), 7.47 (t, $J = 7.9$ Hz, 1H), 7.35 (d, $J = 7.8$ Hz, 1H), 7.27 (s, 1H), 7.22 (d, $J = 9.0$ Hz, 1H), 7.17 (dd, $J = 7.6, 4.8$ Hz, 1H), 3.62 (t, $J = 6.0$ Hz, 2H), 2.27 – 2.06 (m, 2H), 1.67 – 1.47 (m, 2H).

¹³C NMR (100 MHz, CDCl₃) δ 166.5, 161.4, 153.1, 152.0, 143.4, 139.3 (t, $^2J_{C-F} = 27.5$ Hz), 130.0, 123.0, 122.6 (t, $^1J_{C-F} = 243.0$ Hz), 122.2 (t, $^3J_{C-F} = 6.0$ Hz), 119.6, 118.8 (t, $^3J_{C-F} = 6.3$ Hz), 114.4, 62.5, 38.9 (t, $^2J_{C-F} = 27.2$ Hz), 32.1, 19.1 (t, $^3J_{C-F} = 4.3$ Hz).

¹⁹F NMR (376 MHz, CDCl₃) δ -95.59 (t, $J = 16.0$ Hz).

FTIR (neat) ν_{max} : 3232, 2942, 1716, 1590, 1432, 1256 cm^{-1} .

HRMS (APCI) m/z : $[M+H]^+$ calcd. for $C_{17}H_{18}O_4NF_2$, 338.1198; found, 338.1199.



N-(3-(1,1-Difluoro-5-hydroxypentyl)phenyl)acetamide (8):

Prepared according to the General Procedure A using *N*-(3-(Trifluoromethyl)phenyl)acetamide (102 mg, 0.5 mmol, 1 equiv), and 3-buten-1-ol (215 μ L, 2.5 mmol, 5 equiv), potassium formate (126 mg, 1.5 mmol, 3 equiv), thiophenol (5 μ L, 0.05 mmol, 10 mol%) and photocatalyst **P3** (6 mg, 0.01 mmol, 2 mol%) at 100 °C. After 24 h, the reaction was purified according to the General Procedure A (silica gel, 20 – 60% EtOAc/hexanes then 20% MeOH/EtOAc) to provide the desired product as a colorless oil (118 mg, 92 % yield).

R_f: 0.26 (60% ethyl acetate/hexanes)

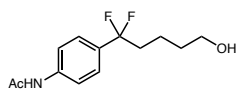
¹H NMR (600 MHz, CDCl₃) δ 8.18 (s, 1H), 7.59 (s, 1H), 7.56 (d, J = 8.3 Hz, 1H), 7.31 (t, J = 7.9 Hz, 1H), 7.16 (d, J = 7.9 Hz, 1H), 3.58 (t, J = 6.0 Hz, 2H), 2.28 (s, 1H), 2.18 – 1.96 (m, 5H), 1.53 (q, J = 7.0, 6.4 Hz, 2H), 1.50 – 1.42 (m, 2H).

¹³C NMR (151 MHz, CDCl₃) δ 169.4, 138.3, 138.1 (t, $^2J_{C-F}$ = 26.7 Hz), 129.3, 122.9 (t, J = 242.5 Hz), 121.3, 120.9 (t, $^3J_{C-F}$ = 6.1 Hz), 116.8 (t, $^3J_{C-F}$ = 6.4 Hz), 62.3, 38.7 (t, $^2J_{C-F}$ = 27.4 Hz), 32.1, 24.5, 19.1.

¹⁹F NMR (376 MHz, CDCl₃) δ -95.18 (t, J = 16.0 Hz).

FTIR (neat) ν_{max} : 3272, 2934, 2873, 1668, 1598, 1555, 1438, 1328, 1169, 1035 cm⁻¹.

HRMS (NSI) m/z : [M+H]⁺ calcd. for C₁₃H₁₈F₂O₂N, 258.1300; found, 258.1301.



***N*-(4-(1,1-difluoro-5-hydroxypentyl)phenyl)acetamide (9):**

Prepared according to the General Procedure A using 1-(phenylethynyl)-3-(trifluoromethyl)benzene (102 mg, 0.5 mmol, 1 equiv), and 3-buten-1-ol (215 μ L, 2.5 mmol, 5 equiv), potassium formate (126 mg, 1.5 mmol, 3 equiv), thiophenol (5 μ L, 0.05 mmol, 10 mol%) and photocatalyst **P3** (6 mg, 0.01 mmol, 2 mol%) at 100 °C. After 24 h, the reaction was purified

according to the General Procedure A (silica gel, 20-60% EtOAc/hexanes then 20% MeOH/EtOAc) to provide the desired product as a colorless oil (112 mg, 87 % yield).

R_f: 0.27 (60% ethyl acetate/hexanes)

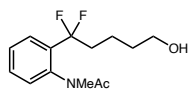
¹H NMR (600 MHz, CDCl₃) δ 7.54 (d, *J* = 8.2 Hz, 2H), 7.46 (s, 1H), 7.40 (d, *J* = 8.3 Hz, 2H), 3.62 (t, *J* = 6.4 Hz, 2H), 2.29 – 2.07 (m, 5H), 1.67 (s, 1H), 1.58 (p, *J* = 6.7 Hz, 2H), 1.54 – 1.45 (m, 2H).

¹³C NMR (151 MHz, CDCl₃) δ 168.7, 139.2, 133.2 (t, ²*J*_{C-F} = 27.1 Hz), 126.0 (t, ³*J*_{C-F} = 6.2 Hz), 123.0 (t, ¹*J*_{C-F} = 242.1 Hz), 119.6, 62.6, 38.9 (t, ²*J*_{C-F} = 27.8 Hz), 32.3, 24.7, 19.2.

¹⁹F NMR (376 MHz, CDCl₃) δ -94.83 (t, *J* = 15.8 Hz).

FTIR (neat) *v*_{max}: 3308, 2933, 2871, 1670, 1604, 1538, 1406, 1368, 1317, 1264, 1182, 1035 cm⁻¹.

HRMS (NSI) *m/z*: [M+H]⁺ calcd. for C₁₃H₁₈F₂O₂N, 258.1300; found, 258.1300.



***N*-(2-(1,1-difluoro-5-hydroxypentyl)phenyl)-*N*-methylacetamide (10):**

Prepared according to the General Procedure A using *N*-methyl-*N*-(2-(trifluoromethyl)phenyl)acetamide (109 mg, 0.5 mmol, 1 equiv), 3-buten-1-ol (215 μL, 2.5 mmol, 5 equiv), potassium formate (126 mg, 1.5 mmol, 3 equiv), thiophenol (5 μL, 0.05 mmol, 10 mol%) and photocatalyst **P3** (6 mg, 0.01 mmol, 2 mol%) at 23 °C. After 24 h, the reaction was purified according to the General Procedure A (silica gel, 30-100% EtOAc/hexanes) to provide the desired product as a colorless oil (106 mg, 78% yield).

R_f: 0.30 (60% ethyl acetate/hexanes)

^1H NMR (600 MHz, CDCl_3) δ 7.62 (dd, $J = 7.8, 1.6$ Hz, 1H), 7.50 (td, $J = 7.5, 1.6$ Hz, 1H), 7.44 (td, $J = 7.6, 1.3$ Hz, 1H), 7.18 (dd, $J = 7.8, 1.3$ Hz, 1H), 3.63 (t, $J = 6.1$ Hz, 2H), 3.19 (s, 3H), 2.24 – 2.09 (m, 2H), 1.77 (s, 3H), 1.64 – 1.52 (m, 4H).

Observed complexity in NMR spectra due to rotameric mixture.

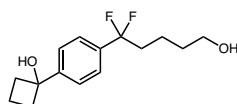
^{13}C NMR (126 MHz, $\text{DMSO}-d_6$) δ 170.1, 142.1, 133.5 (t, $^2J_{\text{C-F}} = 24.7$ Hz), 132.5, 131.2, 129.2, 128.2 (t, $^3J_{\text{C-F}} = 8.1$ Hz), 123.6 (t, $^1J_{\text{C-F}} = 242.2$ Hz), 60.6, 37.9, 37.4 (t, $^2J_{\text{C-F}} = 26.5$ Hz), 32.2, 22.6, 19.4.

Observed complexity in NMR spectra due to rotameric mixture.

^{19}F NMR (282 MHz, CDCl_3) δ -87.66 – -91.49 (m).

FTIR (neat) ν_{max} : 3409, 2932, 2871, 1641, 1450, 1379 cm^{-1} .

HRMS (APCI) m/z : $[\text{M}+\text{H}]^+$ calcd. for $\text{C}_{14}\text{H}_{20}\text{O}_2\text{NF}_2$, 272.1457; found, 272.1457.



1-(4-(1,1-Difluoro-5-hydroxypentyl)phenyl)cyclobutan-1-ol (11):

Prepared according to the General Procedure A using 1-(4-(trifluoromethyl)phenyl)cyclobutan-1-ol (54 mg, 0.25 mmol, 1 equiv), and 3-buten-1-ol (107 μL , 1.25 mmol, 5 equiv), potassium formate (63 mg, 0.75 mmol, 3 equiv), thiophenol (3 μL , 0.025 mmol, 10 mol%) and photocatalyst **P3** (3 mg, 0.005 mmol, 2 mol%) at 100 $^\circ\text{C}$. After 24 h, the reaction was purified according to the General Procedure A (silica gel, 20-60% EtOAc/hexanes) to provide the desired product as a colorless oil (56 mg, 82 % yield).

R_f: 0.52 (60% ethyl acetate/hexanes)

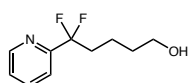
^1H NMR (400 MHz, CDCl_3) δ 7.53 (d, $J = 8.1$ Hz, 2H), 7.45 (d, $J = 8.4$ Hz, 2H), 3.58 (t, $J = 6.1$ Hz, 2H), 2.63 – 2.46 (m, 2H), 2.44 – 2.28 (m, 2H), 2.23 – 1.94 (m, 4H), 1.79 – 1.64 (m, 1H), 1.63 – 1.43 (m, 4H).

¹³C NMR (126 MHz, CDCl₃) δ 148.0, 136.2 (t, ²J_{C-F} = 26.7 Hz), 125.2, 123.1 (t, ¹J_{C-F} = 241.9 Hz), 76.8, 62.5, 38.9 (t, ²J_{C-F} = 27.7 Hz), 37.1, 32.2, 19.1 (t, ³J_{C-F} = 4.2 Hz), 13.1. *1 carbon signal is coincident.*

¹⁹F NMR (376 MHz, CDCl₃) δ -95.14 (t, *J* = 16.1 Hz).

FTIR (neat) ν_{max}: 3314, 2939, 2872, 1540, 1327, 988 cm⁻¹.

HRMS (ESI) *m/z*: [M+Na]⁺ calcd. for C₁₅H₂₀O₂F₂Na, 293.1324; found, 293.1324.



5,5-Difluoro-5-(pyridin-2-yl)pentan-1-ol (12):

Prepared according to the General Procedure A using 2-(trifluoromethyl)pyridine (58 μL, 0.5 mmol, 1 equiv), 3-buten-1-ol (215 μL, 2.5 mmol, 5 equiv), potassium formate (126 mg, 1.5 mmol, 3 equiv), thiophenol (5 μL, 0.05 mmol, 10 mol%) and photocatalyst **P3** (6 mg, 0.01 mmol, 2 mol%) at 23 °C. After 24 h, the reaction was purified according to the General Procedure A (silica gel, 20-80% EtOAc/hexanes) to provide the desired product as a colorless oil (43 mg, 43% yield).

R_f: 0.40 (60% ethyl acetate/hexanes)

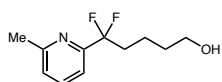
¹H NMR (600 MHz, CDCl₃) δ 8.62 (d, *J* = 4.8 Hz, 1H), 7.78 (t, *J* = 7.8 Hz, 1H), 7.61 (d, *J* = 7.9 Hz, 1H), 7.34 (t, *J* = 6.1 Hz, 1H), 3.61 (t, *J* = 6.4 Hz, 2H), 2.33 (dp, *J* = 16.4, 7.9 Hz, 2H), 2.22 (s, 2H), 1.59 (p, *J* = 6.9 Hz, 2H), 1.51 (p, *J* = 7.6, 7.0 Hz, 2H).

¹³C NMR (151 MHz, CDCl₃) δ 154.9 (t, ²J_{C-F} = 29.3 Hz), 149.4, 137.2, 124.8, 121.7 (t, ¹J_{C-F} = 241.6 Hz), 120.1, 62.3, 36.0 (t, ²J_{C-F} = 25.3 Hz), 32.2, 18.7 (t, ³J_{C-F} = 4.2 Hz).

¹⁹F NMR (376 MHz, CDCl₃) δ -99.06 (t, *J* = 18.5 Hz).

FTIR (neat) ν_{max}: 3343, 2937, 2872, 1592, 1439, 1332, 1180, 994 cm⁻¹.

HRMS (APCI) *m/z*: [M+H]⁺ calcd. for C₁₀H₁₄ONF₂, 202.1038; found, 202.1037.



5,5-Difluoro-5-(6-methylpyridin-2-yl)pentan-1-ol (13):

Prepared according to the General Procedure A using 2-methyl-6-(trifluoromethyl)pyridine (81 mg, 0.5 mmol, 1 equiv), 3-buten-1-ol (215 μ L, 2.5 mmol, 5 equiv), potassium formate (126 mg, 1.5 mmol, 3 equiv), thiophenol (5 μ L, 0.05 mmol, 10 mol%) and photocatalyst **P3** (6 mg, 0.01 mmol, 2 mol%) at 23 $^{\circ}$ C. After 24 h, the reaction was purified according to the General Procedure A (silica gel, 10-60% EtOAc/hexanes) to provide the desired product as a colorless oil (67 mg, 62% yield).

R_f: 0.32 (60% ethyl acetate/hexanes)

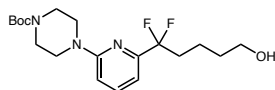
¹H NMR (600 MHz, CDCl₃) δ 7.63 (t, J = 7.8 Hz, 1H), 7.38 (d, J = 7.8 Hz, 1H), 7.17 (d, J = 7.8 Hz, 1H), 3.60 (t, J = 6.5 Hz, 2H), 2.55 (s, 3H), 2.37 (s, 1H), 2.31 (tq, J = 16.5, 7.8, 7.0 Hz, 2H), 1.58 (p, J = 6.8 Hz, 2H), 1.50 (dq, J = 15.5, 7.3 Hz, 2H).

¹³C NMR (151 MHz, CDCl₃) δ 158.6, 154.3 (t, $^2J_{C-F}$ = 29.0 Hz), 137.2, 124.4, 121.8 (t, $^1J_{C-F}$ = 241.8 Hz), 117.0 (t, $^3J_{C-F}$ = 4.7 Hz), 62.3, 36.1 (t, $^2J_{C-F}$ = 25.4 Hz), 32.1, 24.4, 18.7.

¹⁹F NMR (282 MHz, CDCl₃) δ -98.26 (t, J = 16.7 Hz).

FTIR (neat) ν_{max} : 3343, 2938, 2872, 1597, 1462, 1333, 1187, 1037, 994 cm^{-1} .

HRMS (APCI) m/z : [M+H]⁺ calcd. for C₁₁H₁₆ONF₂, 216.1195; found, 216.1194



tert-Butyl 4-(6-(1,1-difluoro-5-hydroxypentyl)pyridin-2-yl)piperazine-1-carboxylate (14):

Prepared according to the General Procedure A using *tert*-butyl 4-(6-(trifluoromethyl)pyridin-2-yl)piperazine-1-carboxylate (166 mg, 0.5 mmol, 1 equiv), 3-buten-1-ol (215 μ L, 2.5 mmol, 5 equiv), potassium formate (126 mg, 1.5 mmol, 3 equiv), thiophenol (5 μ L, 0.05 mmol, 10 mol%) and photocatalyst **P3** (6 mg, 0.01 mmol, 2 mol%) at 23 °C. After 24 h, the reaction was purified according to the General Procedure A (silica gel, 10-60% EtOAc/hexanes) to provide the desired product as a colorless oil (150 mg, 78% yield).

R_f: 0.63 (60% ethyl acetate/hexanes)

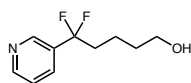
¹H NMR (600 MHz, CDCl₃) δ 7.55 (t, J = 7.9 Hz, 1H), 6.95 (d, J = 7.3 Hz, 1H), 6.67 (d, J = 8.5 Hz, 1H), 3.63 (t, J = 6.4 Hz, 2H), 3.54 (s, 8H), 2.30 (dp, J = 16.3, 7.9 Hz, 2H), 1.70 (s, 1H), 1.61 (p, J = 6.9 Hz, 2H), 1.55 – 1.49 (m, 2H), 1.48 (s, 9H)

¹³C NMR (151 MHz, CDCl₃) δ 158.7, 155.0, 153.0 (t, $^2J_{C-F}$ = 29.4 Hz), 138.5, 121.9 ($^1J_{C-F}$ = 241.3 Hz), 109.2 (t, $^3J_{C-F}$ = 4.8 Hz), 108.1, 80.2, 62.7, 45.0, 43.3 (d, J = 144.7 Hz), 35.8 (t, $^2J_{C-F}$ = 25.3 Hz), 32.5, 28.6, 18.8.

¹⁹F NMR (282 MHz, CDCl₃) δ -96.14 (t, J = 16.2 Hz).

FTIR (neat) ν_{max} : 3436, 2977, 2931, 2865, 1687, 1425, 1243, 905, 726 cm⁻¹.

HRMS (APCI) m/z : [M+H]⁺ calcd. for C₇H₁₀ON, 386.2245; found, 386.2250



5,5-Difluoro-5-(pyridin-3-yl)pentan-1-ol (15):

Prepared according to the General Procedure A using 3-(trifluoromethyl)pyridine (58 μ L, 0.5 mmol, 1 equiv), 3-buten-1-ol (215 μ L, 2.5 mmol, 5 equiv), potassium formate (126 mg, 1.5 mmol, 3 equiv), thiophenol (5 μ L, 0.05 mmol, 10 mol%) and photocatalyst **P3** (6 mg, 0.01 mmol, 2 mol%)

at 23 °C. After 24 h, the reaction was purified according to the General Procedure A (silica gel, 20-80% EtOAc/hexanes) to provide the desired product as a colorless oil (41 mg, 41% yield).

R_f: 0.30 (60% ethyl acetate/hexanes)

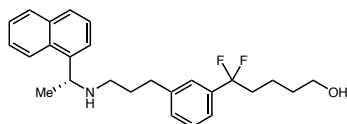
¹H NMR (600 MHz, CDCl₃) δ 8.68 (s, 1H), 8.62 (d, *J* = 5.1 Hz, 1H), 7.76 (d, *J* = 7.9 Hz, 1H), 7.34 (dd, *J* = 8.1, 4.8 Hz, 1H), 3.60 (t, *J* = 6.2 Hz, 2H), 2.21 – 2.09 (m, 2H), 1.56 (d, *J* = 6.9 Hz, 2H), 1.51 (dt, *J* = 9.1, 4.2 Hz, 2H).

¹³C NMR (151 MHz, CDCl₃) δ 150.8, 146.5 (t, ³*J*_{C-F} = 6.3 Hz), 133.3 (t, ²*J*_{C-F} = 27.2 Hz), 133.1 (t, ³*J*_{C-F} = 6.1 Hz), 123.4, 122.1 (t, ¹*J*_{C-F} = 242.7 Hz), 62.1, 38.8 (t, ²*J*_{C-F} = 26.8 Hz), 32.1, 19.0 (t, ³*J*_{C-F} = 4.1 Hz).

¹⁹F NMR (282 MHz, CDCl₃) δ -96.14 (t, *J* = 16.3 Hz).

FTIR (neat) ν_{max}: 3305, 2934, 2872, 1597, 1327, 907, 727 cm⁻¹.

HRMS (APCI) *m/z*: [M+H]⁺ calcd. for C₁₀H₁₄ONF₂, 202.1038; found, 202.1036.



(R)-5,5-difluoro-5-(3-(3-((1-(naphthalen-1-yl)ethyl)amino)propyl)phenyl)pentan-1-ol (16):

Prepared according to the General Procedure A using Cinacalcet freebase (179 mg, 0.5 mmol, 1 equiv), 3-buten-1-ol (430 μL, 5.0 mmol, 10 equiv), potassium formate (126 mg, 1.5 mmol, 3 equiv), thiophenol (5 μL, 0.05 mmol, 10 mol%) and photocatalyst **P3** (6 mg, 0.01 mmol, 2 mol%) at 100 °C. After 24 h, the reaction was purified according to the General Procedure A (silica gel, 20-80% EtOAc/hexanes) to provide the desired product as a colorless oil (126 mg, 61% yield).

R_f: 0.15 (60% ethyl acetate/hexanes)

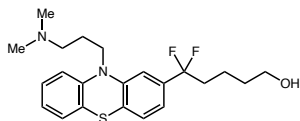
¹H NMR (500 MHz, Chloroform-*d*) δ 8.03 (t, $J = 7.9$ Hz, 2H), 7.92 (dd, $J = 8.2, 1.2$ Hz, 1H), 7.85 (d, $J = 8.2$ Hz, 1H), 7.60 – 7.52 (m, 3H), 7.24 – 7.15 (m, 3H), 7.05 (d, $J = 7.3$ Hz, 1H), 5.08 – 4.99 (m, 1H), 3.60 (t, $J = 6.1$ Hz, 2H), 2.77 – 2.63 (m, 2H), 2.60 – 2.47 (m, 2H), 2.11 (td, $J = 15.9, 7.2$ Hz, 4H), 1.83 – 1.65 (m, 3H), 1.61 – 1.38 (m, 4H).

¹³C NMR (126 MHz, Chloroform-*d*) δ 141.0, 137.4 (t, $J = 26.6$ Hz), 134.0, 131.0, 129.7, 129.5, 129.1 – 128.9 (m), 128.6, 127.0, 126.1, 125.1 (t, $J = 5.9$ Hz), 124.4, 123.2, 122.9 (t, $J = 6.4$ Hz), 121.9, 62.2, 53.6, 46.2, 38.7 (t, $J = 27.4$ Hz), 33.0, 32.2, 28.9, 22.0, 19.3 (t, $J = 4.1$ Hz).

¹⁹F NMR (282 MHz, Chloroform-*d*) δ -94.95 (t, $J = 16.4$ Hz).

FTIR (neat) ν_{\max} : 3329, 3049, 2929, 2860, 1595, 1510, 1444, 1375, 1325, 1264, 1166, 1121, 1013, 901, 860, 799, 779, 734, 703, 608 and 572 cm^{-1} .

HRMS (APCI) m/z : $[\text{M}+\text{H}]^+$ calcd. for $\text{C}_{26}\text{H}_{32}\text{ONF}_2$, 412.2447; found, 412.2448.



5-(10-(3-(dimethylamino)propyl)-10H-phenothiazin-2-yl)-5,5-difluoropentan-1-ol (17):

Prepared according to the General Procedure A using Triflupromazine HCl (194 mg, 0.5 mmol, 1 equiv), 3-buten-1-ol (430 μL , 5.0 mmol, 10 equiv), potassium formate (126 mg, 1.5 mmol, 3 equiv), thiophenol (5 μL , 0.05 mmol, 10 mol%) and photocatalyst **P3** (6 mg, 0.01 mmol, 2 mol%) at 100 $^{\circ}\text{C}$. After 24 h, the reaction was purified according to the General Procedure A (silica gel, 20-80% EtOAc/hexanes) to provide the desired product as a colorless oil (134 mg, 66% yield).

R_f: 0.12 (60% ethyl acetate/hexanes)

¹H NMR (500 MHz, Chloroform-*d*) δ 7.20 – 7.11 (m, 3H), 7.02 (d, $J = 8.0$ Hz, 1H), 6.98 – 6.87 (m, 3H), 3.95 (t, $J = 6.9$ Hz, 2H), 3.57 (t, $J = 5.8$ Hz, 2H), 2.61 – 2.48 (m, 2H), 2.31 (s, 6H), 2.21

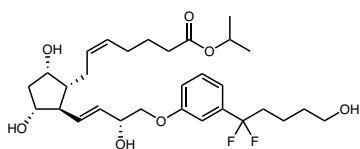
– 2.10 (m, 2H), 2.06 (p, $J = 7.2$ Hz, 2H), 1.52 (dt, $J = 11.6, 6.2$ Hz, 2H), 1.46 (ddt, $J = 15.3, 10.5, 5.1$ Hz, 2H).

^{13}C NMR (126 MHz, Chloroform-*d*) δ 145.3, 144.6, 136.5 (t, $J = 26.9$ Hz), 127.7, 127.6, 125.0, 123.3 (t, $J = 242.8$ Hz), 123.1, 119.5 (t, $J = 6.2$ Hz), 115.8, 112.8 (t, $J = 6.4$ Hz), 61.9, 57.0, 45.2, 45.1, 38.9 (t, $J = 27.6$ Hz), 32.1, 24.7, 19.9 (t, $J = 4.4$ Hz).

^{19}F NMR (282 MHz, Chloroform-*d*) δ -94.23 (t, $J = 15.3$ Hz).

FTIR (neat) ν_{max} : 3348, 2936, 2863, 1598, 1565, 1459, 1443, 1416, 1328, 1287, 1234, 1166, 1131, 1105, 1036, 915, 871, 816, 748, 670, and 648 cm^{-1} .

HRMS (APCI) m/z : $[\text{M}+\text{H}]^+$ calcd. for $\text{C}_{22}\text{H}_{29}\text{ON}_2\text{F}_2\text{S}$, 407.1962; found, 407.1963.



Isopropyl (Z)-7-((1*R*,2*R*,3*R*,5*S*)-2-((*R*,*E*)-4-(3-(1,1-difluoro-5-hydroxypentyl)phenoxy)-3-hydroxybut-1-en-1-yl)-3,5-dihydroxycyclopentyl)hept-5-enoate (18):

Prepared according to the General Procedure A using Travoprost (50 mg, 0.1 mmol, 1 equiv), 3-buten-1-ol (82 μL , 1.0 mmol, 10 equiv), potassium formate (25 mg, 0.3 mmol, 3 equiv), thiophenol (1.1 μL , 0.01 mmol, 10 mol%) and photocatalyst **P3** (1.2 mg, 0.002 mmol, 2 mol%) at 100 $^{\circ}\text{C}$. After 24 h, the reaction was purified using reverse phase preparative HPLC (30-99% MeCN/ H_2O) to provide the desired product as a colorless oil (40 mg, 73% yield).

^1H NMR (500 MHz, Chloroform-*d*) δ 7.33 (t, $J = 7.9$ Hz, 1H), 7.06 (d, $J = 7.7$ Hz, 1H), 7.02 (s, 1H), 6.96 (dd, $J = 8.1, 2.6$ Hz, 1H), 5.78 – 5.70 (m, 2H), 5.66 (ddd, $J = 15.4, 11.4, 6.0$ Hz, 2H), 4.99 (hept, $J = 6.2$ Hz, 1H), 4.54 (tt, $J = 6.8, 3.5$ Hz, 1H), 4.21 (dt, $J = 11.7, 3.8$ Hz, 1H), 4.04 –

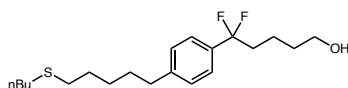
3.87 (m, 3H), 3.63 (t, $J = 6.3$ Hz, 2H), 2.46 – 1.92 (m, 12H), 1.85 – 1.45 (m, 6H), 1.22 (d, $J = 6.3$ Hz, 6H).

^{13}C NMR (126 MHz, Chloroform-*d*) δ 173.7, 158.6, 139.0 (t, $J = 26.6$ Hz), 135.1, 130.8, 129.9, 129.7, 129.1, 122.9 (t, $J = 242.4$ Hz), 118.1 – 117.6 (m), 115.9, 111.7 (t, $J = 6.4$ Hz), 78.2, 73.3, 72.1, 70.9, 67.7, 62.6, 56.1, 50.1, 42.8, 38.9 (t, $J = 27.6$ Hz), 34.1, 32.3, 31.3, 30.1, 26.8, 24.8, 22.0, 19.2 (t, $J = 4.2$ Hz).

^{19}F NMR (282 MHz, Chloroform-*d*) δ -95.31 (t, $J = 16.1$ Hz).

FTIR (neat) ν_{max} : 3384, 2926, 1717, 1588, 1489, 1444, 1374, 1328, 1264, 1179, 1107, 1036, 970, 896, 786, 733, 701, and 667 cm^{-1} .

HRMS (APCI) m/z : $[\text{M}+\text{H}]^+$ calcd. for $\text{C}_{30}\text{H}_{45}\text{O}_7\text{F}_2$, 555.3127; found, 555.3115.



5-(4-(5-(Butylthio)pentyl)phenyl)-5,5-difluoropentan-1-ol (19):

Prepared according to the General Procedure A using butyl(5-(4-(trifluoromethyl)phenyl)pentyl)sulfane (31 mg, 0.1 mmol, 1 equiv), and 3-buten-1-ol (43 μL , 0.5 mmol, 5 equiv), potassium formate (25 mg, 0.3 mmol, 3 equiv), thiophenol (1 μL , 0.001 mmol, 10 mol%) and photocatalyst **P3** (1.2 mg, 0.01 mmol, 2 mol%) at 100 $^{\circ}\text{C}$. After 24 h, the reaction was purified according to the General Procedure A (silica gel, 20-50% EtOAc/hexanes) to provide the desired product as a colorless oil (21 mg, 59 % yield).

R_f: 0.32 (30% ethyl acetate/hexanes)

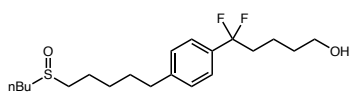
^1H NMR (400 MHz, CDCl_3) δ 7.36 (d, $J = 8.2$ Hz, 1H), 7.20 (d, $J = 7.8$ Hz, 1H), 3.61 (t, $J = 6.3$ Hz, 1H), 2.70 – 2.61 (m, 3H), 2.24 – 1.99 (m, 1H), 1.74 (ddt, $J = 29.5, 15.0, 7.6$ Hz, 3H), 1.60 – 1.38 (m, 3H), 1.01 – 0.92 (m, 2H).

^{13}C NMR (100 MHz, CDCl_3) δ 143.9, 135.0 (t, $^2J_{\text{C-F}} = 26.8$ Hz), 128.5, 125.1 (t, $^3J_{\text{C-F}} = 6.1$ Hz), 123.2 (t, $^1J_{\text{C-F}} = 241.8$ Hz), 62.5, 52.4, 39.0 (t, $^2J_{\text{C-F}} = 27.8$ Hz), 35.4, 32.4, 30.9, 28.5, 24.7, 22.7, 22.2, 19.2, 13.8.

^{19}F NMR (376 MHz, CDCl_3) δ -94.89 (t, $J = 16.1$ Hz).

FTIR (neat) ν_{max} : 3315, 2932, 1677, 1598, 1198, 1038 cm^{-1} .

HRMS (APCI) m/z : $[\text{M-H}]^-$ calcd. for $\text{C}_{20}\text{H}_{31}\text{OF}_2\text{S}$, 357.2058; found, 357.2064.



5-(4-(5-(Butylsulfinyl)pentyl)phenyl)-5,5-difluoropentan-1-ol (20):

Prepared according to the General Procedure A using 1-(5-(Butylsulfinyl)pentyl)-4-(trifluoromethyl)benzene (32 mg, 0.1 mmol, 1 equiv), and 3-buten-1-ol (43 μL , 0.5 mmol, 5 equiv), potassium formate (25 mg, 0.3 mmol, 3 equiv), thiophenol (1 μL , 0.001 mmol, 10 mol%) and photocatalyst **P3** (1.2 mg, 0.01 mmol, 2 mol%) at 100 $^\circ\text{C}$. After 24 h, the reaction was purified according to the General Procedure A (silica gel, 20-70% EtOAc/hexanes) to provide the desired product as a colorless oil (24 mg, 64 % yield).

R_f: 0.22 (30% ethyl acetate/hexanes)

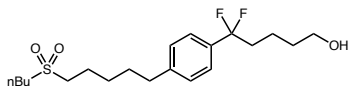
^1H NMR (600 MHz, CDCl_3) δ 7.36 (d, $J = 8.3$ Hz, 2H), 7.21 (d, $J = 7.7$ Hz, 2H), 3.62 (t, $J = 6.4$ Hz, 2H), 2.63 (t, $J = 7.6$ Hz, 2H), 2.50 (t, $J = 7.4$ Hz, 4H), 2.14 (ddt, $J = 16.3, 8.3, 4.3$ Hz, 2H), 1.66 – 1.47 (m, 10H), 1.46 – 1.37 (m, 4H), 0.91 (t, $J = 7.3$ Hz, 3H).

^{13}C NMR (126 MHz, CDCl_3) δ 143.9, 135.0 (t, $^2J_{\text{C-F}} = 26.7$ Hz), 128.5, 125.1 (t, $^3J_{\text{C-F}} = 6.2$ Hz), 123.2 (t, $^1J_{\text{C-F}} = 241.8$ Hz), 62.6, 52.3, 52.3, 39.0 (t, $^2J_{\text{C-F}} = 27.8$ Hz), 35.4, 32.4, 30.9, 28.5, 24.7, 22.7, 22.2, 19.2 (t, $^3J_{\text{C-F}} = 4.1$ Hz), 13.8.

^{19}F NMR (376 MHz, CDCl_3) δ -94.89 (t, $J = 15.9$ Hz).

FTIR (neat) ν_{max} : 3360, 2927, 2858, 1616, 1458, 1327, 1012 cm^{-1} .

HRMS (APCI) m/z : $[\text{M}+\text{H}]^+$ calcd. for $\text{C}_{20}\text{H}_{33}\text{O}_2\text{F}_2\text{S}$, 375.2164; found, 375.2169.



5-(4-(5-(Butylsulfonyl)pentyl)phenyl)-5,5-difluoropentan-1-ol (21):

Prepared according to the General Procedure A using 1-(5-(Butylsulfonyl)pentyl)-4-(trifluoromethyl)benzene (34 mg, 0.1 mmol, 1 equiv), and 3-buten-1-ol (43 μL , 0.5 mmol, 5 equiv), potassium formate (25 mg, 0.3 mmol, 3 equiv), thiophenol (1 μL , 0.001 mmol, 10 mol%) and photocatalyst **P3** (1.2 mg, 0.01 mmol, 2 mol%) at 100 $^{\circ}\text{C}$. After 24 h, the reaction was purified according to the General Procedure A (silica gel, 20-50% EtOAc/hexanes) to provide the desired product as a colorless oil (24 mg, 59 % yield).

R_f: 0.20 (30% ethyl acetate/hexanes)

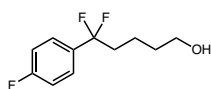
^1H NMR (600 MHz, CDCl_3) δ 7.35 (d, $J = 8.1$ Hz, 2H), 7.18 (d, $J = 8.0$ Hz, 2H), 3.60 (td, $J = 6.3$, 0.8 Hz, 2H), 2.96 – 2.81 (m, 4H), 2.63 (t, $J = 7.6$ Hz, 2H), 2.18 – 2.07 (m, 2H), 1.88 – 1.74 (m, 4H), 1.69 – 1.60 (m, 2H), 1.60 – 1.53 (m, 2H), 1.53 – 1.41 (m, 6H), 0.94 (td, $J = 7.3$, 0.8 Hz, 3H).

^{13}C NMR (126 MHz, CDCl_3) δ 143.9, 135.0 (t, $^2J_{\text{C-F}} = 26.7$ Hz), 128.5, 125.1 (t, $^3J_{\text{C-F}} = 6.2$ Hz), 123.2 (t, $^1J_{\text{C-F}} = 241.8$ Hz), 62.6, 52.3, 52.3, 39.0 (t, $^2J_{\text{C-F}} = 27.8$ Hz), 35.4, 32.4, 30.9, 28.5, 24.7, 22.7, 22.2, 19.2 (t, $^2J_{\text{C-F}} = 4.1$ Hz), 13.8.

^{19}F NMR (376 MHz, CDCl_3) δ -94.92 (t, $J = 16.0$ Hz).

FTIR (neat) ν_{max} : 3318, 3080, 2935, 1675, 1599, 1505, 1326, 1199, 1039, 771 cm^{-1} .

HRMS (ESI) m/z : $[\text{M}+\text{Na}]^+$ calcd. for $\text{C}_{20}\text{H}_{32}\text{O}_3\text{F}_2\text{SNa}$, 413.1932; found, 413.1938.



5,5-Difluoro-5-(4-fluorophenyl)pentan-1-ol (22):

Prepared according to the General Procedure A using 1-fluoro-4-(trifluoromethyl)benzene (82 mg, 0.5 mmol, 1 equiv), 3-buten-1-ol (215 μ L, 2.5 mmol, 5 equiv), potassium formate (126 mg, 1.5 mmol, 3 equiv), thiophenol (5 μ L, 0.05 mmol, 10 mol%) and photocatalyst **P3** (6 mg, 0.01 mmol, 2 mol%) at 100 $^{\circ}$ C. After 24 h, the reaction was purified according to the General Procedure A (silica gel, 10-50% EtOAc/hexanes) to provide the desired product as a colorless oil (52 mg, 48% yield).

R_f: 0.71 (60% ethyl acetate/hexanes)

¹H NMR (400 MHz, CDCl₃) δ 7.45 (dd, J = 8.7, 5.3 Hz, 2H), 7.10 (t, J = 8.7 Hz, 2H), 3.63 (t, J = 6.2 Hz, 2H), 2.27 – 2.05 (m, 2H), 1.63 – 1.43 (m, 4H).

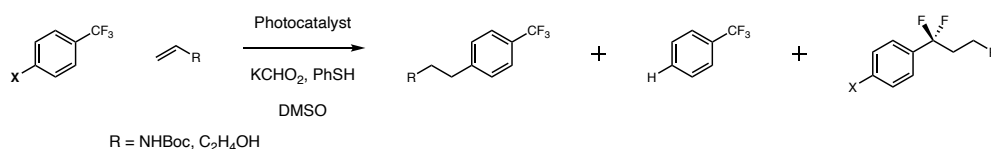
¹³C NMR (126 MHz, CDCl₃) δ 163.4 (d, $^1J_{C-F}$ = 248.7 Hz), 133.4 (td, J_{C-F} = 27.4, 3.3 Hz), 127.1 (dt, J_{C-F} = 8.6, 6.2 Hz), 122.7 (t, $^1J_{C-F}$ = 242.2 Hz), 115.5, 115.4, 62.5, 38.9 (t, $^2J_{C-F}$ = 27.6 Hz), 32.1, 19.0 (t, $^3J_{C-F}$ = 4.2 Hz).

¹⁹F NMR (376 MHz, CDCl₃) δ -94.64 (t, J = 16.1 Hz, 2F), -111.60 (s, 1F).

FTIR (neat) ν_{max} : 3330, 2931, 2874, 1608, 1514, 1327, 1232, 1161, 1035, 838 cm^{-1} .

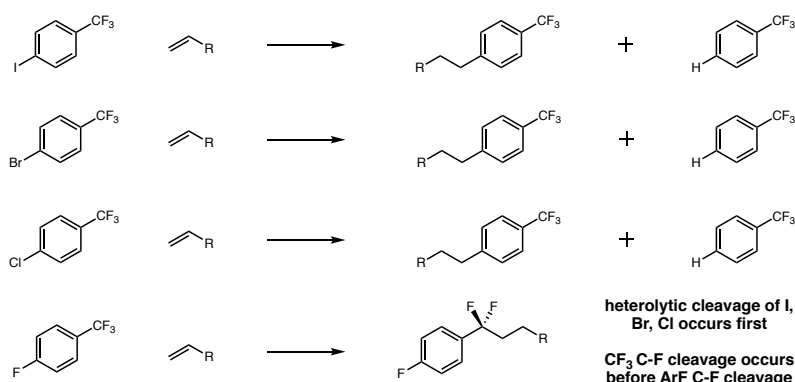
HRMS (APCI) m/z : [M+Cl⁻] calcd. for C₁₁H₁₃OF₃Cl, 253.0613; found, 253.0605.

Selectivity of Heterolytic Cleavage from Table 4.1



Reactions prepared according to General Procedure A with 4-halobenzotrifluoride (0.25 mmol) and alkene (3-buten-1-ol or tert-butyl vinylcarbamate, 0.75 mmol). All reactions with I, Br, and Cl

substituents gave either hydrodehalogenation (3-buten-1-ol) or alkylation via the aryl radical (tert-butyl vinylcarbamate).

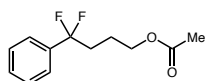


Observed reactivity profile for heterolytic cleavage



Predictable reactivity allows chemoselective reductive couplings

Products from Table 4.2: Defluoroalkylation Alkene Scope



4,4-difluoro-4-phenylbutyl acetate (23):

Prepared according to the General Procedure B using allyl acetate (54 μ L, 0.5 mmol, 1 equiv), α,α,α -trifluorotoluene (3 mL), potassium formate (210 mg, 2.5 mmol, 5 equiv), thiophenol (5 μ L, 0.05 mmol, 10 mol%) and photocatalyst **P3** (6 mg, 0.01 mmol, 2 mol%) at 100 °C. After 24 h, the reaction was purified according to the General Procedure B (silica gel, 5-30% EtOAc/hexanes) to provide the desired product as a colorless oil (73 mg, 64 % yield).

R_f: 0.62 (30% ethyl acetate/hexanes)

¹H NMR (600 MHz, Chloroform-*d*) δ 7.47 (s, 2H), 7.42 (s, 3H), 4.08 (t, $J = 6.4$ Hz, 2H), 2.20 (tt, $J = 16.1, 8.0$ Hz, 2H), 2.03 (s, 3H), 1.81 (p, $J = 6.6$ Hz, 2H).

¹³C NMR (151 MHz, Chloroform-*d*) δ 171.1, 137.2 (t, $J = 26.5$ Hz), 129.9, 128.6, 125.0 (t, $J = 6.2$ Hz), 122.8 (t, $J = 242.3$ Hz), 63.6, 35.9 (t, $J = 28.2$ Hz), 22.2 (t, $J = 4.1$ Hz), 21.0.

^{19}F NMR (282 MHz, Chloroform-*d*) δ -96.10 (t, J = 16.2 Hz).

FTIR (neat) ν_{max} : 2968, 1736, 1451, 1364, 1326, 1232, 1165, 1116, 1019, 973, 763, 730, 697, 661, 624, 605, and 576 cm^{-1} .

HRMS (NSI) m/z : $[\text{M}+\text{Na}]^+$ calcd. for $\text{C}_{12}\text{H}_{14}\text{O}_2\text{F}_2\text{Na}$, 251.08541; found, 251.08543.



5,5-difluoro-5-phenylpentan-1-ol and 4,4-difluoro-4-phenylbutanal (24a):

Prepared according to the General Procedure B using acrolein diethyl acetal (76 μL , 0.5 mmol, 1 equiv), α,α,α -trifluorotoluene (3 mL), potassium formate (210 mg, 2.5 mmol, 5 equiv), thiophenol (5 μL , 0.05 mmol, 10 mol%) and photocatalyst **P3** (6 mg, 0.01 mmol, 2 mol%) at 100 $^{\circ}\text{C}$. After 24 h, the reaction was purified according to the General Procedure B. While no hydrolysis of the acetal was observed during the reaction, upon purification on silica (5 – 10% EtOAc/Hexanes) formation of the aldehyde was observed. Accordingly, the remaining acetal was hydrolyzed in 10 mL of 5:1 THF:1 M HCl (aq), concentrated via rotary evaporation to a colorless oil, and characterized as the corresponding aldehyde (69 mg, 75% yield).

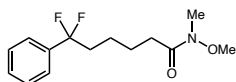
R_f: 0.86 (10% ethyl acetate/hexanes)

^1H NMR (500 MHz, Chloroform-*d*) δ 9.78 (p, J = 0.9 Hz, 1H), 7.50 – 7.40 (m, 5H), 2.70 (t, J = 7.5 Hz, 2H), 2.48 (tdd, J = 16.5, 8.2, 6.8 Hz, 2H).

^{13}C NMR (126 MHz, Chloroform-*d*) δ 199.9, 136.7 (t, J = 26.4 Hz), 130.2, 128.7, 125.0 (t, J = 6.2 Hz), 122.4 (t, J = 242.4 Hz), 37.3 (t, J = 3.2 Hz), 31.7 (t, J = 28.7 Hz), 29.9.

^{19}F NMR (282 MHz, Chloroform-*d*) δ -96.70 (t, J = 16.5 Hz).

FTIR (neat) ν_{max} : 2922, 2848, 2732, 1724, 1451, 1417, 1389, 1322, 1275, 1241, 1169, 1150, 1097, 1073, 1039, 974, 921, 763, 697, 634, 583, and 561 cm^{-1} .



6,6-difluoro-*N*-methoxy-*N*-methyl-6-phenylhexanamide (25):

Prepared according to the General Procedure B using *N*-methoxy-*N*-methylpent-4-enamide (72 mg, 0.5 mmol, 1 equiv), α,α,α -trifluorotoluene (3 mL), potassium formate (210 mg, 2.5 mmol, 5 equiv), thiophenol (5 μ L, 0.05 mmol, 10 mol%) and photocatalyst **P3** (6 mg, 0.01 mmol, 2 mol%) at 100 °C. After 24 h, the reaction was purified according to the General Procedure B (silica gel, 5-25% MeOH/DCM) to provide the desired product as a colorless oil (106 mg, 78 % yield).

R_f: 0.70 (60% ethyl acetate/hexanes)

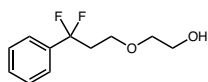
¹H NMR (600 MHz, Chloroform-*d*) δ 7.48 – 7.37 (m, 5H), 3.64 (s, 3H), 3.15 (s, 3H), 2.40 (s, 2H), 2.15 (tt, $J = 16.0, 8.2$ Hz, 2H), 1.66 (p, $J = 7.5$ Hz, 2H), 1.48 (p, $J = 8.3$ Hz, 2H).

¹³C NMR (151 MHz, Chloroform-*d*) δ 174.2, 137.5 (t, $J = 26.7$ Hz), 129.7, 128.5, 125.0 (t, $J = 6.2$ Hz), 123.0 (t, $J = 242.1$ Hz), 61.3, 39.0 (t, $J = 27.6$ Hz), 32.2, 31.7, 24.3, 22.5 (t, $J = 4.0$ Hz).

¹⁹F NMR (282 MHz, Chloroform-*d*) δ -95.59 (t, $J = 16.3$ Hz).

FTIR (neat) ν_{max} : 2939, 1658, 1451, 1415, 1385, 1326, 1172, 1144, 1115, 1069, 980, 921, 846, 763, 730, 698, 658, 625, and 575 cm^{-1} .

HRMS (NSI) m/z : $[M+Cl]^-$ calcd. for $\text{C}_{14}\text{H}_{20}\text{O}_2\text{NF}_2$, 272.1457; found, 272.1458.



2-(3,3-difluoro-3-phenylpropoxy)ethan-1-ol (26):

Prepared according to the General Procedure B using 2-(vinylxy)ethan-1-ol

(44 mg, 0.5 mmol, 1 equiv), α,α,α -trifluorotoluene (3 mL), potassium formate (210 mg, 2.5 mmol, 5 equiv), thiophenol (5 μ L, 0.05 mmol, 10 mol%) and photocatalyst **P3** (6 mg, 0.01 mmol, 2 mol%) at 100 °C. After 24 h, the reaction was purified according to the General Procedure B (silica gel, 10-50% EtOAc/hexanes) to provide the desired product as a colorless oil (71 mg, 66 % yield).

R_f: 0.59 (60% ethyl acetate/hexanes)

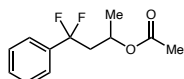
¹H NMR (600 MHz, Chloroform-*d*) δ 7.45 (d, J = 28.6 Hz, 5H), 3.62 (s, 4H), 3.45 (s, 2H), 2.48 (tt, J = 15.6, 6.6 Hz, 2H), 2.05 (s, 1H).

¹³C NMR (151 MHz, Chloroform-*d*) δ 137.1 (t, J = 26.3 Hz), 129.9 (t, J = 1.4 Hz), 128.5, 124.9 (t, J = 6.3 Hz), 122.1 (t, J = 242.4 Hz), 72.1, 65.2 (t, J = 5.1 Hz), 61.7, 39.2 (t, J = 27.5 Hz).

¹⁹F NMR (282 MHz, Chloroform-*d*) δ -94.16 (t, J = 16.0 Hz).

FTIR (neat) ν_{max} : 3411, 2877, 1721, 1451, 1365, 1318, 1255, 1156, 1123, 1062, 960, 920, 890, 812, 762, 733, 697, 659, 627, and 583 cm^{-1} .

HRMS (NSI) m/z : $[\text{M}+\text{Na}]^+$ calcd. for $\text{C}_{11}\text{H}_{14}\text{O}_2\text{F}_2\text{Na}$, 239.0854; found, 239.0852.



4,4-difluoro-4-phenylbutan-2-yl acetate (27):

Prepared according to the General Procedure B using prop-1-en-2-yl acetate (50 mg, 0.5 mmol, 1 equiv), α,α,α -trifluorotoluene (3 mL), potassium formate (210 mg, 2.5 mmol, 5 equiv), thiophenol (5 μ L, 0.05 mmol, 10 mol%) and photocatalyst **P3** (6 mg, 0.01 mmol, 2 mol%) at 100 °C. After 24 h, the reaction was purified according to the General Procedure B (silica gel, 10-30% EtOAc/hexanes) to provide the desired product as a colorless oil (63mg, 55% yield).

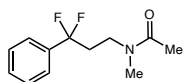
R_f: 0.68 (30% ethyl acetate/hexanes)

¹H NMR (600 MHz, Chloroform-*d*) δ 7.43 (d, J = 17.1 Hz, 5H), 5.21 – 5.01 (m, 1H), 2.55 (ddt, J = 23.3, 15.6, 7.8 Hz, 1H), 2.37 – 2.21 (m, 1H), 1.79 (s, 3H), 1.26 (d, J = 6.2 Hz, 3H).

¹³C NMR (151 MHz, Chloroform-*d*) δ 170.2, 137.0 (t, J = 26.2 Hz), 129.9, 128.6, 125.1 (t, J = 6.4 Hz), 121.7 (t, J = 243.1 Hz), 65.8 (dd, J = 5.4, 3.4 Hz), 44.9 (t, J = 27.6 Hz), 21.1, 21.0.

¹⁹F NMR (282 MHz, Chloroform-*d*) δ -90.45 (ddd, J = 248.7, 15.7, 12.2 Hz), -97.01 (dt, J = 249.4, 17.5 Hz).

FTIR (neat) ν_{max} : 2923, 2853, 1738, 1496, 1451, 1372, 1325, 1241, 1164, 1122, 1069, 1018, 957, 920, 796, 769, 735, 697, 667, 630, and 606 cm^{-1} .



***N*-(3,3-difluoro-3-phenylpropyl)-*N*-methylacetamide (28):**

Prepared according to the General Procedure B using *N*-methyl-*N*-vinylacetamide

(50 mg, 0.5 mmol, 1 equiv), α,α,α -trifluorotoluene (3 mL), potassium formate (210 mg, 2.5 mmol, 5 equiv), thiophenol (5 μL , 0.05 mmol, 10 mol%) and photocatalyst **P3** (6 mg, 0.01 mmol, 2 mol%) at 100 $^{\circ}\text{C}$. After 24 h, the reaction was purified according to the General Procedure B (silica gel, 30-80% EtOAc/hexanes) to provide the desired product as a colorless oil (108 mg, 95 % yield).

R_f: 0.44 (60% ethyl acetate/hexanes)

¹H NMR (500 MHz, Chloroform-*d*) δ 7.55 – 7.33 (m, 5H), 3.47 (dt, J = 16.0, 7.5 Hz, 2H), 2.88 (d, J = 29.7 Hz, 3H), 2.37 (dh, J = 21.5, 7.7 Hz, 2H), 1.99 (d, J = 18.5 Hz, 3H).

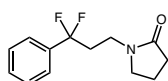
¹³C NMR (126 MHz, Chloroform-*d*) δ 170.6, 170.3, 136.8 (t, J = 26.2 Hz), 136.4 (t, J = 26.1 Hz), 130.2, 129.9, 128.7, 128.5, 124.8 (t, J = 6.2 Hz), 124.6 (t, J = 6.3 Hz), 122.1 (t, J = 242.2 Hz),

121.6 (t, $J = 242.9$ Hz), 44.7 (t, $J = 4.6$ Hz), 42.5 (t, $J = 4.8$ Hz), 37.7 (t, $J = 27.4$ Hz), 36.7, 36.2 (t, $J = 27.3$ Hz), 33.1, 21.8, 21.0.

^{19}F NMR (282 MHz, Chloroform-*d*) δ -95.132 (t, $J = 16.8$ Hz), -96.67 (t, $J = 16.5$ Hz).

FTIR (neat) ν_{max} : 3459, 2937, 1635, 1488, 1451, 1406, 1362, 1325, 1303, 1246, 1208, 1156, 1131, 1058, 1029, 1003, 963, 944, 765, 728, 698, 656, 632, 597, and 578 cm^{-1} .

HRMS (NSI) m/z : $[\text{M}+\text{H}]^+$ calcd. for $\text{C}_{12}\text{H}_{16}\text{ONF}_2$, 228.1195; found, 228.1194.



1-(3,3-difluoro-3-phenylpropyl)pyrrolidin-2-one (29):

Prepared according to the General Procedure B using 1-vinylpyrrolidin-2-one (53 μL , 0.5 mmol, 1 equiv), α,α,α -trifluorotoluene (3 mL), potassium formate (210 mg, 2.5 mmol, 5 equiv), thiophenol (5 μL , 0.05 mmol, 10 mol%) and photocatalyst **P3** (6 mg, 0.01 mmol, 2 mol%) at 100 $^{\circ}\text{C}$. After 24 h, the reaction was purified according to the General Procedure B (silica gel, 30-80% EtOAc/hexanes) to provide the desired product as a colorless oil (106 mg, 89 % yield).

R_f: 0.35 (60% ethyl acetate/hexanes)

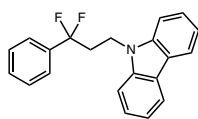
^1H NMR (600 MHz, Chloroform-*d*) δ 7.45 (d, $J = 31.0$ Hz, 5H), 3.47 (t, $J = 7.1$ Hz, 2H), 3.33 (t, $J = 6.9$ Hz, 2H), 2.40 (tt, $J = 15.3, 7.2$ Hz, 2H), 2.30 (t, $J = 8.0$ Hz, 2H), 1.93 (p, $J = 7.5$ Hz, 2H).

^{13}C NMR (151 MHz, Chloroform-*d*) δ 175.0, 136.7 (t, $J = 26.2$ Hz), 130.0, 128.5, 124.8 (t, $J = 6.3$ Hz), 121.9 (t, $J = 242.6$ Hz), 47.3, 36.9 (t, $J = 4.9$ Hz), 36.4 (t, $J = 27.7$ Hz), 30.9, 17.9.

^{19}F NMR (282 MHz, Chloroform-*d*) δ -95.63 (t, $J = 16.2$ Hz).

FTIR (neat) ν_{max} : 3461, 2938, 1675, 1495, 1463, 1450, 1424, 1388, 1318, 1287, 1267, 1246, 1188, 1167, 1104, 1057, 1012, 947, 923, 764, 698, 647, 610, 582, and 562 cm^{-1} .

HRMS (NSI) m/z : $[\text{M}+\text{H}]^+$ calcd. for $\text{C}_{13}\text{H}_{16}\text{ONF}_2$, 240.1195; found, 240.1195.



9-(3,3-difluoro-3-phenylpropyl)-9H-carbazole (30):

Prepared according to the General Procedure B using 9-vinylcarbazole (97 mg, 0.5 mmol, 1 equiv), α,α,α -trifluorotoluene (3 mL), potassium formate (210 mg, 2.5 mmol, 5 equiv), thiophenol (5 μ L, 0.05 mmol, 10 mol%) and photocatalyst **P3** (6 mg, 0.01 mmol, 2 mol%) at 100 °C. After 24 h, the reaction was purified according to the General Procedure B (silica gel, 10-30% EtOAc/hexanes) to provide the desired product as an amorphous white solid (114 mg, 71 % yield).

R_f: 0.76 (30% ethyl acetate/hexanes)

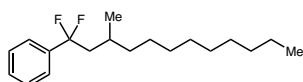
¹H NMR (500 MHz, Acetone-*d*₆) δ 8.12 (d, *J* = 7.7 Hz, 2H), 7.63 – 7.56 (m, 2H), 7.52 – 7.39 (m, 7H), 7.21 (ddd, *J* = 7.8, 6.0, 2.1 Hz, 2H), 4.57 (d, *J* = 7.6 Hz, 2H), 2.81 – 2.68 (m, 1H).

¹³C NMR (126 MHz, Acetone-*d*₆) δ 140.0, 136.5 (t, *J* = 26.0 Hz), 130.2, 129.1, 128.6, 128.4, 125.8, 124.8 (t, *J* = 6.3 Hz), 123.0, 122.3 (t, *J* = 241.7 Hz), 120.2, 119.1, 108.7, 37.0 (t, *J* = 27.2 Hz), 36.5 (t, *J* = 5.2 Hz).

¹⁹F NMR (282 MHz, Acetone-*d*₆) δ -96.63 (t, *J* = 16.2 Hz).

FTIR (neat) ν_{max} : 3046, 1592, 1483, 1450, 1465, 1355, 1387, 1324, 1235, 966, 974, 966, 951, 931, 761, 747, 723, 695, 666, 592, 572, and 528 cm⁻¹.

HRMS (APCI) *m/z*: [M+H]⁺ calcd. for C₂₁H₁₈NF₂, 322.1402; found, 322.1403.



(1,1-difluoro-3-methyldodecyl)benzene (31):

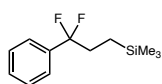
Prepared according to the General Procedure B using 2-methylundec-1-ene (84 mg, 0.5 mmol, 1 equiv), α,α,α -trifluorotoluene (3 mL), potassium formate (210 mg, 2.5 mmol, 5 equiv), thiophenol (5 μ L, 0.05 mmol, 10 mol%) and photocatalyst **P3** (6 mg, 0.01 mmol, 2 mol%) at 100 °C. After 24 h, the reaction was purified according to the General Procedure B (silica gel, 10% toluene/hexanes) to provide the desired product as a colorless oil (139 mg, 94 % yield).

^1H NMR (500 MHz, Chloroform-*d*) δ 7.51 – 7.47 (m, 2H), 7.45 – 7.41 (m, 3H), 2.24 – 2.10 (m, 1H), 2.09 – 1.90 (m, 1H), 1.71 (dq, $J = 12.1, 6.1$ Hz, 1H), 1.40 – 1.16 (m, 16H), 0.96 (d, $J = 6.7$ Hz, 3H), 0.95 – 0.88 (m, 3H).

^{13}C NMR (126 MHz, Chloroform-*d*) δ 138.2 (t, $J = 26.7$ Hz), 129.6 (t, $J = 1.6$ Hz), 128.5, 125.0 (t, $J = 6.3$ Hz), 123.7 (t, $J = 242.9$ Hz), 45.9 (t, $J = 26.1$ Hz), 37.7, 32.1, 29.9, 29.8, 29.8, 29.5, 28.1 (t, $J = 2.7$ Hz), 26.8, 22.9, 20.7, 14.3.

^{19}F NMR (282 MHz, Chloroform-*d*) δ -91.37 (ddd, $J = 244.4, 20.4, 12.8$ Hz), -94.90 (ddd, $J = 244.2, 19.7, 16.5$ Hz).

FTIR (neat) ν_{max} : 2923, 2853, 1451, 1370, 1310, 1255, 1170, 989, 918, 768, 759, 729, 696, 661, 627 and 581 cm^{-1} .



(3,3-difluoro-3-phenylpropyl)trimethylsilane (32):

Prepared according to the General Procedure B using trimethyl(vinyl)silane (73 μ L, 0.5 mmol, 1 equiv), α,α,α -trifluorotoluene (3 mL), potassium formate (210 mg, 2.5 mmol, 5 equiv), thiophenol (5 μ L, 0.05 mmol, 10 mol%) and photocatalyst **P3** (6 mg, 0.01 mmol, 2 mol%) at 100 °C. After 24 h, the reaction was purified according to the General Procedure B (silica gel, 2-5% EtOAc/hexanes) to provide the desired product as a colorless oil (100 mg, 88 % yield).

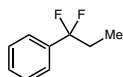
^1H NMR (600 MHz, Chloroform-*d*) δ 7.64 – 7.31 (m, 5H), 2.14 – 2.02 (m, 2H), 0.65 – 0.57 (m, 2H), 0.00 (s, 9H).

^{13}C NMR (151 MHz, Chloroform-*d*) δ 137.6 (t, $J = 26.9$ Hz), 129.6, 128.5, 125.2 (t, $J = 6.2$ Hz), 122.9 (t, $J = 242.3$ Hz), 34.0 (t, $J = 28.9$ Hz), 8.9 (t, $J = 2.7$ Hz), -1.9.

^{19}F NMR (282 MHz, Chloroform-*d*) δ -97.38 (t, $J = 15.7$ Hz).

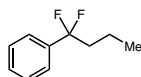
FTIR (neat) ν_{max} : 2952, 1451, 1326, 1247, 1170, 1135, 1022, 972, 917, 891, 828, 761, 723, 695, 668, 650, 598, and 572 cm^{-1} .

HRMS (NSI) m/z : $[\text{M}+\text{Cl}]^-$ calcd. for $\text{C}_{12}\text{H}_{18}\text{O}^{35}\text{ClF}_2\text{Si}$, 279.0789; found, 279.0789.



(1,1-difluoropropyl)benzene (33):

Prepared according to the General Procedure C using ethylene (25 psi), α,α,α -trifluorotoluene (6 mL), potassium formate (420 mg, 5.0 mmol, 1 equiv), thiophenol (10 μL , 0.10 mmol, 2 mol%) photocatalyst **P3** (12 mg, 0.01 mmol, 0.4 mol%), and DMSO (10 mL) at 100 $^\circ\text{C}$. After 24 h, the reaction showed a 65% yield with respect to potassium formate when analyzed by ^{19}F NMR with an internal standard. The reaction was purified according to the General Procedure C (silica gel, 10% benzene-*d*₆/pentane) to provide the desired product as a solution in benzene-*d*₆. The spectral data matched that of commercially available material. (Sigma Aldrich, CAS Number 74185-83-4)



(1,1-difluorobutyl)benzene (34):

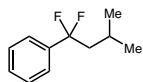
Prepared according to the General Procedure C using propylene (25 psi), α,α,α -trifluorotoluene (6 mL), potassium formate (420 mg, 5.0 mmol, 1 equiv), thiophenol (10 μ L, 0.10 mmol, 2 mol%) photocatalyst **P3** (12 mg, 0.01 mmol, 0.4 mol%), and DMSO (10 mL) at 100 °C. After 24 h, the reaction showed a 68% yield with respect to potassium formate when analyzed by ^{19}F NMR with an internal standard. The reaction was purified according to the General Procedure C (silica gel, 10% benzene- d_6 /pentane) to provide the desired product as a solution in benzene- d_6 .

^1H NMR (500 MHz, Benzene- d_6) δ 7.42 – 7.38 (m, 1H), 7.16 (dt, $J = 4.5, 2.1$ Hz, 2H), 2.01 – 1.89 (m, 1H), 1.44 – 1.33 (m, 1H), 0.76 (t, $J = 7.5$ Hz, 1H).

^{13}C NMR (126 MHz, Benzene- d_6) δ 138.1 (t, $J = 26.7$ Hz), 129.7, 128.6, 125.3 (t, $J = 6.3$ Hz), 123.4 (t, $J = 242.0$ Hz), 41.4 (t, $J = 27.3$ Hz), 16.4 (t, $J = 4.4$ Hz), 13.8.

^{19}F NMR (282 MHz, Benzene- d_6) δ -95.36 (t, $J = 16.2$ Hz).

FTIR (Benzene- d_6) ν_{max} : 2965, 2935, 2877, 1451, 1380, 1326, 1289, 1255, 1166, 1119, 1052, 1013, 980, 920, 892, 863, 812, 761, 727, 696, 659, 623, 587, and 574 cm^{-1} .



(1,1-difluoro-3-methylbutyl)benzene (35):

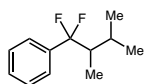
Prepared according to the General Procedure B using 2-Methylprop-1-ene (25 psi), α,α,α -trifluorotoluene (6 mL), potassium formate (420 mg, 5.0 mmol, 1 equiv), thiophenol (10 μ L, 0.10 mmol, 2 mol%) photocatalyst **P3** (12 mg, 0.01 mmol, 0.4 mol%), and DMSO (10 mL) at 100 °C. After 24 h, the reaction showed a 87% yield with respect to potassium formate when analyzed by ^{19}F NMR with an internal standard. The reaction was purified according to the General Procedure B (silica gel, 10% benzene- d_6 /pentane) to provide the desired product as a colorless oil.

¹H NMR (500 MHz, Benzene-*d*₆) δ 7.39 – 7.34 (m, 2H), 7.07 (dd, *J* = 5.0, 1.8 Hz, 3H), 1.87 (td, *J* = 17.2, 6.1 Hz, 2H), 1.79 (dt, *J* = 13.0, 6.5 Hz, 1H), 0.81 (d, *J* = 6.6 Hz, 5H).

¹³C NMR (126 MHz, Benzene-*d*₆) δ 138.5 (t, *J* = 26.7 Hz), 129.6 (t, *J* = 1.6 Hz), 128.6, 125.2 (t, *J* = 6.3 Hz), 123.7 (t, *J* = 242.7 Hz), 47.6 (t, *J* = 26.2 Hz), 23.7 (t, *J* = 3.0 Hz), 23.5.

¹⁹F NMR (282 MHz, Benzene-*d*₆) δ -93.10 (t, *J* = 16.8 Hz).

FTIR (Benzene-*d*₆) ν_{max} : 2965, 2935, 2877, 1451, 1380, 1326, 1289, 1255, 1166, 1119, 1052, 1013, 980, 920, 892, 863, 812, 761, 727, 696, 659, 623, 587, and 574 cm⁻¹.



(1,1-difluoro-2,3-dimethylbutyl)benzene (36):

Prepared according to the General Procedure B using 2-methyl-2-butene (53 μ L, 0.5 mmol, 1 equiv), and α,α,α -trifluorotoluene (3 mL), potassium formate (210 mg, 2.5 mmol, 5 equiv), thiophenol (5 μ L, 0.05 mmol, 10 mol%) and photocatalyst **P3** (6 mg, 0.01 mmol, 2 mol%) at 100 °C. After 24 h, the reaction was purified according to the General Procedure B (silica gel, 10% toluene/hexanes) to provide the desired product as a colorless oil (57 mg, 57 % yield).

¹H NMR (500 MHz, Chloroform-*d*) δ 7.48 – 7.40 (m, 5H), 2.12 (tqd, *J* = 16.9, 7.1, 2.7 Hz, 1H), 1.93 (dqdd, *J* = 13.8, 6.9, 2.7, 0.7 Hz, 1H), 0.97 (d, *J* = 7.1 Hz, 3H), 0.92 (d, *J* = 7.0 Hz, 3H), 0.87 (dt, *J* = 6.8, 1.1 Hz, 3H).

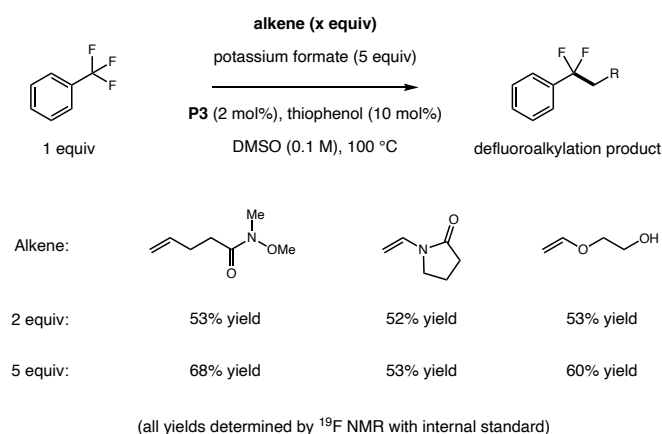
¹³C NMR (126 MHz, Chloroform-*d*) δ 137.7 (t, *J* = 27.0 Hz), 129.5 (t, *J* = 1.6 Hz), 128.4, 125.4 (t, *J* = 6.5 Hz), 125.2 (t, *J* = 247.5 Hz), 46.5 (t, *J* = 24.5 Hz), 26.5 (dd, *J* = 3.1, 1.7 Hz), 22.6, 17.0 (t, *J* = 2.0 Hz), 7.2 (dd, *J* = 5.3, 3.9 Hz).

¹⁹F NMR (282 MHz, Chloroform-*d*) δ -100.61 (ddd, *J* = 1542.6, 243.8, 16.8 Hz).

FTIR (neat) ν_{max} : 2962, 1466, 1450, 1392, 1369, 1314, 1294, 1261, 1193, 1145, 1075, 1059, 1021, 980, 919, 906, 790, 761, 697, 662, 599, and 571.2 cm^{-1} .

Yields of benzotrifluoride with 2 and 5 equiv of select alkenes

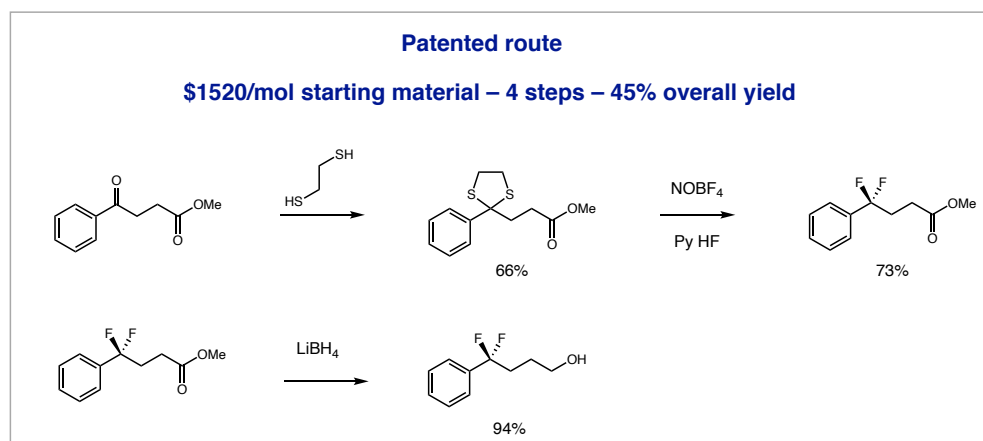
The reaction of benzotrifluoride (0.5 mmol, 1 equiv), photocatalyst P3 (6 mg, 0.01 mmol, 0.02 equiv), alkene (tabulated amounts), and potassium formate (267 mg, 1.5 mmol, 3.0 equiv) were reacted for 24 hours at 100 °C under irradiation of blue LEDs. Fluorobenzene (0.5 mmol, 1 equiv) was added as an internal fluorine standard after the reaction was complete. The yield of each reaction was determined by ^{19}F NMR integration of the characteristic fluorine peaks against the internal standard.



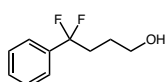
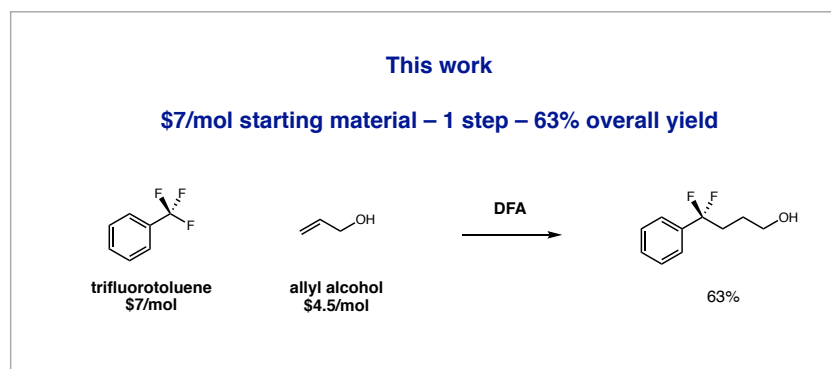
Products from Scheme 4.2: Drug Intermediates and Comparative Routes

Compound 37

Literature Route¹²⁹



This Route: 1 step from cheap commercial materials with an overall yield of 63%



4,4-Difluoro-4-phenylbutan-1-ol (37):

Prepared according to the General Procedure A using allyl alcohol (34 μ L, 0.5 mmol, 1 equiv), trifluorotoluene (3 mL, 25 mmol, 50 equiv), potassium formate (210 mg, 2.5 mmol, 5 equiv), thiophenol (5 μ L, 0.05 mmol, 10 mol%) and photocatalyst **P3** (6 mg, 0.01 mmol, 2 mol%) at 100 $^{\circ}$ C. After 24 h, the reaction was purified according to the General Procedure A (silica gel, 20-50% EtOAc/hexanes) to provide the desired product as a dark oil (59 mg, 63 % yield).

R_f: 0.65 (60% ethyl acetate/hexanes)

^1H NMR (300 MHz, CDCl_3) δ 7.53 – 7.44 (m, 2H), 7.45 – 7.38 (m, 3H), 3.59 (t, $J = 6.4$ Hz, 2H), 2.88 (s, 1H), 2.36 – 2.09 (m, 2H), 1.69 (dtd, $J = 11.4, 7.9, 7.2, 5.5$ Hz, 2H).

^{13}C NMR (75 MHz, CDCl_3) δ 137.2 (t, $^2J_{\text{C-F}} = 26.7$ Hz), 129.7 (t, $J_{\text{C-F}} = 1.7$ Hz), 128.5, 124.9 (t, $^3J_{\text{C-F}} = 6.3$ Hz), 123.1 (t, $^1J_{\text{C-F}} = 242.0$ Hz), 61.7, 35.5 (t, $^2J_{\text{C-F}} = 27.9$ Hz), 25.7 (t, $^3J_{\text{C-F}} = 3.8$ Hz).

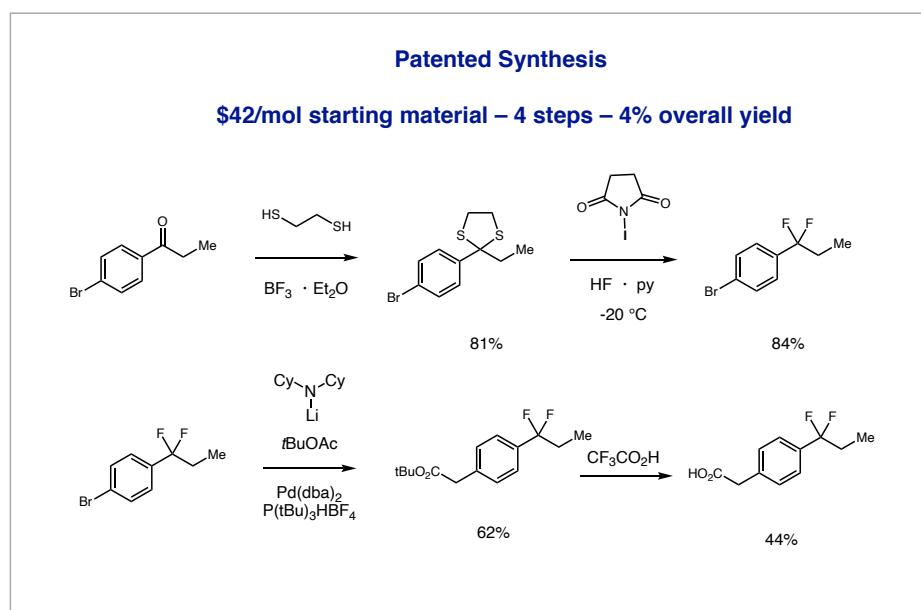
^{19}F NMR (282 MHz, CDCl_3) δ -95.42 (t, $J = 16.5$ Hz).

FTIR (neat) ν_{max} : 3331, 2936, 2879, 1450, 1324, 1058, 975 cm^{-1} .

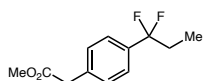
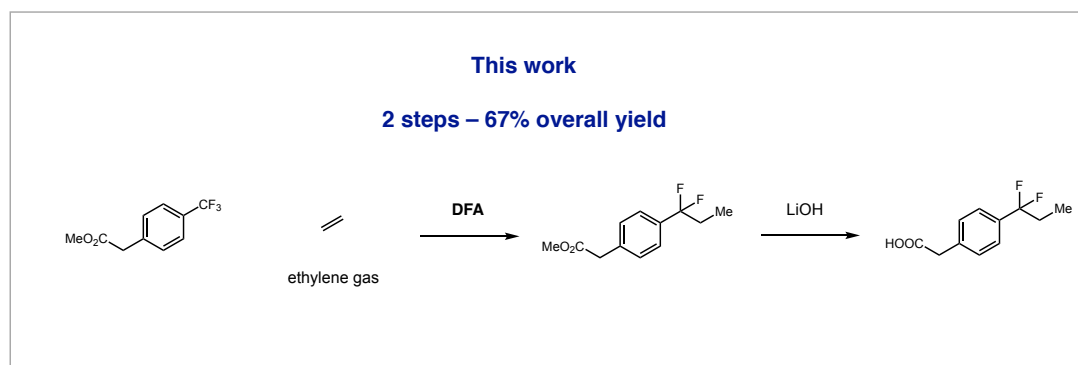
HRMS (APCI) m/z : $[\text{M-H}]^-$ calcd. for $\text{C}_{10}\text{H}_{11}\text{OF}_2$, 185.0783; found, 185.0778.

Compound 40

Literature Route¹³⁰



This Route



Methyl 2-(4-(1,1-difluoropropyl)phenyl)acetate (**40a**):

Prepared according to the General Procedure A using methyl 2-(4-(trifluoromethyl)phenyl)acetate (436 mg, 2 mmol, 1 equiv), and ethylene gas (regulated at 15 psi, see General Procedure C), potassium formate (504 mg, 6 mmol, 3 equiv), thiophenol (20 μL , 0.2 mmol, 10 mol%) and photocatalyst **P3** (25 mg, 0.04 mmol, 2 mol%) at 100 $^{\circ}\text{C}$. After 24 h, the reaction was purified according to the General Procedure A (silica gel, 50% PhMe/hexanes) to provide the desired product as a colorless oil (305 mg, 67 % yield).

R_f: 0.68 (30% ethyl acetate/hexanes)

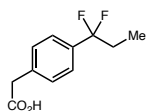
¹H NMR (600 MHz, CDCl_3) δ 7.42 (d, $J = 6.7$ Hz, 2H), 7.33 (d, $J = 7.8$ Hz, 2H), 3.70 (s, 3H), 3.66 (s, 2H), 2.19 – 2.08 (m, 2H), 0.98 (t, $J = 7.5$ Hz, 3H).

¹³C NMR (100 MHz, CDCl_3) δ 171.8, 136.3 (t, $J = 27.0$ Hz), 135.6, 129.4, 125.5 (t, $J = 6.2$ Hz), 122.2 (d, $J = 241.8$ Hz), 52.3 (d, $J = 1.2$ Hz), 41.0, 32.4 (t, $J = 28.5$ Hz), 7.0 (t, $J = 5.1$ Hz).

¹⁹F NMR (376 MHz, CDCl_3) δ -97.42 (t, $J = 16.1$ Hz).

FTIR (neat) ν_{max} : 2983, 2951, 1735, 1436, 1322, 1261, 1161 cm^{-1} .

HRMS (APCI) m/z : $[\text{M}+\text{H}]^+$ calcd. for $\text{C}_{12}\text{H}_{15}\text{O}_2\text{F}_2$, 229.1035; found, 229.1035.



2-(4-(1,1-Difluoropropyl)phenyl)acetic acid (40):

A 5 mL reaction vial was charged with methyl 2-(4-(1,1-difluoropropyl)phenyl)acetate (23 mg, 1 equiv, 0.1 mmol) and LiOH (24 mg, 10 equiv, 1 mmol). The solids were diluted with 1 mL 4:1 THF:H₂O, and stirred at room temperature for 2 h. The reaction mixture was quenched with 1 M HCl (5 mL) and diluted with EtOAc (5 mL). The organics were separated, dried over Na₂SO₄ and concentrated under reduced pressure to provide the desired product as an off white solid (21 mg, 98%).

¹H NMR (500 MHz, CDCl₃) δ 7.43 (d, *J* = 8.1 Hz, 2H), 7.34 (d, *J* = 8.1 Hz, 2H), 3.68 (s, 2H), 2.13 (td, *J* = 16.1, 7.5 Hz, 2H), 0.98 (t, *J* = 7.5 Hz, 3H).

¹³C NMR (126 MHz, CDCl₃) δ 177.31, 136.59 (t, *J* = 27.1 Hz), 134.83, 129.54, 125.54 (t, *J* = 6.2 Hz), 123.4 (t, *J* = 241.9 Hz), 40.81, 32.40 (t, *J* = 28.4 Hz), 6.97 (t, *J* = 5.0 Hz).

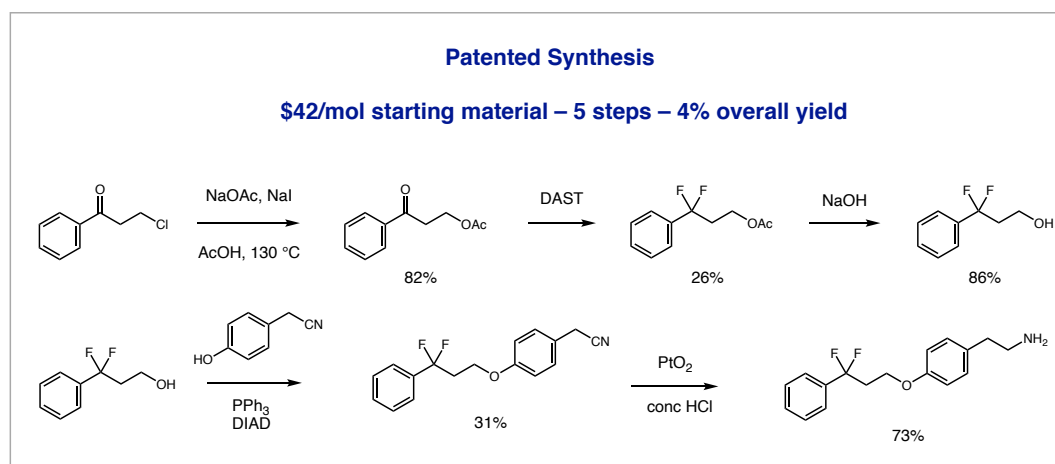
¹⁹F NMR (376 MHz, CDCl₃) δ -97.49 (t, *J* = 16.0 Hz).

FTIR (neat) ν_{max} : 2984, 2944, 1707, 1584, 1416, 1323, 1238, 1095 cm⁻¹.

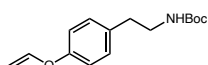
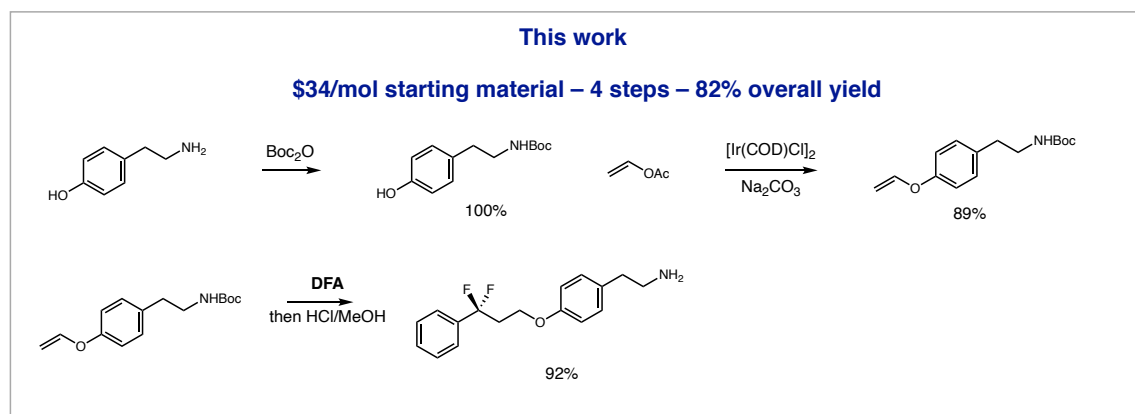
HRMS (APCI) *m/z*: [M-H]⁻ calcd. for C₁₁H₁₁O₂F₂, 213.0733; found, 213.0729.

Compound 44

Literature Route¹³¹



This Route



***tert*-Butyl (4-(vinyloxy)phenethyl)carbamate (46):**

Synthesized according to the procedure of Ishii *et al.*¹⁰²

To a toluene solution (150 mL) of $[\text{IrCl}(\text{cod})]_2$ (1 g, 1 mol%, 1.5 mmol) and Na_2CO_3 (10 g, 0.6 equiv, 90 mmol) were added *tert*-butyl (4-hydroxyphenethyl)carbamate (35 g, 1, equiv, 150 mmol) and vinyl acetate (28 mL, 2 equiv, 300 mmol) under an atmosphere of Ar. The reaction mixture was stirred at 90 °C for 24 h. After quenching with wet ether, and concentration under reduced

pressure, the crude residue was purified by column chromatography (silica gel, 0-10% hexane/EtOAc) to provide the desired compound as an off white amorphous solid (35 g, 89%).

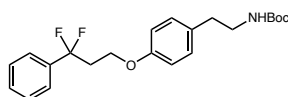
R_f: 0.55 (30% ethyl acetate/hexanes)

¹H NMR (500 MHz, CDCl₃) δ 7.11 (d, *J* = 8.6 Hz, 2H), 6.91 (d, *J* = 8.5 Hz, 2H), 6.59 (dd, *J* = 13.7, 6.1 Hz, 1H), 4.71 (dd, *J* = 13.7, 1.6 Hz, 1H), 4.38 (dd, *J* = 6.1, 1.7 Hz, 1H), 3.31 (q, *J* = 6.8 Hz, 2H), 2.73 (t, *J* = 7.2 Hz, 2H), 1.41 (s, 9H).

¹³C NMR (126 MHz, CDCl₃) δ 155.9, 155.4, 148.3, 133.8, 129.9, 117.2, 94.8, 79.1, 41.9, 35.4, 28.4.

FTIR (neat) ν_{max} : 3362, 2981, 2935, 2875, 1680, 1605, 1526, 1506, 1237 cm⁻¹.

HRMS (APCI) *m/z*: [M+H]⁺ calcd. for C₁₅H₂₂O₃N, 264.1594; found, 264.1596.



5-(4-(5-(Butylsulfonyl)pentyl)phenyl)-5,5-difluoropentan-1-ol (44a):

Small Scale

Prepared according to the General Procedure A using *t*-butyl (4-(vinylloxy)phenethyl)carbamate (67 mg, 0.25 mmol, 1 equiv), trifluorotoluene (1.5 mL, 75 mmol, 50 equiv), potassium formate (105 mg, 0.5 mmol, 5 equiv), thiophenol (3 μL, 0.0025 mmol, 10 mol%) and photocatalyst **P3** (3 mg, 0.005 mmol, 2 mol%) in DMSO (2.5 mL) at 100 °C. After 24 h, the reaction was purified according to the General Procedure A (silica gel, 20-40% EtOAc/hexanes) to provide the desired product as an amorphous white solid (90 mg, 92 % yield).

Large Scale

A 250 mL Schlenk flask was charged with *t*-butyl (4-(vinylloxy)phenethyl)carbamate (3.2 g, 12 mmol, 1 equiv), potassium formate (5 g, 60.0 mmol, 5 equiv), and photocatalyst **P3** (75 mg, 0.12

mmol, 1 mol%). The flask was purged with N₂ three times before the addition of trifluorotoluene (70 mL, 600 mmol, 50 equiv), thiophenol (122 μL, 0.0025 mmol, 10 mol%) and DMSO (120 mL). The flask was then heated to 100 °C in a large oil bath for 24 h under irradiation (blue light, 4 LED arrays). Upon completion, the reaction was diluted with EtOAc (250 mL) and brine (200 mL). The organics were separated, washed with brine (2 x 200 mL) and dried over Na₂SO₄. The crude reaction mixture was purified by flash column chromatography (silica gel, 10-40% EtOAc/hexanes) to provide the desired product as an amorphous off-white solid (4 g, 85%).

R_f: 0.71 (30% ethyl acetate/hexanes)

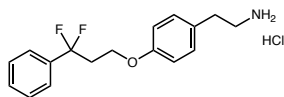
¹H NMR (600 MHz, CDCl₃) δ 7.53 – 7.49 (m, 2H), 7.44 (dd, *J* = 5.3, 2.0 Hz, 3H), 7.07 (d, *J* = 8.1 Hz, 2H), 6.75 (d, *J* = 8.4 Hz, 2H), 4.53 (br. s, 1H), 4.12 (t, *J* = 7.0 Hz, 2H), 3.33 (d, *J* = 6.8 Hz, 2H), 2.87 – 2.46 (m, 4H), 1.43 (s, 9H).

¹³C NMR (100 MHz, CDCl₃) δ 157.1, 156.0, 136.9 (t, *J* = 26.1 Hz), 131.5, 130.0, 129.8, 128.6, 124.9 (t, *J* = 6.3 Hz), 122.0 (t, *J* = 242.4 Hz), 114.7, 79.2, 62.1 (d, *J* = 5.4 Hz), 42.0, 38.9 (t, *J* = 27.6 Hz), 35.4, 28.5.

¹⁹F NMR (282 MHz, CDCl₃) δ -94.51 (t, *J* = 15.4 Hz).

FTIR (neat) ν_{max} : 3337, 3068, 2975, 2931, 1689, 1610, 1509, 1241, 1163, 1051 cm⁻¹.

HRMS (ESI) *m/z*: [M+Na]⁺ calcd. for C₂₂H₂₇O₃NF₂Na, 414.1851; found, 414.1858.



2-(4-(3,3-Difluoro-3-phenylpropoxy)phenyl)ethan-1-amine (44):

A 5 mL reaction vial was charged with *tert*-butyl (4-(3,3-difluoro-3-phenylpropoxy)phenethyl)carbamate (78 mg, 0.2 mmol, 1 equiv) and dissolved in CH₂Cl₂ (1 mL). The reaction mixture was cooled to 0 °C before the dropwise addition of HCl/MeOH (1 mL, made

from 2.5 mL AcCl in 10 mL MeOH). The reaction was stirred for 2 h before being concentrated under reduced pressure to provide the desired product as an off-white solid (65 mg, >99%).

¹H NMR (500 MHz, DMSO-*d*₆) δ 8.20 (br. t, *J* = 23.2 Hz, 2H), 7.59 – 7.53 (m, 2H), 7.52 – 7.48 (m, 2H), 7.16 – 7.09 (m, 2H), 6.86 – 6.75 (m, 2H), 4.05 (t, *J* = 6.4 Hz, 2H), 3.02 – 2.90 (m, 2H), 2.81 (dd, *J* = 9.6, 6.5 Hz, 2H), 2.73 (tt, *J* = 16.5, 6.4 Hz, 2H).

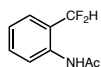
¹³C NMR (126 MHz, DMSO-*d*₆) δ 156.9, 136.2 (t, *J* = 26.0 Hz), 130.1, 129.7, 129.6, 128.6, 124.9 (t, *J* = 6.2 Hz), 122.5 (t, *J* = 241.4 Hz), 114.5, 61.8, 37.5 (t, *J* = 27.1 Hz), 31.9 (t, *J* = 6.5 Hz).

¹⁹F NMR (376 MHz, Methanol-*d*₄) δ -95.30 (t, *J* = 15.9 Hz).

FTIR (neat) ν_{max} : 2960, 1512, 1401, 1145, 1067 cm⁻¹.

HRMS (APCI) *m/z*: [M+H]⁺ calcd. for C₁₇H₂₀ONF₂, 292.1506; found, 292.1507.

Products from Table 4.3: Hydrodefluorination



***N*-(2-(Difluoromethyl)phenyl)acetamide (48):**

Following General Procedure D, the reaction of *N*-(2-(trifluoromethyl)phenyl)acetamide (102 mg, 0.5 mmol, 1 equiv), photocatalyst **P3** (6 mg, 0.01 mmol, 0.02 equiv), and cesium formate (267 mg, 1.5 mmol, 3.0 equiv) at 50 °C provided the product (65 mg, 75% yield) as an amorphous white solid after purification by flash column chromatography on silica (10% – 30% ethyl acetate/hexanes). ¹⁹F NMR of the crude reaction mixture indicated exclusive formation of the Ar–CF₂H product with 0% of the Ar–CFH₂ product.

R_f: 0.71 (60% ethyl acetate/hexanes)

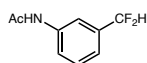
¹H NMR (600 MHz, Chloroform-*d*) δ 8.07 (d, *J* = 8.1 Hz, 1H), 7.55 (s, 1H), 7.49 (t, *J* = 7.7 Hz, 1H), 7.40 (d, *J* = 7.4 Hz, 1H), 7.21 (t, *J* = 7.3 Hz, 1H), 6.66 (t, *J* = 55.0 Hz, 1H), 2.22 (s, 3H).

¹³C NMR (151 MHz, Chloroform-*d*) δ 168.6, 132.0, 127.4 (t, $J = 7.9$ Hz), 124.8, 124.3, 116.0 (t, $J = 237.7$ Hz), 24.8.

¹⁹F NMR (282 MHz, Chloroform-*d*) δ -110.39 (d, $J = 55.0$ Hz).

FTIR (neat) ν_{max} : 3245, 1653, 1558, 1539, 1533, 1521, 1506, 1498, 1489, 1472, 1456, 1436, 1393, 1291, 1028, 757, and 667 cm^{-1} .

HRMS (NSI) m/z : $[M+H]^+$ calcd. for $\text{C}_9\text{H}_{10}\text{ONF}_2$, 186.0725; found, 186.0724.



***N*-(3-(Difluoromethyl)phenyl)acetamide (49):**

Following General Procedure D, the reaction of *N*-(3-(Trifluoromethyl)phenyl)acetamide (102 mg, 0.5 mmol, 1 equiv), photocatalyst **P3** (6 mg, 0.01 mmol, 0.02 equiv), and cesium formate (267 mg, 1.5 mmol, 3.0 equiv) at 50 °C provided the product (65 mg, 70% yield) as an amorphous white solid after purification by flash column chromatography on silica (10% – 30% ethyl acetate/hexanes). ¹⁹F NMR of the crude reaction mixture indicated exclusive formation of the Ar–CF₂H product with 0% of the Ar–CFH₂ product.

R_f: 0.59 (60% ethyl acetate/hexanes)

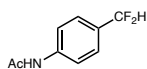
¹H NMR (600 MHz, DMSO-*d*₆) δ 10.14 (s, 1H), 7.89 (s, 1H), 7.66 (d, $J = 8.1$ Hz, 1H), 7.43 (t, $J = 7.9$ Hz, 1H), 7.22 (d, $J = 7.6$ Hz, 1H), 7.01 (t, $J = 55.9$ Hz, 1H), 2.07 (s, 3H).

¹³C NMR (151 MHz, DMSO-*d*₆) δ 168.6, 139.7, 134.5 (t, $J = 22.0$ Hz), 129.3, 121.1, 120.1 (t, $J = 6.2$ Hz), 115.7 (t, $J = 6.3$ Hz), 114.8 (t, $J = 236.2$ Hz), 24.0.

¹⁹F NMR (282 MHz, DMSO-*d*₆) δ -116.63 (d, $J = 55.6$ Hz).

FTIR (neat) ν_{max} : 3430, 1685, 1598, 1559, 1492, 1447, 1373, 1310, 1178, 995, 896, 792, and 667 cm^{-1} .

HRMS (NSI) m/z : $[M+H]^+$ calcd. for $C_9H_{10}ONF_2$, 186.0725; found, 186.0726.



***N*-(4-(Difluoromethyl)phenyl)acetamide (50):**

Following General Procedure D, the reaction of *N*-(4-(Trifluoromethyl)phenyl)acetamide (102 mg, 0.5 mmol, 1 equiv), photocatalyst **P3** (6 mg, 0.01 mmol, 0.02 equiv), and cesium formate (267 mg, 1.5 mmol, 3.0 equiv) at 50 °C provided the product (51 mg, 55% yield) as an amorphous white solid after purification by flash column chromatography on silica (5% – 10% ethyl acetate/hexanes). ^{19}F NMR of the crude reaction mixture indicated exclusive formation of the Ar–CF₂H product with 0% of the Ar–CFH₂ product.

R_f: 0.44 (60% ethyl acetate/hexanes)

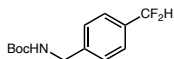
1H NMR (600 MHz, DMSO-*d*₆) δ 10.15 (s, 1H), 7.70 (d, J = 8.2 Hz, 2H), 7.49 (d, J = 8.2 Hz, 3H), 6.94 (t, J = 56.1 Hz, 1H), 2.07 (s, 4H).

^{13}C NMR (151 MHz, DMSO-*d*₆) δ 168.7, 141.5, 128.3 (t, J = 22.4 Hz), 126.4 (t, J = 6.0 Hz), 118.7, 115.0 (t, J = 235.0 Hz), 24.1.

^{19}F NMR (282 MHz, DMSO-*d*₆) δ -107.93 (d, J = 56.1 Hz).

FTIR (neat) ν_{max} : 3301, 2245, 2026, 1971, 1691, 1606, 1542, 1372, 1317, 1263, 1222, 1054, 1029, 1012, 848, 852, and 754 cm⁻¹.

HRMS (NSI) m/z : $[M+H]^+$ calcd. for $C_9H_{10}ONF_2$, 186.0725; found, 186.0726.



***tert*-Butyl (4-(difluoromethyl)benzyl)carbamate (51):**

Following General Procedure D, the reaction of tert-Butyl (4-(trifluoromethyl)benzyl)carbamate (138 mg, 0.5 mmol, 1 equiv), photocatalyst **P3** (6 mg, 0.01 mmol, 0.02 equiv), and cesium formate (267 mg, 1.5 mmol, 3.0 equiv) at 50 °C provided the product (82 mg, 64% yield) as an amorphous white solid after purification by flash column chromatography on silica (2% – 5% ethyl acetate/hexanes). ^{19}F NMR of the crude reaction mixture indicated a 93:7 ratio of the Ar–CF₂H product and the Ar–CFH₂ product (characteristic ^{19}F NMR signal for Ar–CFH₂: (282 MHz, DMSO) δ -201.88 (t, J = 47.7 Hz))

R_f: 0.43 (30% ethyl acetate/hexanes)

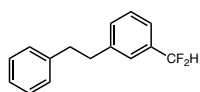
^1H NMR (500 MHz, Chloroform-*d*) δ 7.47 (d, J = 7.8 Hz, 2H), 7.37 (d, J = 7.8 Hz, 2H), 6.63 (t, J = 56.5 Hz, 1H), 4.91 (s, 1H), 4.35 (d, J = 5.2 Hz, 2H), 1.46 (s, 4H).

^{13}C NMR (126 MHz, Chloroform-*d*) δ 156.0, 142.0, 133.6 (t, J = 22.5 Hz), 127.7, 126.0 (t, J = 6.0 Hz), 114.7 (t, J = 238.5 Hz), 79.9, 44.4, 28.5.

^{19}F NMR (282 MHz, Chloroform-*d*) δ -115.57 (d, J = 56.5 Hz).

FTIR (neat) ν_{max} : 3346, 3303, 2984, 2937, 1716, 1703, 1674, 1620, 1541, 1298, 1270, 1153, 1110, 1066, 1051, 1019, 934, 854, 819, 759, 692, 633, and 592 cm⁻¹.

HRMS (NSI) m/z : [M+Na]⁺ calcd. for C₁₃H₁₇O₂NF₂Na, 280.1121; found, 280.1120.



1-(Difluoromethyl)-3-phenethylbenzene (**52**):

Following General Procedure D, the reaction of 1-Phenethyl-3-(trifluoromethyl)benzene (125 mg, 0.5 mmol, 1 equiv), photocatalyst **P3** (6 mg, 0.01 mmol, 0.02 equiv), and cesium formate (267 mg, 1.5 mmol, 3.0 equiv) at 50 °C provided the product (56 mg, 48% yield) as an amorphous white solid after purification by reverse phase preparative HPLC (20% – 50% acetonitrile/water). ^{19}F

NMR of the crude reaction mixture indicated a 77:23 ratio of the Ar–CF₂H product and the Ar–CFH₂ product (characteristic ¹⁹F NMR signal for Ar–CFH₂: (282 MHz, DMSO) δ -203.38 (t, *J* = 48.3 Hz))

R_f: 0.80 (30% ethyl acetate/hexanes)

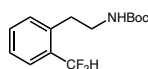
¹H NMR (600 MHz, Chloroform-*d*) δ 7.39 – 7.27 (m, 6H), 7.20 (dd, *J* = 25.0, 7.3 Hz, 3H), 6.62 (t, *J* = 56.6 Hz, 1H), 2.96 (pd, *J* = 9.7, 3.3 Hz, 4H).

¹³C NMR (151 MHz, Chloroform-*d*) δ 142.6, 141.4, 134.6 (t, *J* = 22.1 Hz), 131.0 (t, *J* = 1.8 Hz), 128.8, 128.6, 128.5, 126.2, 125.7 (t, *J* = 6.0 Hz), 123.3 (t, *J* = 6.1 Hz), 115.0 (t, *J* = 238.6 Hz), 37.9, 37.9.

¹⁹F NMR (282 MHz, Chloroform-*d*) δ -110.35 (d, *J* = 56.5 Hz).

FTIR (neat) ν_{max} : 3062, 3027, 2925, 2859, 1602, 1495, 1452, 1373, 1242, 1166, 1083, 1100, 1023, 901, 797, 764, 747, 696, 664, and 551 cm⁻¹.

HRMS (NSI) *m/z*: [M+Cl]⁻ calcd. for C₁₅H₁₄O³⁵ClF₂, 283.0707; found, 283.0706.



***tert*-Butyl (2-(trifluoromethyl)phenethyl)carbamate (53):**

Following General Procedure D, the reaction of *tert*-Butyl (2-(trifluoromethyl)phenethyl)carbamate (145 mg, 0.5 mmol, 1 equiv), photocatalyst **P3** (6 mg, 0.01 mmol, 0.02 equiv), and cesium formate (267 mg, 1.5 mmol, 3.0 equiv) at 50 °C provided the product (68 mg, 50% yield) as colorless oil after purification by reverse phase preparative HPLC (20% – 50% acetonitrile/water). ¹⁹F NMR of the crude reaction mixture indicated a 87:13 ratio of the Ar–CF₂H product and the Ar–CFH₂ product (characteristic ¹⁹F NMR signal for Ar–CFH₂: (282 MHz, DMSO) δ -202.52 (t, *J* = 50.3 Hz))

R_f: 0.40 (30% ethyl acetate/hexanes)

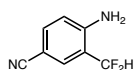
¹H NMR (600 MHz, Chloroform-*d*) δ 7.53 (d, *J* = 7.7 Hz, 1H), 7.42 (t, *J* = 7.5 Hz, 1H), 7.32 (t, *J* = 7.6 Hz, 1H), 7.28 (d, *J* = 7.2 Hz, 1H), 6.81 (t, *J* = 55.3 Hz, 1H), 4.64 (s, 1H), 3.43 – 3.27 (m, 2H), 2.95 (t, *J* = 6.9 Hz, 2H), 1.44 (s, 9H).

¹³C NMR (151 MHz, Chloroform-*d*) δ 156.0, 137.5, 132.6 (t, *J* = 21.1 Hz), 131.0, 130.8, 126.9, 126.5 (t, *J* = 7.1 Hz), 114.4 (t, *J* = 237.7 Hz), 79.5, 41.9, 32.6, 28.5.

¹⁹F NMR (282 MHz, Chloroform-*d*) δ -109.77 (d, *J* = 55.3 Hz).

FTIR (neat) ν_{max} : 3346, 2977, 2933, 1687, 1609, 1585, 1508, 1455, 1391, 1366, 1345, 1269, 1249, 1163, 1128, 1020, 961, 869, 851, 757, 664, 647, and 556 cm⁻¹.

HRMS (NSI) *m/z*: [M+Na]⁺ calcd. for C₁₄H₁₉O₂NF₂Na, 294.1276; found, 294.1277.



4-Amino-3-(difluoromethyl)benzonitrile (54):

Following General Procedure D, the reaction of 4-amino-3-(trifluoromethyl)benzonitrile (93 mg, 0.5 mmol, 1 equiv), photocatalyst **P3** (6 mg, 0.01 mmol, 0.02 equiv), and cesium formate (267 mg, 1.5 mmol, 3.0 equiv) at 23 °C provided the product (55 mg, 65% yield) as an amorphous white solid after purification by reverse phase preparative HPLC (20% – 50% acetonitrile/water). ¹⁹F NMR of the crude reaction mixture indicated a 81:19 ratio of the Ar–CF₂H product and the Ar–CFH₂ product (characteristic ¹⁹F NMR signal for Ar–CFH₂: (282 MHz, DMSO) δ -207.62 (t, *J* = 49.2 Hz))

R_f: 0.59 (60% ethyl acetate/hexanes)

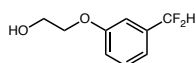
¹H NMR (600 MHz, Chloroform-*d*) δ 7.51 (s, 1H), 7.48 (d, *J* = 8.5 Hz, 1H), 6.73 (d, *J* = 8.5 Hz, 1H), 6.57 (t, *J* = 54.8 Hz, 1H), 4.67 (s, 2H).

^{13}C NMR (151 MHz, Chloroform-*d*) δ 148.6, 135.6, 132.4 (t, $J = 8.2$ Hz), 119.2, 117.6 (t, $J = 21.8$ Hz), 116.8, 115.3 (t, $J = 237.8$ Hz), 100.0.

^{19}F NMR (282 MHz, Chloroform-*d*) δ -114.59 (d, $J = 54.8$ Hz).

FTIR (neat) ν_{max} : 3379, 3254, 2220, 1652, 1646, 1616, 1575, 1540, 1540, 1472, 1328, 1159, 1078, 1014, 911, 830, 766, 667, and 654 cm^{-1} .

HRMS (APCI) m/z : $[\text{M}+\text{H}]^+$ calcd. for $\text{C}_8\text{H}_7\text{N}_2\text{F}_2$, 169.0572; found, 169.0572.



2-(3-(Difluoromethyl)phenoxy)ethan-1-ol (55):

Following General Procedure D, the reaction of 2-(3-(Trifluoromethyl)phenoxy)ethan-1-ol (103 mg, 0.5 mmol, 1 equiv), photocatalyst **P3** (6 mg, 0.01 mmol, 0.02 equiv), and cesium formate (267 mg, 1.5 mmol, 3.0 equiv) at 50 °C provided the product (50 mg, 53% yield) as an amorphous white solid after purification by flash column chromatography on silica (10% – 30% ethyl acetate/hexanes). ^{19}F NMR of the crude reaction mixture indicated exclusive formation of the Ar– CF_2H product with 0% of the Ar– CF_2H_2 product.

R_f: 0.71 (60% ethyl acetate/hexanes)

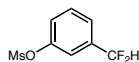
^1H NMR (600 MHz, Chloroform-*d*) δ 7.37 (t, $J = 7.9$ Hz, 1H), 7.10 (d, $J = 7.6$ Hz, 1H), 7.07 (s, 1H), 7.03 (d, $J = 8.4$ Hz, 1H), 6.61 (t, $J = 56.5$ Hz, 1H), 4.14 – 4.11 (m, 2H), 4.00 – 3.97 (m, 2H), 1.99 (bs, 1H).

^{13}C NMR (151 MHz, Chloroform-*d*) δ 159.0, 136.0 (t, $J = 22.3$ Hz), 130.1, 118.5 (t, $J = 6.3$ Hz), 117.2 (t, $J = 1.7$ Hz), 114.6 (t, $J = 239.1$ Hz), 111.5 (t, $J = 6.1$ Hz), 69.5, 61.5.

^{19}F NMR (282 MHz, Chloroform-*d*) δ -110.80 (d, $J = 56.4$ Hz).

FTIR (neat) ν_{max} : 3383, 2941, 2878, 1591, 1494, 1452, 1372, 1325, 1294, 1266, 1185, 1080, 1029, 953, 901, 861, 769, 696, 667, 609, and 549 cm^{-1} .

HRMS (NSI) m/z : $[M+H]^+$ calcd. for $\text{C}_9\text{H}_{11}\text{O}_2\text{F}_2$, 189.0722; found, 189.0720.



3-(Difluoromethyl)phenyl methanesulfonate (56):

Following General Procedure D, the reaction of 3-(trifluoromethyl)phenyl methanesulfonate (120 mg, 0.5 mmol, 1 equiv), photocatalyst **P3** (6 mg, 0.01 mmol, 0.02 equiv), and cesium formate (267 mg, 1.5 mmol, 3.0 equiv) at 23 °C provided the product (50 mg, 45% yield) as a colorless oil after purification by reverse phase preparative HPLC (20% – 50% acetonitrile/water). ^{19}F NMR of the crude reaction mixture indicated exclusive formation of the Ar– CF_2H product with 0% of the Ar– CFH_2 product.

R_f: 0.66 (60% ethyl acetate/hexanes)

^1H NMR (600 MHz, Chloroform-*d*) δ 7.53 (t, $J = 7.8$ Hz, 1H), 7.48 (d, $J = 7.7$ Hz, 1H), 7.46 – 7.39 (m, 2H), 6.66 (t, $J = 56.2$ Hz, 1H), 3.18 (s, 3H).

^{13}C NMR (151 MHz, Chloroform-*d*) δ 149.3, 136.7 (t, $J = 23.0$ Hz), 130.7, 124.7 (t, $J = 6.1$ Hz), 124.5 (t, $J = 1.7$ Hz), 119.5 (t, $J = 6.3$ Hz), 113.6 (t, $J = 240.1$ Hz), 37.8.

^{19}F NMR (282 MHz, Chloroform-*d*) δ -111.65 (d, $J = 56.1$ Hz).

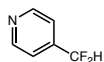
FTIR (neat) ν_{max} : 3035, 2943, 1594, 1491, 1448, 1370, 1322, 1279, 1155, 1121, 1090, 1065, 969, 902, 799, 761, 716, 695, 663, 646, and 583 cm^{-1} .

HRMS (ESI) m/z : $[M+Cl]^-$ calcd. for $\text{C}_8\text{H}_8\text{O}_3\text{ClF}_2\text{S}$, 256.9856; found, 256.9859.

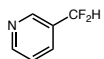


2-(Difluoromethyl)pyridine (57):

Following General Procedure D, the reaction of 2-(trifluoromethyl)pyridine (58 μ L, 0.5 mmol, 1 equiv), photocatalyst **P3** (6 mg, 0.01 mmol, 0.02 equiv), and cesium formate (267 mg, 1.5 mmol, 3.0 equiv) at 23 $^{\circ}$ C provided the product (58% yield vs internal 19 F NMR standard). The spectral data matched that of commercially available material.¹³³ (CAS Number 114468-01-8) 19 F NMR of the crude reaction mixture indicated a 90:10 ratio of the Ar-CF₂H product and the Ar-CFH₂ product (characteristic 19 F NMR signal for Ar-CFH₂: (282 MHz, DMSO) δ -215.25 (t, J = 43.0 Hz))

**4-(Difluoromethyl)pyridine (58):**

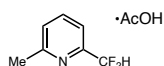
Following General Procedure D, the reaction of 4-(trifluoromethyl)pyridine (58 μ L, 0.5 mmol, 1 equiv), photocatalyst **P3** (6 mg, 0.01 mmol, 0.02 equiv), and cesium formate (267 mg, 1.5 mmol, 3.0 equiv) at 23 $^{\circ}$ C provided the product (43% yield vs internal 19 F NMR standard). The spectral data matched that of commercially available material.¹³⁴ (CAS Number 82878-62-4) 19 F NMR of the crude reaction mixture indicated a 80:20 ratio of the Ar-CF₂H product and the Ar-CFH₂ product (characteristic 19 F NMR signal for Ar-CFH₂: (282 MHz, DMSO) δ -206.12 (t, J = 48.5 Hz))

**3-(Difluoromethyl)pyridine (59):**

¹³³ 2-(Difluoromethyl)pyridine <https://www.sigmaaldrich.com/catalog/product/aldrich/733962>

¹³⁴ 4-(Difluoromethyl)pyridine <https://www.sigmaaldrich.com/catalog/product/aldrich/733261>

Following General Procedure D, the reaction of 3-(trifluoromethyl)pyridine 58 μL , 0.5 mmol, 1 equiv), photocatalyst **P3** (6 mg, 0.01 mmol, 0.02 equiv), and cesium formate (267 mg, 1.5 mmol, 3.0 equiv) at 23 $^{\circ}\text{C}$ provided the product (40% yield vs internal ^{19}F NMR standard). The spectral data matched that of commercially available material.¹³⁵ (CAS Number 76541-44-1) ^{19}F NMR of the crude reaction mixture indicated a 81:19 ratio of the Ar-CF₂H product and the Ar-CFH₂ product (characteristic ^{19}F NMR signal for Ar-CFH₂: (282 MHz, DMSO) δ -206.29 (t, J = 46.6 Hz))



2-(Difluoromethyl)-6-methylpyridine (**60**):

Following General Procedure D, the reaction of 2-methyl-6-(trifluoromethyl)pyridine (81 mg, 0.5 mmol, 1 equiv), photocatalyst **P3** (6 mg, 0.01 mmol, 0.02 equiv), and cesium formate (267 mg, 1.5 mmol, 3.0 equiv) at 23 $^{\circ}\text{C}$ provided the product (71 mg, 64% yield) as a colorless oil after purification by reverse phase preparative HPLC (30% – 99% acetonitrile/water) and acidification of the eluent with conc. HCl. Subsequent hydrolysis of the eluted acetonitrile afforded the acetic acid salt in the title compound. ^{19}F NMR of the crude reaction mixture indicated a 90:10 ratio of the Ar-CF₂H product and the Ar-CFH₂ product (characteristic ^{19}F NMR signal for Ar-CFH₂: (282 MHz, DMSO) δ -220.42 (t, J = 47.9 Hz))

^1H NMR (500 MHz, Deuterium Oxide) δ 8.38 (t, J = 7.9 Hz, 1H), 7.86 (dd, J = 25.1, 7.8 Hz, 2H), 6.99 (t, J = 53.0 Hz, 1H), 2.66 (s, 3H), 1.82 (s, 3H).

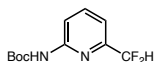
^{13}C NMR (126 MHz, Deuterium Oxide) δ 177.5, 156.2, 147.2, 143.6 (t, J = 27.2 Hz), 130.1, 122.3 (t, J = 5.2 Hz), 109.5 (t, J = 242.3 Hz), 20.9, 19.1.

¹³⁵ 3-(Difluoromethyl)pyridine <https://www.sigmaaldrich.com/catalog/product/aldrich/753173>.

¹⁹F NMR (282 MHz, Deuterium Oxide) δ -120.59 (d, J = 52.9 Hz).

FTIR (neat) ν_{max} : 3122, 2314, 2239, 2125, 1652, 1411, 1342, 1176, 1123, 1057, 780, and 649 cm^{-1} .

HRMS (ESI) m/z : $[\text{M}+\text{Cl}]^-$ calcd. for $\text{C}_9\text{H}_{11}\text{O}_2\text{NCIF}_2$, 238.0452; found, 238.0454.



tert-Butyl (6-(difluoromethyl)pyridin-2-yl)carbamate (61):

Following General Procedure D, the reaction of tert-Butyl (6-(trifluoromethyl)pyridin-2-yl)carbamate (131 mg, 0.5 mmol, 1 equiv), photocatalyst **P3** (6 mg, 0.01 mmol, 0.02 equiv), and cesium formate (267 mg, 1.5 mmol, 3.0 equiv) at 50 °C provided the product (65 mg, 57% yield) as a colorless oil after purification by reverse phase preparative HPLC (20% – 50% acetonitrile/water). ¹⁹F NMR of the crude reaction mixture indicated a 82:18 ratio of the Ar–CF₂H product and the Ar–CFH₂ product (characteristic ¹⁹F NMR signal for Ar–CFH₂: (282 MHz, DMSO) δ -215.27 (t, J = 47.1 Hz))

R_f: 0.85 (60% ethyl acetate/hexanes)

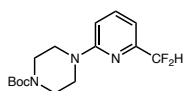
¹H NMR (600 MHz, Chloroform-*d*) δ 7.84 (d, J = 8.4 Hz, 1H), 7.57 (t, J = 7.9 Hz, 1H), 7.05 (d, J = 7.4 Hz, 1H), 6.26 (t, J = 55.6 Hz, 1H), 1.31 (s, 9H).

¹³C NMR (151 MHz, Chloroform-*d*) δ 152.3, 151.9, 151.0 (t, J = 25.7 Hz), 139.5, 114.7 (t, J = 3.6 Hz), 114.2, 113.5 (t, J = 240.4 Hz), 81.6, 28.3.

¹⁹F NMR (282 MHz, Chloroform-*d*) δ -116.63 (d, J = 55.6 Hz).

FTIR (neat) ν_{max} : 3244, 2980, 1733, 1585, 1517, 1466, 1419, 1361, 1291, 1224, 1149, 1109, 1042, 990, 929, 828, 802, 773, 7555, 668, 615, and 558 cm^{-1} .

HRMS (NSI) m/z : $[\text{M}+\text{H}]^+$ calcd. for $\text{C}_{11}\text{H}_{15}\text{O}_2\text{N}_2\text{F}_2$, 245.1096; found, 245.1099.



***tert*-Butyl 4-(3-(difluoromethyl)phenyl)piperazine-1-carboxylate (62):**

Following General Procedure D, the reaction of *tert*-butyl 4-(6-(trifluoromethyl)pyridin-2-yl)piperazine-1-carboxylate (165 mg, 0.5 mmol, 1 equiv), photocatalyst **P3** (6 mg, 0.01 mmol, 0.02 equiv), and cesium formate (267 mg, 1.5 mmol, 3.0 equiv) at 50 °C provided the product (91 mg, 58% yield) as an amorphous white solid after purification by reverse phase preparative HPLC (20% – 50% acetonitrile/water). ^{19}F NMR of the crude reaction mixture indicated a 88:12 ratio of the Ar–CF₂H product and the Ar–CFH₂ product (characteristic ^{19}F NMR signal for Ar–CFH₂: (282 MHz, DMSO) δ -218.18 (t, J = 46.0 Hz))

R_f: 0.76 (60% ethyl acetate/hexanes)

^1H NMR (600 MHz, Chloroform-*d*) δ 7.59 (t, J = 7.9 Hz, 1H), 6.93 (d, J = 7.3 Hz, 1H), 6.70 (d, J = 8.6 Hz, 1H), 6.42 (t, J = 55.9 Hz, 1H), 3.55 (d, J = 8.1 Hz, 8H), 1.48 (s, 9H).

^{13}C NMR (151 MHz, Chloroform-*d*) δ 158.8, 154.9, 151.2 (t, J = 25.5 Hz), 138.7, 114.3 (t, J = 240.2 Hz), 109.2 (t, J = 3.5 Hz), 108.7 (t, J = 1.5 Hz), 80.2, 44.9, 43.8, 42.9, 28.6.

^{19}F NMR (282 MHz, Chloroform-*d*) δ -116.31 (d, J = 55.9 Hz).

FTIR (neat) ν_{max} : 2985, 2931, 2871, 2840, 1675, 1602, 1573, 1475, 1415, 1391, 1369, 1286, 1248, 1217, 1156, 1110, 1031, 988, 961, 865, 797, 775, 755, 732, 670, 626, 614, 562, and 540 cm⁻¹.

HRMS (ESI) m/z : [M+H]⁺ calcd. for C₁₅H₂₂O₂N₃F₂, 314.1675; found, 314.1679.

4.4.6 Computational Details

General Information

All DFT calculations were carried out using the Gaussian 16 software package¹⁰⁶ at the uB3LYP¹⁰⁸ level of theory with the 6-311+G(d,p)¹⁰⁹ basis set unless otherwise stated. The CPCM formalism for the Self Consistent Reaction Field (SCRF) model of solvation was employed in all calculations to account for solvation in DMSO, and the default parameters as implemented in Gaussian were used.

Calculated Reduction Potentials

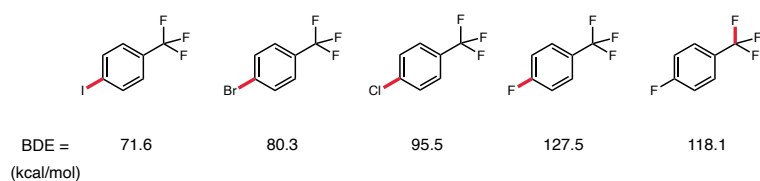
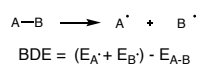
Reduction potentials were calculated using a modified procedure as described by Nicewicz and coworkers.¹⁰⁷ Geometry optimizations were carried out for the reduced and neutral forms of each molecule, and frequency calculations were performed on the minimized structures to ensure no imaginary frequencies existed. Gibbs free energies (G_{298}) were obtained from the calculation and employed in the following equation:

$$E_{1/2}^{0,calc} = -\frac{(G_{298}[reduced]-G_{298}[oxidized])}{n_e\mathcal{F}} - E_{1/2}^{0,SHE} + E_{1/2}^{0,SCE}$$

Where n_e is the number of electrons transferred ($n_e = 1$ for all calculations here), \mathcal{F} is the Faraday constant (value 23.061 kcal mol⁻¹ V⁻¹), $E_{1/2}^{0,SHE}$ is the absolute value for the standard hydrogen electrode (SHE, value = 4.281 V) and $E_{1/2}^{0,SCE}$ is the potential of the saturated calomel electrode (SCE) relative to the SHE in DMSO (value = -0.279V),¹¹⁰ and $G_{298}[oxidized]$ and $G_{298}[reduced]$ are the Gibbs free energies in DMSO obtained from DFT calculations. For example-calculations see the supporting information of the work published by Nicewicz et al.¹⁰⁷

Calculated Bond Dissociation Energies

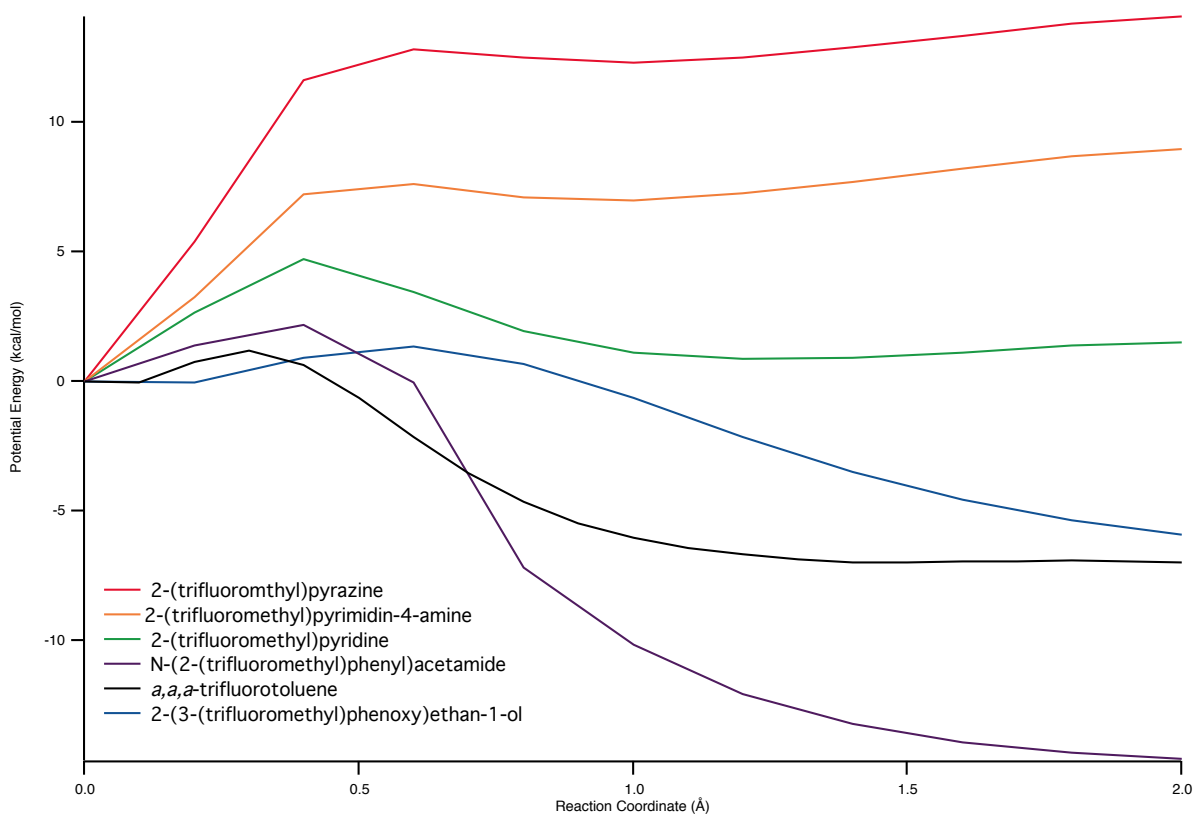
Calculations were carried out at the uM06¹³⁶ level of theory with the 6-311+G(d,p)¹⁰⁹ basis set. Iodine containing molecules, and species pertaining to iodine containing molecules, were carried out using the LanL2DZ basis set. Bond dissociation energies were calculated using the following equation:



Bond Scans

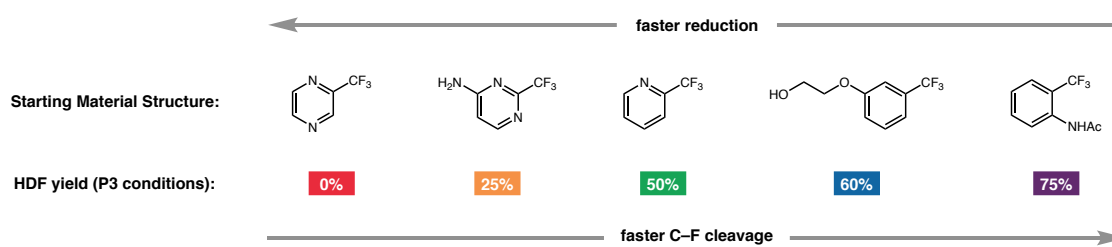
To visualize the thermodynamic barrier of benzylic C–F cleavage the following procedure was employed. Some of the reduced species experience very little or no thermodynamic barrier to cleavage. For these compounds, the geometry of the neutral species was used as the starting geometry but modified to have a charge of -1 and a multiplicity of 2. The potential energy was calculated as the C–F bond was stretched up to 2 Å longer than the starting geometry using uM06/6-31+g(d,p)¹³⁶ level of theory. The relaxed scan was re-optimized every 0.1 Å. The outputs of these calculations were normalized along both axes according to C–F bond length in the neutral species (the starting geometry) then plotted using Igor Pro 8.

¹³⁶ Zhao, Y.; Truhlar, D. G. The M06 Suite of Density Functionals for Main Group Thermochemistry, Thermochemical Kinetics, Noncovalent Interactions, Excited States, and Transition Elements: Two New Functionals and Systematic Testing of Four M06-Class Functionals and 12 Other Function. *Theor. Chem. Acc.* **2008**, *120* (1), 215–241

Figure 4.5 Thermodynamic Profile of C–F bond cleavage in Reduced Trifluoromethylaromatics

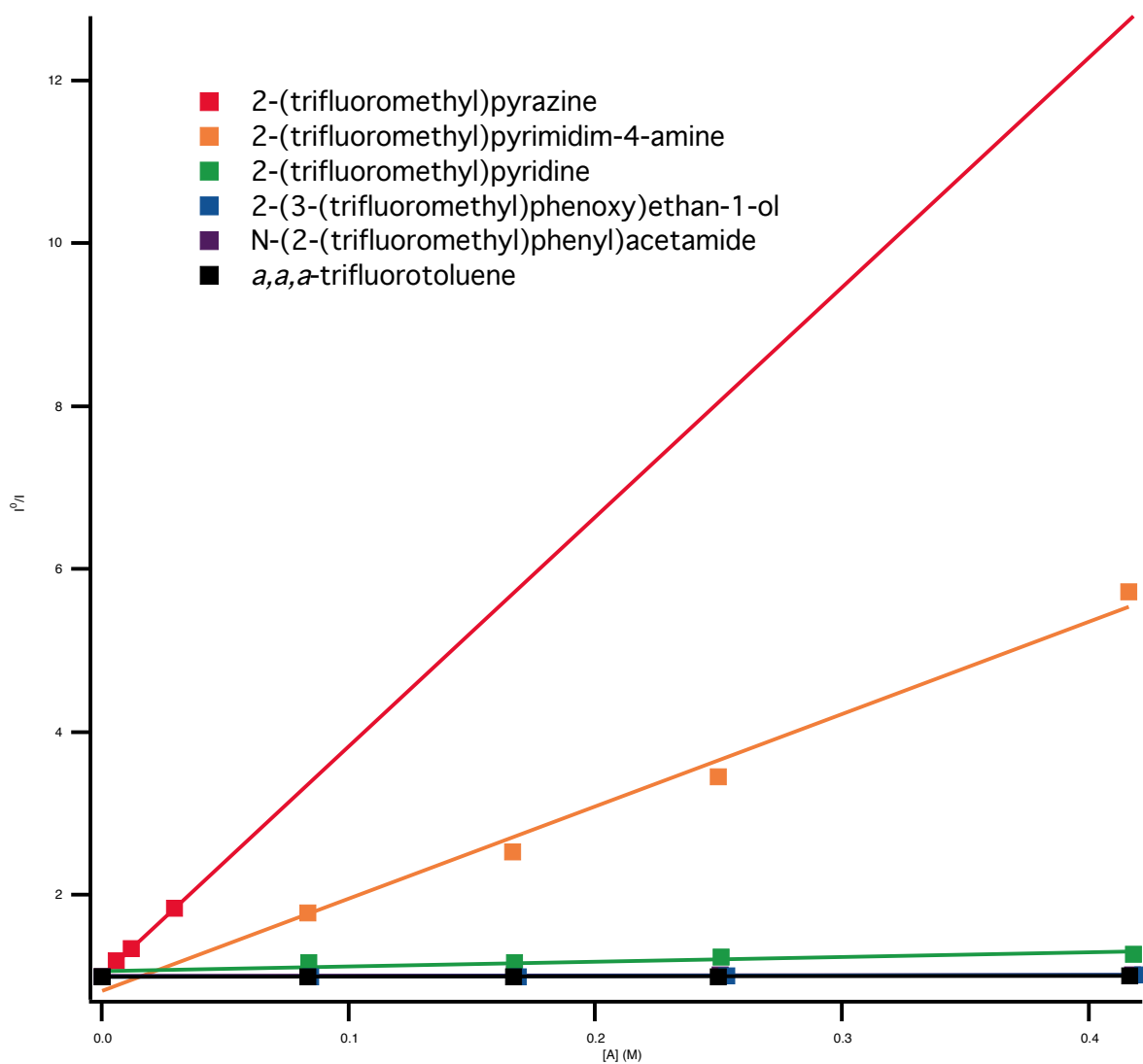
Hydrodefluorination Yields of Calculated Substrates

The reaction of each substrate (0.5 mmol, 1 equiv), photocatalyst **P3** (6 mg, 0.01 mmol, 0.02 equiv), and cesium formate (267 mg, 1.5 mmol, 3.0 equiv) were reacted for 16 hours at 50 °C under irradiation of blue LEDs. Fluorobenzene (0.5 mmol, 1 equiv) was added as an internal fluorine standard after the reaction was complete. The yield of each reaction was determined by ^{19}F NMR integration of the characteristic fluorine peaks against the internal standard.

Figure 4.6 Characterization of the Ideal Substrate

4.4.7 Fluorescence Quenching and Stern-Volmer Plots

All fluorescence measurements were recorded using a Horiba Scientific Dual-FL Fluorometer. Quenching studies were conducted in DMSO at 50 ± 0.5 °C (Peltier temperature controller) with a photocatalyst (Miyake phenoxazine) concentration of 70 μ M. Samples were prepared in Starna quartz cuvettes (3-Q-10-GL14-S) with septum seal caps. Dry N₂ was bubbled through the prepared sample for 5 minutes and allowed to thermally equilibrate in the fluorimeter for an additional 5 minutes before analysis. Raw fluorescence intensity was measured at $\lambda = 500$ nm after excitation at $\lambda = 388$ nm in the quartz cuvettes with a path length of 1 cm and 0.1 second integration. Measurements of the quenchers shown were plotted using Igor Pro 8; data points were fit with a linear trend line.

Substrates**Figure 4.7** Stern Volmer Plots of Select Trifluoromethylaromatics

Compound	[Quencher] (mM)	I ⁰ /I	Coefficients
2-(trifluoromethyl)pyrazine	0	1	$y = a + bx$
2-(trifluoromethyl)pyrazine	5.8	1.2	$a = 1.0145 \pm 0.06$
2-(trifluoromethyl)pyrazine	11.7	1.34	$b = 28.176 \pm 3.75$
2-(trifluoromethyl)pyrazine	29.2	1.83	$\pm 95\%$ confidence interval
2-(trifluoromethyl)pyrimidin-4-amine	0	1	$y = a + bx$
2-(trifluoromethyl)pyrimidin-4-amine	83.2	1.78	$a = 0.82569 \pm 0.508$
2-(trifluoromethyl)pyrimidin-4-amine	166.4	2.53	$b = 11.321 \pm 2.18$
2-(trifluoromethyl)pyrimidin-4-amine	249.6	3.45	$\pm 95\%$ confidence interval
2-(trifluoromethyl)pyrimidin-4-amine	416.1	5.72	
2-(3-(trifluoromethyl)phenoxy)ethan-1-ol	0	1	$y = a + bx$
2-(3-(trifluoromethyl)phenoxy)ethan-1-ol	84.4	1	$a = 0.99518 \pm 0.0163$
2-(3-(trifluoromethyl)phenoxy)ethan-1-ol	168.8	0.99	$b = 0.054371 \pm 0.0693$
2-(3-(trifluoromethyl)phenoxy)ethan-1-ol	253.1	1.01	$\pm 95\%$ confidence interval
2-(3-(trifluoromethyl)phenoxy)ethan-1-ol	421.9	1.02	
N-(2-(trifluoromethyl)phenyl)acetamide	0	1	$y = a + bx$
N-(2-(trifluoromethyl)phenyl)acetamide	83.5	1.02	$a = 1.0127 \pm 0.027$
N-(2-(trifluoromethyl)phenyl)acetamide	167	1.03	$b = 0.028402 \pm 0.116$
N-(2-(trifluoromethyl)phenyl)acetamide	250.6	1.02	$\pm 95\%$ confidence interval
N-(2-(trifluoromethyl)phenyl)acetamide	417.6	1.02	
2-(trifluoromethyl)pyridine	0	1	$y = a + bx$
2-(trifluoromethyl)pyridine	83.6	1.17	$a = 1.0647 \pm 0.135$
2-(trifluoromethyl)pyridine	167.2	1.17	$b = 0.58759 \pm 0.576$
2-(trifluoromethyl)pyridine	250.8	1.24	$\pm 95\%$ confidence interval
2-(trifluoromethyl)pyridine	418	1.28	
α,α,α -trifluorotoluene	0	1	$y = a + bx$
α,α,α -trifluorotoluene	83.3	1.0029	$a = 0.99883 \pm 0.00848$
α,α,α -trifluorotoluene	166.6	1.0009	$b = 0.023275 \pm 0.0364$
α,α,α -trifluorotoluene	249.9	1.0002	$\pm 95\%$ confidence interval
α,α,α -trifluorotoluene	416.7	1.0115	

Other Reaction Components

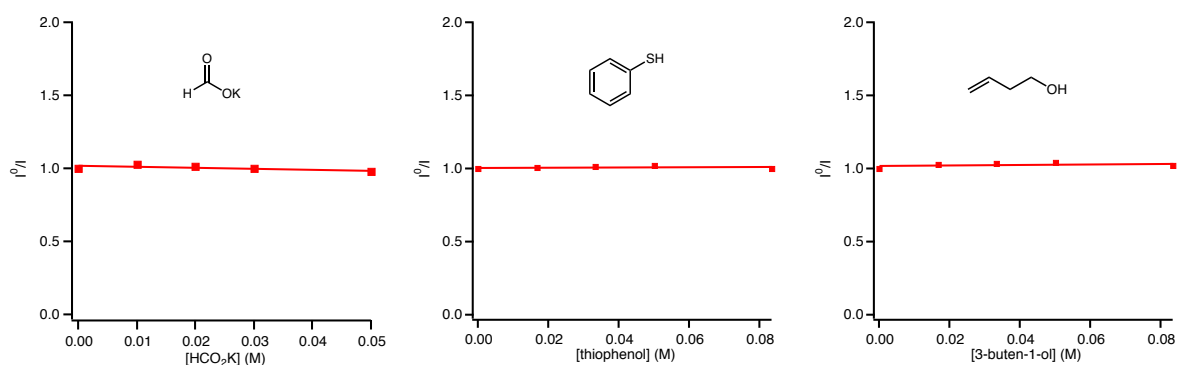


Figure 4.8 Stern Volmer Plots of Other Reaction Components

Compound	[Quencher] (mM)	I^0/I	Coefficients
potassium formate	0	1	$y = a + bx$
potassium formate	10.0	1.03	$a = 1.0185 \pm 0.0765$
potassium formate	20.0	1.02	$b = -0.0071607 \pm 0.0312$
potassium formate	30.0	1.02	$\pm 99\%$ confidence interval
potassium formate	50.0	1.00	
thiophenol	0	1	$y = a + bx$
thiophenol	16.7	1.01	$a = 1.0057 \pm 0.0452$
thiophenol	33.4	1.02	$b = 0.0020272 \pm 0.0184$
thiophenol	50.1	1.02	$\pm 99\%$ confidence interval
thiophenol	83.5	1.00	
3-buten-1-ol	0	1	$y = a + bx$
3-buten-1-ol	16.7	1.03	$a = 1.0148 \pm 0.0703$
3-buten-1-ol	33.4	1.04	$b = 0.005300 \pm 0.0287$
3-buten-1-ol	50.1	1.04	$\pm 99\%$ confidence interval
3-buten-1-ol	83.5	1.02	

Chapter 5:
Reductive Mineralization of Perfluoroalkyl
Substances using Visible Light

Abstract: We've developed photoredox conditions capable of degrading perfluorooctanoic acid and number of its derivatives. These specific polyfluorinated alkanes have largely been phased out industrially in light of their potential toxicity and environmental impact. Accordingly, they're no longer considered suitable for use in consumer products even most industrial uses. Even so, PFOS and its derivatives have been detected in water supplies and is known to bioaccumulate in humans. Large stockpiles of the chemicals remain in storage with no resourceful method for destruction or recycling. We've found, in line with previous reports, that highly reducing conditions lead to the eventual mineralization of these materials. Here we report the detailed characterization of PFOA decomposition employing visible light photoredox as a controlled and sustainable method for PFAS mineralization.

5.1 Introduction

Perfluoroalkylated substances (PFAS) have without question had an enormous impact as commercial materials. The umbrella term PFAS, refers to a number of compounds that are utilized industrially and in everyday consumer products to bolster chemical resistance or physical durability. The applications of these substances range from nonstick cookware and stain resistant clothing to high-performance firefighting foams.

Perfluoroalkyl substances are also persistent organic pollutants that have been detected on a global scale. Their use as industrial surfactants in the production of Teflon (Dupont; PTFE), Scotchgard (3M; PFOSA), and other culinary products has been implicated as a major point of exposure for which breakdown products like perfluorooctanoic acid (PFOA) and perfluorosulfonic acid (PFOS) enter the bloodstream of many Americans. Because humans cannot break down these PFAS, they accumulate and can remain in the body for over a decade, posing a serious health risk for those with repetitive exposure. Likewise, these products are persistent environmental

contaminants, left over from industrial pollution and obsolete film-forming firefighting foams. Heavily affected areas have contaminated water supplies that serve as another significant point of exposure.

In light of these concerns, the Stockholm Convention—focused on persistent organic pollutants—has called for the restricted production of these materials and focus has been placed on removing the contaminants from affected areas. While efficient methods to concentrate these toxins from water have been developed, there are currently no viable methods for their chemical degradation on large scale. Accordingly, the current state of the art for disposal is incineration at temperatures above 1000 °C.¹³⁷ (Figure 5.1)

Although chemical degradation of PFASs has been reported by enzymatic biotransformation,¹³⁸ (electro)chemical oxidation,¹³⁹ sonication,¹⁴⁰ and/or incineration,¹³⁷ these technologies currently suffer from very long reaction times (days to weeks), poor efficiency, and poorly characterized byproducts.¹⁴¹ We posit that due to the extremely electron-deficient nature of PFASs, catalytic reduction represents a logical method of the controlled, predictable degradation

¹³⁷ (a) TSANG, W.; BURGESS, D. R.; BABUSHOK, V. On the Incinerability of Highly Fluorinated Organic Compounds. *Combust. Sci. Technol.* **1998**, *139* (1), 385–402; (b) Vecitis, C. D.; Park, H.; Cheng, J.; Mader, B. T.; Hoffmann, M. R. Treatment Technologies for Aqueous Perfluorooctanesulfonate (PFOS) and Perfluorooctanoate (PFOA). *Front. Environ. Sci. Eng. China* **2009**, *3* (2), 129–151

¹³⁸ (a) Colosi, L. M.; Pinto, R. A.; Huang, Q.; Weber, W. J. J. Peroxidase-Mediated Degradation of Perfluorooctanoic Acid. *Environ. Toxicol. Chem.* **2009**, *28* (2), 264–271; (b) Luo, Q.; Lu, J.; Zhang, H.; Wang, Z.; Feng, M.; Chiang, S.-Y. D.; Woodward, D.; Huang, Q. Laccase-Catalyzed Degradation of Perfluorooctanoic Acid. *Environ. Sci. Technol. Lett.* **2015**, *2* (7), 198–203

¹³⁹ (a) Lin, H.; Niu, J.; Ding, S.; Zhang, L. Electrochemical Degradation of Perfluorooctanoic Acid (PFOA) by Ti/SnO₂-Sb, Ti/SnO₂-Sb/PbO₂ and Ti/SnO₂-Sb/MnO₂ Anodes. *Water Res.* **2012**, *46* (7), 2281–2289; (b) Ochoa-Herrera, V.; Sierra-Alvarez, R.; Somogyi, A.; Jacobsen, N. E.; Wysocki, V. H.; Field, J. A. Reductive Defluorination of Perfluorooctane Sulfonate. *Environ. Sci. Technol.* **2008**, *42* (9), 3260–3264

¹⁴⁰ (a) Cheng, J.; Vecitis, C. D.; Park, H.; Mader, B. T.; Hoffmann, M. R. Sonochemical Degradation of Perfluorooctane Sulfonate (PFOS) and Perfluorooctanoate (PFOA) in Groundwater: Kinetic Effects of Matrix Inorganics. *Environ. Sci. Technol.* **2010**, *44* (1), 445–450; (b) Lv, H.; Wang, N.; Zhu, L.; Zhou, Y.; Li, W.; Tang, H. Alumina-Mediated Mechanochemical Method for Simultaneously Degrading Perfluorooctanoic Acid and Synthesizing a Polyfluoroalkene. *Green Chem.* **2018**, *20* (11), 2526–2533; (c) Wang, N.; Lv, H.; Zhou, Y.; Zhu, L.; Hu, Y.; Majima, T.; Tang, H. Complete Defluorination and Mineralization of Perfluorooctanoic Acid by a Mechanochemical Method Using Alumina and Persulfate. *Environ. Sci. Technol.* **2019**, *53* (14), 8302–8313

¹⁴¹ Qu, Y.; Zhang, C.; Li, F.; Chen, J.; Zhou, Q. Photo-Reductive Defluorination of Perfluorooctanoic Acid in Water. *Water Res.* **2010**, *44* (9), 2939–2947

of PFASs.¹⁴² Strategies for reductive defluorination of PFASs have been successful, but they currently require superstoichiometric metal reductants or extensive irradiation with high intensity UV light (254 nm). To address these challenges, we've aimed to develop a unique approach to PFAS processing where an organic-based catalytic system (no precious or toxic metals would be needed) that requires only formate and visible light as stoichiometric inputs. Detailed characterization of decomposition pathways will enable the effective and predictable decomposition of PFASs.

Recently the Jui group has developed a number of defluorinative methods in which very strong C–F bonds are broken for functionalization. In doing so we have identified a series of systems that accomplish very challenging reduction events (previously achievable only through the use of dissolving metal reductants). These systems utilize visible light, formic acid salts, and organic chromophores to activate fluorinated organic substances through a radical polar crossover mechanism.

The carbon–fluorine bonds that make these compounds useful also make them extremely challenging to deconstruct. We questioned if the conditions we've developed for the modification of trifluoromethylaromatics could be used to invoke decomposition of PFAS. This would offer a controlled decomposition amenable to characterizing

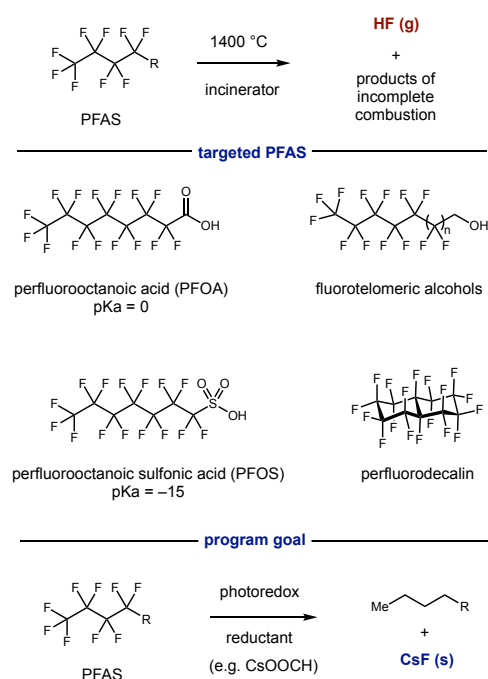


Figure 5.1 Disposal of perfluorinated substances requires extremely high temperatures

¹⁴² Ross, I.; McDonough, J.; Miles, J.; Storch, P.; Thelakkat Kochunarayanan, P.; Kalve, E.; Hurst, J.; S. Dasgupta, S.; Burdick, J. A Review of Emerging Technologies for Remediation of PFASs. *Remediat. J.* **2018**, *28* (2), 101–126

the decomposition products. Additionally the use of visible light to drive decomposition of PFAS would offer a sustainable and safe alternative to the methods currently in use.

5.2 Results and Discussion

We began our experimentation by submitting a number of PFAS to the reductive conditions our group developed for the defluoroalkylation of unactivated trifluoromethylaromatics.¹⁴³ The reactions contain only an organophotoredox catalyst, **P3**, and a stoichiometric reductant, cesium formate. Under these conditions, we observed no reaction from perfluorodecalin and perfluorooctanesulfonic acid. Contrarily, we found that PFOA and its derivative, perfluoro-N,N-diphenyloctanamide **1**, reacted forming a number of new fluorinated products over 24 hours.

We first looked at the octanamide derivative in hopes of identifying these degradation products and then identifying their order of appearance. When the crude reaction mixture was placed under vacuum, the proceeding ¹⁹F NMR indicated that all but one of the products from the reaction were volatile and been evaporated. The remaining product contained only one fluorine and was isolated in 20%

yield and identified as fluoroacetamide **2**

(Figure 5.2) This fragment indicates cleavage occurs between C2 and C3, in line with

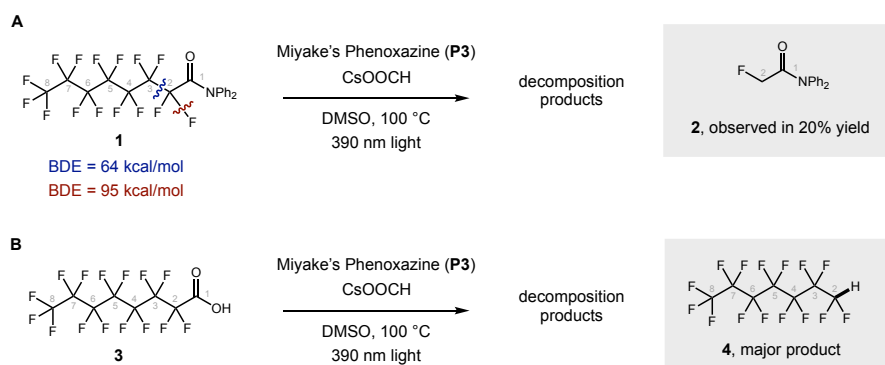


Figure 5.2 Controlled decomposition and characterization of PFAS using photoredox

¹⁴³ Vogt, D. B.; Seath, C. P.; Wang, H.; Jui, N. T. Selective C–F Functionalization of Unactivated Trifluoromethylarenes. *J. Am. Chem. Soc.* **2019**, *141* (33), 13203–13211

our DFT studies that implicate this as the weakest bond in the molecule. Presumably this cleavage is driven by the injection of a single electron into the LUMO of the perfluorinated alkane. Subsequent rearrangement and expulsion of an anionic fragment and an open shell fragment would yield this product after subsequent defluorination. Investigation of this proposal using DFT and isotopic labeling is underway.

Concurrently, we investigated whether this mechanistic characterization translated to PFOA itself. To study the individual products from the complex reaction mixture we employed a solvent combination (1:1 v:v MeCN:DMSO) that produced only a single product over the course of 8 hours (which was consistent with the major product of the initial conditions). By ^{19}F NMR the product contained a $-\text{CF}_2\text{H}$ moiety so we prepared a number of genuine standards¹⁴⁴ in order to identify the exact length of the fragment. Contrary to our initial suspicion that the fragment being formed reflected the C2–C3 of the acetamide derivative, we positively identified the major product as the 7-carbon chain, **4**. (Figure 5.2b) This product instead indicated a C1–C2 fragmentation. Fragmentation in this way is both uncommon and surprising under reducing conditions. To aid in the ongoing investigation of these decomposition mechanisms and help elucidate why they may be different, we've turned to DFT and isotopic labeling studies. Specifically, for PFOA, we're interested in why the C1–C2 cleavage takes preference to the expected C2–C3 cleavage. We're also interested in elaborating on the nature of fragmentation (i.e. where are the charges localized after heterolytic cleavage and from where does the H of the $-\text{CF}_2\text{H}$ moiety originate).

¹⁴⁴ These standards were prepared by hydrodehalogenation of the commercial perfluoroiodides using conditions reported by our group for hydrodefluorination. See Chapter 4 and 5.4.3 Procedures and Characterization Data, pg 296 for further details.

5.3 Conclusions

While we've only begun our experimentation with PFAS, we believe that the conditions described offer an advantage for studying reductive decomposition pathways. Using visible light to invoke decomposition has allowed us to operate under relatively mild conditions and observe and characterize discrete intermediates.

5.4 Supporting Information

5.4.1 General Information

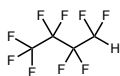
All reactions were set up on the bench top and conducted under nitrogen atmosphere while subject to irradiation from blue LEDs (Kessil 390 nm). Photoredox catalyst P3 was prepared according to literature procedures.¹²⁵ Metal formates were purchased from Sigma-Aldrich chemicals co. Perfluorinated substances were purchased from Sigma-Aldrich chemicals co. or prepared from literature procedures.

5.4.2 General Analytical Information

All NMR spectra were obtained on an INOVA 400 MHz NMR. Chemical shifts (δ) are internally referenced to fluorobenzene (δ -113.5 ppm) for ^{19}F NMR and the residual protio solvent for ^1H NMR. (CDCl_3 : δ 7.26 ppm for ^1H NMR and 77.2 ppm for ^{13}C NMR; CD_3OD : δ 3.31 ppm for ^1H NMR and 49.1 ppm for ^{13}C NMR; THF-d_8 : δ 3.58 ppm for ^1H NMR and 67.6 ppm for ^{13}C NMR; $(\text{CD}_3)_2\text{CO}$: δ 2.05 ppm for ^1H NMR and 29.84 ppm for ^{13}C NMR; C_6D_6 : δ 7.16)

5.4.3 Procedures and Characterization Data

Preparation of Fluorocarbon Fragment Standards



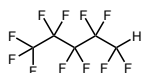
1,1,1,2,2,3,3,4,4-nonafluorobutane:

An oven-dried screw-top test tube equipped with a stir bar was sealed with a PTFE/silicon septa and cooled to room temperature under N_2 atmosphere. The tube was charged with photocatalyst **P3** (2 mol%, 6 mg) and cesium formate (5 equiv, 444 mg). The atmosphere was exchanged by applying vacuum and backfilling with N_2 (this process was conducted a total of three times). Under

N_2 atmosphere, the tube was charged with 1,1,1,2,2,3,3,4,4-nonafluoro-4-iodobutane (1 equiv, 123 mg) and separately degassed, d_6 -DMSO (0.1 M, 5 mL) via syringe. The nitrogen line was removed, and the resulting mixture was stirred at 1200 RPM for 24 hours under irradiation with a blue LED maintained at 23 °C with air cooling. The crude reaction mixture was analyzed directly by 1H and ^{19}F NMR. The crude reaction mixture was used as a stock solution of authentic standard to identify fragments from PFOA degradation.

1H NMR (399 MHz, DMSO- d_6) δ 7.24 (dd, J = 50.0, 5.2 Hz, 1H).

^{19}F NMR (376 MHz, DMSO- d_6) δ -75.96 (t, J = 9.2 Hz), -122.53 (t, J = 7.8 Hz), -124.89 (ddd, J = 13.8, 9.2, 5.1 Hz), -133.87 – -134.14 (m).

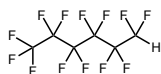


1,1,1,2,2,3,3,4,4,5,5-undecafluoropentane:

An oven-dried screw-top test tube equipped with a stir bar was sealed with a PTFE/silicon septa and cooled to room temperature under N_2 atmosphere. The tube was charged with photocatalyst **P3** (2 mol%, 6 mg) and cesium formate (5 equiv, 444 mg). The atmosphere was exchanged by applying vacuum and backfilling with N_2 (this process was conducted a total of three times). Under N_2 atmosphere, the tube was charged with 1,1,1,2,2,3,3,4,4,5,5-undecafluoro-5-iodopentane (1 equiv, 198 mg) and separately degassed, d_6 -DMSO (0.1 M, 5 mL) via syringe. The nitrogen line was removed, and the resulting mixture was stirred at 1200 RPM for 24 hours under irradiation with a blue LED maintained at 23 °C with air cooling. The crude reaction mixture was analyzed directly by 1H and ^{19}F NMR. The crude reaction mixture was used as a stock solution of authentic standard to identify fragments from PFOA degradation.

1H NMR (399 MHz, DMSO- d_6) δ 7.26 (dd, J = 49.9, 5.2 Hz, 1H).

^{19}F NMR (376 MHz, $\text{DMSO-}d_6$) δ -80.50 (t, J = 9.7 Hz), -124.08 (h, J = 8.5, 7.8 Hz), -126.25 – -126.41 (m), -129.06 – -129.19 (m), -138.52 – -138.81 (m).

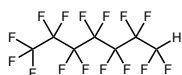


1,1,1,2,2,3,3,4,4,5,5,6,6-tridecafluorohexane:

An oven-dried screw-top test tube equipped with a stir bar was sealed with a PTFE/silicon septa and cooled to room temperature under N_2 atmosphere. The tube was charged with photocatalyst **P3** (2 mol%, 6 mg) and cesium formate (5 equiv, 444 mg). The atmosphere was exchanged by applying vacuum and backfilling with N_2 (this process was conducted a total of three times). Under N_2 atmosphere, the tube was charged with 1,1,1,2,2,3,3,4,4,5,5,6,6-tridecafluoro-6-iodohexane (1 equiv, 223 mg) and separately degassed, d_6 -DMSO (0.1 M, 5 mL) via syringe. The nitrogen line was removed, and the resulting mixture was stirred at 1200 RPM for 24 hours under irradiation with a blue LED maintained at 23 °C with air cooling. The crude reaction mixture was analyzed directly by ^1H and ^{19}F NMR. The crude reaction mixture was used as a stock solution of authentic standard to identify fragments from PFOA degradation.

^1H NMR (399 MHz, $\text{DMSO-}d_6$) δ 7.24 (tt, J = 50.1, 5.3 Hz, 1H).

^{19}F NMR (376 MHz, $\text{DMSO-}d_6$) δ -80.39 (t, J = 9.6 Hz), -122.98 (d, J = 15.2 Hz), -123.32, -126.03 (td, J = 13.8, 5.0 Hz), -128.94 (dq, J = 13.7, 6.6, 5.2 Hz), -138.60 (ddt, J = 50.3, 8.8, 4.4 Hz).



1,1,1,2,2,3,3,4,4,5,5,6,6,7,7-pentadecafluoroheptane:

An oven-dried screw-top test tube equipped with a stir bar was sealed with a PTFE/silicon septa and cooled to room temperature under N₂ atmosphere. The tube was charged with photocatalyst **P3** (2 mol%, 6 mg) and cesium formate (5 equiv, 444 mg). The atmosphere was exchanged by applying vacuum and backfilling with N₂ (this process was conducted a total of three times). Under N₂ atmosphere, the tube was charged with 1,1,1,2,2,3,3,4,4,5,5,6,6,7,7-pentadecafluoro-7-iodoheptane (1 equiv, 248 mg) and separately degassed, *d*₆-DMSO (0.1 M, 5 mL) via syringe. The nitrogen line was removed, and the resulting mixture was stirred at 1200 RPM for 24 hours under irradiation with a blue LED maintained at 23 °C with air cooling. The crude reaction mixture was analyzed directly by ¹H and ¹⁹F NMR. The crude reaction mixture was used as a stock solution of authentic standard to identify fragments from PFOA degradation.

¹H NMR (399 MHz, DMSO-*d*₆) δ 7.25 (tt, *J* = 50.1, 5.2 Hz, 1H).

¹⁹F NMR (376 MHz, DMSO-*d*₆) δ -80.26 (t, *J* = 9.5 Hz), -121.87 – -122.45 (m), -122.60 – -122.92 (m), -122.98 – -123.32 (m), -125.75 – -125.99 (m), -128.69 – -129.05 (m), -138.42 – -138.67 (m).

Decomposition of PFAS

An oven-dried screw-top test tube equipped with a stir bar was sealed with a PTFE/silicon septa and cooled to room temperature under N₂ atmosphere. The tube was charged with photocatalyst **P3** (2 mol%, 6 mg) and cesium formate (5 equiv, 444 mg). The atmosphere was exchanged by applying vacuum and backfilling with N₂ (this process was conducted a total of three times). Under N₂ atmosphere, the tube was charged with the PFAS (1 equiv) and separately degassed, *d*₆-DMSO (0.1 M, 5 mL) via syringe. The nitrogen line was removed, and the resulting mixture was stirred at 1200 RPM for 24 hours under irradiation with a blue LED maintained at 100 °C in a shallow oil

bath. The crude reaction mixture was analyzed directly by ^1H and ^{19}F NMR. A number of synthesized standards were added to the crude reaction mixture to identify components via ^{19}F NMR.

Slower Decomposition of PFAS

An oven-dried screw-top test tube equipped with a stir bar was sealed with a PTFE/silicon septa and cooled to room temperature under N_2 atmosphere. The tube was charged with photocatalyst **P3** (2 mol%, 6 mg) and cesium formate (5 equiv, 444 mg). The atmosphere was exchanged by applying vacuum and backfilling with N_2 (this process was conducted a total of three times). Under N_2 atmosphere, the tube was charged with the PFAS (1 equiv) and separately degassed, 1:1 (v:v) DMSO:MeCN (0.1 M, 5 mL) via syringe. The nitrogen line was removed, and the resulting mixture was stirred at 1200 RPM for 8 hours under irradiation with a blue LED maintained at 100 °C in a shallow oil bath. The crude reaction mixture was analyzed directly by ^1H and ^{19}F NMR. A number of synthesized standards were added to the crude reaction mixture to identify components via ^{19}F NMR.

^{19}F NMR Spectra of Crude Reaction Mixtures

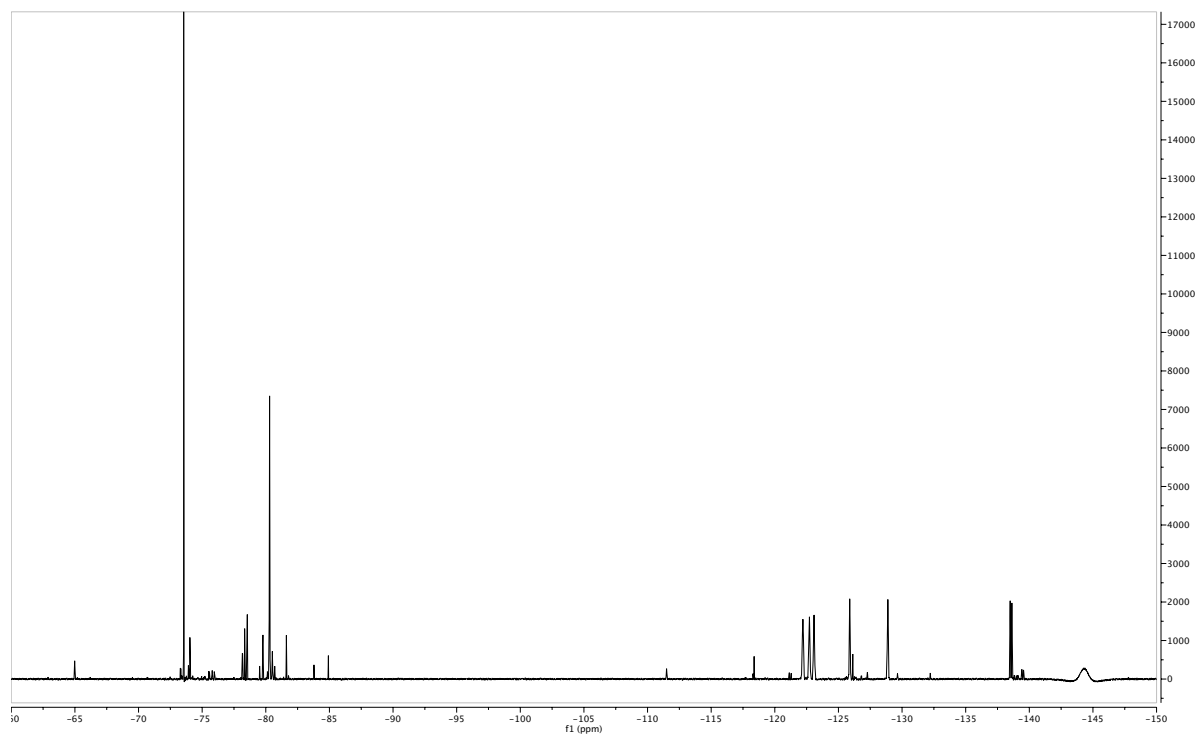
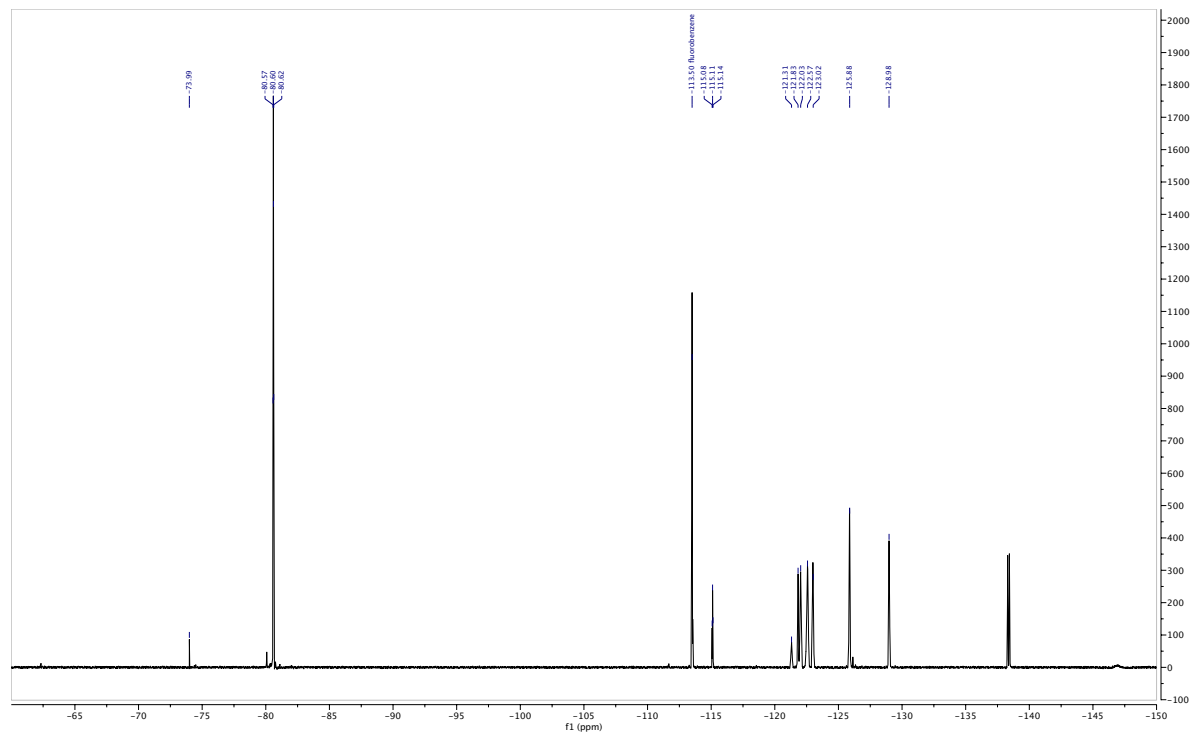
Figure 5.3 ^{19}F NMR of PFOA Degradation Products (DMSO, 100 °C, 24 hours)**Figure 5.4** ^{19}F NMR of PFOA Degradation Products (DMSO:MeCN, 100 °C, 8 hours)

Figure 5.5 ^{19}F NMR of PFOA Degradation Products (DMSO:MeCN, 100 °C, 8 hours) with added 1,1,1,2,2,3,3,4,4,5,5,6,6,7,7-pentadecafluoroheptane standard (no new peaks)

